eman ta zabal zazu

Universidad del País Vasco
Euskal Herriko Unibertsitatea

(cc) 2021 Jon Ander López Ibarra (cc by-nc 4.0)

Department of Control and Systems Engineering

Doctoral program in Control Engineering, Automation and Robotics

eman ta zabal zazu

Universidad del País Vasco
Euskal Herriko Unibertsitatea

Intelligent and Self-adaptive strategies for improved energy management in fleets of vehicles

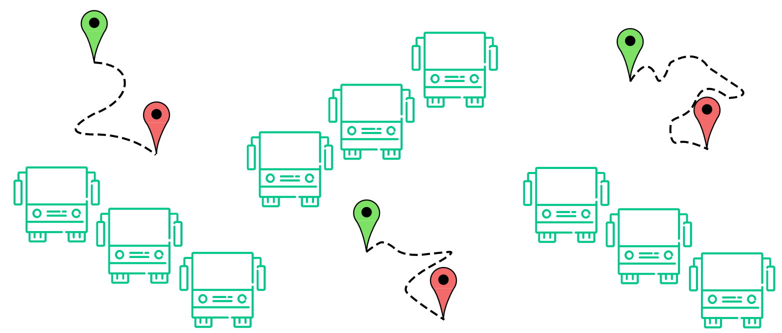

Author: **Jon Ander López Ibarra**

Supervised by: Dr. Haizea Gaztañaga (IKERLAN)

Prof. Haritza Camblong (UPV-EHU)

Doctoral Thesis 2021

This thesis was funded by and carried out at

ikerlan

MEMBER OF BASQUE RESEARCH
& TECHNOLOGY ALLIANCE

Acknowledgements

Heldu da, heldu da hainbestetan pentsatu dudan momentu hau eta egia esan, amaiera izanik nik ikusten dut hasiera baten moduan. Milaka oroitzapen etortzen zaizkit burura bide honetan bizi izan ditudanak eta hainbeste pertsona eskerrak emateko lerro batzuetan. Espero det honen parte izan zareten guztiok gustuko izatea.

Eta hasteko, ez dut ikusten modu hoberik zugandik jaso dudan laguntza guztiagatik, nigan konfiatzeagatik eta nola ez zure aholku baliotsu guztiengatik Haizea. Nik uste bide honetan zehar eramaten dudan gauza baliotsuenetarikoa eman didazula, pertsona moduan haztea. Ahaztu barik esker mila ematea asteburuetan zehar zuzentzen pasatako denbora guzti horrengatik eta emandako aholku oso baliotsuengatik. Eta zelan ez oroitzea zutaz Haritza, eskerrik asko beti laguntzeko prest izateagatik, aholku guztiengatik eta emandako kofidantzagatik bide gonetan zehar.

Bide honen hasiera ez zen hasi bide zuzenengatik, baina askotan esaten dudan moduan, tesiak ez daukate bide zuzenik, baizik eta bide korapilatsu bat. Eta korapilo bakoitzean tesia berezi egiten duen bizitazun, esperientzia eta pertsonak daude. Beraz, hasiera hasieratik hasita, Ikerlan-eko biltegiratze taldeko guztioi eskerrak eman nahi dizkizuet. Izan nuen korapilo honengatik ez balitz izango, seguru naiz nire tesia ez zela izango honela bideratuta. Eta orain bai, hasieran egon zinen lehenengo pausuak ematen laguntzen eta irakatsitako guztiagatik eskerrak eman nahi dizkizut Maitane. Zuri ere Egoitz, zure amaiera bizi izan nuelako nire hasieran eta lerro hauek idazterakoan momentu horiek etortzen zaizkit burura eta zure alboan egonda irakatsi zenidan guztiagatik, beti ateratzen zen gai interesgarriren bat. Nola ahaztu Iñigo eta Mikel, baterien guruak izanik, nituen milaka zalantza eta egonezin argitzeagatik, bene benetan liluratzen nau mundu honek.

Se fue soltando el nudo y surgió el siguiente reto con un nuevo planteamiento de tesis y nueva gente a mi lado. Como olvidarme de ti al escribir estas líneas

Victor. Esta tesis es también parte tuya por haberme transmitido y enseñado tanto. Como ya he dicho, la tesis no es un camino recto y con tu marcha se creo otro nudo. Baina korapilo berri hau alboan nuen jendearekin ez zen hain handia egin. Momentu honetan jaso nuen beroagatik eskerrak eman nahi dizkizuet Igor, Jon eta Haizea. Eta nola ez, kudeaketa talde honetan zaudeten pertsona guztiei. Andoni, ezin ahaztu zutaz, emandako animo guztiengatik eta laguntza behar izan dudanean hor egoteagatik, esker mila. Nerea, zuzenean hasten naiz zure izena izaten, guztia badakizulako eta albotik nire tesia bizi izan duzulako, bai Ikerlan-en eta bai atzerrian, plazer bat izan zen zurekin lan egitea hain erronkatsu izan zen zure master tesian, harro nago zutaz. Como no mencionarte aquí Pilar, por todas las enseñanzas y consejos aportados te quería dar las gracias. Milaka eztabaida mamitsu horiengatik eta falta zaizkigunak, mila esker Josu, pertsona paregabea zara. Eta eztabaidetaz hitzegiten, Aitor zu etortzen zara ere nire burura eta eskerrak eman nahi dizkizut gauzei hainbeste buelta ematen laguntzeagatik. Eta zelan ahaztu nire alboan egon zareten dokotoregai bezala Amaia, Mattin, David eta Iñigo, eta sartu zareten doktoregai eta ikasle guztiei Eneko, Markel, Olatz eta Mikel eskerrik asko bide honetan alboan egoteagatik.

Next jump in this fruitful path was to the north of Europe, to Finland to be more concise. I would like to thank all colleagues from VTT Electrical Powetrains and Storage team for all the learnings. Special thanks to Mikaela for receiving and supporting me during my stay in VTT. Also to Santhosh, Joel, Yancho, Petr, Pekka, Mikko, Mehrnaz and Marco thanks a lot for making the research stay so special and share with me both the technical and personal side from you. Special thanks to all the people that I met in the different conferences such as Pablo, Winfred, Maude, Paulo, Daniel...

I would like to give special thanks to all the jury members and external reviewers for being part of this thesis, and for all their valuable comments. Special mention to Maude, for all the support.

Zelan ahaztu zutaz Bea, korapilo honen zati handiak bizi izan dituzulako eta hauek desegiten ere lagundu didazulako beti irrifarre batekin eta guztirako irtenbide bat aurkituz. Mila mila esker bihotz bihotzez alboan egoteagatik bide honetan eta aguantatu duzun guztiagatik.

Y por último, agradecer a mi familia por todo vuestro apoyo. Sin vosotros esto no hubiese sido posible. Aunque a veces lejos, siempre me he sentido cerca y es por eso que haya podido llegar al final de este camino tan enrevesado. Podéis sentiros orgullosos de ello porque todo esto va por vosotros.

Eskerrik asko danori,
Jon Ander

Abstract

Title: Intelligent and self-adaptive strategies for improved energy management in fleets of vehicles.

In the last years, the automotive industry is undergoing a major transformation. Internal combustion vehicles are being replaced by more sustainable electrified vehicles. Despite the higher number of light vehicles, electric buses are surging faster than any other type of vehicle. The investment cost of electrified buses is higher than conventional diesel buses. However, the lower operation costs of electrified vehicles, has opened up new challenges to improve the energy efficiency further. One of the main challenge is the efficient management of the available power sources. Hybrid and fuel cell buses have a broader number of degrees of freedom compared to battery electric buses, due to the multiple onboard power sources. The power sources energy division is performed based on the energy management strategy.

To achieve and ensure the compensation of the initial extra cost, the total cost of ownership optimization minimizing the operation costs is crucial. The new trend of digitalization makes possible to perform the correct total cost of ownership management, by means of monitoring the vehicles operation and tracing the evolution throughout the vehicle lifetime. In addition, the available operation data of a whole fleet elevates the management level to the fleet level. The fleet level point of view opens up new degrees of freedom to explore. The new degrees of freedom together with the unlimited computational resources by means of digitalization cloud computing, allows to go a step further in the energy management field.

The main challenge of this thesis is "to obtain an integrated solution to manage energetically a fleet of vehicles optimizing the total cost of ownership of the whole fleet, while ensuring that the vehicle service requirements are fulfilled in terms of the planned battery lifetime by means of learning based energy management strategy". To face this challenge on the one hand, a novel learning based energy management strategy based on the adaptive neuro-fuzzy inference system technique conscious of the battery aging has been developed. Learning based energy management strategies allow to merge the short-term power/energy management to obtain close results to the dynamic programming operation, together with the buses battery state of health long-term management.

On the other hand, a hierarchical fleet energy management strategy has been proposed, which integrates the learning based energy management strategy as a holistic approach for the fleet and vehicle management. Within the framework of this approach, new degrees of freedom have been discovered and applied from the fleet level point. The first bus-to-route fleet management adapts each bus operation to each route. The second route-to-bus fleet re-organization, manages the most critical buses batteries lifetime. The third technique updates the learning based energy management strategy to adapt the operation to the new conditions of the bus throughout the fleet lifetime.

The learning based energy management strategy has been evaluated under different scenarios. The obtained results have shown close results to the dynamic programming optimization. The real-time validation of the learning based energy management strategy has been performed in a hardware-in-the-loop, which proves the ability to run the learning based energy management strategy in real-time. The developed solution for plug-in hybrid electric buses has been demonstrated to be directly applicable for fuel cell hybrid electric buses.

The developed hierarchical fleet energy management strategy has been studied in two case studies. The first case study a fleet of buses with LTO battery chemistry without replacement has been analyzed. As second case study, a fleet of buses with NMC battery chemistry with periodically planned battery replacements has been evaluated. For these two scenarios, a fleet buses battery lifetime evaluation plan has been defined. The correct compliance of the developed battery lifetime plan together with the fleet energy management techniques application of bus-to-route, route-to-bus and energy management strategy update, ensure improving the total cost of ownership of the whole.

Key words: Fleet energy management, energy management strategy, battery, fuel cell, dynamic programming, neuro-fuzzy, plug-in hybrid electric bus, fuel cell electric bus.

Laburpena

Titulua: Estrategia adimentsu eta auto-moldakorrak auto floten energia kudeaketa aurreratuentzat.

Autoen industria eraldaketa sakona jasaten hari da azkeneko urteetan. Errekuntza autoak ordezkatzen ari dira auto elektrifikatu jasangarriagoengatik. Auto arinen kopurua handiagoa izan arren, autobus elektrikoan dira azkarren garatzen hari den teknologia. Autobus elektrifikatuen inbertsioa, diesel autobusena baino handiagoa da, aldiz, autobus elektrifikatuen operazio kostu baxuek, energia efizientzia hobetzeko erronka berriak sortu dira. Erronka nagusietako bat energia iturrien kudeaketa efizientea da. Arlo honetan, autobus hibrido eta hidrogenozko autobusek, bateriadun autobusek baino askatasun maila gehiago dituzte, autobusetan daramaten energia iturri anizkoitzengatik. Energia iturrien energia zatiketa energia kudeaketa estrategiekin gauzatzen da.

Hasierako inbertsioaren konpentsazioa ziurtatzeko, jabetzaren guztizko kostuaren optimizazioa operazio kostuak murrizten, ezinbestekoa da. Digitalizazioaren joera berriak jabetzaren guztizko kostuen kudeaketa ahalbidetzen du, ibilgailuen operazioa monitorizatuz eta hauen bizitza osoan zehar. Gainera, flota osoaren operazio datuak izatea ahalbidetzen du kudeaketa maila flota mailara igotzea. Flota mailako ikuspuntuak, kudeaketa energetikorako askatasun gradu kopuruak handitzen ditu. Askatasun gradu berriek, hodeiko errekurtso konputazional "mugagabeekin" batera, aurrera pausu bat ematea ahalbidetzen dute kudeaketa energetikoaren alorrean.

Tesi honen erronka nagusia, "autoen flota bat energetikoki kudeatzeko soluzio integrala bat lortzea, flota mailako jabetzaren guztizko kostua optimizatuz, ziurtatzen planifikatutako baterien bizitzak lortzen direla, ikasketan oinarritutako energia kudeaketa estrategikoen bidez". Erronka hau gauzatzeko alde batetik, ikasketan oinarrituriko energia kudeaketa estrategia berri bat garatu da, inferentzia sistema neuro-lauso moldakorra den teknikaz baliatuz, baterien degradazioaz kontziente dena. Ikasketan oinarrituriko energia kudeaketa estrategiek ahalbidetzen dute epe motzeko potentzia/energia kudeaketa gauzatzea programazio dinamikoaren pareko emaitzak lortuz, autobusen baterien bizitzaren epe luzeko kudeaketarekin bateratzea.

Bestaldetik, floten kudeaketa energetikoa gauzatzeko estrategia jerarkiko bat proposatu da, ikasketan oinarrituriko estrategia integratzen duena, flota eta ibilgailu mailako kudeaketa holistikoa egiteko. Garatutako egitura honekin, flota mailako askatasun maila berriak aurkitu eta aplikatu dira. Lehenengo autobusa-ibilbide floten kudeaketa teknika, autobusaren operazioa ibilbide bakoitzera egokitzen du. Bigarren ibilbide-autobusera floten kudeaketa teknika, flotaren berrantolaketa kudeatzen du, autobus baterien bizitza kritikoenak orekatuz. Hirugarren flota mailako teknika ikasteko energia kudeaketa estrategia eguneratzen du, autobusen bizitza osoan zehar ematen diren egoera berriei operazioa moldatzeko.

Ikasketan oinarrituriko estrategia energetikoa, egoera ezberdinetan ebaluatu egin da. Lortutako emaitzak programazio dinamikoaren antzeko emaitzak izan dira. Ikasketan oinarrituriko estrategia energetikoaren denbora-errealeko erabilera frogatu egin da, hardware begizta batetan. Autobus entxufagarrientzat garatu den ikasketan oinarrituriko estrategia energetikoaren aplikagarritasun zuzena hidrogenozko autobusetan frogatu da.

Floten kudeaketa energetikoa gauzatzeko estrategia jerarkiko bi ikasketa kasuetan analizatu egin da. Lehenengo kasua LTO bateria duten autobus flota bat analizatu da, zeinean bateria aldaketarik ez den ematen. Bigarren kasua NMC bateria duten autobus flota bat analizatu da, zeinean bateria aldaketak ematen diren. Bi ikasketa kasu hauetarako, flotaren baterien bizitza plan bat garatu da. Plan honen betetze zuzena ematen bada, floten kudeaketa tekniken batera, flotaren jabetzaren guztizko kostuaren hobetzea ziurtatzen da.

Hitz gakoak: Flota energia kudeaketa, energia kudeaketa estrategia, bateria, erregai pila, programazio dinamikoa, neuro-lausoa, autobus hibrido entxufagarriak, hidrogenozko autobus hibridoak.

Resumen

Título: Estrategias inteligentes y auto-adaptativas para gestión energética mejorada en flotas de vehículos.

La industria de la automoción esta sufriendo una gran transformación. Los vehículos de combustión están siendo reemplazados por vehículos electrificados más sostenibles. A pesar del mayor número de vehículos ligeros, los autobuses eléctricos son el tipo de vehículo que más rápido está creciendo. El coste de inversión de los autobuses electrificados es mayor comparado a los autobuses convencionales de diesel. Sin embargo, los menores costes de operación de los vehículos electrificados, han creado nuevos retos para la mejora de la eficiencia energética. Uno de los mayores retos es la correcta gestión de las fuentes de alimentación disponibles. En este sentido, los autobuses híbridos y autobuses de hidrógeno tienen más grados de libertad, debido a las múltiples fuentes de alimentación abordo del vehículo. La división energética de las fuentes de alimentación es llevada a cabo por la estrategia de gestión energética.

Para lograr y asegurar la compensación de la inversión inicial, la optimización del coste total de propiedad minimizando los costes de operación es crucial. La nueva tendencia de digitalización posibilita realizar la correcta gestión del coste total de propiedad, monitorizando la operación de los vehículos y trazando la evolución a lo largo de la vida del vehículo. La disponibilidad de los datos de operación de toda la flota posibilita elevar el nivel de gestión a nivel de flota. El punto de visto a nivel de flota crea nuevos grados de libertad para explorar. Los nuevos grados de libertad junto con los recursos computacionales ilimitados debido a la computación en la nube, posibilita dar un paso adelante en el campo de la gestión energética.

El objetivo principal de esta tesis es "obtener una solución integral para gestionarl energéticamente una flota de vehículos optimizando el coste total de propiedad, mientras se asegura que la planificación de vida útil de las baterías se cumple por medio de estrategias de gestión energéticas basadas en el aprendizaje. Para hacer frente a este reto por un lado se ha desarrollado una innovadora estrategia de gestión energéticas basada en el aprendizaje aplicando la técnica neuro-difusa y consciente de la vida de la batería. Las estrategias de gestión energéticas basadas en el aprendizaje posibilitan la gestión a corto plazo de la potencia/energía obteniendo resultados próximos a la programación dinámica, junto con la gestión a largo plazo del estado de salud de la baterías.

Por otro lado, se ha propuesto una estrategia energética jerárquica de gestión de flotas que integra la estrategia de gestión energética basada en el aprendizaje para gestionar de una manera holística tanto la flota como el vehículo. En el marco de este método, se han descubierto nuevos grados de libertad y aplicados desde el punto de vista de la gestión de flota. La primera técnica de gestión de flota denominada autobús-a-ruta, adapta la operación de cada autobús para cada ruta. La segunda técnica denominada ruta-a-autobús, toma decisiones para la re-organización de la flota gestionando de este modo las vidas de baterías de autobuses más críticas. La tercera técnica de gestión de flota actiualiza las estrategias de gestión energéticas basadas en el aprendizaje para adaptar la operación de los autobuses a lo largo de la vida.

La estrategia de gestión energética basada en el aprendizaje ha sido analizado en diferentes escenarios. Los resultados obtenidos son cercanos a los obtenidos mediante la programación dinámica. Se ha validado la operación de la estrategia en tiempo real en un "hardware-in-the-loop". Se ha demostrado la aplicació directa de la solución desarrollada para autobuses híbridos enchufables en autobuses de hidrógeno.

La estrategia energética jerárquica de gestión de flotas se ha analizado en dos casos de estudio. El primer caso de estudio se ha analizado una flota de autobuses con la química de baterías LTO evitando reemplazos. En el segundo caso de estudio se ha analizado una flota de autobuses con la química de baterías NMC con reemplazos periódicos planificados. Para estos dos casos de estudio se ha realizado una planificación de evaluación de vida de las baterías. El correcto cumplimiento del plan de vida de las baterías junto con la aplicación de las técnicas de gestión energética aseguran la mejora del coste total de propiedad de toda la flota.

Palabras clave: Gestión energética de flota, estrategia de gestión energética, batería, pila de combustible, programación dinámica, neuro-difuso, autobús híbrido enchufable, autobús de hidrógeno.

Abbreviations

AFC Alkaline Fuel Cell

ANFIS Adaptive Neuro Fuzzy Inference System

BMS Battery Management System

BEB Battery Electric Bus

BOL Beginning Of Life

BT Battery

CC Constant Current

CD-CS Charge-Depleting Charge-Sustaining

CHA Charge

CV Constant Voltage

DC Direct Current

DCH DCHDischarge

DOD Depth of Discharge

DP Dynamic Programming

EB Electric Bus

EDLC Electric Doubled-Layer Capacitor

EG Electric Generator

EMS Energy Management Strategy

EOL End Of Life

EU European Union

EV Electric Vehicle

EM Electric Motor

ESS Energy Storage System

FC Fuel Cell

FCHEB Fuel Cell Hybrid Electric Bus

FEC Full Equivalent Cycles

FL Fuzzy-Logic

GS Gen-Set

GPS Global Position System

GHG Greenhouse Gas

HIL Hardware-in-the-Loop

HDV Heavy-Duty Vehicle

HEB Hybrid Electric Bus

HEV Hybrid Electric Vehicle

HESS Hybrid Energy Storage System

ICE Internal Combustion Engine

ITS Intelligent Transportation System

LCO Lithium Cobalt Oxide

LMO Lithium Manganese Oxide

LFP Lithium Nickel Cobalt Aluminium Oxide

LTO Lithium Titanate Oxide

MCFC Molten Carbonate Fuel Cell

NMC Lithium Nickel Manganese Cobalt Oxide

NCA Lithium Nickel Cobalt Aluminium Oxide

OB Optimization-Based

OER Oxygen Excess Ratio

PAFC Phosphoric Acid Fuel Cell

PEMFC Proton Exchange Membrane Fuel Cell

PHEB Parallel Hybrid Electric Bus

P-HEB Plug-in Hybrid Electric Bus

RB Rule-Based

RMSE Root Mean Square Error

SHEB Series Hybrid Electric Bus

SOC State of Charge

SOFC Solide Oxide Fuel Cell

SOH State of Health

TCO Total Cost of Ownership

UC Ultra-Capacitor

V2I Vehicle-to-Infrastructure

V2V Vehicle-to-Vehicle

List of Symbols

Symbol	Description	Unit
$a_{cyc}(k)$	Vehicle acceleration	$\left[\frac{m}{s^2}\right]$
$\alpha(k)$	Vehicle slope angle	$[°]$
α_{cha}	Recharging time constant	$[-]$
α_{H_2}	Hydrogen mass consumption cost function weigth	$[-]$
β_{H_2}	Fuel cell oxygen excess ratio cost function weigth	$[-]$
C_{BT}	Battery pack nominal capacity	$[Ah]$
C_{BTkWh}	Battery cost	$\left[\frac{€}{kWh}\right]$
$C_{fuel/t}$	Annual fuel price	$\left[\frac{€}{l}\right]$
$C_{kW/t}$	Referential annual power cost of the grid	$\left[\frac{€}{kW}\right]$
$C_{kWh/t}$	Referential annual energy cost of the grid	$\left[\frac{€}{kWh}\right]$
c_{rf}	Rolling coefficient	$[-]$
c_x	Drag coefficient	$[-]$
$\triangle mF_{ICE}(U(k))$	Fuel mass consumption determined by the split factor	$\left[\frac{kg}{s}\right]$
$\triangle x_{ref}$	State of charge current difference from a reference state of charge	$[-]$

dr	Discount rate	$[\%]$
$DR_{BT/t}$	Depreciation rate of the Battery (BT) per year	$\left[\frac{\%}{year}\right]$
$dw_{drsft}(k)$	Angular acceleration of the drive-shaft	$\left[\frac{rad}{s^2}\right]$
$dw_{wh}(k)$	Angular acceleration of the wheel	$\left[\frac{rad}{s^2}\right]$
E_{BT}	Energy of the battery pack	$[kWh]$
E_{cha}	Energy absorbed from the grid	$[kWh/day]$
$E_{charged}$	Charged energy definition	$[kWh]$
$\eta_{EM}(k)$	Efficiency of the electric motor	$[\%]$
η_{Tr}	Efficiency of transmission	$[\%]$
E_{usable}	Battery usable energy	$[kWh]$
$F_a(k)$	Aerodynamic drag force	$[N]$
$F_g(k)$	Gravitational force	$[N]$
f_{H_2}	Daily hydrogen consumption	$\left[\frac{kg}{day}\right]$
$F_i(k)$	Inertial force	$[N]$
f_{ICE}	Daily fuel consumption	$\left[\frac{l}{day}\right]$
$F_r(k)$	Rolling resistance force	$[N]$
A_f	Frontal area of the vehicle	$[m^2]$
$F_T(k)$	Force acting on the wheels	$[N]$
g	Gravity constant	$\left[\frac{m}{s^2}\right]$
γ	Final drive ratio	$[-]$
γ_{BT}	Battery lifetime	$[years]$
γ_{cal}	Battery cycling lifetime	$[years]$
γ_{cyc}	Battery calendar lifetime	$[years]$
$I_{BT}(k)$	Current to be provided by the battery pack	$[A]$

$I_{BT_{max}}$	Maximum current limit of the battery pack	$[A]$
$I_{BT_{min}}$	Minimum current limit of the battery pack	$[A]$
$ievt$	Depth of discharge events	$[-]$
$I_FCout(k)$	Current to be provided by the the fuel cell	$[A]$
J_{EM}	Electric motor jerk	$\left[\frac{m}{s^3}\right]$
J_{FCHEB}	Fuel cell hybrid electric bus cost function	$[-]$
J_{P-HEB}	Plug-in hybrid electric bus cost function	$[-]$
k_{cs}	Global factor to cold starts	$[-]$
λ_{O_2}	Fuel cell oxygen excess ratio	$[-]$
LL_{ievt}	Battery lifetime lost	$[-]$
L_{route}	Route distance	$[km]$
m_{BT}	Weigth of the battery pack	$[kg]$
m_{cellBT}	Number of battery cell strings	$[-]$
M_{H_2}	Molar mass of hydrogen	$\left[\frac{g}{mol}\right]$
$mf_{ICE}(k)$	Instantaneous fuel mass flow	$\left[\frac{kg}{s}\right]$
m_{veh}	Curb weigth	$[kg]$
m_{pass}	Average weight per person	$[kg]$
m_{tot}	Force acting on the wheels	$[kg]$
n	Number of training epochs	$[-]$
N	Route length	$[-]$
n_{cellBT}	Number of battery cells in series	$[-]$
n_{cellFC}	Number of cells in the stack	$[-]$
NE_{ievt}	Number of depth of discharge events	$[-]$
NE_{ievt}^{max}	Number of maximum depth of discharge events	$[-]$

n_{pass}	Number of passengers onboard the bus	$[kg]$
$n_{round-tripsday}$	Number of completed round trips in a day	$[-]$
Op_{year}	Yearly operation days	$\left[\frac{\text{day}}{year}\right]$
$\omega_{EM}(k)$	Electric motor rotational speed	$\left[\frac{rad}{s}\right]$
$\omega_{EM_{max}}$	Electric motor maximum rotational speed limit	$\left[\frac{rad}{s}\right]$
$\omega_{EM_{min}}$	Electric motor minimum rotational speed limit	$\left[\frac{rad}{s}\right]$
$\omega_{GS}(k)$	Genset rotational speed	$\left[\frac{rad}{s}\right]$
$\omega_{GS_{max}}$	Genset maximum rotational speed limit	$\left[\frac{rad}{s}\right]$
$\omega_{GS_{min}}$	Genset minimum rotational speed limit	$\left[\frac{rad}{s}\right]$
$P_{BT}(k)$	Power target for the battery pack	$[W]$
$P_{cha}(k)$	Power of the charger	$[kW]$
$P_{dem}(k)$	Total power demand during vehicle operation	$[W]$
$P_{EM}(k)$	Power target for the electric motor	$[W]$
$P_{FC}(k)$	Power target for the fuel cells	$[W]$
$P_{FC_{max}}$	Fuel cell maximum power limit	$[W]$
$P_{FC_{min}}$	Fuel cell minimum power limit	$[W]$
$P_{FCout}(k)$	Power provided by the the fuel cell	$[W]$
$P_{GS}(k)$	Power target for the genset	$[W]$
$P_{GSout}(k)$	Power provided by the genset in the training process	$[W]$
$P_{GStarget}(k)$	Power provided by the genset in the optimization process	$[W]$
$P_{max_{aux}}$	Maximum auxiliary consumption	$[kW]$
R_{BT}	Battery pack internal resistance	$[\Omega]$
R_{BTcell}	Battery cell internal resistance	$[\Omega]$

ρ_{air}	Air density	$\left[\frac{kg}{m^3}\right]$
ρ_{fuel}	Volumetric density of diesel	$[kg/l]$
$RMSE$	Root mean square error	$[-]$
r_{wh}	Wheel radius	$[m]$
$SOC_{BT}(k)$	State of charge of the battery	$[\%]$
SOH_{BT}	State of health of the battery	$[\%]$
t	Current year	$[years]$
T	Study scenario duration	$[years]$
t_{cha}	Bus recharging time	$[s]$
TCO_{P-HEB}	Total cost of ownership for plug-in hybrid electric buses	$\left[\frac{€}{lifetime}\right]$
TCO_{FCHEB}	Total cost of ownership for fuel-cell hybrid electric buses	$\left[\frac{€}{lifetime}\right]$
$T_{drsft}(k)$	Torque in the drive-shaft	$[Nm]$
$T_{EM}(k)$	Torque in the electric motor	$[Nm]$
$T_{EM_{max}}$	Maximum electric motor torque limit	$[Nm]$
$T_{EM_{min}}$	Minimum electric motor torque limit	$[Nm]$
$T_{GS}(k)$	Torque in the genset	$[Nm]$
$T_{GS_{max}}$	Maximum genset torque limit	$[Nm]$
$T_{GS_{min}}$	Minimum genset torque limit	$[Nm]$
$T_{ICE}(k)$	Torque in the internal combustion engine	$[Nm]$
T_s	Time step	$[s]$
$T_{wh}(k)$	Torque in the wheel	$[Nm]$
$U(k)$	Power sources split factor	$[-]$
$u_{f,max}$	Maximum split factor constrain	$[-]$

$u_{f,min}$	Minimum split factor constrain	$[-]$
$U_{BT}(k)$	Battery pack equivalent open-circuit voltage	$[V]$
V_{OCBT}	Cell ideal open circuit voltage source	$[V]$
$w_{drsft}(k)$	Rotational speed of the drive-shaft	$\left[\frac{rad}{s}\right]$
W_{H_2}	Fuel-cell hydrogen consumption	$[g/s]$
W_x	Weight applied to the state of charge difference factor	$[-]$
$w_{wh}(k)$	Wheel rotational speed	$\left[\frac{rad}{s}\right]$
x_0	Initial state of charge constrain	$[\%]$
$x_{f,max}$	Maximum state of charge constrain	$[\%]$
$x_{f,min}$	Minimum state of charge constrain	$[\%]$
x_{final}	Final state of charge constrain	$[\%]$
ζ_{BT}	Battery utilization constant	$[-]$

Scientific contributions

Within this research project, several scientific contributions to the literature were published. These are listed below.

JOURNAL ARTICLES:

a. **J. A. López-Ibarra**, N. Goitia-Zabaleta, V.I. Herrera, H. Gaztañaga and H. Camblong, 2020. Battery aging conscious intelligent energy management strategy and sensitivity analysis of the critical factors for plug-in hybrid electric buses. eTransportation 5, 100061. https://doi.org/10.1016/j.etran.2020.100061

b. **J. A. López-Ibarra**, H. Gaztañaga, A. Saez-de-ibarra and H. Camblong, 2020. Plug-in hybrid electric buses total cost of ownership optimization at fleet level based on battery aging. Applied Energy 280, 115887. https://doi.org/10.1016/j.apenergy.2020.115887

CONFERENCE ARTICLES:

c. **J. A. López-Ibarra**, H. Gaztañaga, A. Saez-de-ibarra and H. Camblong, *Hardware-in-the-Loop Experimental Validation of a Learning based Neuro-Fuzzy Energy Management Strategy for Plug-in Hybrid Electric Buses*, in IEEE Vehicle Power and Propulsion Conference (VPPC), Gijón, 2020.

d. **J. A. López-Ibarra**, H. Gaztañaga, A. Anttila, P. Rahkola, M. Ranta and M. Pihlatie, *Electric Bus Forward and Backward Models Validation Methodology Based on Dynamometer Tests Measurements*, in IEEE Vehicle Power and Propulsion Conference (VPPC), Gijón, 2020.

e. **J. A. López-Ibarra**, H. Gaztañaga, Y. Todorov and M. Pihlatie, *Learning Based Energy Management Strategy Offline Trainers Comparison for Plug-in*

Hybrid Electric Buses, in IEEE Vehicle Power and Propulsion Conference (VPPC), Gijón, 2020.

f. B. Falcon Mendoza, V. Herrera-Pérez, **J. A. López-Ibarra**, H. Gaztañaga, and H. Camblong, *Fuzzy based Predictive Control for Optimal Energy Management in Hybrid Urban Buses*, in IEEE Vehicle Power and Propulsion Conference (VPPC), Gijón, 2020.

g. **J. A. López-Ibarra**, N. Goitia-Zabaleta, A. Milo, H. Gaztañaga, and H. Camblong, *Battery and Fuel Cell Aging Conscious Intelligent Energy Management Strategy for Hydrogen Hybrid Electric Buses*, in Transport Research Arena 2020, Helsinki.

h. **J. A. López-Ibarra**, N. Goitia-Zabaleta, A. Milo, H. Gaztañaga, and H. Camblong, *Intelligent and Adaptive Fleet Energy Management Strategy for Hybrid Electric Buses*, in IEEE Vehicle Power and Propulsion Conference (VPPC), Hanoi, 2019.

i. **J. A. López-Ibarra**, N. Goitia-Zabaleta, A. Milo, H. Gaztañaga, and H. Camblong, *Adaptive Energy Management Strategy for a Hybrid Shunter Locomotive*, in IEEE Vehicle Power and Propulsion Conference (VPPC), Hanoi, 2019.

j. M. Lucu, **J. A. López-Ibarra**, E. Martinez-Laserna, I. Gandiaga and H. Camblong, *Development of a self-adaptive cycle ageing model for li-ion batteries using machine learning methods*, in Electric Vehicles Symposium, Lyon, 2019.

k. J. Olmos, **J. A. López-Ibarra**, V. I. Herrera, and H. Gaztañaga, *Analysis of Optimal Charging Points Location and Storage Capacity for Hybrid and Full Electric Buses*, in International conference on Ecological Vehicles and Renewable Energies, Monaco, 2019.

l. **J. A. López-Ibarra**, A. Milo, V. I. Herrera, H. Gaztañaga, and H. Camblong, *Bus-to-Route and Route-to-Bus Approaches in Hybrid Electric Buses Fleet for Battery Lifetime Extension*, in International conference on Ecological Vehicles and Renewable Energies, Monaco, 2019.

m. **J. A. López-Ibarra**, V. I. Herrera, M. Lucu, N. Goitia-Zabaleta, H. Gaztañaga, and H. Camblong, *Battery Ageing Conscious Intelligent Energy Management Strategy for Hybrid Electric Buses*, in International conference on Ecological Vehicles and Renewable Energies, Monaco, 2019.

n. **J. A. López-Ibarra**, V. Herrera, A. Milo, H. Gaztañaga, and H. Camblong, *Energy Management improvement based on Fleet Learning for Hybrid Electric Buses*, in IEEE Vehicle Power and Propulsion Conference (VPPC), Chicago, 2018

SOFTWARE REGISTRATION:

o. H. Gaztañaga, **J. A. López-Ibarra** and A. Saez-de-ibarra, *PLATAFORMA DIGITALIZADA PARA LA MEJORA ENERGÉTICA DE FLOTAS DE AUTOBUSES ELÉCTRICOS E HÍBRIDOS*.

BOOK CHAPTER:

p. **J. A. López-Ibarra**, V. Herrera, A. Milo, H. Gaztañaga, and H. Camblong, *Energy Management improvement based on Fleet Digitalization Data Exploitation for Hybrid Electric Buses*, in Computational Intelligence and Optimization Methods for Control Engineering Energy, Springer Nature Switzerland AG 2019, 2019, ch. 14, pp 319-353.

p. **J. A. López-Ibarra**, H. Gaztañaga, J. Olmos, A. Saez-de-Ibarra and H. Camblong, *Plug-in Hybrid Electric Buses with Different Battery Chemistries Total Cost of Ownership Planning and Optimization at Fleet Level based on Battery Aging*, in Intelligent Control and Smart Energy Management Renewable Resources and Transportation, Springer Optimization and Its Applications Series (Accepted)

Patent:

p. **J. A. López-Ibarra**, and H. Gaztañaga *Vehicle fleet management method*, Application number EP21382101.0 (Under review).

Contents

List of Tables

List of Figures

General introduction

Transport is one of the most impacting sectors regarding Greenhouse Gas (GHG) emissions. In 2016, it caused 20% of GHG emissions in Europe. With the goal of tackling the road transport emissions, the automotive industry has had a mind shift looking for more sustainable and emission free alternative solutions. In this regard, city buses are positioned as potential candidates for alternative technologies market, due to favorable operational characteristics.

The urban road transport decarbonization process is being addressed with the integration of the available commercial solutions of full-electric and hybrid buses solutions. One of the main challenge regarding the technology election is based on the efficient utilization of the power sources and Energy Storage System (ESS) according to the power demand level. In this regard Hybrid Electric Buses (HEBs) have a wider number of degrees of freedom compared to Battery Electric Buses (BEBs), since they are composed of two or more power sources. This allows to have the control of the available power sources based on the Energy Management Strategy (EMS), which manages the operation.

In addition to the higher number degrees of freedom, the developments on HEBs pave the way for the oncoming Fuel Cell Hybrid Electric Buses (FCHEBs) integration. The architectural similarities between the HEB and FCHEB makes HEB an ideal intermediate step solution. These similarities allow to apply directly HEBs developments regarding energy management into FCHEBs. The current FCHEB technological maturity and market penetration level, holds back the massive integration. However, it is foreseen a hydrogen technology price decrease, with the hydrogen market penetration growth. In a near future the scenario of road transport, due to the variety of integrated technological solutions, will be composed of mixed fleets.

Not only FCHEBs integration is a challenging process, but also HEBs integration. The main challenge is the higher investment costs beside conventional diesel buses. On the pro side, the lower operational costs of HEBs, together with the high yearly driven distances, compensate the manufacturing extra costs. As a result, the Total Cost of Ownership (TCO) economic performance improvement indicator plays a key role in the transport electrification process.

Breaking down the TCO calculation and identifying the energy efficiency related factors, the operation cost and carbon-taxes cost factors are the costs that are considered to be manageable. As it has been aforementioned the operation costs are manageable by means of the HEBs degrees of freedom and the ability to manage those variables with the EMS.

The integration of the new developments of digitalization into the automotive industry allows a continuous monitoring of the operation of the vehicles, cloud data storage, and cloud-computing. The "unlimited" data storage and resources allow to develop more sophisticated and advanced EMSs based on artificial intelligence. In addition to that, the available operation data of all the vehicles enables to analyze the different energetic behaviors and opens new ways and levels to further improve the TCO.

On the one hand, the learning based EMSs open up new possibilities of management. Learning based EMSs permits to consider and combine consumption minimization short-term objectives with other long-term targets that directly impact to the TCO. A crucial long-term target that affects on the TCO is the battery lifetime and respective number of replacements. The BT lifetime is shorter than the bus service lifetime. This fact demands replacement of the BT to fulfill the bus service requirements. By means of the learning based EMS the BT lifetime can be managed together with the consumption minimization.

On the other hand, the capability to monitor the vehicles operation of a fleet allows to step up an upper level point of view, the fleet level. The fleet level enables to develop fleet management techniques. The current available fleet management approaches are focused on traffic jam avoidance, vehicle diagnostics, itinerary planning, and charging scheduling. Fleet energy management is identified as a gap in the literature with potential for further improvement of the TCO at fleet level. This upper level management development combined with the new possibilities of the learning based EMSs for optimizing and managing the TCO at vehicle and fleet levels are identified as the main challenges to be tackled. The main challenge of this Ph.D. thesis is:

To obtain an integrated solution to manage energetically a fleet of vehicles optimizing the TCO the whole fleet, while ensuring that the vehicle service requirements are fulfilled in terms of the planned battery lifetime by means of learning based energy management strategies.

To face this identified challenge, the objective of this Ph.D. thesis is:

To develop a methodology to optimize and manage the total cost of ownership for fleets of vehicles

Besides the main objective of this thesis, other particular objectives proposed in the present study are:

- Developing an artificial intelligence **learning based energy management strategy for plug-in hybrid electric buses conscious of the battery aging**.
- Validating the replicability and develop a **learning based energy management strategy for fuel cell hybrid electric buses conscious of the battery and fuel-cell aging**.
- Exploring and applying **the new degrees of freedom derived from the fleet level point of view**.

This document is structured in 5 chapters.

In the first chapter, the state-of-the-art review of electrified buses focusing on hybridization is presented. The analysis is performed from the powertrain, vehicle management, and fleet management standpoints. Furthermore, available commercial solutions are reviewed. Finally, the main gaps identified in the literature are also reported. The identified gaps are the baseline to define the research plan adopted in this Ph.D. thesis.

In the second chapter, the novel hierarchical EMS for TCO management at fleet level is introduced. The hierarchical architecture is composed of three levels. The inner part contains the online learning based EMS. In this level, the management of the available power sources is carried out onboard the bus. The onboard integrated EMS is designed at the immediate upper level in the cloud. Based on a neuro-fuzzy technique, the EMS is defined learning from the global optimal solutions. In the highest management level, the operation of the whole fleet is optimized based on the fleet TCO. The decisions taken define the fleet re-organization and the online operation EMS update throughout the bus lifetime. These decisions are based on the evaluated battery lifetime of the fleet, aiming at meeting the planned TCO requirements.

In the third chapter, the proposed vehicle level EMS design and real-time implementation onboard the bus are thoroughly described and analyzed. The novel approach of the vehicle level EMS is a learning-based EMS. The developed solution is a particular contribution of the Ph.D. thesis as depicted in Fig. 1. This advance EMS is composed of a dynamic programming global optimization technique and the neuro-fuzzy based learning technique. The basis of the utilized techniques are introduced in this chapter. The novel learning based EMS has been evaluated into two case studies: a Plug-in Hybrid Electric Bus (P-HEB) and a FCHEB. The results obtained with the two topologies have been analyzed and compared.

In the fourth chapter the proposed novel hierarchical EMS methodology for the TCO management at fleet level is thoroughly described and evaluated. The vehicle level analysis is elevated to fleet level in this chapter. This analysis is the main contribution of the present Ph.D. thesis, as shown in Fig. 1. The fleet level energy management covers the identified gap in the literature. Two fleets of buses case studies are analyzed throughout the whole lifetime, evaluating every stage of the hierarchical EMS. The obtained results of the two fleets are analyzed and compared.

In the fifth chapter the general conclusions and contributions of this Ph.D. thesis are presented. To lend continuity to the research, some possible future lines

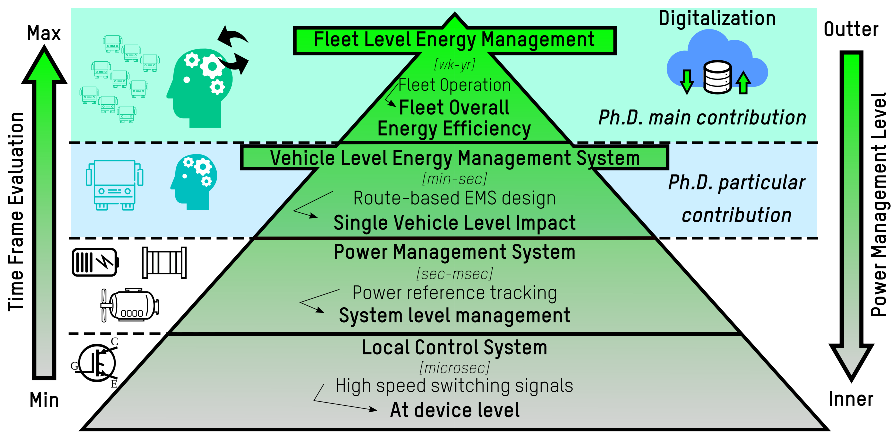

Figure 1: Energy Management hierarchy.

related to the topic addressed in this Ph.D thesis are presented.

To provide an overview of the content and facilitate the comprehension of the document structure, the Ph.D. organization is depicted in Fig. 2.

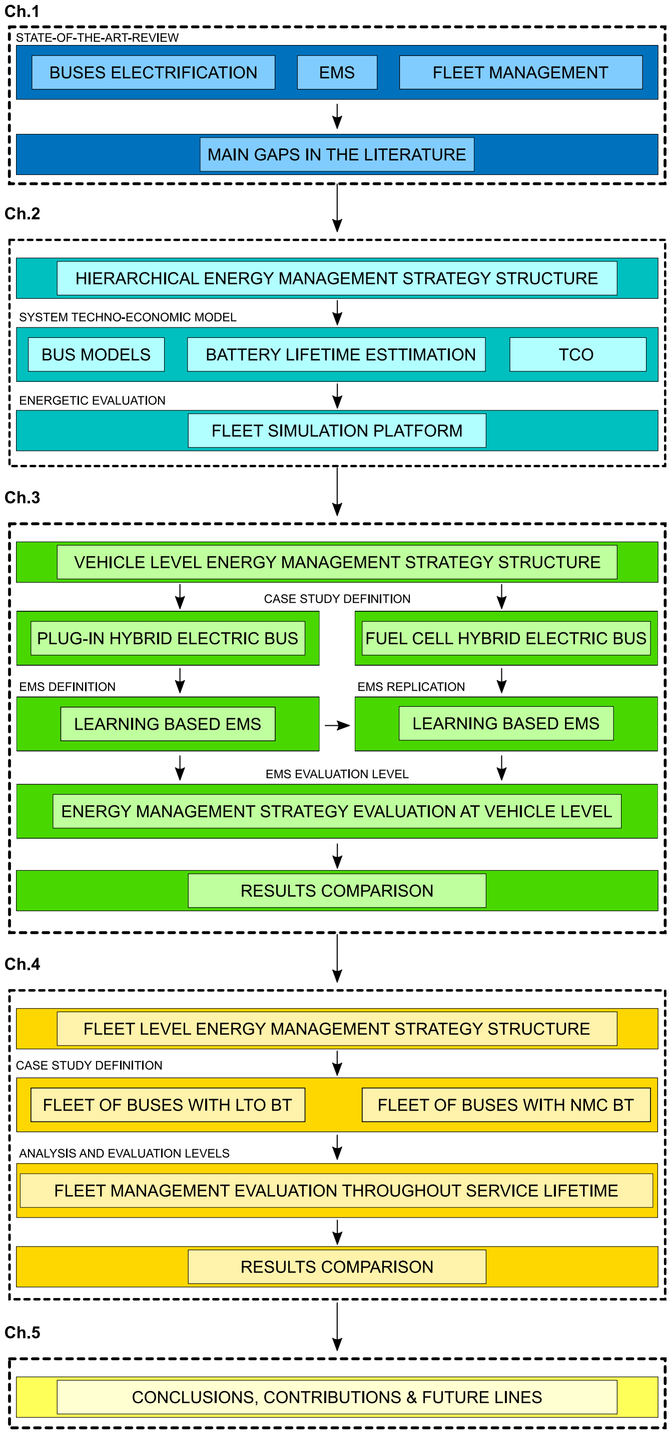

Figure 2: Ph.D thesis organization.

1

State-of-the-art

Summary

In this first chapter the state-of-the-art review of electrified buses is presented. The analysis is performed from the powertrain, vehicle management, and fleet management standpoints. Furthermore, available commercial solutions are reviewed. Finally, the main gaps identified in the literature are also reported. These gaps serve as a baseline to define the research plan adopted in this Ph.D thesis.

1.1 Introduction

The growing concern in regard to GHG emissions issue has derived on a mind shift in the automotive industry, looking for more sustainable and greener solutions. The road transport was responsible of the 72.1% of total transport GHG emissions in 2016, as depicted in Fig. 1.1-A [1].

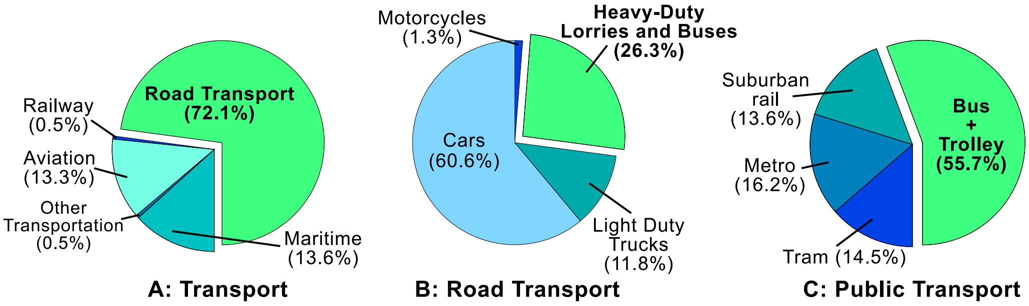

Figure 1.1: European public urban transport pollution and utilization breakdown.

Light duty vehicles have been in the spotlight, almost neglecting the Heavy-Duty Vehicle (HDV) impact. HDVs emit a quarter of the road transport GHG emissions as depicted in Fig. 1.1-B. In addition, despite the more restrictive standards regarding GHG emissions (EURO VI) limiting the Internal Combustion Engine (ICE) operation, HDV emissions have been constantly growing between from 1990 to 2010 [2].

The more restrictive EURO VI GHG emission standards are limiting the

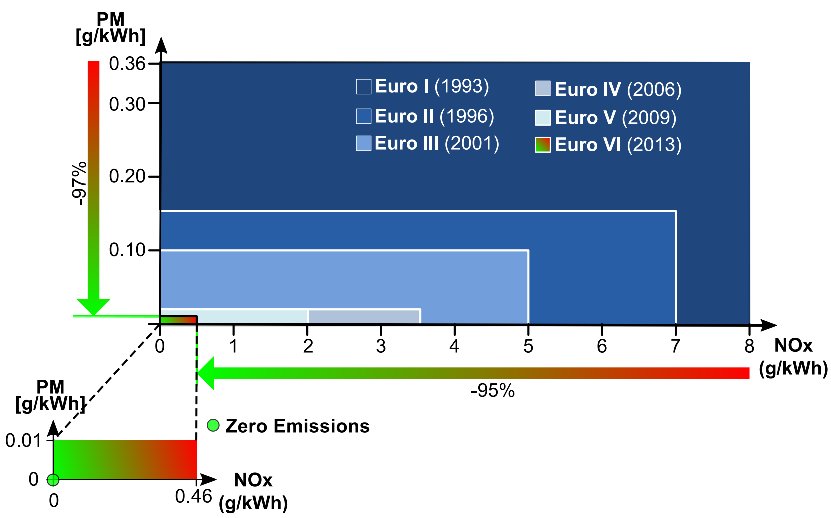

Figure 1.2: EURO standard GHG emission limitations.

transport emissions nearly to zero, as depicted in Fig. 1.2. Moreover, due to the high pollution concentration in some cities, zero emissions zones have been implemented with a tendency to increase over the years.

Analyzing the level of pollution impact of lorries and buses is different. The most worrying zones are urban areas, due to the high pollution and congestion levels, where commonly buses are running around 16 hours a day. Moreover, buses are the most used type of public transport, with nearly 56% of journeys in Europe in 2014, as shown in Fig. 1.1-C [3]. The European bus fleets lay out, still in 2015, was composed of nearly 50% of the vehicles with Euro III or older ICEs [4]. Moreover, nowadays about the 98% of the lorries in Europe rely on diesel [5]. To fulfill the scheduled reduction of 30% of CO2 emissions for HDVs by 2030, from the CO2 levels of 2019 [5], a renewal of the road transport fleets to a more sustainable fleet is needed.

The transport decarbonization challenge is seen to be spearheaded by public transport, owing to the favorable driving characteristics [6]. As a result, several studies have been performed on the subject of analyzing the available alternative technologies, pointing out hybrid electric buses (HEBs) and full electric buses as the most viable options [7–9]. The fact that buses are running in a predefined route facilitates the battery sizing and driving range issue. Moreover, these type of buses are much more efficient than diesel buses in stop-and-go operation mode.

Among the available alternative technologies, HEBs are found as the intermediate step between conventional and BEB, having the closest manufacturing costs to conventional diesel buses and offering improved energy efficiencies [7–10]. However, due to the reduced energy storage system and the resulting constrained use of it, HEBs show similar polluting behavior to conventional buses regarding the environmental footprint [10]. Therefore, the target for the full decarbonization of urban road transport must be addressed with the deployment of the available full electric buses solutions.

The lithium-ion BTs price decrease (price drop of around 79% since 2010 [11]) has placed BEBs as the widespread storage system solution [8, 9], in regard to full electric buses. However, to reach the zero-emissions target of public transport, wider range of solutions are required to meet the most demanding and longer routes requirements [12, 13]. In this respect, FCHEBs are suitable solutions for covering these kind of routes. The main drawback of FCHEBs is still the lack of hydrogen refueling stations and the high price of the Fuel Cells (FCs).

The closest solution to FCHEBs and the main competitors of full electric buses are P-HEB, due to the technical characteristics and lower manufacturing cost [14–16]. The larger BT capacities than in HEBs and the additional flexibility degree of charging allow to harness the BT utilization, increasing the zero emission zone range. In addition, the advances in P-HEBs will pave the way for the oncoming FCHEBs implementation, as the topologies and degrees of freedom are similar, being the developed P-HEBs EMSs applicable directly on FCHEBs [17, 18].

All the aforementioned powertrains have in common the higher investment costs beside conventional diesel buses, making the integration of alternative solutions a challenging process. On the pro side, the lower operational costs of P-HEBs and BEBs, together with the high yearly driven distances help to compensate the manufacturing extra costs [6, 9, 10, 19] This fact is yet not the case for the FCHEBs. To evaluate the offset cost, the TCO calculation plays a key role on the transport electrification process [9, 12].

The TCO calculation is determined with known conditions, which vary throughout the bus lifetime and generate uncertainties on the TCO, as it has been evidenced in the literature [12, 20, 21]. The main reason is the high sensitivity of the TCO to the operational aspect [9, 12, 21]. A technical proposal is the continuous monitoring of the vehicles operation, by means of the new opportunities of digitalization. Indeed, this monitoring allows to have the fleet overall view, having an additional degree of freedom and point of view to process, analyze, and make decisions, with the aim of managing and further improving the overall fleet TCO.

Digitalization is the process of providing vehicles with sensors to acquire information, storing this information in the cloud, and analyzing the data [22]. This new trend enables to monitor the energetic operation of each vehicle from a local and fleet point of view. Consequently, the decision making for the fleet TCO management can be carried out from an upper level of the whole fleet overview. Based on this decision, the lower level decision making for the EMS design of each bus is performed from the fleet and local points of view. The main challenge for the TCO management at fleet level and the digitalization is the large data volume to be managed by fleet managers. Consequently, new automated and advanced tools are needed for the data analysis and decision making, becoming a thriving area of research [23, 24].

1.2 Electric and Hybrid Electric Buses

Nowadays automotive manufacturers have shifted the production focus to more efficient and sustainable solutions. Electrification of vehicles is being the tendency that most of the automotive manufacturers are adopting. Consequently new powertrains and ESSs solutions have been developed [25]. However, the new technology adoption has not progressed directly from ICE based vehicles to pure Electric Vehicles (EVs). There has been a transitional technology, Hybrid Electric Vehicle (HEV). This technology is more efficient and less polluting than combustion vehicles and with a smaller ESS than EVs.

As an overview, among the available alternative technologies, HEB are found as the intermediate step between conventional and BEB, having the closest manufacturing costs to conventional diesel buses and offering improved energy efficiencies [7–10]. Hybrid is a term used to refer to vehicles powered by at least two power sources. The most usual combination is composed by an ICE and an Electric Motor (EM) connected to a battery. This combination takes advantage of both conventional ICE vehicles and BEBs. HEBs have a superior mileage beside BEBs, as a result of the combination of two or more power sources. As a consequence of this combination, HEBs have more flexibility to supply the power demand compared to conventional and BEBs. This flexibility allows to operate the ICE in the optimal conditions, reducing the fuel consumption beside conventional vehicles [14, 24]. However, due to the reduced ESS and the resulting constrained use of it, HEBs show similar polluting behavior to conventional buses regarding the environmental footprint [10]. Setting the target for the full decarbonization of urban road transport, it has to be addressed with the deployment of the available full electric buses solutions.

Among the full electric solutions BEBs and FCHEBs are found. As it has been aforementioned, BEBs are actually commercially available and widespread solution. With the aim of covering all type of routes a wider range of solutions is needed. At this point FCHEBs are the near future solution for covering the most demanding routes. However, nowadays P-HEBs are the best alternative to FCHEB. The powertrains similarities provide both architectures similar characteristics. The current developments on P-HEB are an investment for the FCHEBs, since they are directly applicable.

The recent technological developments on vehicle electrification has broaden the possible solutions. This makes to have a wide range of different electric and hybrid vehicles powertrains. In addition, regarding the ESS size, ICE, and EM rate, different hybridization levels are identified in the literature. Therefore, in the following sections the classifications concerning powertrain and hybridization levels are detailed, finishing with an overview of available commercial hybrid and electric buses.

1.2.1 Powertrain Architectures

In the literature, HEBs composed of a Gen-Set (GS) and a BT are generally grouped into three categories [14], regarding the powertrain elements (power electronics, power sources and propulsion systems) architecture.

- Parallel Hybrid Electric Buses: EM and the ICE are rotating at the same speed imposed by the wheels.
- Series Hybrid Electric Buses: The series configuration is only driven by an EM.
- Series-Parallel Hybrid Electric Buses: This configuration is a combination of both parallel and series.

Following with the hybrid buses, but this time composed of a FC and a BT pack, two powertrain types are differentiated. The classification has been determined following the previous HEBs classification criteria of categorizing the powertrains based on the powertrain elements. The most simple structure is the series FCHEB, working as a range extender. The parallel FCHEB has an increased flexibility, since both the FC and the BT are able to provide the power demand.

Finally, in the case of BEBs, powertrains architectures can be classified by the type of transmission, by the locations and the number of EMs or by combinations of ESSs [26]. Therefore, in the following subsections the three HEBs powertrain architectures are described and an overview of the main Electric Buses (EBs) architectures is carried out.

1.2.1.1 Series Hybrid Buses

Series Hybrid Electric Bus (SHEB) is considered to be a purely EB with a range extender. Therefore the series powertrain architecture integrates an EM to drive the vehicle. The energy is provided by an ESS and a GS (composed by an ICE and a electric generator), which is used to extend the driving range of the ESS, as shown in Figure 1.3. All the elements are electrically connected to a DC bus through power electronics (inverters and converters). Consequently the power split is determined based on the power demand. This electrical connection allows to increase the operation modes, summarized in Fig. 1.3 as 7 different operation modes.

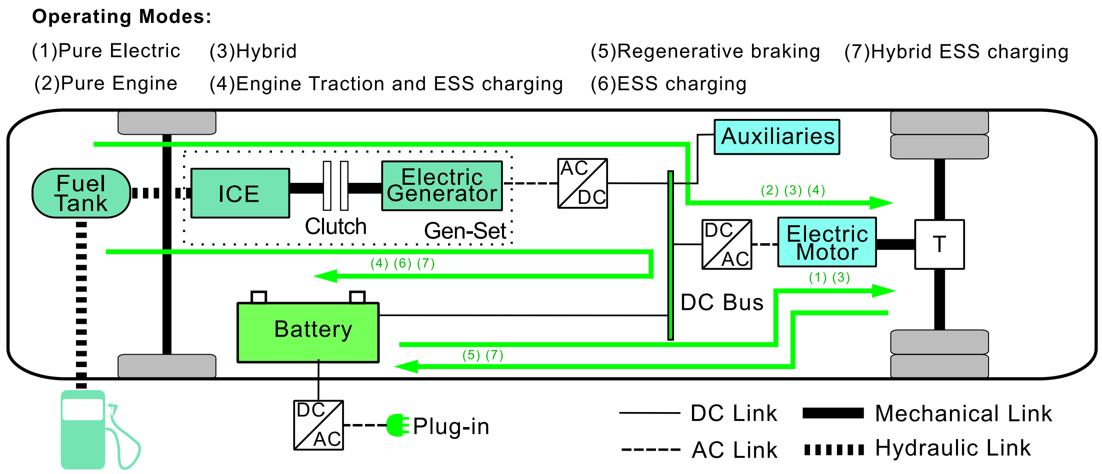

Figure 1.3: Series powertrain architecture.

This powertrain architecture includes several advantages. The ICE operation is independent of the traction motor. Thereby, the ICE is designed to operate in the optimal operation conditions, increasing the efficiency and reducing the fuel consumption. The ICE drives the generator to generate electricity, determined by the power demand. The generator charges the ESS and powers the EM. This gives the opportunity to make a more intensive use of the ESS, avoiding deep cycles. The electric drive allows to operate without any mechanical transmissions, decreasing the mechanical looses [14, 27, 28].

The advantage of having more flexibility to supply the electricity becomes a drawback, as the three machines (EM, ICE and generator) need to be designed to supply the full power of the vehicle. This impacts directly on the price, weight, and size. In highway operation, owing to electrical losses, the overall efficiency is reduced. Thus, SHEB are the most efficient for stop-and-go urban and city driving [28].

1.2.1.2 Parallel Hybrid Buses

In contrast to SHEBs, Parallel Hybrid Electric Buses (PHEBs) are considered to be conventional combustion vehicles with an additional path. Therefore, an ICE and an EM drive the vehicle, as shown in Fig. 1.4. Both machines are connected to a mechanical transmission, rotating simultaneously. Consequently, the torque demand is determined by the torque split factor. To increase the operating modes, both machines can supply either individually or coupled. Compared to the SHEB operation modes, the PHEB is less flexible, showing 5 operation modes as indicated in Fig. 1.4.

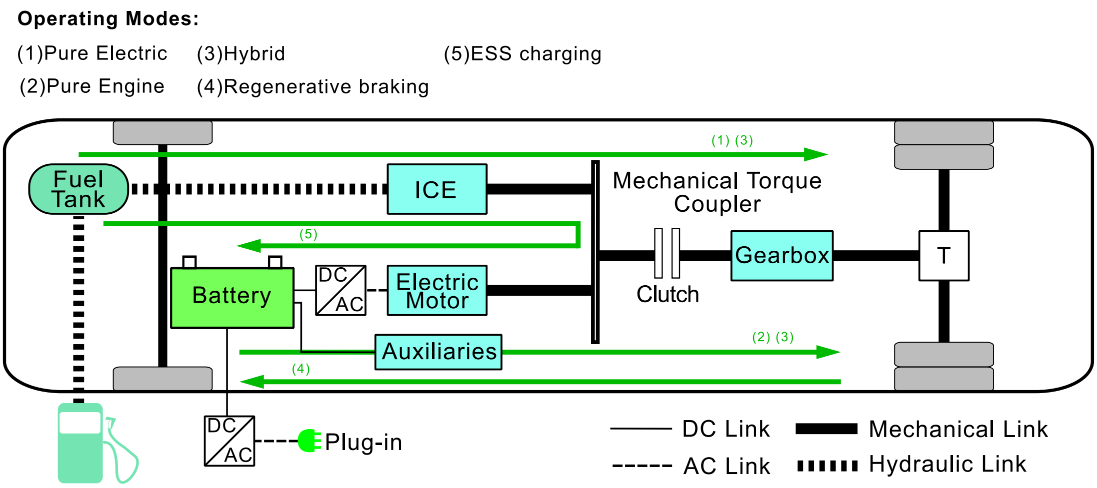

Figure 1.4: Parallel powertrain architecture.

The parallel configuration strengths, opposite to the series configuration, derive from the highway operation. In high rotation speed or cruising during long distances the efficiency is improved. The flexibility of having two traction machines, allows to downsize the EM, as the torque demand can be provided by both machines.

Weaknesses of PHEBs, are mainly related to the limitation of the ESS use. ESS can only be charged by regenerative breaking and cruising operation. The ESS is subjected to deeper cycles. The efficiency is lower at low rotational speeds. This kind of architecture has been widely adopted by European vehicle manufacturers [29].

1.2.1.3 Series-Parallel Hybrid Vehicles

The series-parallel architecture combines both aforementioned configurations, having all elements of both configurations, as shown in Fig. 1.5. Therefore, the mechanical and electrical connections are doubled. This configuration gives the electrical and mechanical flexibilities of SHEB and PHEB respectively. The number of operation modes are the same as the SHEB. However, the number of paths for the power transmission are higher.

As a result of the combination of both configurations, there are multiple operating modes. The extra flexibility of this type of powertrain is the main

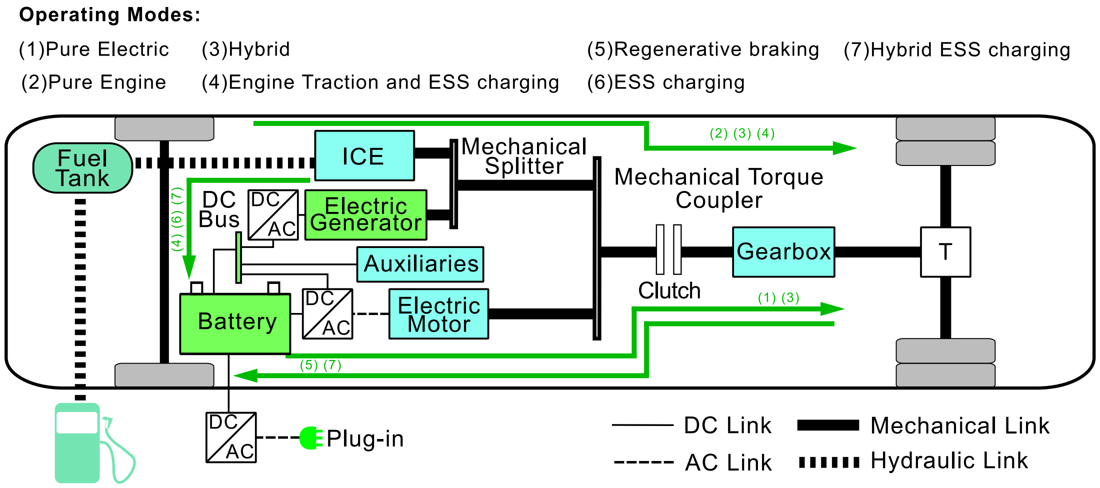

Figure 1.5: Series-parallel powertrain architecture.

advantage. However, the control algorithm is more complex, due to the several operating modes and energy flows to obtain the best energetic performance [14]. Moreover, the amount of extra elements increases also the cost.

1.2.1.4 Series Fuel-Cell Hybrid Electric Buses

Series FCHEBs architecture is composed of a FC and a BT in series, as shown in Fig. 1.6. The FC acts as a range extender, feeding the BT at constant power. The constant and stable power operation of the FC is the best, owing to the FC low dynamics. On the contrary the power peaks are provided by the BT. In addition, the FC reaches the maximum efficiency at partial loads [30]. The operation flexibility is very limited and just 2 operation modes are possible, as

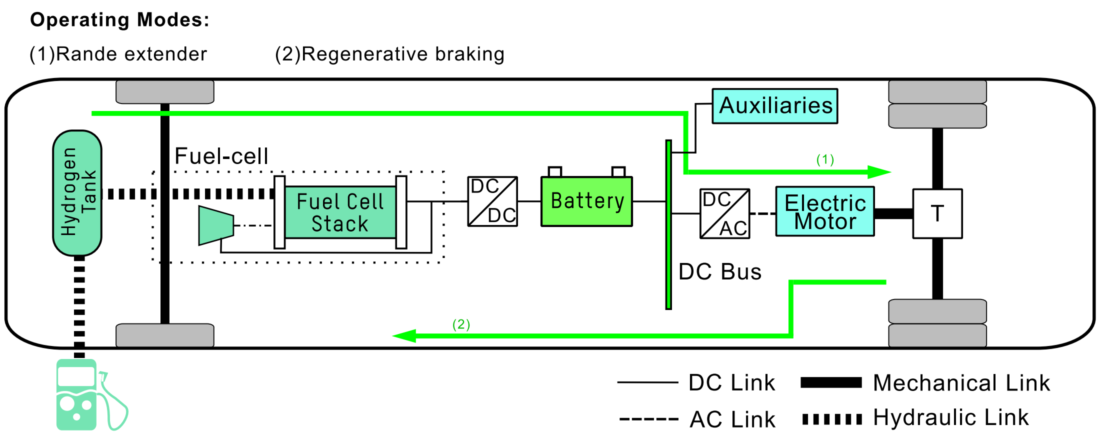

Figure 1.6: Series Fuel-Cell Hybrid Electric Bus powertrain architecture.

shown in Fig. 1.6.

The series FCHEB configuration is very simple. The complexity of the EMS is low, since there is not a power split to manage. This type of configuration is usually a non plug-in one. The BT is charged from the regenerative energy recovery and from the FC continued supply of hydrogen [30]. It is noteworthy the efficiency decrease, due to the fact that the BT is in the middle between the FC and the EM.

1.2.1.5 Parallel Fuel-Cell Hybrid Electric Buses

The parallel FCHEBs have the same power elements as the series FCHEB, but the distribution is different. In this type of architecture, the FC and the BT are connected in parallel, as shown in Fig. 1.7. Both power elements can fulfill the power demand. The common operation of this type of architecture is based on supplying the power to the EM and auxiliaries by the FC system and the transient power is provided by the BT system. Due to the less use of the BT, the size is smaller than the series FCHEB topology. The operation modes are the same as the series HEB, having 7 operation modes, as depicted in Fig. 1.7.

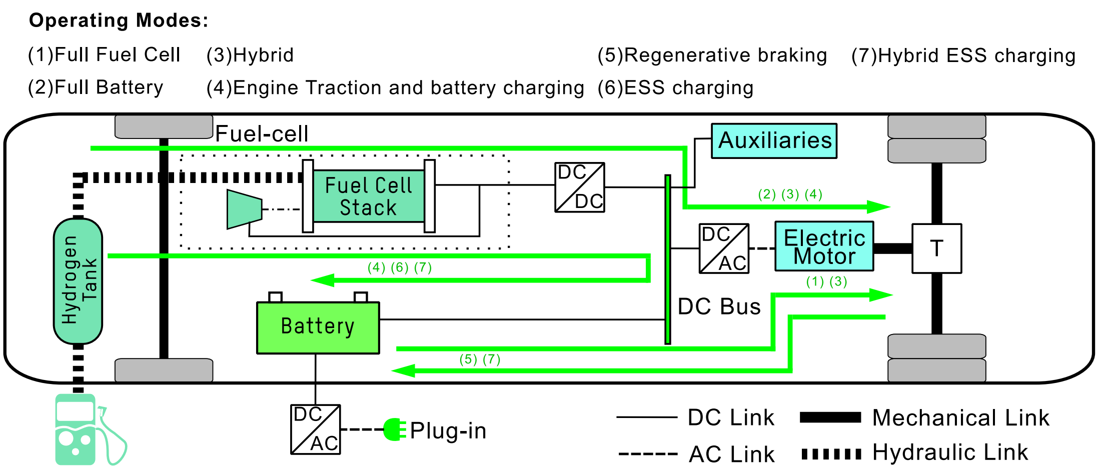

Figure 1.7: Parallel Fuel-Cell Hybrid Electric Bus powertrain architecture.

It is the most common architecture found in the literature. The reached efficiency is higher than the series architecture [30]. It is usually equipped with a plug-in. On the contrary to the series architecture, the EMS requires a much more complex design, with the aim of fulfilling the energy demand in the most efficient way [31]. In addition, apart from the hydrogen consumption efficiency, the FC safe operation has to be managed.

1.2.1.6 Electric Buses

Figure 1.8 depicts the 3 main powertrains with their corresponding operation modes.

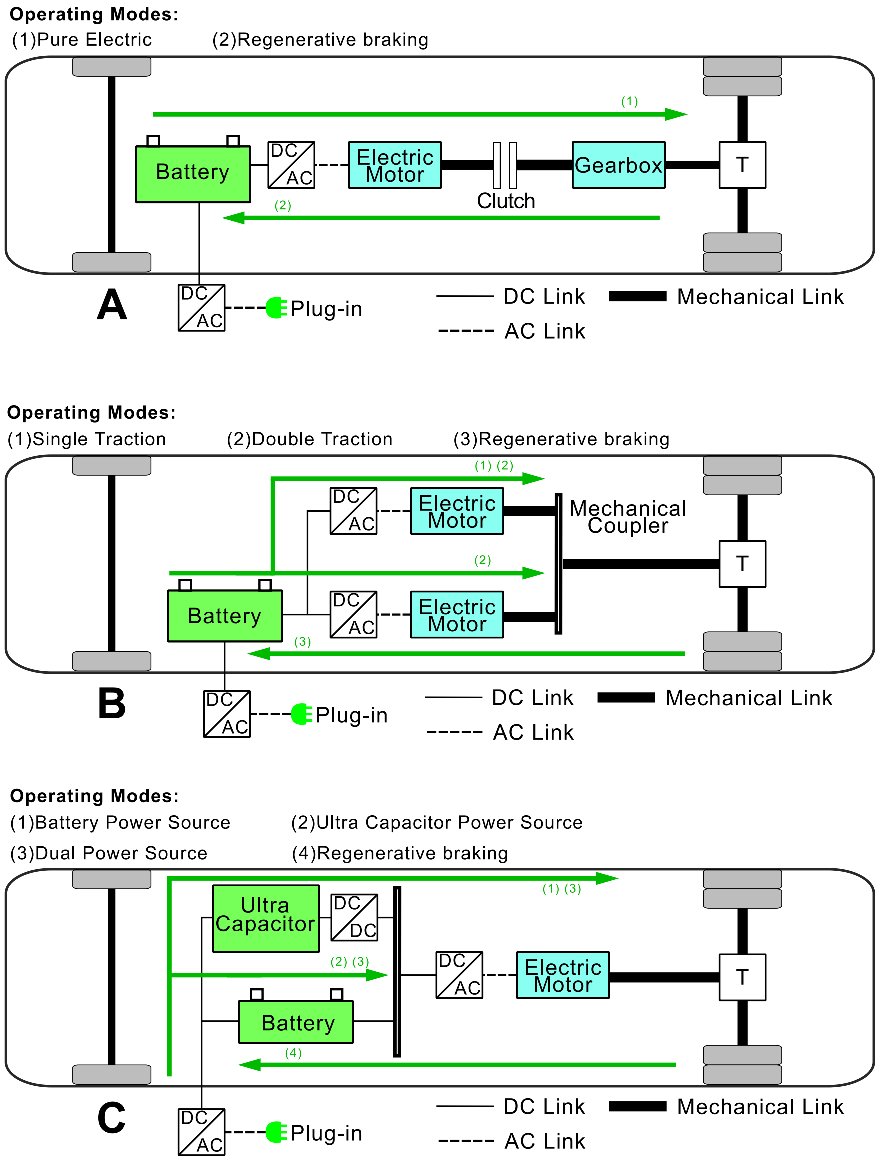

Figure 1.8: **A** Single Motor (optional gearbox) **B** Dual Motor **C** Dual energy storage system.

- ***Single Motor without gearbox***: This is the simplest and widely employed powertrain by automotive manufacturers. There is absence of gears, commonly merging the EM, the main reduction gear, and differential in a compact package. The absence of gears enables to reach higher speed without mechanical help as depicted in Fig. 1.9 zone a [26]. High torques are given at low speeds in zone b, being the highest torques given in zone c at zero speed. On the contrary, the ICE has run at idle speed (around 800 rpm) with the clutch help. Beside ICE, the EM can achieve an efficiency of the 85%. However, when driving at low speed, the EM can only provide a portion of its maximum power, needing to increase the EM size [26].

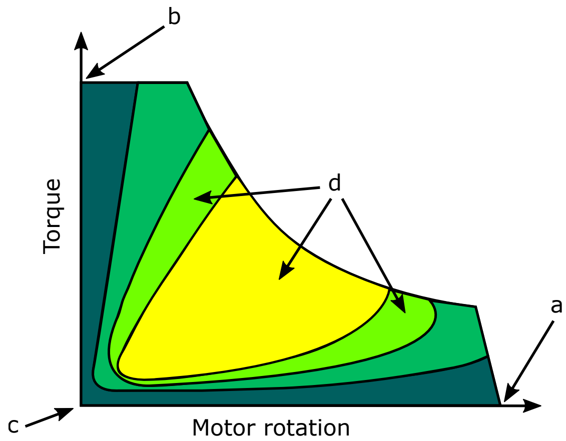

Figure 1.9: Electric Motor Torque-Speed Efficiency Map.

- ***Single Motor with gearbox***: The previously mentioned EM oversize at low speeds drawback is improved with this architecture. The behavior at low speed improves providing the EM with 2 gears. Consequently, the fuel economy is increased around 2-5% [26].

- ***Dual Motor***: Providing the EB powertrain with 2 or more EMs, the layout flexibility increases. In addition, this powertrain either with 2 or 4 EMs, it allows to run in front, rear, or all wheel-drive [26].

- ***Dual ESS***: This powertrain is a combination of high energy density ESS (commonly batteries) and high power density ESS (commonly Ultra-Capacitors (UCs)). This type of powertrain allows to use batteries with lower power density and higher energy density, overcoming the power need with the UCs [32].

1.2.2 Hybridization Levels

Hybridization level is determined by the ratio between the power provided by the ESS and the total power demand of the bus. Therefore, this level is directly related to the size of the ESS, EM and ICE. In Fig. 1.10, the five hybridization levels identified in the literature with their main characteristics are shown [29, 33, 34].

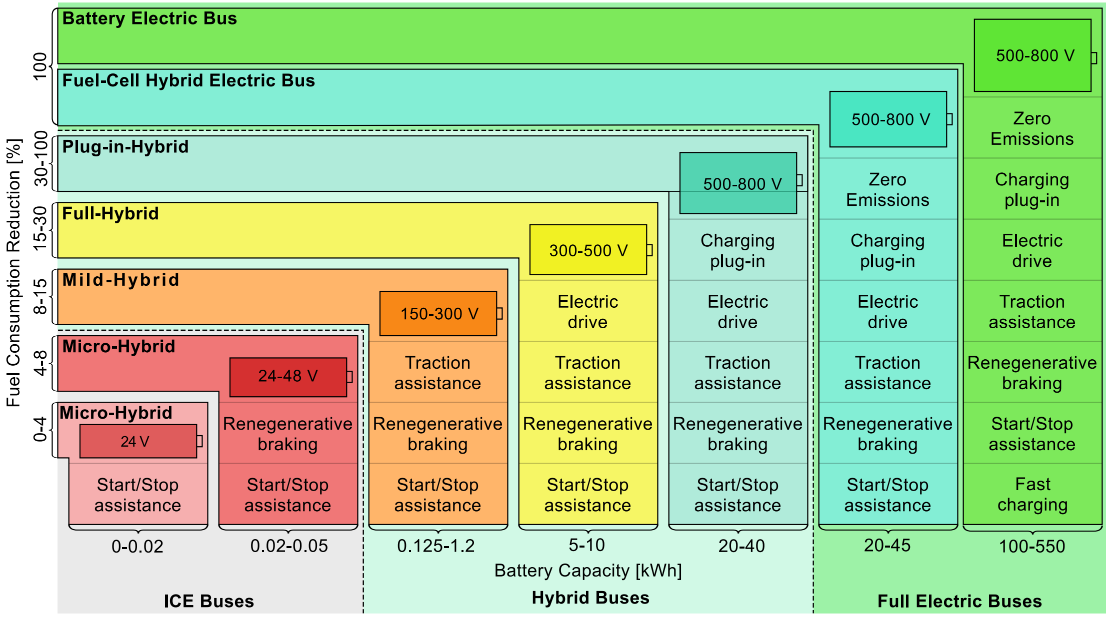

Figure 1.10: Hybridization levels.

An overview of the five hybridization levels with their main characteristics is made in the following lines:

- **Micro-Hybrid**:

The micro-hybrid level presents the lowest hybridization level. The main function of the ESS is to turn on the ICE. It does not provide neither assistance nor traction to the wheels. When the bus stops, the ESS supplies the power auxiliaries demand. The process for cranking again the ICE is by pressing the clutch. The only way of recharging the ESS is given during driving through regenerative braking. Therefore, the ESS is sized for meeting the start-stop function. Further developments for this hybridization level include switching off the ICE while driving at constant speed (sailing) on the highway [29].

- **Mild-Hybrid**:

This hybridization level acquires the micro-hybrid characteristics, adding an extra function. Beside micro-hybrid buses, this hybridization level integrates an extra motor having the ability to assist the drive train. This extra function helps to minimize the fuel consumption, assisting the drivetrain when the fuel consumption is high, especially during acceleration. The only way of recharging the ESS is both by regenerative braking or actively by the ICE. As a result, the ESS is sized related to the power requirements for meeting the assisted drive demands [29].

- **Full-Hybrid**:

As well as the aforementioned mild-hybrid bus, this hybridization level also obtains the lower hybridization level's functions. Additionally, this hybridization provides pure electric driving, being able to operate at zero emission mode. For this extra function, a higher EM and ESS size is needed. The electric operation is used when the ICE operation efficiency is low (at low speed). The way of recharging the battery is identical to the mild-hybrid bus, regenerative braking and actively by the ICE. As a result, the pure electric driving range is very limited. The best operation performance is obtained from urban driving [29].

- **Plug-in-Hybrid**:

Plug-in-hybrid buses are placed on the highest hybridization level. The functions of this hybridization level are identical to the ones of full-hybrid buses. However, the ESS size is increased significantly beside lower hybridization levels. This is due to a more charging flexibility degree, as the ESS can be charged either during driving (regenerative braking and ICE charging) or directly from the grid. As a result, the pure electric driving mode range is extended.

- **Fuel-Cell Hybrid Electric**:

Entering to the zero emission zone, at the top of the hybridization level classification, hydrogen buses are found. This type of buses are grouped inside the full electric buses group, since the bus is operated based on hydrogen and BTs. Giving that green hydrogen is used and the electricity to recharge the BTs is generated from renewable energy sources, the FCHEB is a zero emission vehicle.

- **Battery Electric**:

The pure electric bus is placed on the opposite side of the combustion. The pure electric bus has zero emissions full operation. Consequently, the ESS has the largest size and it could be charged by regenerative braking or directly from the grid.

1.3 Power Sources for Transport Electrification

As a result of the wide range of different buses architectures and hybridization levels, there exists an appropriate power source device for each solution. The power sources are core elements for BEBs and HEBs. In the case of BEBs, the BT is the most expensive part with 50% of the bus cost. For FCHEB and HEBs the BT is a significant part of the cost, reaching values of 39% of the cost of the bus [35]. Furthermore, power sources have shorter lifetime than power electronic systems. This way, they are a bottleneck in the lifetime of the bus. Moreover, BT pack replacements are required and this affects significantly the operation costs during the vehicle lifetime [36, 37], increasing the TCO. Therefore, it can be said that the BT lifetime is closely related to the vehicle operation. Therefore, the appropriate selection and sizing is crucial for EBs and HEBs design [29].

Depending on the application of the type of bus, different ESSs are selected. Commonly, power sources for transport electrification are optimized for energy or power purposes. The power source used for energy applications are electrochemical (BTs) and chemical (FCs) power sources. On the contrary, in the case of power applications, the most used ones are electrochemical (BTs) and electrical (UC) ESSs. However, a single power source has difficulties to meet both requirements: energy and power. As a result, new Hybrid Energy Storage System (HESS) concepts have been developed.

Electrochemical ESSs are the oldest form of electricity storage and power source for transport electrification. BTs developments have been mainly driven

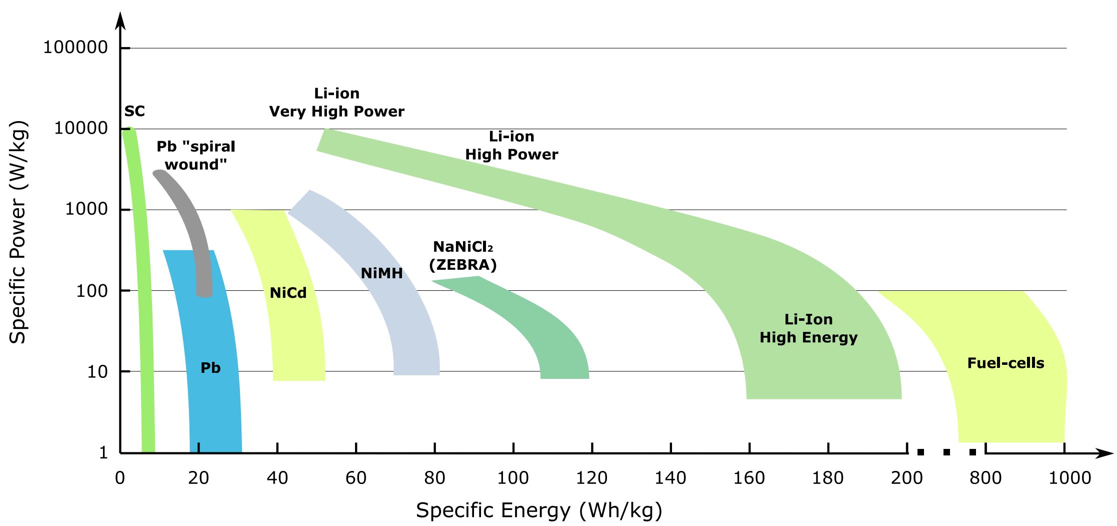

Figure 1.11: ESSs commonly used for EBs.

by researching on different ways to increase the energy density. Starting with lead-acid cells in the 1850s', nickel-cadmium cells in 1890s' and nickel metal hybrid cells in 1960's. Finally, adopting lithium-ion battery as the current storage system chemistry since 1991 [38], as shown in Figure 1.11 [29]. This adoption was driven by two main factors: technical characteristics and cost reductions (nearly 79 % drop from 2010 to 2017 [11]). Regarding technical characteristics, lithium element is the most electropositive (-3.04 V) as well as the lightest (equivalent weight M=6.94 g/mol and specific gravity =0.53 g/cm3) metal [39]. Moreover, lithium batteries do not present memory effect and the self-discharge rate is very low. Those advantages leads lithium BTs to become the widely adopted technology by vehicle manufacturers.

In the following lines, the utilized ESSs in the automotive industry are reviewed: Lithium batteries, UC, HESSs and FCs are detailed.

1.3.1 Lithium-ion Batteries

Lithium-ion batteries are classified as rechargeable or secondary batteries. In lithium-ion batteries electricity is stored in chemical form and the electricity it is produced through an electrochemical reaction process. Lithium-ion batteries are basically composed of two electrodes (anode and cathode), an electrolyte, a separator and a case [40]. Most of the EBs and HEBs applications require high energy densities. As a result, researchers have carried out new combinations of cathode, anode and electrolyte primary functional components, to obtain higher energy densities. Therefore, "lithium-ion batteries" is an umbrella term for a variety of material combinations used to form batteries [29]. Anode mostly is composed of graphite carbon (C) - which allows to reach higher potentials. However, for applications that require longer lifetimes and safer levels, lithium titanate (LTO) is used, instead of C anodes [29, 41].

Lithium-ion batteries are classified acccording to each cathode and anode material. The cathode materials usually contain manganese (LMO), cobalt (LCO), iron-phosphate (LFP), or mixtures such as $LiNiMnCo$ (NMC) and $LiNiCoAlO_2$ (NCA). This classification is shown in Table 1.1, with an overview of the main characteristics.

In the following lines, a study of the aforementioned lithium-ion BTs is carried out.

Table 1.1: Lithium-ion different chemistries.

CATHODE	LCO	LMO	NCA	LFP	NMC	NMC
ANODE	C	C	C	C	C	LTO
Optimized for	Energy	Power	Energy	Power	Energy	Cycle Life
Nominal Voltage [V]	3.6	3.7	3.65	3.2-3.3	3.6-3.7	2.3
Specific Energy [Wh/kg]	175-240	100-150	175-240	60-120	150-220	70-75
Specific Power [W/kg]	1000	4000	1000	4000	1000	4000
Safety risk	Highest	Moderate	Serious	Unreactive	Moderate	Moderate
Buses [33, 34]	-	-	-	BYD Enviro	Iveco E-WAY Mercedes eCitaro	Solaris

- **Lithium Cobalt Oxide (LCO)**:

LCO is the most mature (starting in 1991) and the first commercial lithium-ion battery [42]. It is normally not used in vehicle applications, though its energy density is relatively good. It is relatively expensive, due to the high cost of cobalt. However, the main disadvantage for EBs implementation is that LCO is the most reactive and has the lowest thermal runaway temperature (150°C) of lithium-ion batteries [42]. At elevated temperatures, LCO decomposes and produces oxygen, reacting exothermically with organic materials within the cell [41].

- **Lithium Manganese Oxide (LMO)**:

LMO is less expensive and significantly more tolerant to abuse than LCO [42]. The oxygen release is minimum, the thermal response being determined by the anode and electrolyte reactions. Thus, stable electrolytes at high voltages are used. Due to its characteristics, LMO is more commonly used in EV applications than LCO. As an example Tesla is using this type of chemistry [43].

- **Lithium Nickel Cobalt Aluminium Oxide (LFP)**:

Although LFP batteries have low specific energy, their specific power is high. LFP operating voltage range is lower than other cathode chemistries composed with a C anode. This leads to a lifetime increase. In addition, it does not release oxygen. Consequently, it is the safest lithium-ion battery and widely used by vehicle manufacturers [41, 42].

- **Lithium Nickel Manganese Cobalt Oxide (NMC)**:

NMC is safer and less expensive than LCO. The capacity is defined by the upper voltage cut off, which is usually acceptable. This chemistry has high energy densities and it is commonly used for energy purpose applications. Therefore, NMC is used for EBs applications [42].

- **Lithium Nickel Cobalt Aluminium Oxide (NCA)**:

NCA main advantage is the high specific energy density. However, as the voltage operation range is high, NCA is about as safe as LCO. Nevertheless, some vehicle manufacturers use this chemistry for their high energy density [42].

- **Lithium Titanate Oxide (LTO)**:

LTO main advantage is the high specific power density. It has the lowest voltage, which allows to reach the highest lifetime. LTO BT specific energy density is low and it is the most expensive chemistry. However, it is a very widely used technology [42].

1.3.2 Ultra Capacitors

UCs have the capacity to store and deliver energy at high currents in a short period of time. Therefore, they have very high specific power densities (approximately 1000-2000 W/kg) with an efficiency up to 95%. However, the energy density of UCs is much lower than lithium-ion batteries, as shown in 1.11. They have the longest lifetime period of the ESSs [40]. Moreover, as UCs are not very sensitive to temperature, they require minimal maintenance and can face long operation periods. These features fit with some HEBs and EBs applications, such as those that need extra power for rapid acceleration or hilling, regenerative braking energy storage, and fast charging. As a result, UCs are widely used as ESS by vehicle manufacturers [29, 33, 34, 40].

As well as lithium-ion batteries, there exist two different UC classes, Electric Doubled-Layer Capacitor (EDLC) and pseudo-capacitors. EDLC are the most used ones, as they have higher power density than pseudo-capacitors. Pseudo-capacitors store the energy in the electrochemical form, having higher energy density than EDLCs. However, due to the chemical reactions, the lifetime decreases [44].

As it has been aforementioned, UCs are widely used by vehicle manufacturers. As an example the micro-hybrid Mazda-6 model uses a UCs, to enable regenerative braking on 12 V start-stop systems. Regarding buses applications, the ADL Enviro400 mild bus and the ADL Enviro400H full hybrid bus are equipped with

UCs [29, 33, 34, 40].

1.3.3 Hydrogen Fuel-Cells

FCs are electrochemical elements that covert the chemical fuel in electricity without a combustion process. Hydrogen FCs are the most popular and commercially available on the market; however, methanol or ethanol have been also used as fuels. The process for producing electricity is called electrolysis. From a combination of hydrogen and oxygen, electricity is produced [45].

Different classifications criteria are defined in the literature according to the different parameters of FC, such as the electrolyte type, type of exchanged ion, type of reactants, operating temperature or pressure. Commonly, the most used classification criteria is based on the electrolyte type, as it has been seen in Tab. 1.2 [45–47].

The first FC type is Alkaline Fuel Cell (AFC) that works at relatively low temperature, low weight and simple operation. The second FC is Phosphoric Acid Fuel Cell (PAFC) working at higher temperatures (150-200 ºC) than the AFC. This allows to combine the electrical system with heat recovery, thus increasing the efficiency. However, the power density is low [47]. The most flexible and promising technology is the Proton Exchange Membrane Fuel Cell (PEMFC). This technology has the lowest operation temperature (between 65-85ºC) and the highest power density [45, 47]. Finally, Molten Carbonate Fuel Cell (MCFC) and Solide Oxide Fuel Cell (SOFC) technologies are the FC with the highest operation temperature. The high operation temperature allows to reach a total combined efficiency (electricity and heat) of 85% and 75-80% for the MCFC and SOFC respectively.

Table 1.2: FC classification according to the electrolyte.

Fuel-Cell Type	**Operation Temperature** [$\check{z}C$]	**Power Density**	**Fuel cell Efficiency**	**Lifetime [hours]**	**Application Area**	**Fuel Options**
AFC	50-230	High	50-60	>10000	Space	Hydrogen
PAFC	150-220	Low	40-50	>40000	Distributed power	Hydrogen, Natural Gas, Diesel
PEMFC	65-85	Very high	30-70	>40000	Transport, portable	Hydrogen, Natural Gas, Diesel
MCFC	600-700	Medium	40-60	>40000	Distributed power	Hydrogen
SOFC	500-1000	Low	40-70	>30000	Base load power	Hydrogen, Natural Gas, Diesel

From the different technologies, for buses applications, the PEMFC is the best technological choice and the only one used in transport applications. The low operation temperature with the high power density combination allows to operate a FC on board the bus. The main drawbacks of this FC are the need of platinum as a catalyst, the difficulty of water management and the use of pure hydrogen as fuel [47].

The development of FCHEBs have gained market attraction in the last few years. Nowadays, the main bus manufacturers have developed or they are manufacturing FCHEB models. Caetano bus manufacturer has developed with Toyota the 12 meters H2 City Gold bus. Solaris has also developed the Solaris Urbino 12 hydrogen bus with around 300 km driving range. Finally, Van Hool has also a FCHEB solution in its A330 FC bus model.

1.3.4 Hybrid Storage Systems

There is no power source meeting all the EB requirements. Therefore combinations and hybridizations of different ESSs are done to broaden the EBs capabilities. These hybridizations are electronically combined. These combinations are commonly made to increase both power and energy characteristics [40].

1.4 Commercially Available Electrified Solutions

A market research has been performed, aiming at having an overview of the commercially available electrified buses. The widest range of solutions have been encountered for BEBs and HEBs. However, there is a clear growing tendency of the available FCHEBs solutions.

1.4.1 Battery Electric Buses

Table 1.3 depicts the great step forward that BEBs have faced in the last years. The report [48] gives the global main manufacturers whole report. The ESSs sizes are within the range of 94-380 kWh, with a driving range up to 560 km. Most

Table 1.3: Full Electric Buses market overview.

OEM	Model	Bus Architecture	ESS Type	ESS Size [kW]	Electric Range [km]	Charging Technology	Sold Units
Proterra	*Catalyst FC*	DM 2 gears	LTO	94-126	80-100	PLG/PTG/WRL	100
	Catalyst CR	or	NMC	220-330	220-310		
	Catalyst E2	SM PM 2 gears		440-660	405-560		
BYD	*8 meters*	DM	LFP	160	200	PLG	80 in Europe in 2015-2016
	Double decker			340	240		
	10.8 meters			320	260		
	12 meters			270-380	210-300		
	18 meters			270	170	PLG/PTG	
Yutong	*Yutong E12*	SM	LFP	324	-	PLG	35.000 in 2015-2016
Zhongtong Bus	*LCK6122EVG*	SM	LFP	350	250	PLG	20.000 in 2015-2016
Solaris	Urbino 9.9	SM	LFP/ LTO	160	200	PLG/PTG	5
	Urbino 12	SM/DM		240	266		93
	Urbino 18	SM		240	185		5
Volvo	*7900*	SM 2 Gears	LFP	76	96	PTG	11
Irizar	*ie2*		NaNiCl (ZEBRA)	376	250	PLG	13
Van Hool	*Exqui.City 18m*	SM	LFP	215	120	PLG/PTG	40
VDL Bus & Coach	Citea LLE-99		NMC	180	-	PTG	67
	Citea SLF - 120		LTO/NMC	63-240	-		
	Citea SLF - 180		NMC	63-180	-		
Optare	Solo EV		LFP	270		PLG	56
	Metrocity EV			205			13
	Versa EV						13
	Metrodecker			-	-		-

of the buses are pulled by a single motor. However, there is a growing tendency of developing dual motor buses with 2 gears, with the aim to improve the EMs efficiency. The plug-in charging technology still dominates. However, due to the fast charging boost, the pantograph solution is growing rapidly.

Regarding the ESS, as the BEBs need larger batteries for higher driving ranges, there is no bus with UCs. The main utilized ESS chemistries are similar to the ones utilized in HEBs, being the safest LFP and LTO. However, due to the high energy density characteristics to achieve higher driving ranges, some manufactures use NMC.

1.4.2 Hybrid Electric Buses

Table 1.4 depicts the current market overview with the main manufacturers of HEBs solutions. The most adopted bus architecture is the series because it is more suitable than the parallel architecture for stop-and-go city driving, as it is pulled by an EM. On the contrary, the parallel architecture is mainly pulled by an ICE, having the best efficiency at high speeds. As a result, it is more suitable for extra urban routes than the series architecture, making use of the EM at low speeds. It is noteworthy that the buses with the largest ESS (ESS range 19-32 kWh) are plug-in HEBs, as there is a more intensive use of the ESS. Consequently, this hybridization level has the highest fuel savings - up to 75%.

Most of the full-hybrid buses power sources are UCs within a range of 0.4-0.5 kWh. This hybridization level does not need to be recharged from the grid, as the regenerative braking and the GS in the case of series configuration is sufficient

Table 1.4: Hybrid Electric Buses market overview.

OEM	**Model**	**Bus Architecture**	**Hybridization Level**	**ESS Type**	**ESS Size** [kWh]	**Fuel Savings** [%]
Man	*Lion's City Hybrid*	Series	Full Hybrid	UC	0.4	30
Mercedes-Benz	*Citaro G Bluetec Hybrid*	Series	Full Hybrid	UC	2 [Ah]	8.5
Vectia	*Veris.12 Hybrid+*	Series	Plug-in	LTO	24	
Volvo	*7900 Hybrid*	Parallel	Plug-in	LFP	19	75
Solaris	*Urbino 18 DIWA Hybrid*	Parallel	Full Hybrid	UC	0.5	20
Iveco	*Urbanaway bus*	Series	Full Hybrid	LFP	11	40
Orion	*Hybrid Electric Bus*	Series	Plug-in	Li	32	
Scania	Citywide LE Hybrid	Parallel	Full Hybrid	Li	1.2	20-25

to recharge the ESS. Regarding the ESS chemistry, the most used ones are the safest, NMC, LTO and LFP.

1.4.2.1 Fuel-Cell Hybrid Electric Buses

The available solutions for FCHEBs are fewer compared with the available solutions for HEBs and BEBs, as shown in Tab. 1.5 [33, 34, 49]. However in the last years, bus manufacturers are starting to bet for hydrogen solutions. All the buses have PEMFCs with power ranges between 70 kW up to 120 kW. Regarding the BT chemistry, LTO is the most utilized BT type, due to high power density. The BT capacities are ranged from 24 kWh up to 30 kWh.

Table 1.5: Hybrid Electric Buses market overview.

OEM	**Model**	**Fuel Cell**		**ESS**		**Motor**
		Module	**Module power [kW]**	**Chemistry**	**Energy [kWh]**	**type**
Solaris	*Urbino 12 Hydrogen*	Ballard FCmove-HD	70	LTO	30	In-wheel
Daimler EVO Bus	*Citaro Fuel Cell hybrid 12*	AFCC	2x60	-	-	-
Caetano	*Citaro G Bluetec Hybrid*	Toyota FC	-	LTO	29-44	Central PEM
Van Hool	*A330 fuel cell*	Ballard FCveloCity-HD	85	-	24-36	Central PEM

1.5 Energy Management Strategies

The hybrid bus operation rely strongly on the suitable and efficient power/torque split among the available sources. The complex energy division calculation is solved based on the EMS, focusing on the maximization of the overall efficiency and minimization of the operation costs [24]. A management strategy is defined as an algorithm, which is a set of instructions or laws regulating the overall operation and power flow of the system. Fig. 1.12 [50, 51] depicts the different levels of the management architecture of vehicles with the evaluation period and the application of each level.

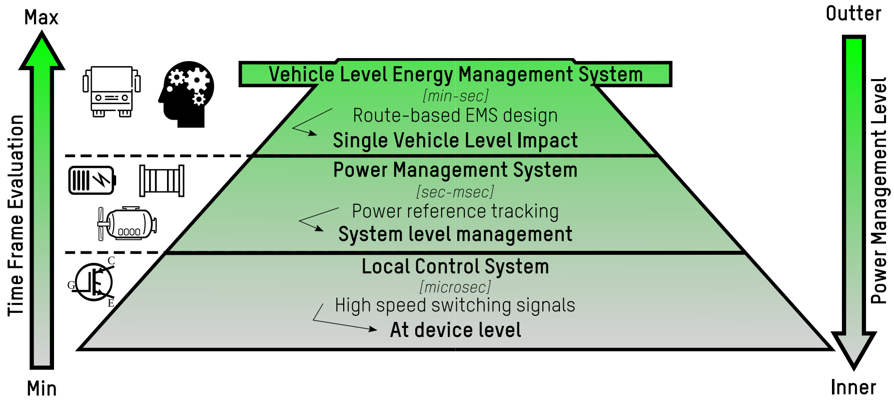

Figure 1.12: Management architechture of vehicles.

In the following lines, an overview from the innermost to the outermost level is described:

- ***Local Control System***: The function of the local control system is to generate switching signals, to control the modulation. These high speed switching signals are generated by microprocessors according to the torque/current input [50].

- ***Power Management System***: This management level determines the power set points between the multiple power sources according to the operation limits. To prevent the multiple power sources misuse, policies are applied (such as ESS over-discharging and over charging method and motor current and power limits). Power management system's inputs came from the LEMS [50].

- ***Vehicle Level Energy Management Strategy***: Vehicle level energy management strategy level has a longer time frame evaluation period than the aforementioned levels and it is the outermost level of the architecture. This level is the one which plans the vehicle dynamics, operation targets and power sources split factor. The strategic planning is applied to each individual local bus [50].

The vehicle level EMS plays a key role to ensure the correct system performance in terms of fuel economy and GHG emissions, in each local vehicle. Therefore, transport EMSs have been topic of interest for several years, with the aim of improving the energy efficiency of each vehicle [14].

1.5.1 Energy Management Strategies Classification

Traditionally in the literature the proposed EMSs at vehicle level have been classified as Rule-Based (RB) and Optimization-Based (OB) EMSs, as shown in Fig. 1.13 [15, 51]. As a brief overview, on the one hand, RB EMSs are generally designed for specific driving cycles and operating conditions, having limited adaptability to the real changing conditions. On the other hand, despite the good results achieved with OB EMSs, the future driving conditions need to be known or predicted and commonly they require high computational efforts, making more difficult the online on-board implementation [14, 15, 24]. Therefore, the effective design of an EMS is a complex task, since in real driving conditions the energy uncertainties and disruptions are tough to predict [15, 52]. In the following lines a review of the different EMSs is carried out.

1.5.1.1 Rule-Based Energy Management Strategies

These strategies rely on a set of rules to take actions on controllable sources. These rules are designed based on human expertise, intuition, and/or mathematical models, commonly with the drawback of not having prior knowledge of the driving cycle. The main advantage of these strategies is the low computational cost, being widely used for real-time EMSs. Rule-based strategies are divided into two subgroups, deterministic and fuzzy logic methods.

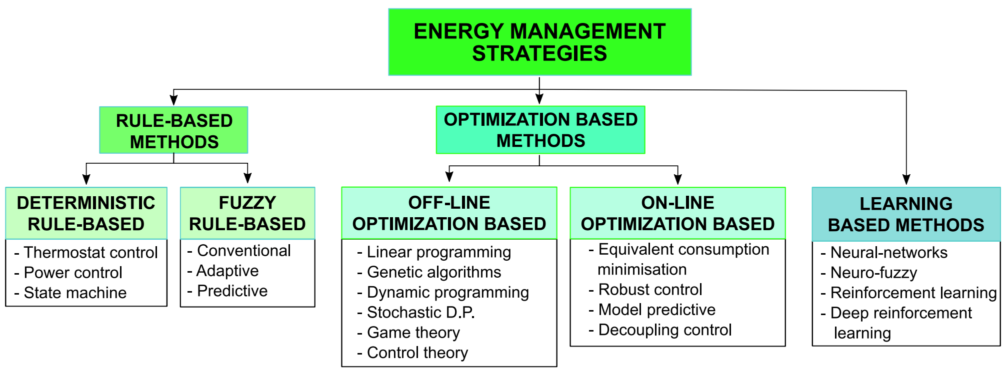

Figure 1.13: EMS strategies classification.

Deterministic methods require a wide knowledge of the application, as they are based on the human experiences and knowledge[28, 51]. These methods are suitable for low levels of hybridization. However, as the rules are obtained from selected driving cycles, they are not optimal solutions for real-life driving conditions [24]. The most used RB techniques are thermostat control, power control and state machine. Want *et. al* [53] proposed three different EMSs for PHEBs, pure electric, charge-depleting and charge-sustaining, managing the energy based on thresholds. Similarly, a RB EMS with a look up table was proposed in [54].

For more complex models or even for those systems that cannot be modeled, Fuzzy-Logic (FL) is an appropriate solution. These methods are also based on predefined rules, implemented in a map-based format. Therefore, the improvement margin is wider than with deterministic methods [24, 51]. FL is performed based on the following three main steps:

1. **Fuzzification**: scalar values are transformed to fuzzy values.
2. **Inference engine**: fuzzified measurements are used to evaluate the control rules stored in the fuzzy rule-base.
3. **Defuzzification**: the fuzzified response is processed to obtain a crisp value.

In the literature plenty of FL EMSs have been proposed [55–59] for energy management in hybrid vehicles with energy storage system (ESS) based on SC [60], BT [61] and hybrid ESS [62]. Herrera *et. al* proposed a FL EMS for a P-HEB and tested it into a Hardware-in-the-Loop (HIL) platform in real time, aiming at evaluating the real-time operation of the FL [58]. Chen *et. al* developed a FL EMS for FCHEBs, with the aim of maintaining the BT State of Charge (SOC), satisfying the FC dynamic constraints [57].

1.5.1.2 Optimization Based Energy Management Strategies

The OB strategies rely on analytical or numerical algorithms to take actions, resulting being more accurate than rule-based approaches [24]. These algorithms are based on minimization/maximization of a cost function to obtain the global optimum of a predefined driving cycle. The optimization method can be split into two subgroups [24, 51]: off-line and on-line optimization methods.

Off-line optimization methods are usually used as benchmarks or design purposes, as they are off-line implemented to a fixed driving cycle. It is noteworthy the Dynamic Programming (DP) approach from the different off-line optimization methods. The main reason for this is because it is commonly used as a baseline for different proposed approaches [24, 28, 51, 63, 64]. Since OB off-line methods cannot be applied online, in the literature there exist several approaches that use optimization techniques to design RB EMSs and implement them in real-time [65–69].

It is noteworthy the proposed EMS by Liang *et. al* based on correctional DP, for P-HEBs targeting to combine fuel efficiency improvement and drivability [65]. Based on multi-objective genetic algorithms, Herrera *et. al* proposed an EMS for managing a P-HEB with hybrid ESS, BT and UC, aiming at optimizing the daily operating cost [69].

On the contrary, *on-line optimization methods* are considered as sub-optimal problems. This is due to the fact that the optimizations are applied instantaneously, instead of applying the whole predefined route. For a wider optimization, some optimization methods include driving profile predictions, varying the effectiveness of the accuracy of the prediction model [24, 51]. Nowadays, these driving profile prediction models have been improved implementing the recent advances in Intelligent Transportation System (ITS) [15]. These new techniques are based on acquiring traffic or road condition information via telematics from sources such as Vehicle-to-Vehicle (V2V) or Vehicle-to-Infrastructure (V2I) [24, 28].

Johannesson *et. al* developed model predictive control to define the optimal split factor and schedule the charging and discharging of the ESS [70]. Similarly, also based on model predictive control, Guo *et. al* proposed a bi-level EMS to decouple the components into two levels [71]. The outer level defines the optimal speed and the inner level defines the optimal split factor of the power sources.

1.5.1.3 Learning Based Energy Management Strategies

Nowadays, a new trend is to provide vehicles with sensors, enabling to monitor the operation of each vehicle. This process is known as vehicles digitalization and lies on the data acquisition, data storage, computation and data analysis in the cloud [22, 24]. The cloud-computing system allows to have "unlimited" resources, widening possibilities of optimizing the EMS through global methods [24]. In addition, by means of cloud-computing, historical operation data exploitation is a valuable input to provide enough information and further improve the EMS design [24, 72, 73]. As a result, learning based EMSs have been emerged, learning from a data-base and gaining the ability to self-adapt to changing real driving conditions [15].

In the literature, several learning based EMSs have been published. Khayyam *et. al* [74] proposed an EMS based on 3 fuzzy controls tuned based on a hybrid adaptive neural-fuzzy inference system (ANFIS) genetic algorithm. Ozatay *et. al* [73] developed a cloud based system, aiming at feeding back the driver the optimized driving guidelines. A data-base with the optimal speed profile operation by means of dynamic programming (DP) was used to train neural networks and implement it in the vehicle as EMS [75–77]. In addition, Tian *et. al* improved this approach by implementing two neuro-fuzzy systems, one for the target state of charge (SOC) and another for the genset output [16].

Based on the Global Position System (GPS) information, Chen *et. al* developed a hierarchical clustering technique for identifying the driving cycle to determine the EMSs to apply [78]. The EMSs are designed specifically for each route. Yang *et. al* [79] exploited the compiled information offline, aiming at clustering 6 different driving behaviors and modelling them based on a Markov chain. The online part was based on a super vector machine, for identifying the recognized driving behaviors and applying the developed EMS for each driving behavior. Hu *et. al* [15] developed a deep reinforcement learning based EMS, learning from the torque and SOC operation. Liu *et. al* developed a Markov chain combined Q-learning technique, used to speed-up the markov chain [80] and a reinforcement learning algorithm with the aim to minimize the fuel consumption [81].

1.5.2 Energy Management Strategies Trends

Focusing on P-HEBs and FCHEBs, several EMSs have been proposed in the literature for different purposes, such as the thermal energy management [10, 82], optimal sizing of ESSs [58] and fuel economy [62, 83].

A wider range of conditions will allow to learn from the changing conditions, improving the EMS adaptiveness to driving disruptions. However, the majority of the existing literature aim to improve the operation costs of the P-HEBs and FCHEBs, mostly focused on fuel or hydrogen efficiency, limiting the BT or the PEMFC lifetime [30, 84, 85]. Despite the BT prices have been decreasing, they still have a great impact on the TCO [30, 37, 86]. Due to this fact, health conscious EMSs are gaining popularity in the EMS design.

BT pack replacements are required aiming at meeting the buses planned service lifetime. These replacements affect significantly to the operation costs during the vehicle lifetime [36, 37], increasing the TCO. Concerning BTs, some studies pointed out values up to 39 % of the BT price on the buses total price [35].

These replacements are previously planned for the TCO determination and they have to be met [87]. Therefore, aiming at minimizing the operation costs as well as meeting the BT and/or PEMFC aging constraints, BT lifetime has to be managed, with the aim of optimizing and further improving the TCO.

For bus manufacturers, the developed initial EMS for fulfilling the efficiency operation goals is a significant point. Due to this fact, the majority of the existing literature aiming at improving the operation costs of P-HEBs and FCHEBs are focused on fuel or hydrogen efficiency, limiting the BT and FC lifetime [30, 84, 85]. However, the conditions used for the initial EMS vary throughout the bus lifetime. Therefore, an update of the initially designed EMS will adapt the EMS to new situations.

For the correct updating of the EMS, the continuous operation monitoring is needed. This need is fulfilled with the new vehicles digitalization trend, which allows to have the possibility to analyze the current operation and take action to correct it, if required [86].

The operation information with the needed BT and PEMFC advanced knowledge will allow to manage the BT and PEMFC lifetime, going a step further on the EMS. In this regard, new techniques for managing the BT aging are needed, due to the fact that BT replacements are directly related to the TCO. Consequently, the operation management conscious of the BT aging will allow to further improve the TCO. In the following lines, the state-of-the-art review of the available BT aging conscious EMS for P-HEBs and FCHEBs are presented.

1.5.2.1 BT Aging Conscious Energy Management Strategies for P-HEBs

A suitable and efficient P-HEBs power split among the GS and the BT becomes a complex problem due to the several variables to be considered such as road conditions, remaining energy and economic issues in the short and long term. Furthermore, if the BT aging management is included in the optimization problem, it becomes even more complex. To solve this issue, advanced techniques and knowledge of the BT and its end application are needed to determine an efficient and techno-economic trade-off between minimizing fuel consumption and managing BT usage [86, 88].

The BT lifetime is affected by two degradation methods: calendar aging and cycling of the BT [89]. On the one hand, the calendar aging is determined by fixed years. When the BT arrives to the calendar aging years limit, it arrives to the BT End Of Life (EOL). Therefore, it is a degradation that is not manageable during the operation. On the other hand, cycling degradation is given by the different stress factors. The identified main stress factors are temperature, middle SOC, C-rate charging, C-rate discharging and depth of discharge (DOD) [88, 89]. These factors are manageable and have to be maintained within the operation constraints provided by the manufacturer or managed according to the BT utilization.

The P-HEBs BT temperature has to be maintained constant within the recommended operation levels with the help of the heating and cooling system. The correct temperature operation of the BT avoids unexpected fast degradation. The temperature management rises the auxiliary consumption, but this extra consumption can be optimized [86]. Regarding C-rate levels, as long as that the defined operation charging and discharging maximum and minimum C-rates are fulfilled, there is not extra degradation owing due to this factor. Finally, DOD and middle SOC have to be managed, aiming at maximizing or minimizing the BT lifetime. Dealing with hybrid propulsion systems, several EMSs have been proposed in the literature with a multi-objective strategy to minimize fuel consumption, the capacity loss and extend the BT lifetime [90, 91].

To maximize the lifetime of the hybrid system, many researchers have explored health-conscious EMSs to take care of the potential degradation of the BT system. For instance, Ravey *et. al* applied genetic algorithm to optimize the parameters of a fuzzy logic controller according to a cost function [92]. Instead of designing a set of rules for the fuzzy-logic, the optimization-based EMS solve the health management problem by finding the optimal solution of the cost function. In another research, Santucci *et. al* presented a model predictive control for a parallel HEV with HESS [93]. This HESS consists of both UC and BT, where the UC is used for absorbing the power peaks. To quantify the improvements obtained by the ESS hybridization, BT degradation is evaluated. Jin *et. al* developed a fuzzy logic controller where the BT aging is evaluated [94]. A real-time management strategy based on model predictive control has been proposed by Gomozov *et. al*, in which the BT power variation and SOC limits are considered in the cost function to minimize its degradation [95]. Sockel *et. al* proposed a model predictive control EMS based on future behaviors predictions enhancing the BT lifetime of plug-in hybrid electric vehicles [96]. Recent approaches such as the one proposed by Xie *et. al* developed a pontryagin's minimum principle based EMS taking into account the trade-off between BT degradation and fuel consumption minimization.

[88]. Using the desired SOC reference constructed with the optimal Depth of Discharge (DOD), the trade-off between BT degradation and fuel consumption is optimized based on a model predictive control.

In the recent proposed approaches, BT aging management have gained importance in the EMS design. On the contrary, as it is stated in [30], the health conscious EMS design is still a challenging issue. Most of the researchers propose an initial EMS designed for the bus initial conditions with a set of boundaries. These boundaries focus on the instantaneous power/energy management of the hybrid powertrains, without considering any updates of the EMS within the bus lifetime. Throughout the bus lifetime, bus conditions vary and the BT SOH must be evaluated periodically. In this context, BT aging conscious EMS has to be updated and re-designed according to this new status [30].

In this regard, multi-objective strategies have been proposed, such as the works proposed by Ma *et. al* and Herrera *et. al* [69, 97]. Based on genetic algorithms, they tune the fuzzy-logic membership functions taking into account the BT degradation. Yue *et. al* [30], proposed a health conscious EMS update based on SOH decision-making. In this research, the update and EMS re-optimization are done also based on GA. Other researchers have modeled the DP cost function with the aiming at minimizing the BT degradation. However, DP computation is heavy for online implementation [30] reason why DP is mostly used for evaluation, comparison and as analysis tool [30, 98, 99].

The reviewed strategies do not consider the state of health (SOH) of the BT as an input. The SOH is a valuable information, which enables the maximization of the BT lifetime in a long-term scope [86]. As it has been aforementioned, the BT State of Health (SOH) and degradation are closely related to the DOD. High SOCs directly lead to a faster BT degradation. P-HEBs initial SOCs are the highest reached SOCs during the operation. This is the reason for not defining the initial SOC at 100% and setting at lower levels -around 80-90% SOCs-. Having a fixed initial SOC, the final SOC definition determines the DOD. The DOD and consequently the final SOC are directly linked to the trade-off between fuel consumption and BT degradation. As a result, the correct design of an optimal final SOC is critical for the lifetime BT management [88].

1.5.2.2 BT Aging Conscious Energy Management Strategies for FCHEBs

The reviewed advances in P-HEBs are indirectly paving the way for the oncoming FCHEBs implementation, as the topologies and degrees of freedom are similar. The developed EMS for P-HEBs are directly applicable on FCHEBs [17, 18]. The direct application of the P-HEBs EMSs developments with the expected TCO drop around 30-50% for FCHEBs by 2030 are helping to increase hydrogen bus popularity [12].

Setting the starting point at the P-HEBs, BT aging conscious EMSs state-of-the-art, the management techniques and BT knowledge apply directly FCHEBs aging conscious EMSs. However, if the FC aging management is included in the problem, it becomes even more complex. As a quick answer to this problem, a fair balance between the BT and FC utilization has to be determined, based on advanced techniques, knowledge of the PEMFC, BT and the bus application.

Focusing on the PEMFC stress factors, the load dynamics is the most critical factor regarding its lifetime management. Under load changes in the PEMFC, the chemical reactions inside the FC are accelerated. The chemical reactions, acceleration leads into an oxygen consumption increase and a stack voltage decrease. The element that controls the oxygen injection into the cathode is the compressor, the auxiliary element of PEMFC that consumes the most of the energy (up to 20%) and causes the voltage drop when more oxygen is needed [100]. The needed oxygen is measured by the Oxygen Excess Ratio (OER). In the literature, it is known that the highest FC output power is achieved between 2 and 2.5 OER [81, 100]. However, a bigger OER does not mean a better condition, as the compressor parasitic consumption increases, reducing the FC output power. Therefore, in the current literature, a steady OER value of 2 is considered as optimal [101]. The OER drop could be transformed in an oxygen starvation, with a consequent hot spot or burn on the surface of a membrane, causing permanent PEMFC damage [100, 101].

To tackle this problem, the OER in the cathode has to be maintained greater than 1, with an accurate control of the air-feed system. However, the OER control during transient state, is delimited by the manifold and air compressor dynamics, the delivered power increase limitation and a correct management of the demanded power is a crucial issue [100–102] .

In the literature, several approaches have been proposed. Fletcher *et. al* proposed an EMS based on the optimal operation obtained with stochastic DP optimization. Aiming at enhancing the FC lifetime, the cost function was modeled taking into account the cell degradation [84]. Sundström and Stefanopoulou presented a deterministic DP based EMS, taking into account the SOC, OER of the FC and the hydrogen consumption in the cost function [102]. Yue *et. al* published a thorough review of published health conscious energy management strategies for FC hybrid electric vehicles, concluding that a gap exists between implemented ageing mechanisms and BT and PEMFC lifetime aging conscious EMS [30]. Wang *et. al* have carried out a wide of different works in the filed of FC hybrid electric powertrains, with the aim to maximize FC lifetime [103–105].

1.6 Fleet Management Techniques

In the recent years, automotive industry is equipping smart vehicles with a set of sensors to monitor operation variables [23]. In addition, vehicle interconnection and data compilation and transmission through the cloud have been developed. These smart vehicle features and extra elements have allowed to go a step further in the energy management hierarchy, adding an additional higher level comparing with the aforementioned management levels architecture of vehicles shown in Figure 1.12 [50, 51].

Fleet management is identified as the highest level of the management hierarchy. Its main objective is to analyse, process and make decisions based on the processed data. The data volume needed for the analysis is high, therefore, this level has the longest evaluation time frame (weeks or even years). In contrast to the vehicle level EMS [50, 51], the fleet management has a wider scope and manages the whole fleet. As a result, it is the outermost level of evaluation. A wider scope allows to compare the behavior of each vehicle in the fleet, learning from those with the best energetic behavior. Thus, the aim is to improve the whole fleet energy efficiency, reducing the operation and maintenance costs. The current vehicle level EMS design approaches are commonly optimized once and no comparisons are made with other vehicles. The fleet management level allows to collect the data from all vehicles from a fleet and identify the vehicles with the best energetic behavior.

In the literature, several fleet management system approaches have been identified, with different purposes [14, 24]. However, no information has been found about fleet energy management techniques in the literature. The main identified purposes are focused on the following areas: traffic jams avoidance, vehicle diagnostics, itinerary planning and charging regulation and scheduling [24].

The first use of telematics was focused on vehicle positioning. Thong *et. al* developed a pioneering fleet management system for location accuracy improvement and exploit this information to avoid traffic jams [106]. In addition to that, in [107], Balaji *et. al* developed a smart traffic lights time optimization approach to avoid traffic jams. Likewise, HomChaudhuri *et. al* proposed a hierarchical control for management with two levels of sharing information. The higher level is based on the traffic lights information and traffic information (provided by the surrounding vehicles). This information is used to predict the velocity and choose the target velocity with the best fuel efficiency. The lower level based on this information controls the power split factor of the hybrid vehicle by applying the energy consumption minimization strategy [108].

In the automotive industry, vehicle diagnostics for predictive maintenance has been the driving force in digitalization implementation. J. Grantner *et. al* proposed an intelligent vehicle health diagnostics method based on fuzzy logic, updating the fuzzy rules from cluster extraction of the fleet data [109]. In regards to the fleet BT data exploitation Haycock *et. al* proposed a BT monitoring approach, aiming at evaluating the BT utilization and improving the TCO regarding the leasing economic model [110]. Likewise, Barré *et. al* proposed a methodology for clustering EVs according to each operation, with the aim of improving the BT state of health (SOH) estimation [111]. Nuhic *et. al* developed a battery SOH monitoring with degradation prognosis that learns from fleet data [112].

Other topic of research, based on data exploitation is the green itinerary planning. In the literature, several approaches have been proposed [113–116]. It is worth mentioning the approach of Mehar *et. al* proposing an extension of the EcoDrive green itinerary planning service [115] for EVs providing several paths taking into account the following information: (i) Road cartography: elevation, (ii) Driving perturbations: traffic congestions, unexpected events and driver habits, (iii) Vehicle features: weight, BT type and engine efficiency map, (iv) Weather conditions: air friction, wind speed and temperature.

Recharging infrastructure optimization at fleet level has also been a topic of research, particularly applied to urban mobility, due to the fact that the profiles are predefined. The compilation and process of the information of the recharging operation widens the opportunities of the recharging management. Qin *et. al* exploited the compiled information with the aim of minimizing the charging station queues [117]. In an attempt to go a step further on recharging management, Hill *et. al* proposed a vehicle-to-grid (V2G) fleet model. This model shows that with BT operation monitoring, the shallow cycles are avoided. Consequently, the BT lifetime increases, making more profitable the V2G at fleet level. Lastly, Rogge *et. al* [6] addressed the challenges of range limitation and required charging time, developing a methodology for the charging infrastructure planning.

With regards to fleet data exploitation, in [118], Wittmann *et. al* proposed a holistic framework. This approach covers from the fleet tracks data acquisition to the evaluation. The data is acquired from a smart phone application and a data logger. Consequently, this data is processed filtering the tracks and ordering them according to the selected features such as distance, average speed and driving behavior. Finally, the data is evaluated making use of different developed tools. It is noteworthy the developed data analysis tool used to simulate electric vehicle's energy consumption. However, this approach is not focused on a methodology for fleet energy management.

1.7 Conclusions and Main Gaps Found in the Literature

In the present state-of-the-art, the background knowledge in the topic of electrified buses have been reviewed. This last section has the intention to collect and highlight the challenges of the field of urban road transport electrification and the main gaps the literature, with the aim of exploiting new resources by means of the digitalization. The identified highlights and gaps serve as basis for the developments of this Ph.D thesis.

Firstly, the different available bus types according to the powertrain architecture and hybridization level have been analyzed. This analysis allows to explore the main components of the powertrain and acquire the basic knowledge for identifying the degrees of freedom for each topology. Among the available powertrains, P-HEBs and FCHEBs have been identified as the most promising technologies with the highest number of degrees of freedom for their control pursuing the efficiency improvements. The higher BT size allows to increase the power sources utilization flexibility. Therefore, this Ph.D thesis developments have been addressed towards P-HEBs and FCHEBs powertrains efficiency improvements.

The appropriate ESS selection for the different hybridization levels and powertrain architectures is crucial for the TCO improvement. From the available ESS portfolio, for the specific P-HEBs and FCHEBs applications, lithium-ion BTs and FCs have been identified. On the one hand, regarding the lithium-ion existing chemistries LFP, NMC and LTO are the most used ones. From the aforementioned three options, LFP has been dismissed, for being a BT optimized for power purpose, but with worse technical characteristics than the LTO BT. Therefore, in this Ph.D thesis NMC energy application BT and LTO power application BT have been selected for the studied powertrains. On the other hand, the FC selection among the available technologies has been a straight forward decision, since the only viable technology for the FCHEB is the PEMFC. Based on the market research for the FCHEB application, LTO BT technology has been selected.

The higher upfront costs beside conventional buses hinders the integration of P-HEBs and FCHEBs. The main attractiveness of these type of buses is their lower operational costs, that together with the high yearly driven distances help to compensate the initial investment cost. The way to evaluate the offset cost is based on the TCO calculation, which plays a key role in the electrified buses integration viability study.

Nowadays, digitalization appears as a new trend that allows to acquire information, store this information in the cloud, analyze and compute this data in the cloud with "unlimited" resources. Targeting to explore and exploit the new digitalization opportunities, a state-of-the-art review has been carried out analyzing the existing different management techniques. The operation monitoring of the vehicle allows to analyze the efficiency behavior into depth. The combination of the capability to have operation data and new learning based EMSs allows to optimize the operation further. The learning based EMSs permit to consider and combine consumption minimization short-term objective with the long-term BT lifetime management.

Optimizing the TCO of the vehicle and the BT lifetime further and respective BT replacements management are crucial. The management combination of the short-term and long-term managements has been identified as a gap in the literature. In addition, the proposed EMSs are designed based in the bus initial conditions with a set of boundaries focused on the instantaneous power/energy management. Due to the lack of a short and long-term management combination, no updates are considered throughout the bus lifetime. The bus conditions vary and BT SOH has to be evaluated periodically, needing tools to combine the short-term and long-term management.

For covering this gap, learning based EMSs have been identified as the main candidates to exploit cloud-computing resources. By means of cloud-computing, DP global optimizations of the routes and the data motorization can be performed. Afterwards, real-time replication of the global optimization and onboard integration is achieved, designing FL EMSs based on neuro-fuzzy technique. For covering the long-term target, not only the fuel or hydrogen consumption has been taken into account, but also BT and/or PEMFC lifetime. In this regard, the identified learning based EMS has utilized and extend aiming at developing a learning-based BT aging conscious EMS. The manageable stress factors of the BT and/or PEMFC have been determined.

Finally, this state-of-the-art review shows a clear gap for fleet energy management techniques. A need of developing tools to manage fleets energetically in regard to fleet energetic efficiency improvement and further optimize the TCO, with the aim of exploiting the upcoming opportunities in this thriving area of research. In this regard, an energetic fleet management methodology to optimize and manage the TCO for fleets of vehicles should be developed.

2

Fleet Level Hierarchical Energy Management Strategy

Summary

In this chapter, the proposed fleet level hierarchical EMS is introduced. A specific case study is also presented, in which the proposed approach has been evaluated. This case study is composed of 10 routes, evaluating different powertrains. The plug-in hybrid electric and fuel cell hybrid electric bus powertrains are defined with the respective battery aging models. To energetically and economically evaluate the presented case study, a fleet simulation tool has been developed in MATLAB, which is detailed in this chapter. Finally, the utilized total cost of ownership economic model is described.

2.1 Structure of the Hierarchical Energy Management Strategy

In this section, the proposed fleet level TCO optimization methodology is introduced. An outlook of the developed hierarchical decision maker and different management levels from the inside out is carried out. The proposed hierarchical decision maker from the fleet to the bus scheme, shown in Fig. 2.1, is composed of three levels. It pursues the energetic management of a fleet of vehicles from the fleet commissioning until the fleet service lifetime, aiming at optimizing the TCO of the whole fleet.

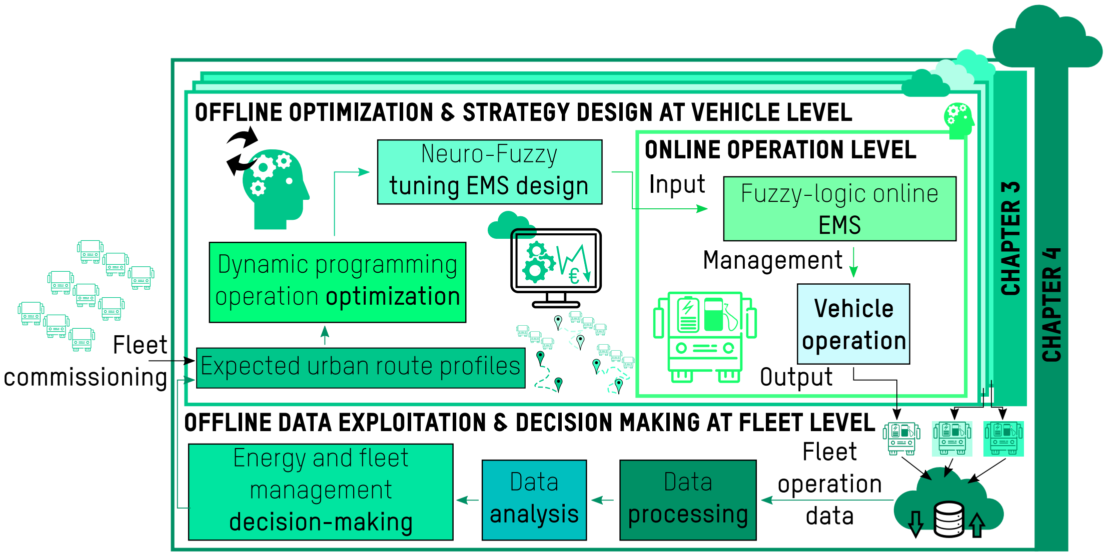

Figure 2.1: Proposed hierarchical decision maker from the fleet to the bus scheme.

The inner and first level is integrated in each vehicle. The *online operation* onboard of each vehicle is carried out. This level is composed of the EMS, which manages in real-time the vehicle sources and loads to obtain the required performance by the driver. The onboard integrated EMS is fuzzy-logic strategy. It aims to manage the split-factor of the available power sources of the bus. Each EMS implemented in each vehicle is designed according to the upper levels.

The online EMS design is based on the *offline optimization and strategy design at vehicle level*. As the name of the level indicates, this second level is offline and remotely performed in the cloud. Concerning the EMS design structure, on the one hand, the optimization used for feeding the learning technique is a DP global optimization method. Each vehicle operation is optimized with the aim of maximizing the efficiency and optimizing the TCO according to each route. On the other hand, the learning technique part is based on a neuro-fuzzy learning technique, which is used for automatically tuning and determining the rules of the online fuzzy-logic strategy. In this way, the online EMS is designed with the aim of replicating the optimal operation obtained from the DP optimization.

The optimization modeling allows to design an EMS based on the TCO and BT aging analysis, since the operation obtained from the DP optimization is used as a reference for the EMS design in terms of the available power sources split factor usage. The decision for the optimization scenario definition is taken on the *offline data exploitation and decision making at fleet level*, performed as well in the cloud. This decision for the optimization modeling is made based on the outlook of the whole fleet and affects to the inner levels. The compiled fleet operation data is processed and analyzed. And based on the current status of the fleet in terms of TCO and BTs SOH, decisions are taken for further improving the TCO.

The proposed hierarchical EMS has been evaluated in a specific case study composed of 10 routes and for 3 different bus powertrains presented in Sec. 2.2. With the aim of energetically evaluating fleets of vehicles with the proposed EMS, a dedicated simulation platform has been developed. The bus models integrated in the simulation platform are introduced in Sec. 2.3, with the respective BT cells aging models in Sec. 2.4. This simulation is in depth described in Sec. 2.5. It enables to make studies at vehicle level and at fleet level, consequently allowing to evaluate the technical and economical range of improvement in both levels. Finally, the TCO is presented in Sec. 2.6, a calculation for economically evaluating the case study.

The briefly introduced *online operation* and *offline optimization and strategy design at vehicle level* are further detailed and evaluated in Chapter 3. Continuously in Chapter 4, the *offline data exploitation and decision making at fleet level* is explained and evaluated in depth.

2.2 Studied Fleet Scenario Overview

The analysis of this thesis has been in reliance of a fleet composed of 10 buses running on the routes shown in Fig. 2.2. The urban routes have been generated from a data-base of standardized driving cycles and adapted to a bus driving behavior [119].

Each driving profile represents one round-trip of the length shown next to every route reference. The daily operation of each bus is considered to be 16 hours. This operation varies, with the aim of fulfilling the planned daily round-trips. In Tab. 2.1 the routes round-trip distance, mean speed, aggressiveness and duration characteristics are given.

Table 2.1: Routes characteristics.

Route	**Distance** $[km]$	**Mean speed** $[km/h]$	**Aggressiveness** $[m/s^2]$	**Duration** $[s]$
1	14.25	26.77	0.07	1917
2	20.44	25.57	0.07	2879
3	9.18	13.84	0.20	2387
4	13.63	20.58	0.14	2385
5	15.48	17.80	0.09	3129
6	18.58	27.00	0.05	2479
7	32.17	28.23	0.04	4103
8	29.63	28.53	0.05	3741
9	17.29	23.45	0.08	2655
10	12.16	17.77	0.16	2465

As a brief analysis of the routes, the following information is noteworthy. Route 3 is the shortest route with 9.18 km each round-trip with the lowest mean speed and the highest aggressiveness. The high aggressiveness is a sign of route in the city center, being a route composed of acceleration and deceleration peaks. The shortest route in kilometers is not matching with the shortest in duration. Route 1 is accomplished in the shortest time. It has a mixture of acceleration, decelerations and cruising speed.

The longest route with the highest time to be accomplished is route 7. As analyzed before, the shortest route corresponds to the lowest mean speed. However, route in this case route 8 has the highest mean speed but it is not the longest. Route 7 takes more time to fulfill the route and consequently, covers longer distance. It is noteworthy that both routes have low aggressiveness (low acceleration and deceleration repetitions) and high cruising speeds, a characteristic that increases the mean speed and driven distance.

In this thesis, three type of buses have been modeled: LTO BT based P-HEB,

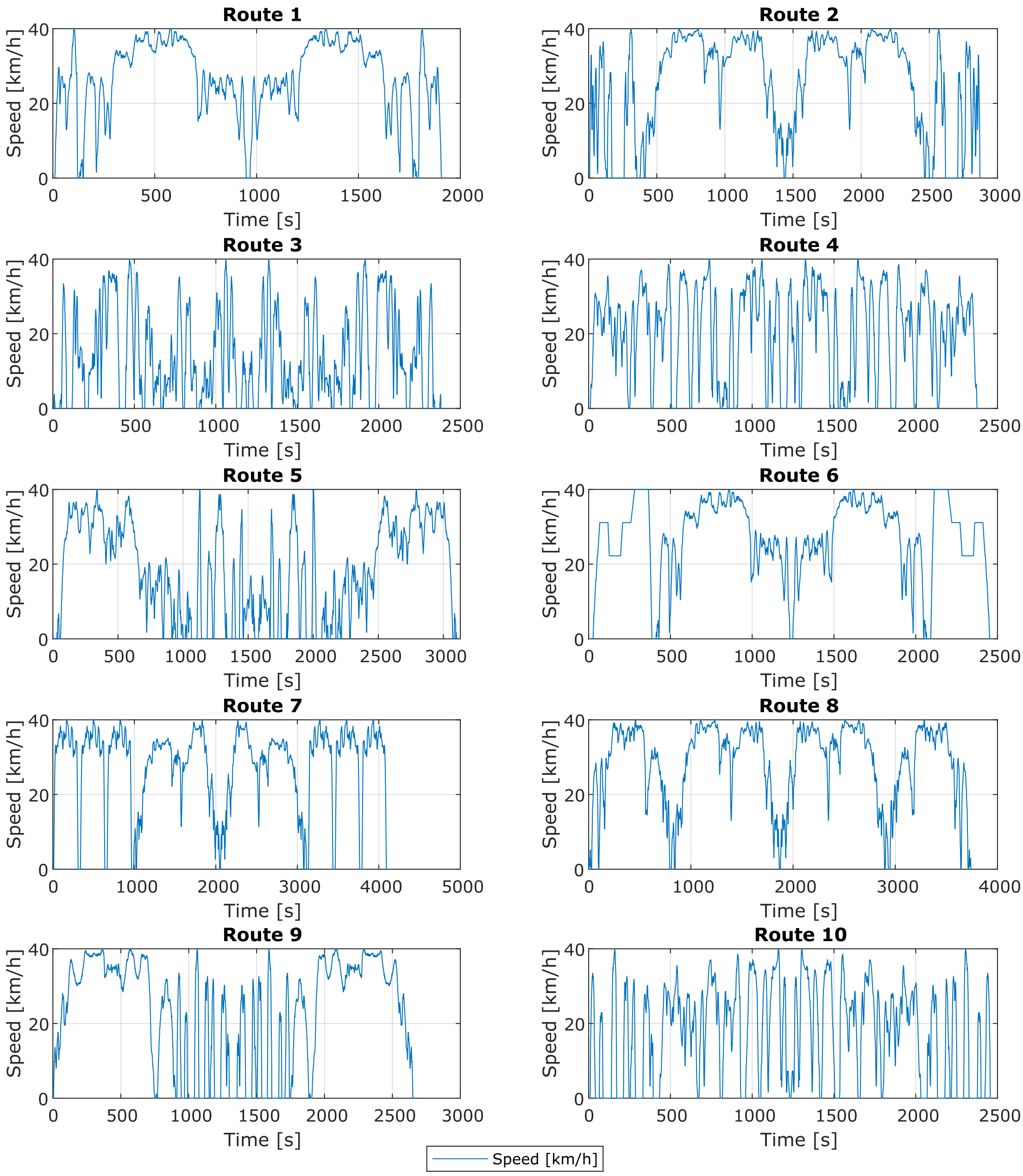

Figure 2.2: Fleet routes speed profiles.

NMC BT based P-HEB, and LTO BT and PEM fuel cell based FCHEB. The component's models are described in Section 2.3. Regarding the power sources, the powertrain elements have been designed according to bus data [31, 86, 87].

The LTO chemistry BT pack has been chosen for bus model 1 with the aim of evaluating a power purpose BT pack. This type of BT chemistry has longer lifetime than NMC chemistry, as shown later in Fig. 2.13. The technical characteristics are shown in Tab. 2.2. With the aim of studying a BT pack for energy application, bus model 2 has been equipped with a NMC BT. The characteristics of this P-HEB are shown in Tab. 2.3.

Table 2.2: Bus model 1: LTO BT based P-HEB.

Elements		Parameters	Units
Electric Motor Power		196.5	kW
Auxiliary demand minimum/maximum		12/18	kW
Genset Power		160	kW
Battery Pack	Chemistry	LTO	-
	Series cells	260	-
	Cells branches	2	-
	Battery pack mass	266	kg
	Power charge/discharge	168/192	kW
	Energy	23.92	kWh

Table 2.3: Bus model 2: NMC BT based P-HEB.

Elements		Parameters	Units
Electric Motor Power		196.5	kW
Auxiliary demand minimum/maximum		12/18	kW
Genset Power		160	kW
Battery Pack	Chemistry	NMC	-
	Series cells	162	-
	Cells branches	1	-
	Battery pack mass	166	kg
	Power charge/discharge	96/192	kW
	Energy	23.98	kWh

In addition to the two P-HEBs, a FCHEB has also been considered. This powertrain has been used with the aim of proving the replication of the developed EMSs for the P-HEB in the FCHEB. In Tab. 2.4, bus model 3 characteristics are shown.

Table 2.4: Bus model 3: LTO and PEM fuel cell based FCHEB.

Elements		Parameters	Units
Electric Motor Power		196.5	kW
Auxiliary demand minimum/maximum		8/16	kW
Fuel Cell	Type	PEM	-
	Fuel Cell Power	2x60	kW
	Fuel Cell auxiliary consumption	500	W
	Oxygen excess ratio upper limit ($n_{O_2}^{lim}$)	1.7	-
	Stack Cells (n_{cell})	381	-
Battery Pack	Chemistry	LTO	-
	Series cells	305	-
	Cells branches	2	-
	Battery pack mass	312	kg
	Power charge/discharge	196/224	kW
	Energy	28.06	kWh

2.3 Bus Models

The electrical model of the powertrain elements has been developed for the quasi-static simulation method. This simulation method is a non causal, discrete-state model where the signals flow from the drive cycle through the powertrain elements one way [63]. Therefore, the used formulation has been based on backward or "effect-cause" approach. The power is calculated at each discrete step following a predefined speed profile going upstream through the vehicle components [27]. To standardize the power flow direction, the adopted sign convention has been positive power when there is an electrical power demand or mechanical traction and negative when there is an electrical power absorption or mechanical braking.

The developed P-HEB and FCHEB models with each respective EMS are shown in Figs. 2.3 [87] and 2.4 [31] respectively. Each element of each powertrain is described in the following lines.

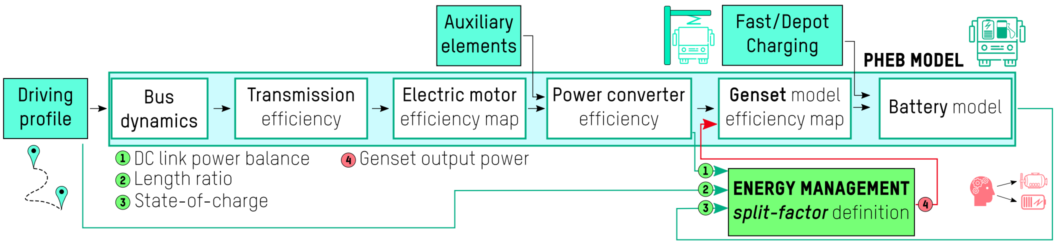

Figure 2.3: P-HEB powertrain model scheme.

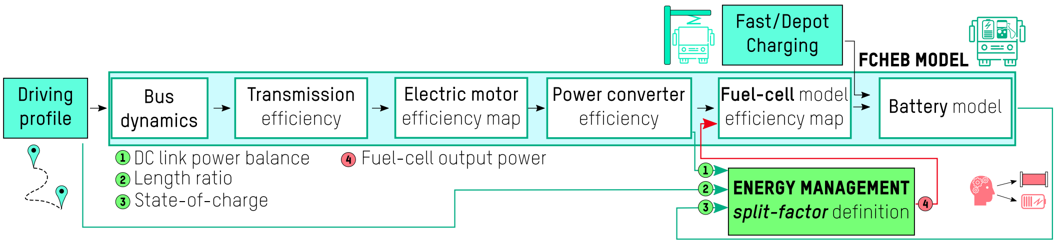

Figure 2.4: FCHEB powertrain model scheme.

2.3.1 Bus Dynamics

Bus dynamics are calculated in the same way for both powertrains, P-HEB and FCHEB. In the quasi-static simulation, the inputs to the vehicle model are the speed $v_{cyc}(k)$ $[\frac{m}{s}]$, acceleration $a_{cyc}(k)$ $[\frac{m}{s^2}]$ and the slope angle $\alpha(k)$ $[°]$ of the predefined route [27]. From these profiles, the backward simulation is applied, starting from the calculation of the force acting on the wheels (F_T $[N]$), at each discrete state k defined as follows [27, 120]:

$$F_T(k) = F_a(k) + F_g(k) + F_i(k) + F_r(k) \tag{2.1}$$

where $F_a(k)$ $[N]$ is the aerodynamic drag force, $F_g(k)$ $[N]$ the gravitational force, $F_i(k)$ $[N]$ the inertial force and $F_r(k)$ [N] the rolling resistance force (depicted in Fig. 2.5), at each discrete state k. They are defined as follows:

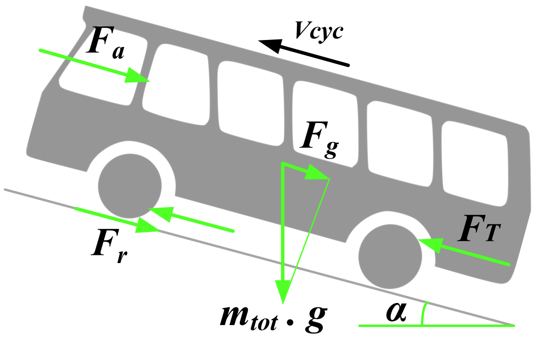

Figure 2.5: Forces acting on the bus during driving.

$$F_a(k) = 0.5 \cdot \rho_{air} \cdot A_f \cdot c_x \cdot v_{cyc}^2(k) \tag{2.2}$$

$$F_g(k) = m_{tot} \cdot g \cdot sin(\alpha(k)) \tag{2.3}$$

$$F_i(k) = m_{tot} \cdot a_{cyc}(k) \tag{2.4}$$

$$F_r(k) = c_{rf} \cdot m_{tot} \cdot g \cdot cos(\alpha(k)) \tag{2.5}$$

where the parameters are defined in Tab. 2.5.

The total mass of the vehicle can be defined as:

$$m_{tot} = m_{veh} + m_{BT} + m_{pass} \cdot n_{pass} \tag{2.6}$$

where m_{veh} $[kg]$ is the empty bus weight, m_{BT} $[kg]$ is the BT weight, m_{pass} $[kg]$ is the average weight per person (assumed to be 75 kg) and n_{pass} is the number of

Table 2.5: Bus model characteristics.

Parameter	Symbol	Value	Unit
Air density	ρ_{air}	1.1	$\frac{kg}{m^3}$
Curb weigth	m_{veh}	12500	kg
Drag coefficient	c_x	0.8	$-$
Frontal area	A_f	8.67	m^2
Gravity constant	g	9.81	$\frac{m}{s^2}$
Rolling coefficient	c_{rf}	0.008	$-$
Wheel radius	r_{wh}	0.487	m

passengers (considered to be as reference case 35 passengers of a maximum of 70 passengers) [120].

From the bus dynamic model calculation, the outputs are the wheel rotational speed $w_{wh}(k)$ $\left[\frac{rad}{s}\right]$, angular acceleration $dw_{wh}(k)$ $\left[\frac{rad}{s^2}\right]$ and the required torque in the wheel $T_{wh}(k)$ $[Nm]$ calculated as follows:

$$w_{wh}(k) = \frac{v_{cyc}(k)}{r_{wh}} \tag{2.7}$$

$$dw_{wh}(k) = \frac{a_{cyc}(k)}{r_{wh}} \tag{2.8}$$

$$T_{wh}(k) = F_T(k) \cdot r_{wh} \tag{2.9}$$

2.3.2 Transmission Model

The transmission consists on the elements placed between the motor and the drive wheel axle. For the case of P-HEB and FCHEB configurations, the tractive force is the EM. Since the EM is more flexible than the ICE in a wider rotational speed ranges, there is no need of a gear-box. It is connected to the transmission through a final drive ratio. The final drive ratio transforms a certain rotational speed into a different speed, with the aim of making the most of the EM efficiency [27].

The inputs are the outputs of the dynamic model, i.e., $w_{wh}(k)$, $a_{wh}(k)$ and $T_{wh}(k)$. As a result, the rotational speed of the drive-shaft $w_{drsft}(k)$ $\left[\frac{rad}{s}\right]$, acceleration of the drive-shaft $dw_{drsft}(k)$ $\left[\frac{rad}{s^2}\right]$ and the required torque in the drive-shaft $T_{drsft}(k)$ $[Nm]$ are recalculated as shown in the following lines:

$$w_{drsft}(k) = w_{wh}(k) \cdot \gamma(k) \tag{2.10}$$

$$dw_{drsft}(k) = dw_{wh}(k) \cdot \gamma(k) \tag{2.11}$$

$$T_{drsft}(k) = \frac{T_{wh}(k)[+]}{\gamma(k) \cdot \eta_{Tr}} + \frac{T_{wh}(k)[-] \cdot \eta_{Tr}}{\gamma(k)} \tag{2.12}$$

where γ $[-]$ is the final drive ratio and η_{Tr} $[\%]$ the efficiency of transmission model [27].

As it has been aforementioned, the traction is only provided by the EM $T_{EM}(k)$ $[Nm]$. The EM power supply is divided between the BT and GS in the case of the P-HEB and between the BT and FC in the case of the FCHEB, needing to feed the total power demand $P_{dem}(k)$ $[W]$.

$$T_{EM}(k) = T_{drsft}(k) + dw_{drsft}(k) \cdot J_{EM} \tag{2.13}$$

$$P_{dem}(k) = w_{drsft}(k) \cdot T_{EM}(k) \tag{2.14}$$

where J_{EM} $\left[\frac{m}{s^3}\right]$ is the electric motor jerk.

2.3.3 Split Factor

The information obtained from the transmission model sets the required tractive demand in the backward model. This demand has to be satisfied by each vehicle, combining as energetically and economically efficient as possible the power sources. The combination of the power sources use is determined by the split factor according to the integrated EMS in the bus. For the P-HEB and FCHEB configurations, the power $P_{dem}(k)$ has to be split in a different way.

As it has been aforementioned, the P-HEB and FCHEB configurations are only driven by the EM. In this case, the split factor is defined by the power demand $P_{dem}(k)$ $[W]$, as the series configuration is electrically coupled by the electric DC bus. This factor is divided in the case of the P-HEB between the BT power $P_{BT}(k)$ $[W]$ and the GS power $P_{GS}(k)$ $[W]$, as represented in Eq. 2.15. The GS is composed by an ICE (speed controlled) and an electric generator (torque controlled).

$$P_{dem}(k) = \begin{cases} P_{GS}(k) = P_{dem}(k) \cdot (1 - U(k)) \\ P_{BT}(k) = P_{dem}(k) \cdot U(k) \end{cases} \tag{2.15}$$

In the case of the FCHEB, the split factor is divided between the BT power $P_{BT}(k)$ $[W]$, and the FC power $P_{FC}(k)$ $[W]$, as represented in Eq. 2.16.

$$P_{dem}(k) = \begin{cases} P_{FC}(k) = P_{dem}(k) \cdot (1 - U(k)) \quad [W] \\ P_{BT}(k) = P_{dem}(k) \cdot U(k) \quad [W] \end{cases} \tag{2.16}$$

2.3.4 Electric Motor

As it has been aforementioned, both power train configurations use the EM for traction purposes. The efficiency of the EM $\eta_{EM}(k)$ $[\%]$ is calculated by means of the $w_{drsft}(k)$ and $T_{EM}(k)$ parameters, based on the efficiency map shown in Fig. 2.6 [121]. The EM model output is the required electric power $P_{EM}(k)$ $[kW]$ defined as follows [120]:

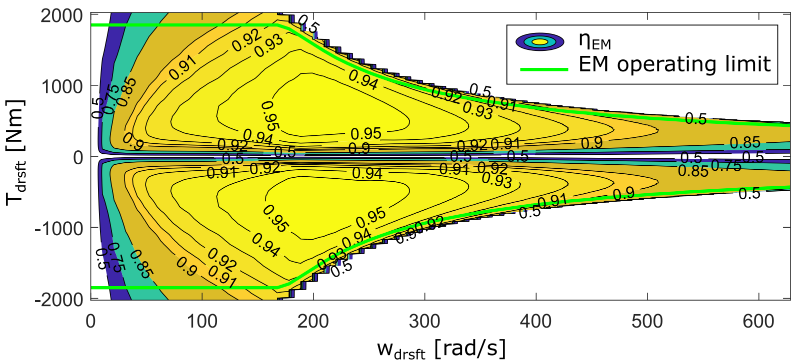

Figure 2.6: EM efficiency map.

When $w_{drsft}(k) > 0$ and $T_{EM}(k) > 0$, (traction mode):

$$P_{EM}(k) = \frac{w_{drsft}(k) \cdot T_{EM}(k)}{10^3 \cdot \eta_{EM}(k)(w_{drsft}(k),\ T_{EM}(k))} \tag{2.17}$$

When $w_{drsft}(k) > 0$ and $T_{EM}(k) < BT0$, (regenerative mode):

$$P_{EM}(k) = \frac{w_{drsft}(k) \cdot T_{EM}(k) \cdot \eta_{EM}(k)(w_{drsft}(k),\ T_{EM}(k))}{10^3} \tag{2.18}$$

2.3.5 Genset

The GS is a power element of the P-HEB and composed of an ICE and an electric generator. Both elements are mechanically connected by a clutch. The GS has been modeled based on efficiency and consumption maps. The dynamics related to the GS are not addressed in this thesis.

The GS model in this thesis has been obtained from a commercial diesel motor of VOLVO used in hybrid buses applications and commercial EG for transport applications, and their efficiency maps are shown in Figs. 2.7 and 2.8B respectively [121]. From the interpolation of fuel consumption map shown in Fig. 2.8A, the instantaneous fuel mass flow $mf_{ICE}(k)$ $\left[\frac{kg}{s}\right]$ consumed at each discrete state k is calculated as follows [27, 120],

$$mf_{ICE}(k) = f(w_{drsft}(k),\ T_{ICE}(k)) \tag{2.19}$$

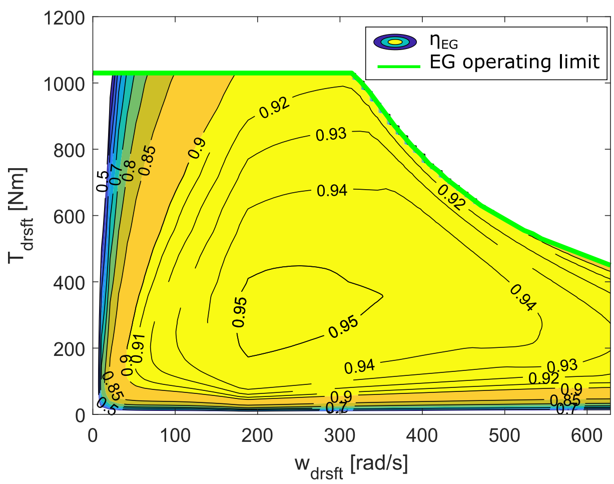

Figure 2.7: EG efficiency map.

The GS operation has been previously optimized in a prior research to identify the most efficient operation points for the whole power operation range of the GS as shown in Fig. 2.9 [120, 121].

The GS model input is the power target $P_{GS}(k)$ $[kW]$ determined by the split factor of Eq. 2.17. Fig. 2.9 curve has been included in the model to obtain (depending on the power demanded to the GS input and including the inverter efficiency) the instantaneous targets for the ICE rotational speed and corresponding mechanical torque [120, 121].

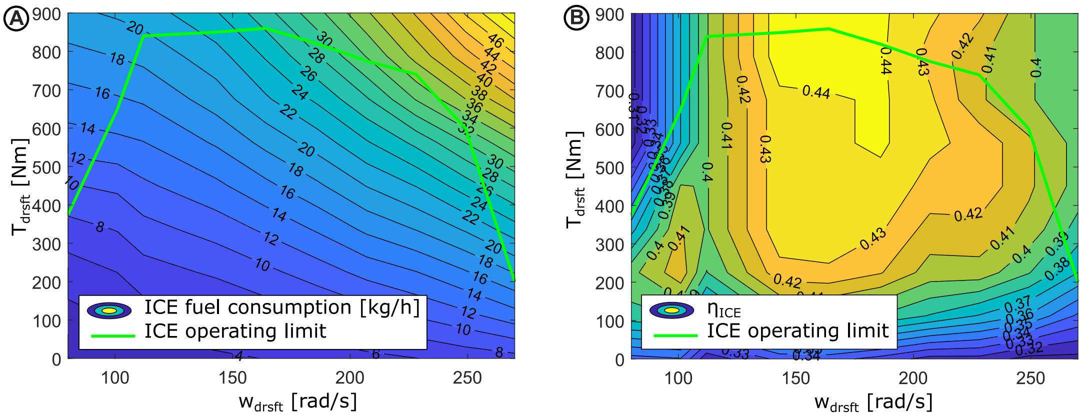

Figure 2.8: ICE fuel consumption and efficiency maps.

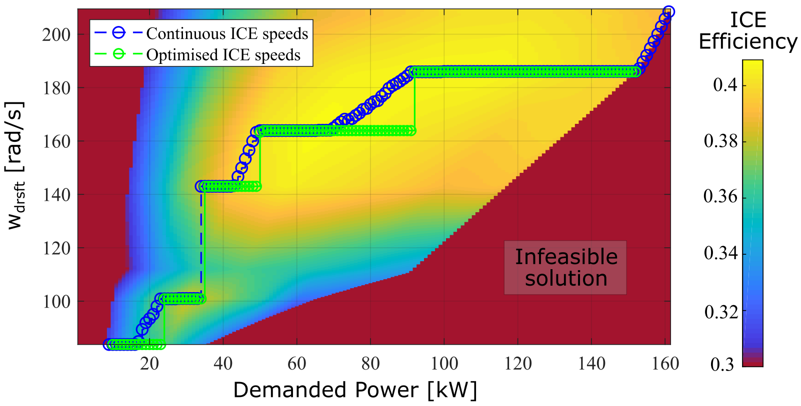

Figure 2.9: GS optimal operation curve and efficiency map.

2.3.6 Fuel Cell

The FC system consists of a FC stack, an air compressor and other auxiliary balancesof plant devices, such as power conditioning units, humidifier and cooling module [101]. The FC model has been obtained from [102]. The air compressor is modeled as a single element, since it is the auxiliary element that consumes the most. In this model it is fed directly from the FC. Therefore, in the FC output power curve shown in Fig. 2.10A [31], the air compressor power consumption has been considered. Other auxiliaries have been taken into account with a constant power consumption reaching 500 W.

The backward simulation technique, the input of the FC model is the power to be provided by the FC $P_{FCout}(k)$ $[W]$, defined by the EMS with the split factor determination. Derived from the FC output power, (by means of FC output power curve shown in Fig. 2.10A) FC output current is obtained $I_FCout(k)$ $[A]$. Derived from the FC output current, by means of the hydrogen consumption and FC

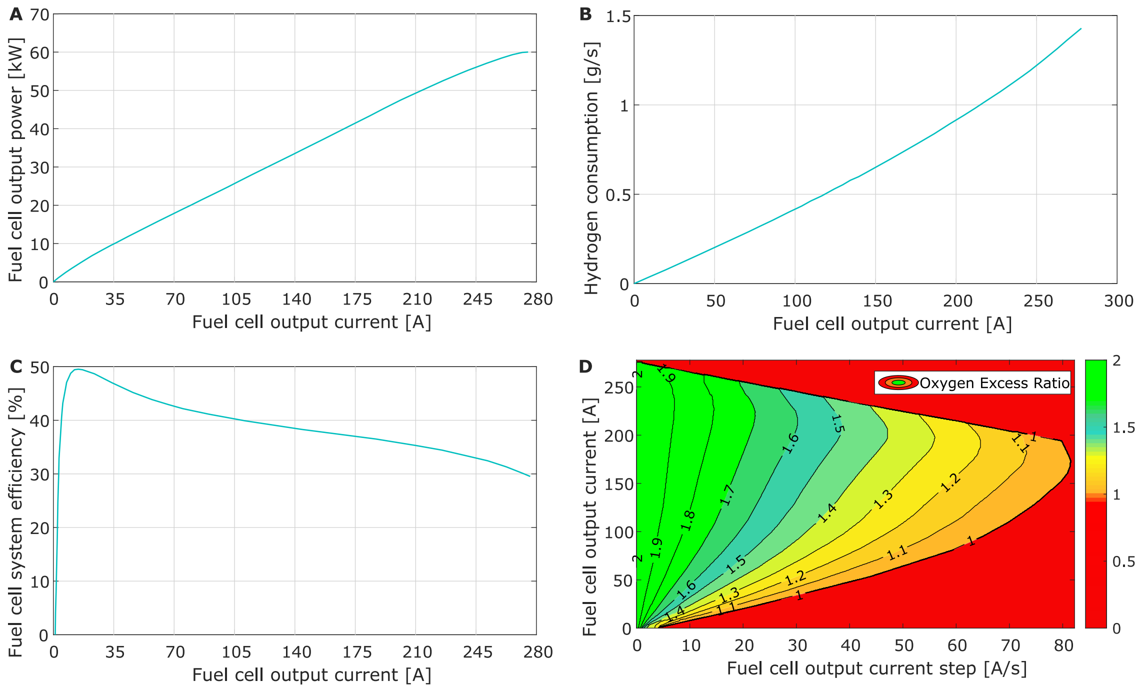

Figure 2.10: Fuel-cell model. A: FC output current and output power. B: FC hydrogen consumption. C: FC efficiency. D: FC oxygen excess ratio.

system efficiency curves (shown in Figs. 2.10B and C, respectively) the hydrogen consumption W_{H_2} $[g/s]$ and FC system efficiency are obtained.

The FC stack current $I_{stack}(k)$ $[A]$ is calculated as follows:

$$I_{stack}(k) = \frac{2 \cdot F \cdot W_{H_2}(k)}{n_{cellFC} \cdot M_{H_2}} \tag{2.20}$$

where F is the Faraday's constant, n_{cellFC} the number of cells in the stack and M_{H_2} $\left[\frac{g}{mol}\right]$ is the molar mass of hydrogen.

In the literature, it is known that the highest FC output power is achieved between 2 and 2.5 OER [100]. However, a bigger OER does not mean a better condition, as the compressor parasitic consumption increases, reducing the FC output power. Therefore, in the current literature, a steady OER value of 2 is considered as optimal [101].

Under load changes of the FC, the chemical reactions inside the FC are accelerated. The chemical reactions acceleration lead into an oxygen consumption increase and stack voltage decrease. This issue could derive in an oxygen starvation, with a consequent hot spot or burn in the surface of a membrane, causing permanent FC damage [100, 101].

To tackle this problem the OER in the cathode has to be maintained greater than 1, with an accurate control of the air-feed system. However, the OER control during transient state is delimited by the manifold and air compressor dynamics. These dynamics have been considered based on the FC cathode OER map, shown in Fig. 2.10D [100–102].

2.3.7 Auxiliary Loads

The auxiliary loads containing the air conditioning, air compressor, cooling pump, power steering and lights are represented as a minimum and maximum mean consumption: 12 kW and 18 kW for the P-HEB and 8 kW and 16 kW for the FCHEB. The FCHEB auxiliaries are lower, due to the heat recovery system implementation. The auxiliary loads can be powered by the BT and the GS for the P-HEB and by the BT and FC for the FCHEB.

2.3.8 Battery

Both buses, powertrains use the same BT model. The BT cell is represented by an ideal open circuit voltage source (V_{OCBT} $[V]$) in series with the internal resistance (R_{BTcell} $[\Omega]$). It has been assumed that a string contains n_{cellBT} BT cells in series and the BT pack groups m_{cellBT} strings in parallel [120].

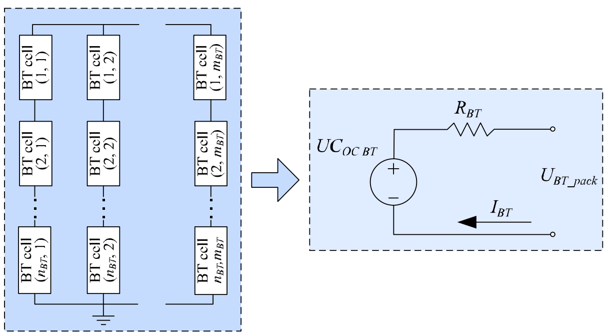

Figure 2.11: Battery pack electric model.

For the state of charge (SOC) estimation of the BT ($SOC_{BT}(k)$), the Coulomb counting method has been used [122]. In this modeling, the BT current ($I_{BT}(k)$[A]) is calculated at each sampling (k), as follows:

$$I_{BT}(k) = \frac{U_{BT}(SOC_{BT}(k))}{2 \cdot R_{BT}} - \frac{\sqrt{U_{BT}(SOC_{BT}(k))^2 - 4 \cdot R_{BT} \cdot P_{BT}(k)}}{2 \cdot R_{BT}} \quad (2.21)$$

where $U_{BT}(k)$ $[V]$ is the BT pack equivalent open-circuit voltage and $R_{BT}(k)$ $[\Omega]$ is BT pack the equivalent internal resistance of the BT, at pack level. The BT model input is the BT pack power target $P_{BT}(k)$ [W] generated by the EMS split factor.

The SOC is updated at each sample as follows:

$$SOC_{BT}(k+1) = SOC_{BT}(k) - \frac{I_{BT}(k+1)}{C_{BT} \cdot 3600} \cdot 100 \quad (2.22)$$

where C_{BT} $[Ah]$ is the BT pack nominal capacity.

The parameters for the cells modeling are shown in Tab. 2.6. NMC and LTO type chemistries have been chosen due to the application characteristics. NMC chemistry is mostly used for energy applications, since the specific energy is high, 149 Wh/kg. On the contrary, LTO chemistry is used for power applications with lower specific energy, in this case 90 Wh/kg.

Table 2.6: Electrical parameters of BT cells.

Nickel Manganese Cobalt Oxide (NMC) [86, 123, 124]		**Lithium titanate oxide (LTO) [121, 125]**	
Nom. voltage	3.7 V	Nom. voltage	2.3 V
Nom. capacity	40 Ah	Nom. capacity	20 Ah
Int. resistance	0.8 $m\Omega$	Int. resitance	0.53 $m\Omega$
Max C-rate disch/ch	8/4 *C-rate*	Max C-rate disch/ch	8/7 *C-rate*
Specific energy	149 Wh/kg	Specific energy	90 Wh/kg
Calendar lifetime	8 $years$	Calendar lifetime	15 $years$

2.4 BT Lifetime Estimation

In this section the BT lifetime (γ_{BT} $[years]$) and the method of the calculation of the number of replacements are described. For this calculation, BT calendar degradation and BT cycling degradation methods have been taken into account.

$$\gamma_{BT} = min\Big[\gamma_{cal}, \gamma_{cyc}\Big] \quad (2.23)$$

where γ_{cal} $[years]$ is the number of years by means of the calendar degradation and γ_{cyc} $[years]$ the degradation by means of the BT operation. The calendar degradation is a fixed value for each chemistry, and these values are given in Tab. 2.6. However, the BT cycling degradation has to be evaluated based on the process described in the following lines.

BT cycling degradation is calculated based on a Rainflow cycle counting algorithm [126] and Wöhler curve-based method [120]. The Wöhler curve-based method is a fatigue analysis commonly used for BT aging estimations [127–129].

The Wöhler method lies on the number of NE_{ievt} events -in this case DOD- that can occur until the BT reaches its EOL

The lifetime lost (LL_{ievt}) calculation is done by the relation of the accounted (NE_{ievt}) and the maximum number of events (NE_{ievt}^{max}) that the BT can withstand, expressed as follows:

$$LL_{ievt} = \frac{NE_{ievt}}{NE_{ievt}^{max}} \tag{2.24}$$

The NE_{ievt} are accounted by means of the Rainflow algorithm (Fig. 2.12 [120]), with steps of 1% of DOD.

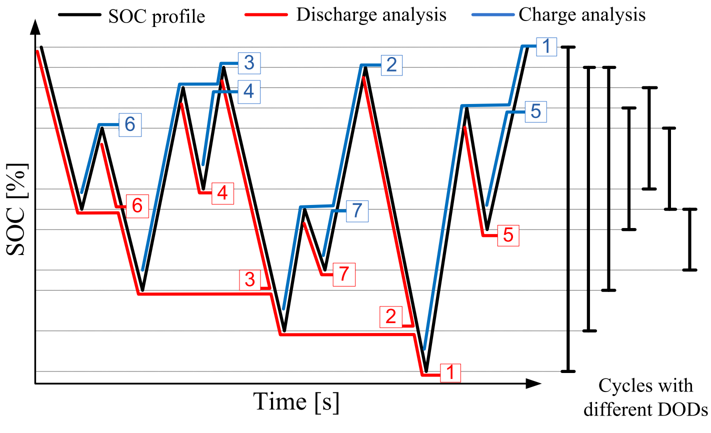

Figure 2.12: Rainflow charging/discharging cycle counting algorithm.

The NE_{ievt}^{max} are extracted from Wöhler curves of NMC and LTO chemistries shown in Fig. 2.13 and extracted from [130]. For the Wöhler curve of the NMC chemistry, the number of Full Equivalent Cycles (FEC) from 0 to 30 has been limited to 10000 based on our knowledge. In this way, the micro-cycles will be limited.

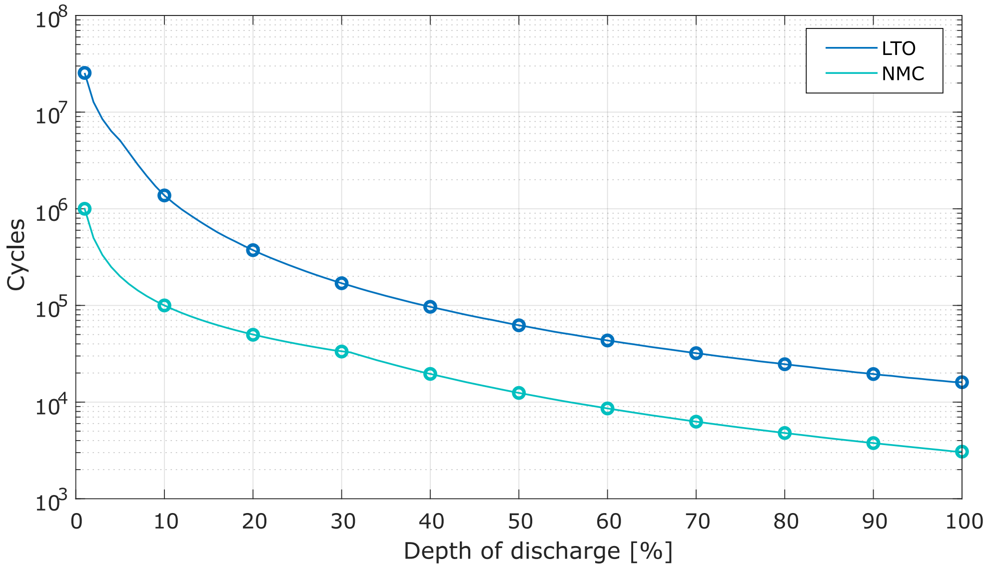

Figure 2.13: LTO and NMC Wöhler curves.

For determining the total lifetime loss (LL) in the whole range of DODs (from 0 to 100%), the sum of all the events in the cycling evaluated period has to be calculated as follows [120]:

$$LL = \sum_{ievt} LL_{ievt} \tag{2.25}$$

Finally, considering the evaluated SOC profile's time period with the inversion of LL, the total cycling lifetime (γ_{cyc}) can be calculated, typically defined in years:

$$\gamma_{cyc} = \frac{1}{\sum_{ievt=1}^{100} \left(\frac{NE_{ievt}}{NE_{ievt}^{max}} \right)} \tag{2.26}$$

2.5 Fleet simulation platform

The introduced P-HEB and FCHEB models have been implemented into a vehicle and fleet simulation platform developed in the framework of this Ph.D thesis. The graphic interface of this platform is shown in Fig. 2.14 which is the main window.

This simulation platform serves as a tool that allows evaluating a fleet of vehicles from the energetic and economic point of view. Therefore, this platform gives the flexibility to evaluate different routes and P-HEB, FCHEB and BEB vehicle types.

In the main window of the fleet simulation platform, as depicted in Fig. 2.14, the route information to evaluate is shown. In here, the available information of the routes to analyze are the distance, maximum speed, aggressiveness, energy demand, minimum and maximum SOC, fuel or hydrogen consumption, BT consumption and BT aging.

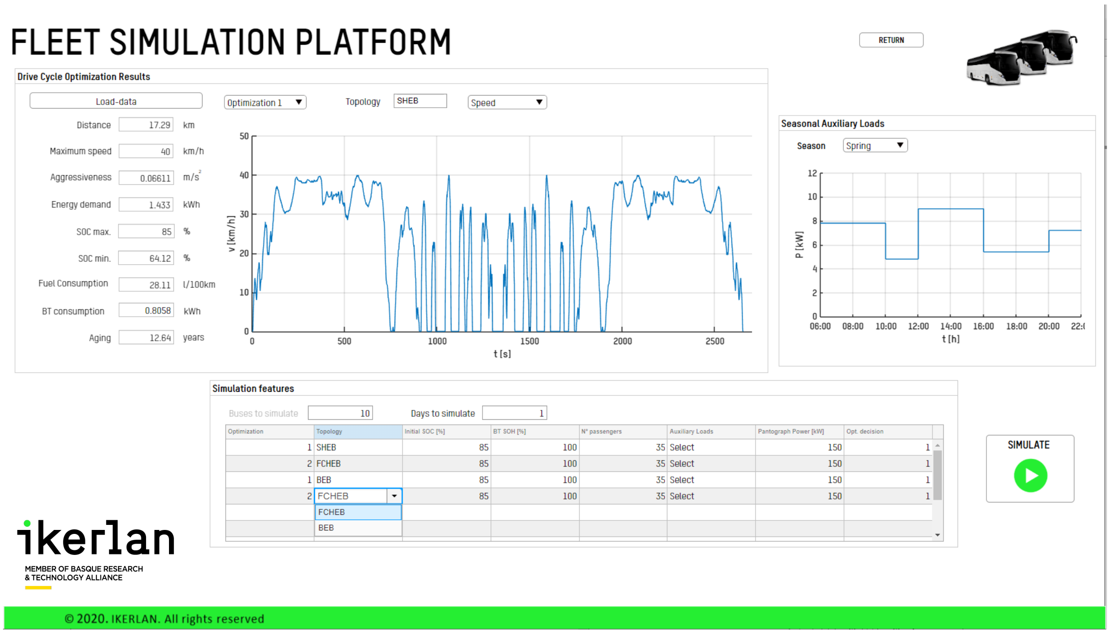

Figure 2.14: Developed fleet simulation platform.

From the available routes, the fleet simulation platform allows to create mixed fleets and analyze the vehicle operation with different EMSs, auxiliary consumption levels, charger powers or mean number of passengers. Once the fleet operation is obtained, it gives the ability to analyze the obtained techno-economically.

2.6 Total Cost of Ownership

Both the P-HEB and FCHEB have higher investment costs than conventional buses. However, as it has been aforementioned, the high yearly driven distances of buses and the lower operational costs help to compensate the BT, FC and manufacturing extra costs [6, 9, 10, 19]. The solution feasibility study has to be determined based on the calculation of the TCO, as it is the economic performance indicator, which includes the cost of investment, insurance, infrastructure, maintenance, driver, operation, carbon-taxes and EOL [12, 121, 131].

From the above-mentioned factors forming the TCO, two different groups have been differentiated from the energetic manageability point of view: fixed and manageable costs. Figure 2.15 shows both groups of factors. Once the bus is under operational conditions, on the one hand, cost of investment, insurance, infrastructure, maintenance and driver costs have been taken as constant, since they cannot be managed from an energetic point of view. On the other hand, operation costs can be managed with direct impact on the carbon taxes. As shown in Figure 2.15, the previously analyzed degrees of freedom regarding the P-HEB [86] and FCHEB [31] controllability are the fuel or hydrogen consumption, the power and energy charging costs, the energy storage system utilization and the consequent number of replacements.

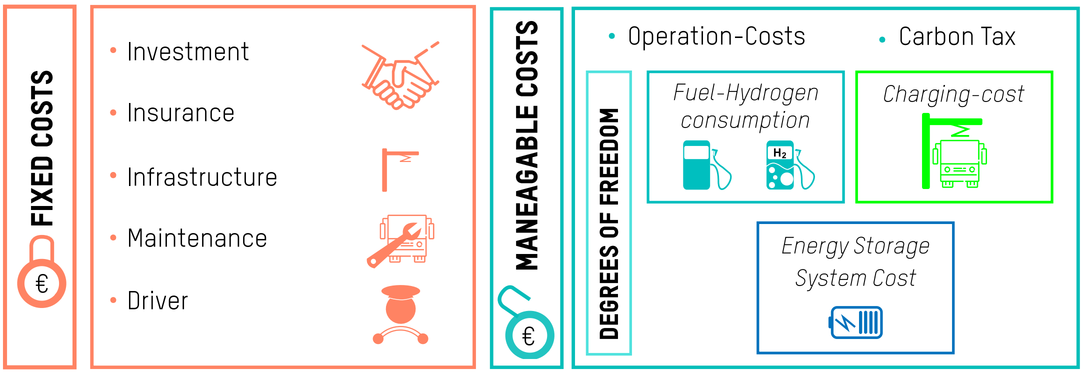

Figure 2.15: Total cost of ownership fixed and manageable costs overview.

The variables that differentiate the P-HEB and FCHEB in terms of TCO are the fuel and hydrogen consumption respectively. The TCO calculation for the P-HEB and FCHEB is described in the following lines.

The TCO calculation for P-HEB, $TCO_{P-HEB}\left[\frac{€}{lifetime}\right]$, has been carried out based on the aforementioned manageable costs obtaining the following equation [9, 19],

$$TCO_{P-HEB} = \sum_{t=1}^{T} \frac{(f_{ICE} \cdot C_{fuel/t} \cdot Dev_{fuel} + E_{cha} \cdot C_{kWh/t}) \cdot Op_{year}}{(1+dr)^T} + \\ + C_{kW/t} \cdot P_{cha} + \frac{C_{BTkWh} \cdot E_{BT} \cdot DR_{BT/t}}{(1+dr)^T} \tag{2.27}$$

where T is the scenario duration $(years)$, t the current year, $f_{ICE}\left[\frac{l}{day}\right]$ the fuel consumption, $C_{fuel/t}\left[\frac{€}{l}\right]$ the annual fuel price, $E_{cha}[kWh/day]$ the energy absorbed from the grid, $C_{kWh/t}\left[\frac{€}{kWh}\right]$ the referential annual energy cost of the grid, $Op_{year}\left[\frac{\text{day}}{year}\right]$ the yearly operation days, $C_{kW/t}\left[\frac{€}{kW}/year\right]$ the annual cost of the power, P_{cha} $[kW]$ the power of the charger, $C_{BTkWh}\left[\frac{€}{kWh}\right]$ the BT initial price, E_{BT}[kWh] the BT pack energy, $DR_{BT/t}\left[\frac{\%}{year}\right]$ depreciation rate of the BT per year and $dr[\%]$ the discount rate.

The fuel consumption, f_{ICE} $[l/day]$, is obtained with:

$$f_{ICE} = \frac{\sum_{k=1}^{p} mf_{ICE}(k) \cdot k_{cs}}{\rho_{fuel}} \cdot n_{round-trips \quad day} \quad \left[\frac{l}{day}\right] \tag{2.28}$$

where p is the driving cycle length in seconds, k_{cs} $[-]$ the global factor to cold starts, ρ_{fuel} $[kg/l]$ the volumetric density of diesel and $n_{round-tripsday}$ $[-]$ the number of completed round trips in a day.

The energy absorbed from the grid $E_{cha}[kWh/day]$ is calculated from the recharged power and the power of the charger P_{cha} $[kW]$ is calculated based utilized power in the charger. Finally, the BT replacements number is calculated following the methodology presented in Sec. 2.4.

The TCO calculation for the FCHEB, TCO_{FCHEB} $\left[\frac{€}{lifetime}\right]$, is calculated in the same way for the P-HEB, replacing the fuel consumption by the hydrogen consumption as follows:

$$\begin{aligned} TCO_{FCHEB} = \sum_{t=1}^{T} & \frac{(f_{H_2} \cdot C_{H_2/t} \cdot Dev_{H_2} + E_{cha} \cdot C_{kWh/t}) \cdot Op_{year} + C_{kW/t} \cdot P_{cha}}{(1+dr)^T} + \\ & + \frac{C_{BT} \cdot E_{BT} \cdot DR_{BT/t}}{(1+dr)^T} \quad \left[\frac{€}{lifetime}\right] \end{aligned} \tag{2.29}$$

The hydrogen consumption f_{H_2} $[kg/day]$ is obtained from the following equation:

$$f_{H_2} = \sum_{k=1}^{p} W_{H_2}(k) \cdot n_{round-trips} \quad \left[\frac{kg}{day}\right] \tag{2.30}$$

Finally, in Table 2.7 the applied techno-economic parameters for the TCO calculations are summarized [7, 10, 13, 121, 132–138].

Table 2.7: Total cost of ownership parameters.

	Acronym	**Value**	**Unit**	**Reference**
Global factor to cold starts	k_{cs}	1.15	–	[120]
Volumetric density of diesel	ρ_{fuel}	0.832	kg/l	[120]
Fuel cost	C_{fuel}	0.95	€$/l$	[135]
Diesel fuel price development	Dev_{fuel}	2.3	$\%/year$	[135]
Hydrogen cost (1% market penetration)	C_{H_2}	11.12	€$/kg$	[138]
Hydrogen cost (10% market penetration)	C_{H_2}	8.16	€$/kg$	[138]
Hydrogen cost (30% market penetration)	C_{H_2}	7.51	€$/kg$	[138]
Hydrogen cost (75% market penetration)	C_{H_2}	6	€$/kg$	[13, 138]
Hydrogen cost (ideal scenario)	C_{H_2}	5	€$/kg$	[13]
Hydrogen price development	Dev_{fuel}	Fixed	-	[138]
Energy electricity cost	C_{kWh}	0.139	€$/kWh$	[135]
Power electricity cost	C_{kW}	25.9	€$/kW/year$	[10]
Electricity price development	Dev_{Elect}	3.7	$\%/year$	[135]
Yearly operation days	Op_{year}	330	€$/kW/year$	[134][1]
Bus service life	$P_{FleetEOL}$	12	$year$	[10]
NMC BT low cost scenario	C_{BTkWh}	550	€$/kWh$	[137]
NMC BT medium cost scenario	C_{BTkWh}	800	€$/kWh$	[121, 133]
NMC BT high cost scenario	C_{BTkWh}	1000	€$/kWh$	[136]
LTO BT low cost scenario	C_{BTkWh}	700	€$/kWh$	[137]
LTO BT medium cost scenario	C_{BTkWh}	1000	€$/kWh$	[121, 133]
LTO BT high cost scenario	C_{BTkWh}	1500	€$/kWh$	[136]
BT depreciation rate	$DR_{BT/t}$	-20	% in 12 years	[132, 137] [1]
Discount rate	dr	2.2	%	[135]

[1] Own estimation

3

Vehicle Level Artificial Intelligence Learning Based Energy Management Strategy

Summary

This chapter presents the proposed vehicle level energy management strategy design and real-time implementation. The optimization and artificial intelligence based learning techniques background and method are explained. For evaluating the vehicle level energy management strategy, two case studies have been analyzed. On the one hand, the plug-in hybrid electric bus energy management strategy has been evaluated in simulation and in a hardware-in-the-loop platform for a specific route. On the other hand, the developed energy management strategy has been replicated for a fuel cell hybrid electric bus and analyzed with a different route.

3.1 Structure of the Vehicle Level Energy Management Strategy

The proposed vehicle level EMS is an intelligent and adaptive battery aging conscious EMS, aiming at making compatible the fuel and hydrogen consumption with the management of the BT lifetime. This approach is split into two main blocks, the offline learning based EMS design and the online operation level as shown in Fig. 3.1.

It is composed of two levels, as it has been aforementioned in Sec. 2.1. The offline learning based EMS design shown at the left hand of Fig. 3.1 is composed of a DP optimization and a learning based neuro-fuzzy technique. The aim of the EMS design is to first optimize the operation of a bus driving on a specific route and generate a data-base with the different auxiliary consumptions. Hence, the EMS is designed by means of a neuro-fuzzy technique trained and tested with the generated optimized data-sets.

The core of the online operation level is a fuzzy-logic based EMS, as shown in the right hand of Fig. 3.1 [87]. The EMS is composed of different fuzzy-logic structures, divided by the length-ratio. Each structure is used according to the placement of the bus in the route. The EMS defines the optimized GS power for the P-HEB or FC power for the FCHEB defining the corresponding power split factor.

In Sec. 3.2 the offline optimization and strategy design at vehicle level is

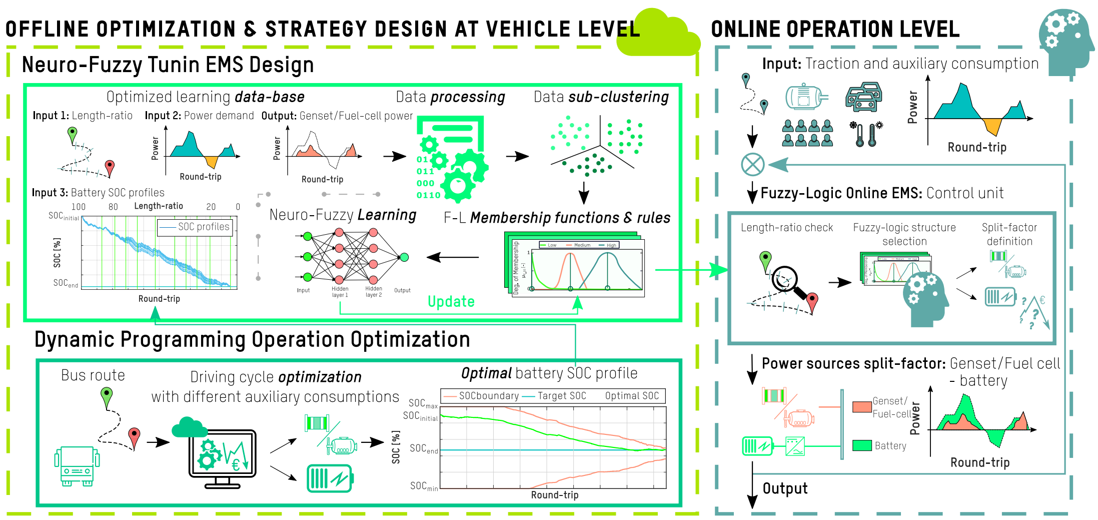

Figure 3.1: Vehicle level energy management strategy structure.

described. This section is split into two subsections. First, the DP global optimization and cost functions are defined. It is worth mentioning here, that a specific cost function has been develop for the P-HEB and another for the FCHEB. Following the optimization technique definition, the neuro-fuzzy based learning method is explained. The same learning technique inputs have been used for all the bus models. However, the output for the P-HEB is the GS power and for the FCHEB the FC power. In Sec. 3.3 the online operation is presented in detail.

Once the proposed strategy has been described, the chapter is completed by evaluation dedicated sections. The vehicle level EMS is evaluated for the P-HEB topology in Sec. 3.4 and for the FCHEB topology in Sec. 3.5. The P-HEB EMS has also been tested into a HIL platform, with the aim of testing the real-implementation of the proposed approach.

3.2 Offline Optimization & Strategy Design at Vehicle Level

At this stage, the EMS is designed offline, based on a DP optimization and a neuro-fuzzy technique. The objective of the learning based EMS design is to develop a replication of the DP optimal operation of the bus operating in a specific route, by means of the split factor of the power sources.

3.2.1 Dynamic Programming Optimization

DP global optimization has been used to determine buses optimal operations and performances, which implies less emissions and efficiency optimization, using Bellman's DP algorithm [139]. This approach has been commonly used as a baseline for benchmarking the proposed new EMSs for HEVs and for off-line optimization [24, 64].

Two cost functions and optimization constraint scenarios have been defined, one for P-HEBs and the other one for FCHEBs.

P-HEB cost function and constraints

The optimization for the P-HEB problem is based on the fuel consumption minimization and BT utilization management. This management is carried out based on the following cost function (J_{P-HEB}) :

$$J_{P-HEB} = min_{u_k \in U_k} \sum_{k=0}^{N-1} \triangle mf_{ICE}(U(k)) \cdot (\triangle x_{ref} \cdot w_x) \cdot T_s \tag{3.1}$$

where $\triangle mF_{ICE}(U(k))$ is the fuel mass consumption (determined by the torque power split factor U), $\triangle x_{ref}$ the SOC current difference from a reference SOC and w_x the weight applied to the SOC difference factor. All the calculations are carried out at each time step (T_s=1 s), within the urban route length (N). The dynamic system has been modeled with a single state variable, BT SOC, achieving the best trade-off between accuracy and computational efficiency [140]. The implemented constraints are explained in the following lines:

$$\begin{cases} x(0) = x_0 \\ x(end) = x_{final} \\ x(k_f)\epsilon[x_{f,min}, x_{f,max}] \\ u(k_f)\epsilon[u_{f,min}, u_{f,max}] \\ x(k)\epsilon\chi(k) \subset \Re^n \\ u(k)\epsilon\chi(k) \subset \Re^m \end{cases} \tag{3.2}$$

where $x(0)$ sets the initial SOC, $x(end)$ sets the final SOC, $x(k_f)$ and $u(k_f)$ set the SOC and split factor boundary of the optimization and $x(k)$ and $u(k)$ constraint the SOC and split factor values to real values.

The split factor at the initial point, is set from $U = [-1, 1]$. For the case of series configuration considered in this study, the power demand (P_{dem} [W]) is split, as shown in Eq. 3.3. This factor determines the power split between the BT power (P_{BT} [W]) and the GS power (P_{genset} [W]).

$$P_{dem}(i) = \begin{cases} P_{Genset}(i) = P_{dem}(i) \cdot (1 - U(i)) \\ P_{BT}(i) = P_{dem}(i) \cdot U(i) \end{cases} \tag{3.3}$$

Based on this equation, $U = 1$ defines full electric mode; $U < 1$ & $U > 0$ defines hybrid mode; $U = 0$ defines full ICE mode and $U = -1$ defines full ICE mode recharging the BT.

In the first stage, the operation of the bus in a specific driving cycle is optimized in terms of efficiency and cost, based on DP [139]. Optimizations are carried out using different auxiliary consumption demands, in the range starting from the minimum to the maximum of the mean auxiliary power demands. These optimizations give the information of the optimal split factor between the GS and the BT to fulfill the power demand for each auxiliary consumption.

In addition, the following powertrain constraints are defined in the bus model optimization [87]:

$$\begin{cases} I_{BT_{min}} \leq I_{BT}(k) \leq I_{BT_{max}} \\ T_{GS_{min}} \leq T_{GS}(k) \leq T_{GS_{max}},\ \omega_{GS_{min}} \leq \omega_{GS}(k) \leq \omega_{GS_{max}} \\ T_{EM_{min}} \leq T_{EM}(k) \leq T_{EM_{max}},\ \omega_{EM_{min}} \leq \omega_{EM}(k) \leq \omega_{EM_{max}} \end{cases} \tag{3.4}$$

where $I_{BT}(k), T_{GS}(k), \omega_{GS}(k), T_{EM}(k)$ and $\omega_{EM}(k)$ represent respectively the BT current, GS torque, GS rotational speed, EM torque and EM rotational speed with each respective limits at each discrete state k.

FCHEB cost function and constraints

The cost function for the FCHEB has been developed with the aim of minimizing the hydrogen consumption and the OER variation, and hence to maximize the FC lifetime. Indeed, the start-stop cycles, idling time, load variation and high and low current FC demand are managed based on this cost function.

$$J_{FCHEB} = min_{u_k \in U_k} \sum_{k=0}^{N-1} (W_{H_2}(U(k) \cdot \alpha_{H_2}) + \beta_{H_2} \cdot \triangle\lambda_{O_2}(k)) \cdot T_s \qquad \triangle\lambda_{O_2} = \begin{cases} \lambda_{O_2}, & \lambda_{O_2} < \lambda_{O_2}^{lim} \\ 0, & \lambda_{O_2} \geq \lambda_{O_2}^{lim} \end{cases} \tag{3.5}$$

where $W_{H_2}(U(k))$ is the hydrogen mass consumption (determined by the power split factor U), $\lambda_{O_2}(k)$ the OER of the fuel cell, and α_{H_2} and β_{H_2} are the respective weights. All the calculations are carried out at each time step k (T_s=1 s), within the urban route length (N). The split factor at the initial point is set from $U = [-1, 1]$. For the case of parallel configuration, this factor determines the power split between the BT and FC. The implemented constraints are the same defined in Eq. 3.2

The split factor is limited in the range of $U = [-1, 1]$. In the case of the FCHEB configuration, the power demand (P_{dem} [W]) is split, as shown in Eq. 3.6, between the BT power (P_{BT} [W]) and the FC power (P_{FC} [W]).

$$P_{dem}(i) = \begin{cases} P_{FC}(i) = P_{dem}(i) \cdot (1 - U(i)) \\ P_{BT}(i) = P_{dem}(i) \cdot U(i) \end{cases} \tag{3.6}$$

Based on this equation, $U = 1$ defines full electric mode (only BT); $U < 1$ & $U > 0$ defines hybrid mode; $U = 0$ defines full FC mode and $U = -1$ defines full FC mode recharging the BT. In addition, the following powertrain operation constraints have been defined in the bus model optimization:

$$\begin{cases} I_{BT_{min}} \leq I_{BT}(k) \leq I_{BT_{max}} \\ P_{FC_{min}} \leq P_{FC}(k) \leq P_{FC_{max}} \\ T_{EM_{min}} \leq T_{EM}(k) \leq T_{EM_{max}}, \ \omega_{EM_{min}} \leq \omega_{EM}(k) \leq \omega_{EM_{max}} \end{cases} \tag{3.7}$$

where $SOC(k), I_{BT}(k), P_{FC}(k), T_{EM}(k)$ and $\omega_{EM}(k)$ represent the battery SOC, battery current, FC power, electric motor torque and electric motor rotational speed with each respective limits at each discrete state k.

Final SOC definition

For the DP optimizations, the proposed approach is focused on P-HEBs and FCHEBs. The initial SOC in the literature is set as 85 % [120]. The final SOC has been established based on the level of demand of the route, with the goal of recharging the BT to reach the initial SOC within the recharging time. The recharging time $t_{cha}[s]$ has been determined according to the route distance $L_{route}[km]$, as follows,

$$t_{cha} = L_{route} \cdot \alpha_{cha} \tag{3.8}$$

where α_{cha} is a constant empirically obtained for each bus technology that aims to achieve a BT depletion among all the route. For the case of the LTO BT, α_{cha} has been determined as 9 and for the NMC BT it has been determined as 22.

Once the recharging time is set, the energy to be charged, $E_{cha}[kWh]$, is calculated as follows:

$$E_{charged} = P_{cha} \cdot 1000 \cdot \tfrac{t_{cha}}{3600} - P_{max_{aux}} \cdot 1000 \tfrac{t_{cha}}{3600} \tag{3.9}$$

where $P_{max_{aux}}$ $[kW]$ is the maximum auxiliary consumption with the aim of calculating the energy to be charged in the worst scenario.

The usable energy E_{usable} $[kWh]$ in the BT is calculated based on the BT energy E_{BT} $[kWh]$, current BT SOH, SOH_{BT} [%], BT utilization constant, ζ_{BT}, and initial SOC, x_0 [%], as follows:

$$E_{usable} = \left(E_{BT} \cdot \frac{SOH_{BT}}{100} \cdot \zeta_{BT} \right) \cdot \frac{x_0}{100} \tag{3.10}$$

Finally, the maximum discharged energy in the BT is calculated with the difference of Eqs. 3.10 and 3.9, the final SOC x_{final} [%] is calculated as follows:

$$x_{final} = \frac{E_{usable} - E_{charged}}{E_{BT} \cdot \frac{SOH_{BT}}{100}} \cdot 100 \tag{3.11}$$

Having the constraint and optimal operation defined, a data-base is built, with the different auxiliary consumptions, within the minimum and maximum auxiliary consumptions, with steps of 1 kW. The decision of optimizing the operation for different auxiliary consumption was based on a previous study [86], since the auxiliary power consumption was identified as a critical factor for buses management. In this way, for each route a data-base with global optimal operations is built.

3.2.2 Neuro-fuzzy Learning Technique

The training procedure has been carried out based on a neuro-fuzzy technique, more specifically on the ANFIS learning technique from MATLAB. From this point on, the learning technique is denominated ANFIS. The training process has been performed following the intelligent decision maker process shown in Fig. 3.2.

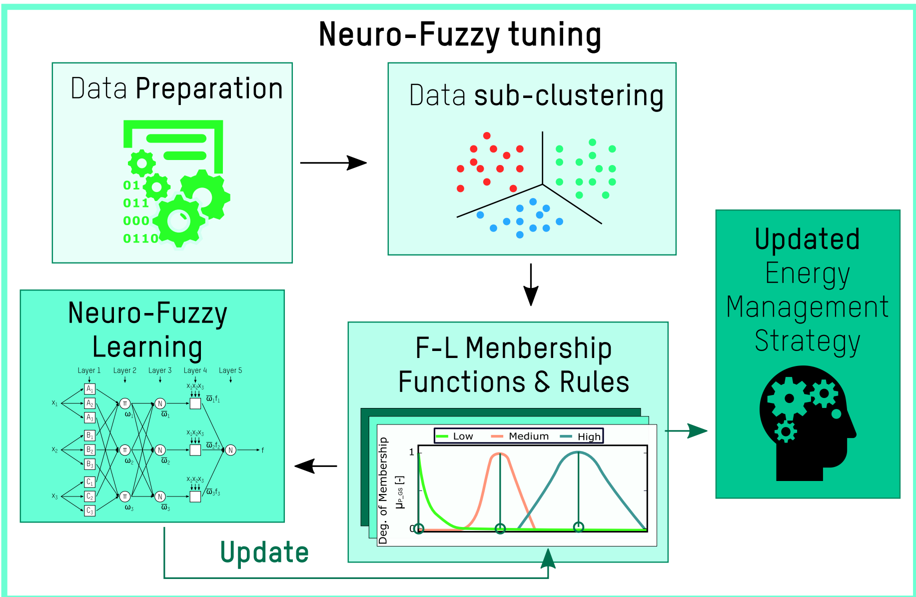

Figure 3.2: Intelligent Decision Maker.

In the data preparation stage, the previously built data-base in the optimization stage explained in Sec. 3.2 is preprocessed. The data-base is composed of the determined ANFIS training inputs and outputs. From the previously developed work [141], the number of inference systems have been reduced from 5 to 3, having the SOC, the length-ratio and the power demand as inputs and the GS power or FC power as the output. The output definition, determined the split factor between the available power sources for the P-HEB and FCHEB applications respectively. The inputs reduction has been carried out based on a variable correlation study, dismissing those variables with correlation. Each input and output of the described data-base is firstly normalized within $[0, 1]$.

The normalized data-base is split into different stages, divided in accordance to the route distance ratio and the amount of data of each set. A first approach has been carried out with 10 % length-ratio steps division. For having homogeneous data-sets, for those sets larger than the others, the 10 % distance ratio has been split into two 5 % step sets.

Once the data is processed, the ANFIS initial fuzzy-logic design has been generated based on subtractive-clustering technique of the datasets [142]. At this second data sub-clustering, the initial membership function design, number of outputs and rules are defined.

At the ANFIS learning stage, the initial membership functions and rules are trained based on the ANFIS technique, with the aim of tuning the membership functions and refining the proposed first rules. It is worth mentioning that from the obtained optimal operations, around 80% is used for the training process and 20% for the testing process of the developed ANFIS based EMS.

ANFIS technique was developed by Jang and improved by Sugeno and Kang [143, 144]. This technique is used for learning from a data-base and tuning the fuzzy inference system [74]. In this work the aforementioned data-base has been used for the learning and tuning process. The technique for the ANFIS tuning stage is a hybrid learning algorithm in conformity with back-propagation and least-squares-type methods, as shown in Fig. 3.3. The main reasons for using the hybrid method have been the training speed, the error avoidance with the support of the second algorithm and the smarter networks training based on supervised learning [74].

The ANFIS architecture is composed of 5 layers. The nodes x, y and z in layer 1 represent the system inputs that are the SOC, the length-ratio and the power demand respectively. The node in layer 5 refers to the system output GS power or FC power for the P-HEB and FCHEB applications respectively. The reduction of inputs, i.e., from 5 to 3, speeds up the learning process, maintaining the accuracy

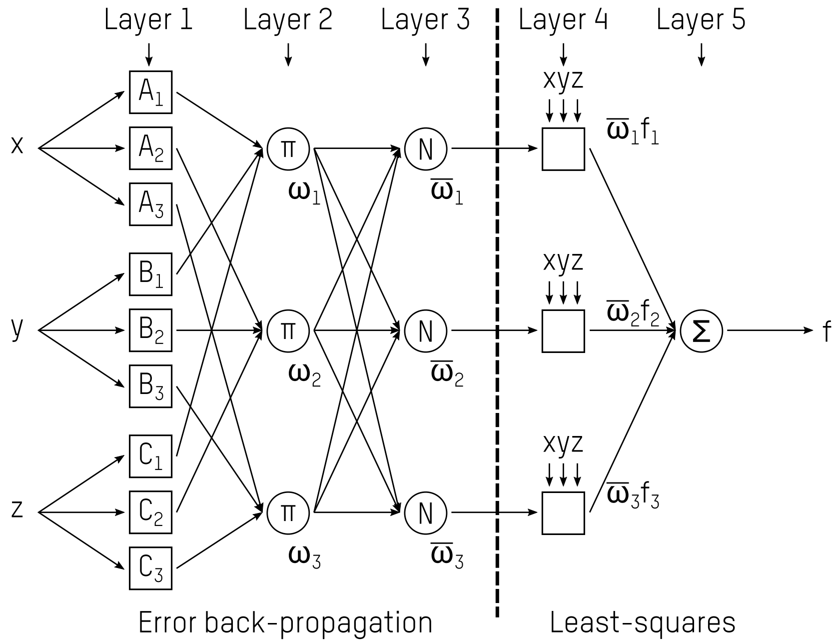

Figure 3.3: ANFIS architecture.

level. The output of each layer is expressed in Eq. 3.12.

$$\begin{cases} O_i^1 = \mu_{Ai} = e^{-\left(\frac{x-a}{b}\right)^2}, \quad i = 1,2,3 \\ O_i^2 = \omega_i = \mu_{A_i}(x) \cdot \mu_{B_i}(y) \cdot \mu_{C_i}(z), \quad i = 1,2,3 \\ O_i^3 = \bar{\omega}_i = \frac{\omega_i}{\sum_{j=1}^{i} \omega_i}, \quad i = 1,2,3 \\ O_i^4 = \bar{\omega}_i F_i = \bar{\omega}_i(p_i x + q_i y + r_i z + m_i), \quad i = 1,2,3 \\ O_i^5 = F = \sum_{j=1}^{3} \bar{\omega}_i f_i = \frac{\sum_{j=1}^{3} \omega_i f_i}{\sum_{j=1}^{3} \omega_i} \end{cases} \tag{3.12}$$

Layer 1 $O_i^1 = \mu_{Ai}$ is an adaptive layer where the fuzzification process is carried out according to the chosen membership function type, in this case Gaussian functions. In Eq. 3.12, x is one of the input variables and $\{a, b\}$ are the parameters defining the bell-shaped node. Layer 2 $O_i^2 = \omega_i$ is a fixed layer where each rule weight is determined multiplying each node by the input signals. Layer 3 $O_i^3 = \bar{\omega}_i$ is a fixed layer where each rule weight is normalized with the sum of all rules. Layer 4 $O_i^4 = \bar{\omega}_i f_i$ is an adaptive layer where p, q, r, m fuzzy set design parameters are determined. Layer 5 $O_i^5 = F$ is a fixed layer where the output is computed, also known as sugeno defuzzification process [143].

Finally from the intelligent decision maker, the designed sugeno type fuzzy-logic EMS is obtained. From this point on, the designed fuzzy-logic EMS is denominated ANFIS based EMS. The ANFIS based EMS is implemented in the vehicle for managing the power sources in real-time. The online EMS operation is explained in the following section.

3.3 Online Operation at Vehicle Level

At this level, the ANFIS based EMS is operated in real-time onboard the bus. The inputs for the EMS are the current power demand, the current length-ratio and the current BT SOC. Based on the EMS power split factors are determined: the GS and BT for the P-HEB and the FC and BT for the FCHEB.

The ANFIS based EMS is composed of four steps, as shown in Fig. 3.4.

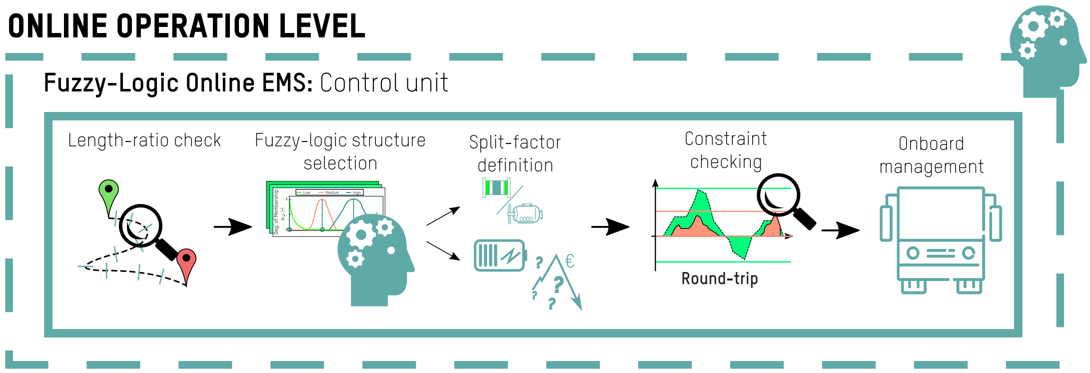

Figure 3.4: ANFIS based EMS structure.

In the first step the length-ratio is checked. Based on this information, the corresponding FL structure is defined. According to the current FL structure defined in the second step, in a third step, depending on the current power demand, length-ratio and SOC of the BT, the split factor (U) is determined, with the aim of fulfilling the power demand. For the case of the P-HEB, the GS output power is determined and for the FCHEB, the FC output power is determined. This EMS is executed every second.

To ensure the correct operation of the buses, in the last step the operation constraints are applied. In the case of the P-HEB, the constraints shown in Eq. 3.4 are applied.

As regards the FCHEB, the constraints shown in Eq. 3.7 have been defined for a safe operation.

3.4 EMS Evaluation in a Plug-in Hybrid Electric Bus Case-Scenario

In this section, the developed and previously presented vehicle level EMS is evaluated for a P-HEB application. This evaluation has been carried out for the P-HEB with LTO BT (with characteristics described in Tab. 2.2), driving on route 4, which is depicted in Fig. 3.5.

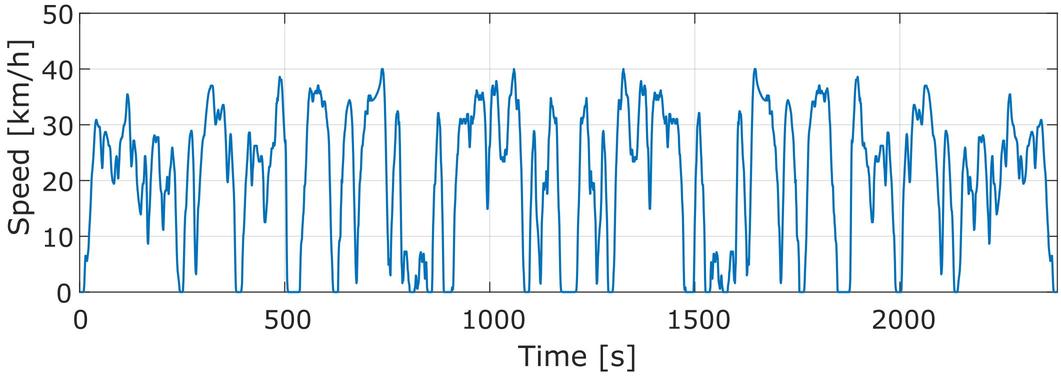

Figure 3.5: Route 4 speed profile.

In the subsequent first subsection, the learning based EMS offline design process is carried out. The optimized DP operation for the different auxiliary consumptions is used as data-set for the ANFIS technique. The ANFIS based training and testing for the aforementioned route are analyzed.

The designed ANFIS based EMS based on the offline learning based approach has been validated at simulation level in Matlab and experimentally in a HIL platform. The simulations and emulations have been performed in a core i7-6600 CPU with 2.60 GHz and 2.80 GHz with 8 GB of RAM memory computer.

3.4.1 Learning based Energy Management Strategy Evaluation

A data-base has been generated applying the DP optimization for route 4 and obtaining the optimal profiles for the following variables: power demand, BT SOC and output GS power. In addition to these optimized variables, the length-ratio is used as a reference in the training process.

The obtained optimal profiles for the 16 kW mean auxiliary consumption case are shown in Fig. 3.6. The length-ratio splits the optimized data into data-sets and it is used as an input variable to identify the bus placement at every sample time. The power demand and BT SOC are the other two inputs that compose the data-base. The output variable is the GS output power, the variable that determines the split factor of the P-HEB.

With the same approach applied for the 16 kW auxiliary consumption, the

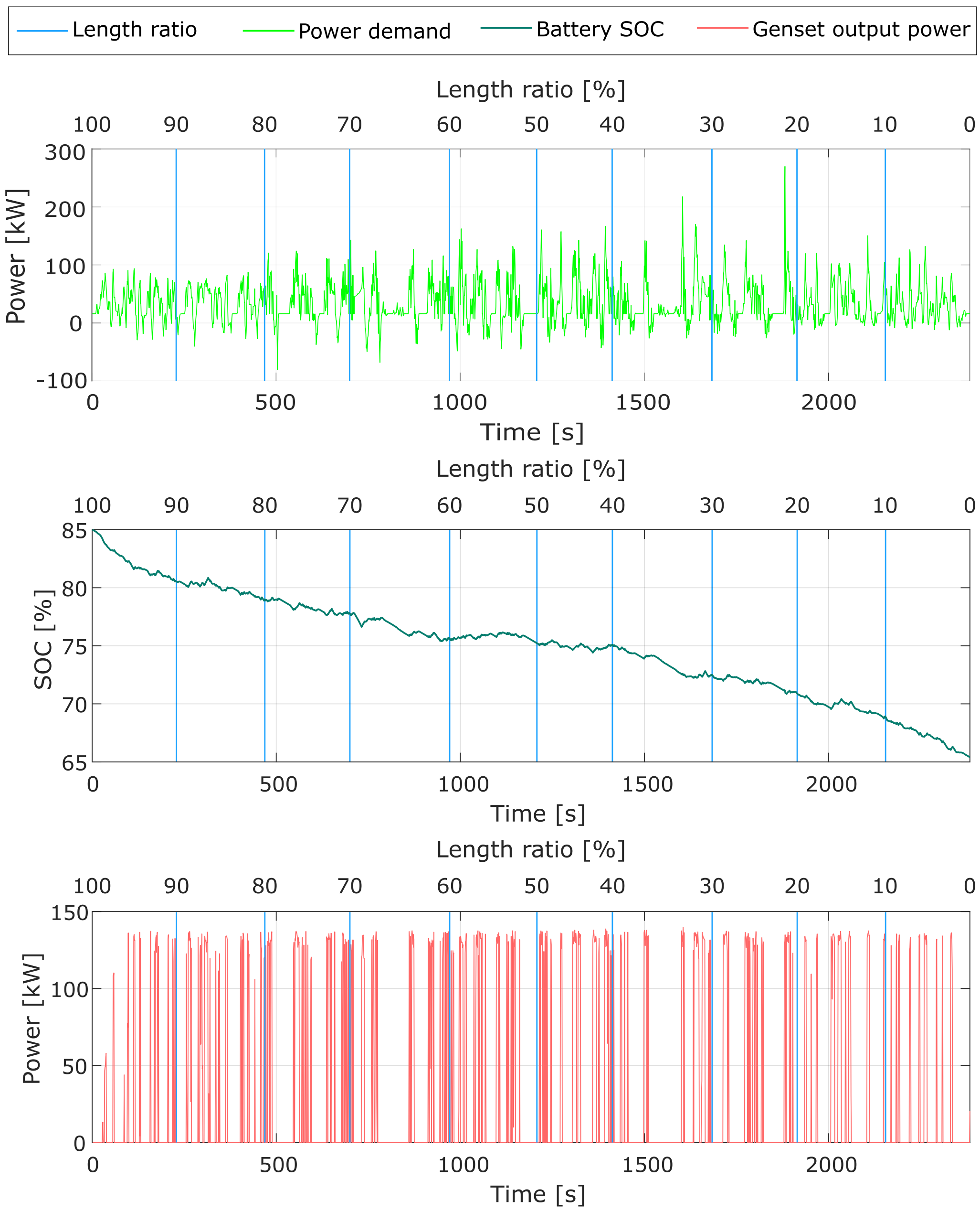

Figure 3.6: Route 4 with 16 kW mean auxiliary consumption: power demand, BT SOC and GS power output profiles, all split by the length-ratio.

complete data-base is generated with the optimal operation of 7 optimizations, for different mean auxiliary consumptions. The mean auxiliary consumptions are comprised between the minimum and the maximum auxiliary consumptions, 12 kW and 18 kW respectively.

Therefore, the example of the optimization process shown in Fig. 3.6 is repeated for the 7 mean auxiliary consumptions. From this optimization, 7 optimized SOC profiles, power demands and output GS powers are obtained, for the 7 mean auxiliary consumptions. The length-ratios is used as a reference in all variables. These 7 optimizations conform the previously stated data-base.The obtained 7 optimal SOC profiles are shown in Fig. 3.7. They are actually used as a reference when evaluating the developed EMS accuracy.

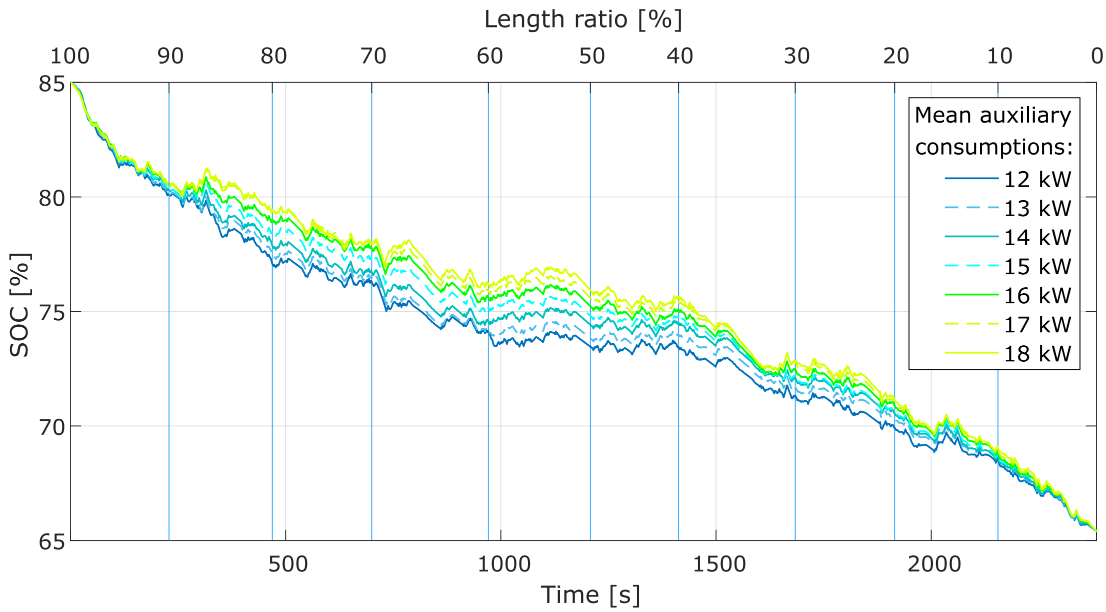

Figure 3.7: DP optimized SOC profiles for different auxiliary consumptions.

Once the data-base is generated, the data-sets have to be determined. For this decision, the amount of data for each 10% length-ratio step is analyzed. For the present case study, the total amount of data reaches 16,688 data points. In Tab. 3.1, the amount of data for each data set is given in the second column. It is noteworthy that the data is homogenized for all the data-sets. When the data-sets are determined, the ANFIS based EMS is designed based on the training and testing process of the ANFIS learning technique. For this, from the divided data-sets, part of the data is used for the training process (around 80%) and the rest is used for test (around the 20%). The way to evaluate the training and testing process is by means of the Root Mean Square Error (RMSE), calculated as follows:

$$RMSE = \sqrt{\frac{1}{n}\sum_{i-1}^{n}(y_i - \tilde{y}_i)^2} = \sqrt{MSE} = \sqrt{\frac{1}{n}\sum_{i-1}^{n}(P_{GSout}(k) - P_{GStarget}(k))^2} \quad (3.13)$$

where n stands for the number of training epochs, $P_{GSout}(k)$ is the obtained GS power and $P_{GStarget}(k)$ is the GS power training target.

Table 3.1: Training, testing and data errors.

Length	**All Data**	**Training Data**		**Testing Data**	
Ratio [%]	**Data**	**Data**	**RMSE**	**Data**	**RMSE**
[100-90)	1,603	1,336	0.035	267	0.059
[90-80)	1,680	1,400	0.029	280	0.043
[80-70)	1,617	1,348	0.015	269	0.028
[70-60)	1,897	1,581	0.018	316	0.028
[60-50)	1,659	1,383	0.023	276	0.031
[50-40)	1,435	1,196	0.010	239	0.050
[40-30)	1,897	1,581	0.040	316	0.052
[30-20)	1,617	1,348	0.016	269	0.041
[20-10)	1,680	1,400	0.011	280	0.014
[10-0)	1,603	1,336	0.029	267	0.040

Regarding the EMS evaluation, as it has been aforementioned, most of the data is used for the training process. The RMSE evaluation shows a higher error for the testing than for the training, as shown in Tab. 3.1. This is a regular result in the training and testing that indicates that the training overfitting is avoided. The obtained trained FL structures are shown in Appendix B for this particular case study as example of the length-ratio from 100% to 90%.

With the aim of validating the developed ANFIS based EMS accuracy, a Matlab simulation has been performed. The achieved improvement and the ability to replicate DP operation applying the ANFIS based EMS has been evaluated for the different existing mean auxiliary consumptions. On the one hand, the proposed EMS has been compared with the DP global optimization results to benchmark the ANFIS based EMS. On the other hand, it has been compared with the Charge-Depleting Charge-Sustaining (CD-CS) EMS to show the achieved improvement compared with a commercially and non-advanced solution.

The obtained fuel consumptions with the mentioned 3 approaches (ANFIS based EMS, DP optimization and CD-CS) are shown in Tab. 3.2. It should be noted that for the 7 auxiliary consumption the ANFIS based EMS has the same behavior in terms of fuel consumption, remaining higher that the DP optimization and lower than the CD-CS EMS.

The obtained difference from the DP optimization to the proposed ANFIS EMS approach is within the range of 7.14-10.99 %. At this point, it is worth mentioning that the obtained results in terms of fuel consumption with the ANFIS based EMS are really close to the DP optimal fuel consumption. Regarding the percentage decrease comparing the CD-CS EMS and the ANFIS EMS, it ranges from 5.25 % up to 6.86 %. This evaluation justifies the range of improvement at vehicle level for all the mean auxiliary consumption applying the ANFIS, proving the stability to reach fuel consumption minimization compared with the CD-CS EMS.

Table 3.2: Fuel efficiency technical evaluation of route 4 with all the possible auxiliary consumptions.

Mean Auxiliary consumption [kW]	**fuel consumption [l/100 km]**			**DP**	**ANFIS vs**
	DP optimization	**ANFIS based EMS**	**CD-CS EMS**	**Error [%]**	**CD-CS diFF. [%]**
12	30.48	33.83	36.32	10.99	6.86
13	31.82	34.82	37.07	9.43	6.07
14	33.17	36.66	38.20	10.52	4.03
15	34.50	37.54	39.66	8.81	5.35
16	35.85	38.81	40.96	8.26	5.25
17	37.16	40.05	42.56	7.78	5.90
18	38.49	41.24	43.63	7.14	5.48

In addition to the obtained fuel consumption minimization results shown in Tab. 3.2, a power demand and split analysis for the 16 kW auxiliary consumption has been performed. First, the P-HEB ANFIS based EMS management power split between the BT and GS has been analyzed and depicted in Fig. 3.8. It is important to highlight that the at some points GS provides higher power than the required for fulfilling the power demand. This behavior is due to the highest efficiency at high powers. The power exceed is used to recharge the BT. Regarding the BT behavior, it covers the lowest power demands and helps the GS to fulfill the demand when it is too high to be provided only by the GS.

With the aim of evaluating the capability of the ANFIS based EMS to follow the optimized GS output power and obtained optimal SOC by the DP profile,

The capability of the ANFIS based EMS to follow the optimized GS output power and BT SOC has been analyzed in route 4 with a mean auxiliary consumption of 16 kW. This analysis aims to evaluate the trained and tested

Figure 3.8: Power demand split between the BT and GS.

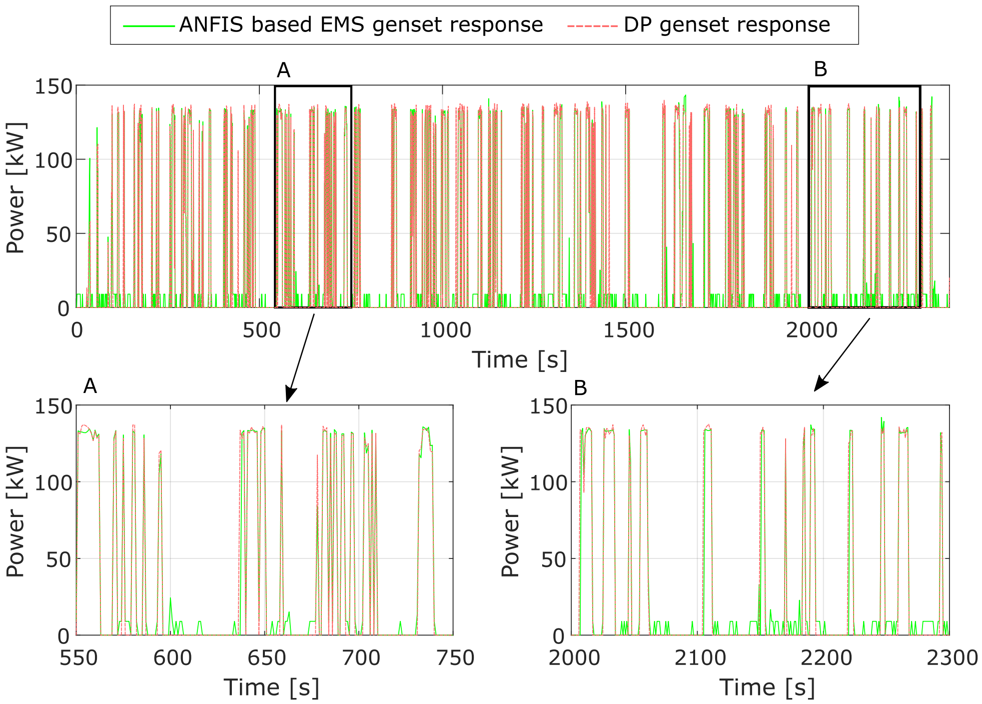

Figure 3.9: GS output power response for the DP optimization and for the ANFIS EMS.

rules and membership functions behavior.

The obtained GS output response of the ANFIS based EMS compared to the DP optimization is shown in Fig. 3.9. In this figure two zooms have been done (Fig. 3.9 A and B) to evaluate in an easier way. It is worth noting that the achieved GS output power with the ANFIS based EMS replicates the DP optimization over all the route. This replication behavior allows to reach a similar fuel consumption compared to the DP optimization.

The SOC profile comparison is another key point to check the developed EMS capability of replicating the DP operation. In Fig. 3.10, the obtained DP SOC profile compared to the ANFIS EMS with the obtained error are shown. The achieved similar behaviors between the DP and ANFIS EMSs, as shown in Fig. 3.10. The obtained maximum error difference has been up to 0.41 % with a mean error of -0.048 %.

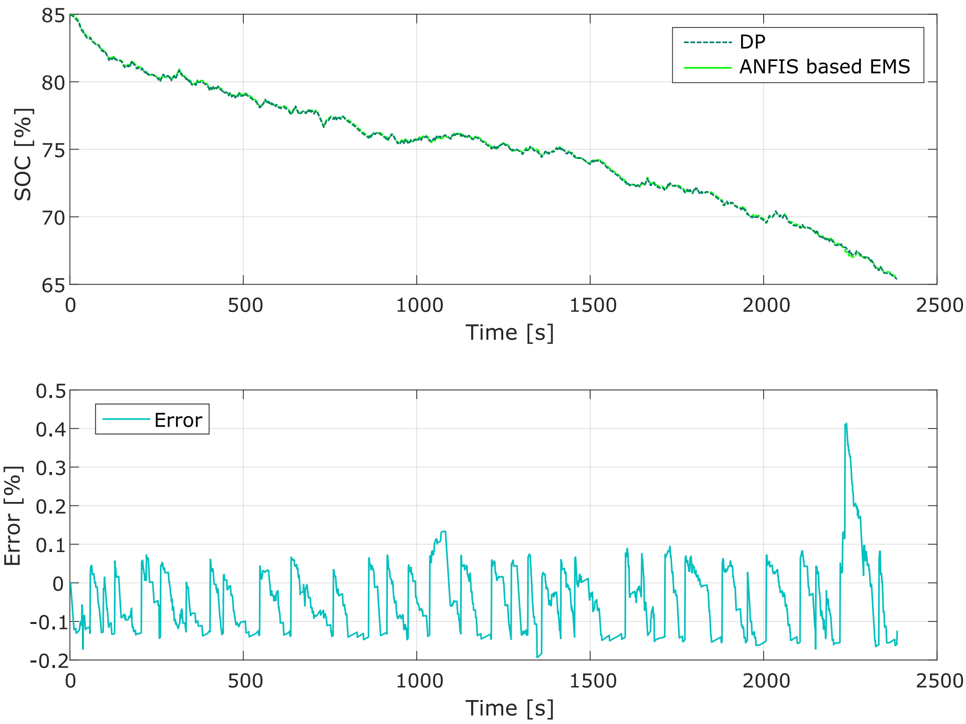

Figure 3.10: DP SOC profile compared to ANFIS based EMS and error.

3.4.2 Real-Time experimental validation of the Learning based Energy Management Strategy

The objective of this subsection is to present the validation results that demonstrate that the developed fuzzy-logic based EMS are implementable and can be executed in real-time, which is crucial for its future application in real vehicle [145]. The direct implementation and validation of the EMS at bus level is a costly and time consuming process. HIL approach is an intermediate step in the implementation and validation process between the simulation and the real application [58]. The HIL platform allows to validate the EMS implemented into a Management Unit, operating the emulated P-HEB power flows in real-time.

The developed HIL platform [58] allows a flexible and reduced cost experimental validation [146]. The power flows on the 700 V DC busbar of the powertrain of the considered P-HEB are emulated and controlled by the Emulation Unit in the HIL platform, as shown in Fig. 3.11. This emulation allows to validate the proposed learning based EMS implemented in the Management Unit in real-time, before the integration in the bus, as an intermediate step.

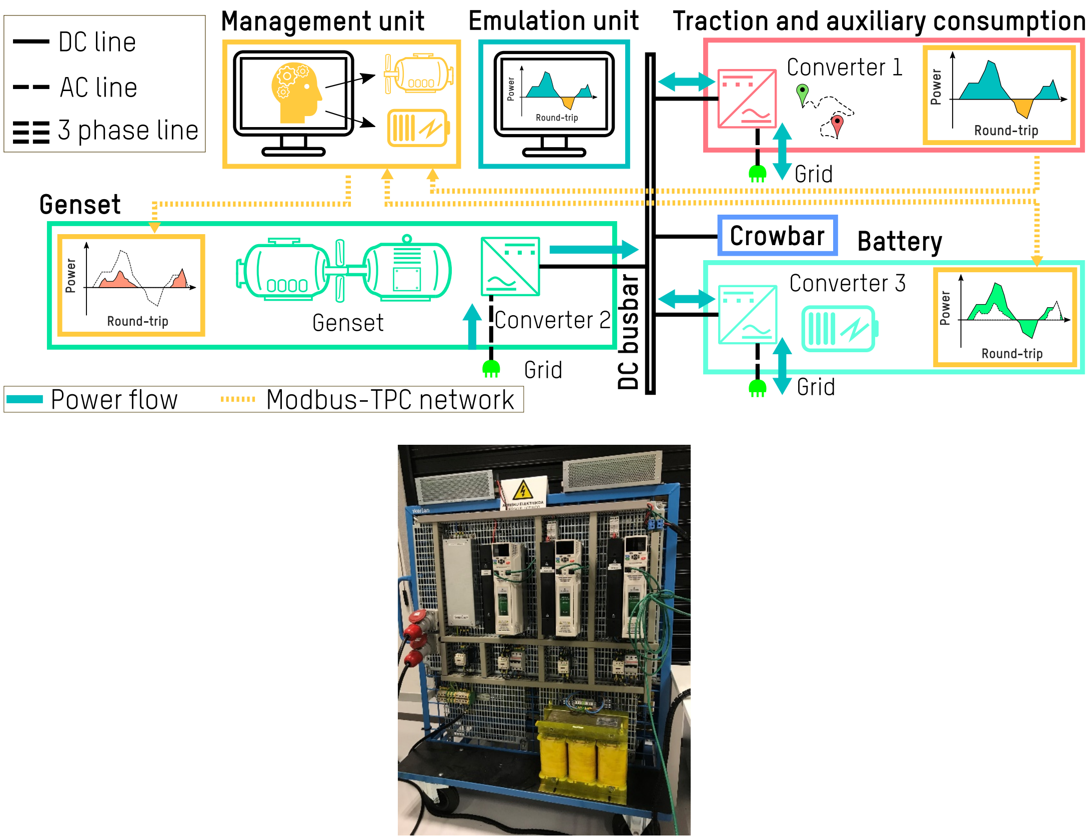

Figure 3.11: Architecture of the HIL platform (up) and picture of the test-bench (down).

The developed HIL is composed of scaled converters up to 18 kW, 700 V DC bus and a crowbar, shown in Fig. 3.11. The traction and auxiliary consumption power demands are emulated with converter 1. Regarding the power components, the GS is emulated by converter 2 and the BT is emulated with converter 3, configured to inject and absorb power to/from the DC busbar. It is the only converter configured in voltage control mode in order to maintain constant the voltage in the DC busbar. With the aim of carrying out the power sources management in real-time, the developed FL EMS has been implemented into the Management Unit.

The system power request in the DC busbar is determined according to the power calculation from the driving profile in Fig. 3.5 and the auxiliary consumption. This information is processed by the Emulation Unit that is communicated with the power components based on a communication network under MODBUS TCP/IP protocol.

The previously described EMS, implemented in the Management unit, determines the GS and BT power split factor according to the current power demand, length-ratio and SOC of the BT. The power demand information flow is communicated via TCP/IP protocol to the GS and BT, with the aim of fulfilling the traction and auxiliary consumption power demand.

For performing the emulations a core i7-6600 CPU with 2.60 GHz and 2.80 GHz with 8 GB of RAM memory computer has been used, where the management and emulation units have been implemented.

3.4.2.1 Learning Based Energy Management Strategy Real-Time Validation

The emulated bus has been the aforementioned P-HEB with 16 kW auxiliary consumption, running on the described route 4.

For describing the power behavior with the proposed EMS approach, two time frames have been chosen and zoomed from the whole round-trip, as shown in Fig. 3.12 and 3.13. It is worth noting that the provided power with the GS is above the demanded power when the power demand is high, as shown in Fig. 3.12. The ICE best efficiency is given at high power rates. Therefore, the DP optimization and consequently the ANFIS based EMS replicates this behavior. The GS use is divided optimally within the whole round-trip. Please take note that it is assumed that the GS withstands the required power dynamics.

Regarding the battery power, it fulfills the power demand when the demand is low. In addition, the BT provides the required power peaks that the GS is not able to fulfill.

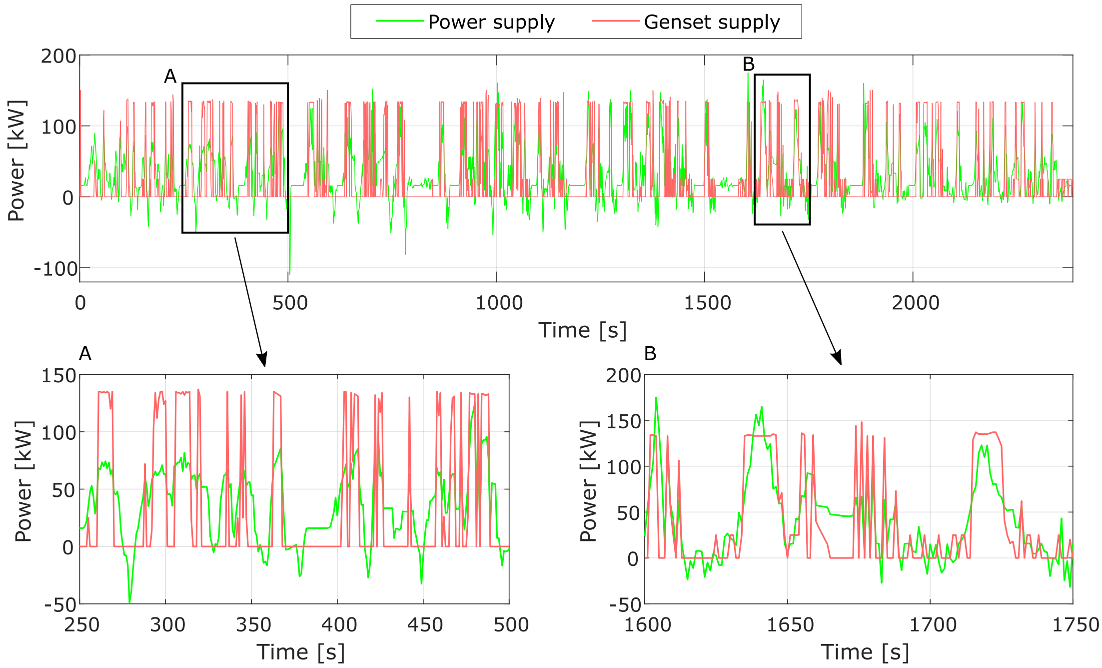

Figure 3.12: Power demand and provided power with the GS using the ANFIS based EMS experimental results.

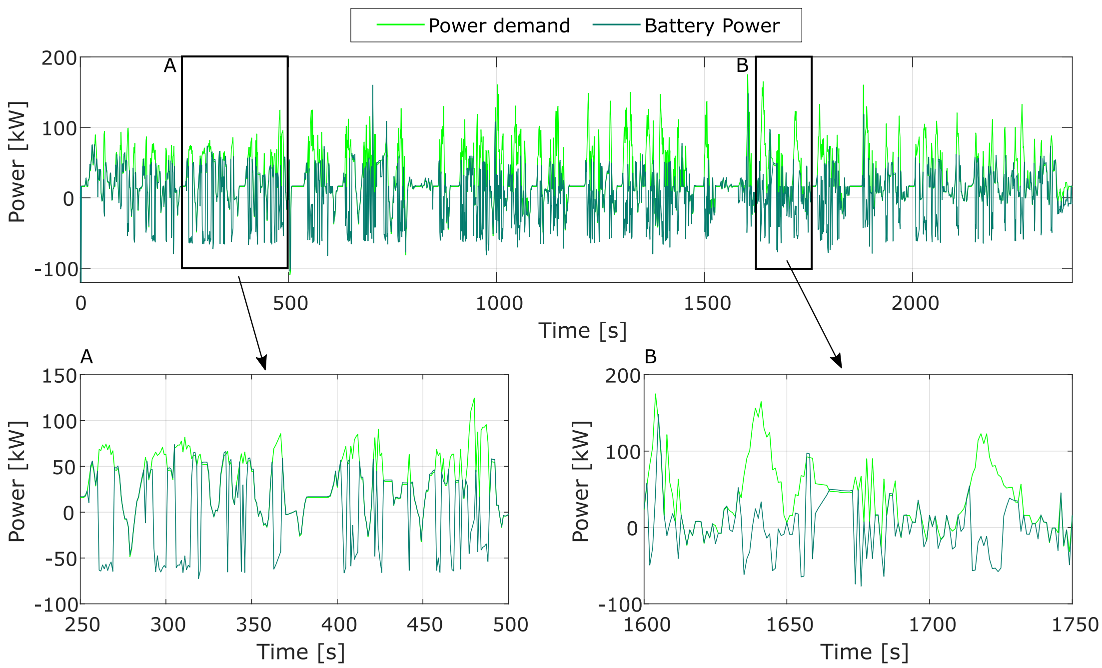

Figure 3.13: Power demand and provided power with the battery using the ANFIS based EMS experimental results.

3.4.2.2 Learning Based Energy Management Strategy Experimental Comparison

For further analyzing the ANFIS based EMS, the obtained results have been compared with the DP optimization results and with the experimental results obtained with a CD-CS EMS. This comparison allows to evaluate the effectiveness of the ANFIS based EMS and its improvement range compared to the conventional EMS solutions.

Firstly, SOC profile is compared with the one obtained with the DP optimization. As it is observed in Fig. 3.14, the proposed EMS follows the DP optimization SOC profile with a mean error of 0.14 %, due to the energy demand difference between the optimization and emulation. The maximum obtained error has been up to 1.06 %. It should be emphasized that the DP optimization and the developed ANFIS based EMS discharge the BT around all the round trip.

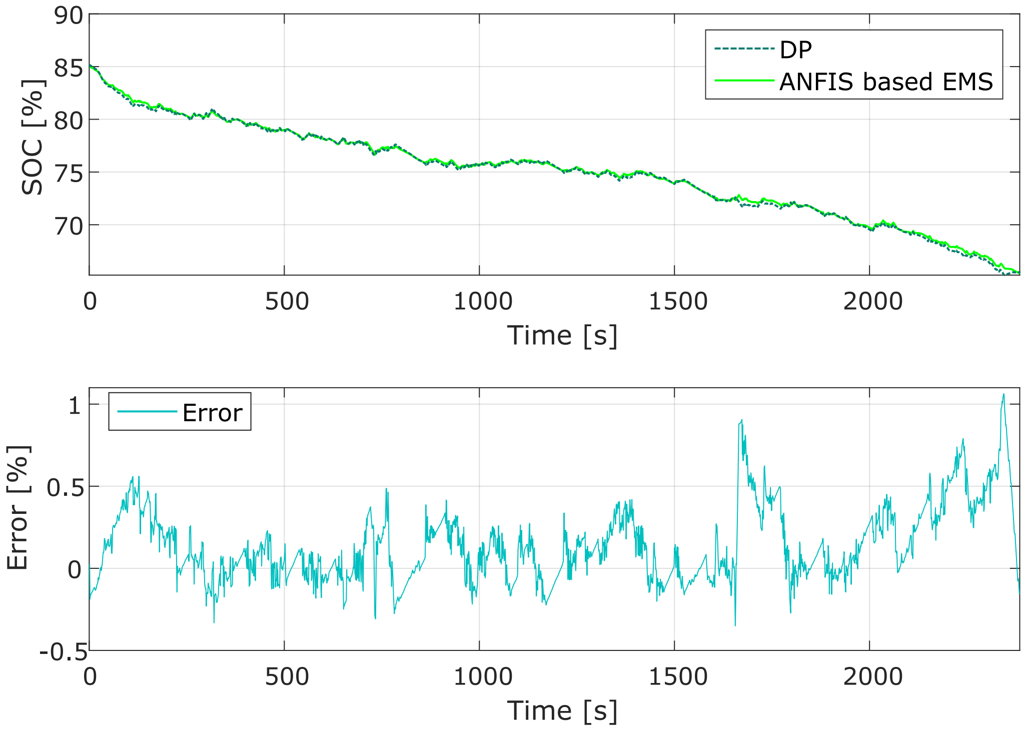

Figure 3.14: Battery SOC profile (up) and error (down) for the DP optimization and ANFIS EMS experimental results.

Regarding the GS utilization within the DP and ANFIS based EMS comparison, in Fig. 3.15, two time frames have been chosen, to compare and evaluate. The GS utilization among the route is replicated closely to the optimal operation. This behavior allows also to replicate the SOC depletion, as shown in

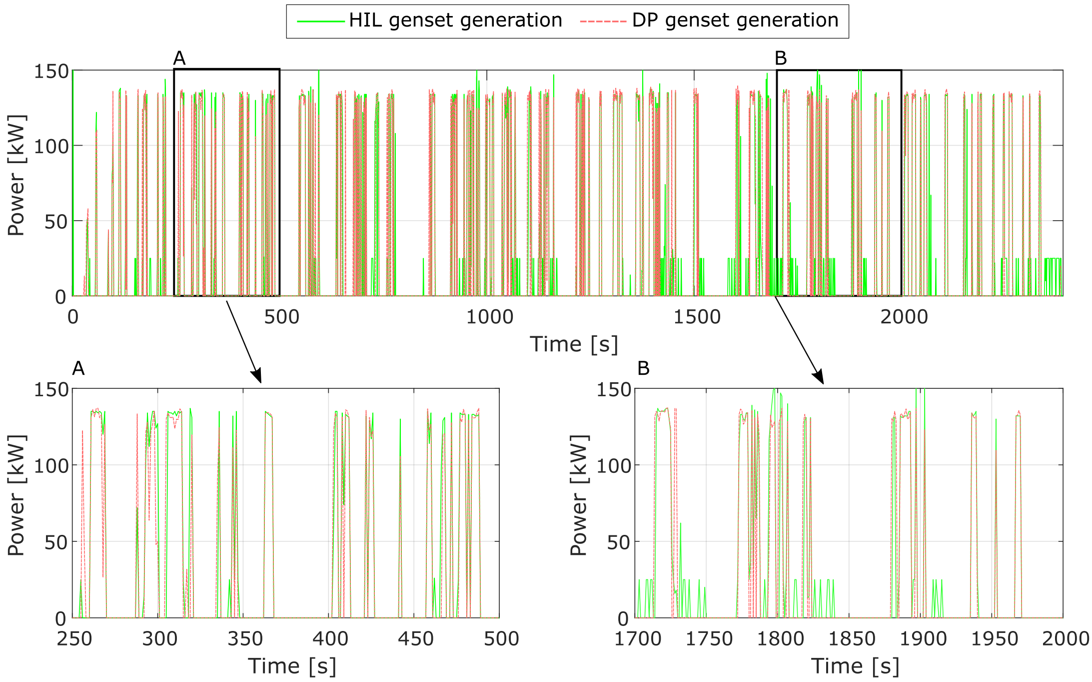

Figure 3.15: GS power operation of the ANFIS based EMS experimental results compared to the DP optimal operation.

Fig. 3.14.

With reference to the CD-CS EMS, this EMS uses the BT until the minimum SOC target is reached. After reaching the minimum SOC, all the power demand is provided by the GS and the SOC is sustained, as shown in Fig. 3.16.

Finally, the power sources behavior has been analyzed, applying the CD-CS, which results are depicted in Figs. 3.17 and 3.18. In the first part, the P-HEB is driven in BT depleting mode and in the last part with the GS in charge sustaining mode. It may be noted that the reduced BT power demands in the CD-CS, as it is used just for covering the power demand.

The obtained results for the ANFIS based EMS and CD-CS EMS have been analyzed in terms of fuel consumption and then compared to DP. The obtained fuel consumption with DP global optimization has been of 35.85 l/100km. Compared to the ANFIS based EMS, which offers a consumption of 38.61 l/100km, a difference of 7.41 % has been obtained.

Finally, it may be noted that the proposed approach decreases the fuel consumption of 7.3% compared to the CD-CS strategy. The experimentally obtained fuel consumption value in the HIL platform, has been 41.65 l/100km, calculated based on the GS efficiency maps.

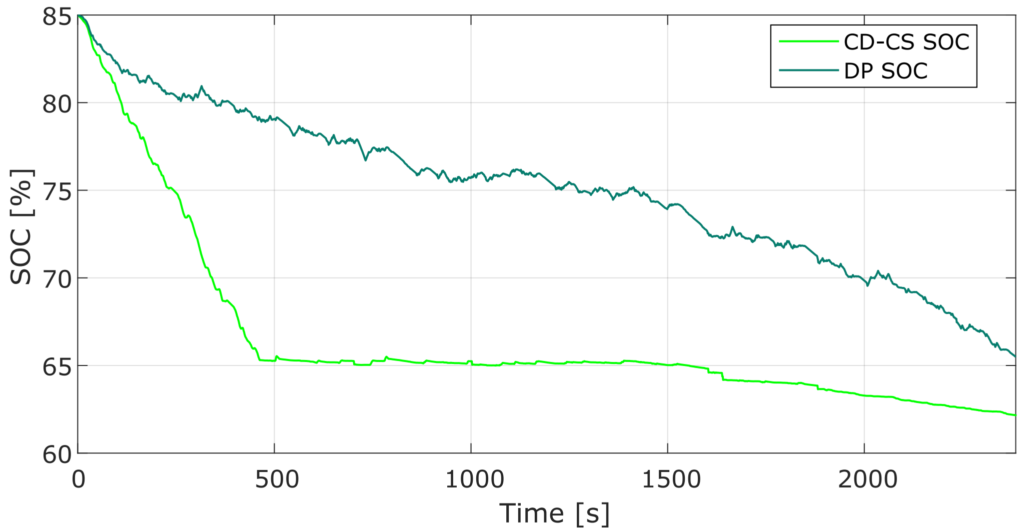

Figure 3.16: Battery SOC profile for the CD-CS EMS experimental results with the DP optimal solution.

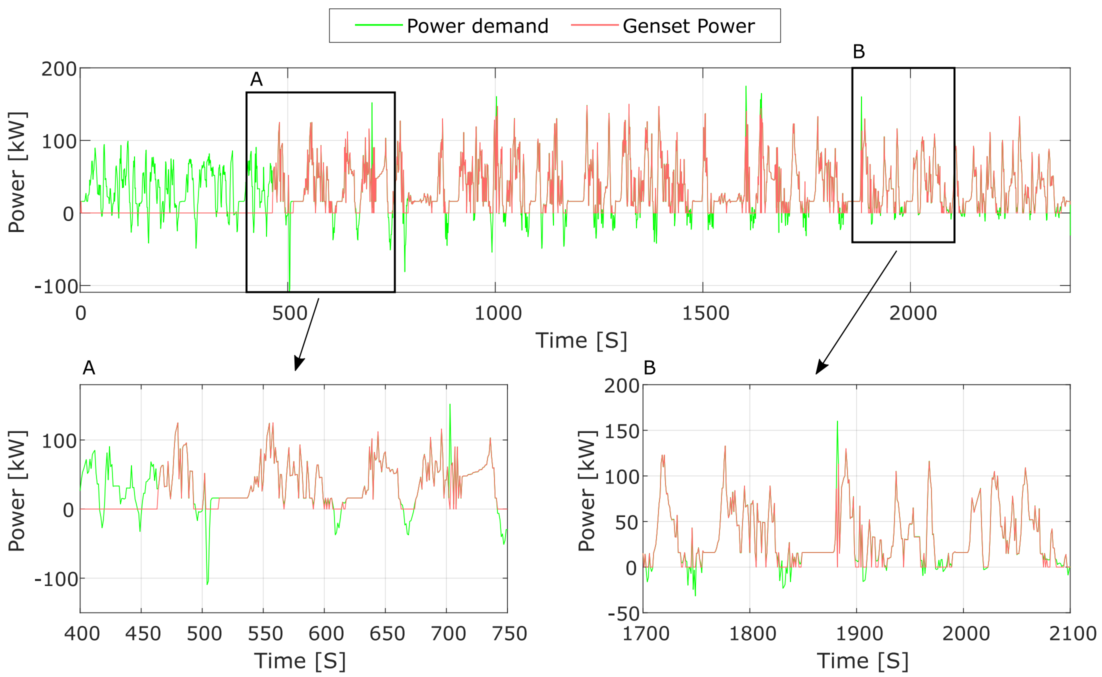

Figure 3.17: Experimentally obtained power demand and GS power for the CD-CS experimental results.

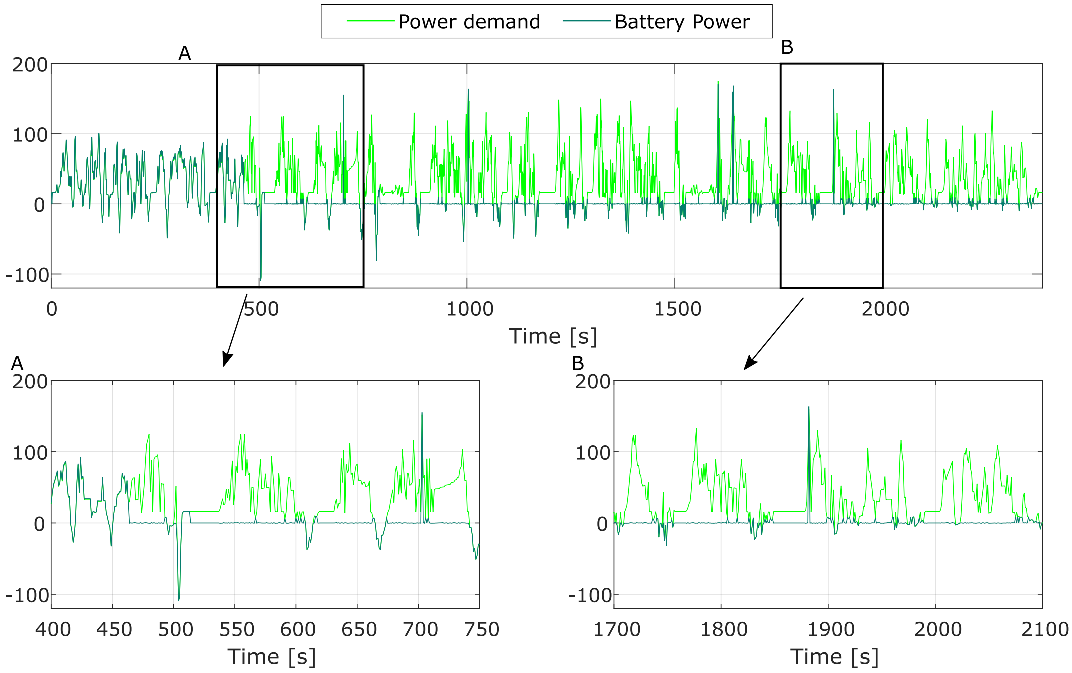

Figure 3.18: Power demand and provided power with the BT for the CD-CS EMS experimental results.

3.5 EMS Replication and Evaluation in a Fuel Cell Hybrid Electric Bus Case-Scenario

The objective of this section is to replicate the proposed ANFIS based EMS for a parallel FCHEB considering the parameters listed in 2.4, as shown in Fig. 3.19. As it has been aforementioned in Sec. 1.5.2.2, the advances in P-HEBs in terms of EMS, as the topologies and degrees of freedom are similar and directly applicable on FCHEBs.

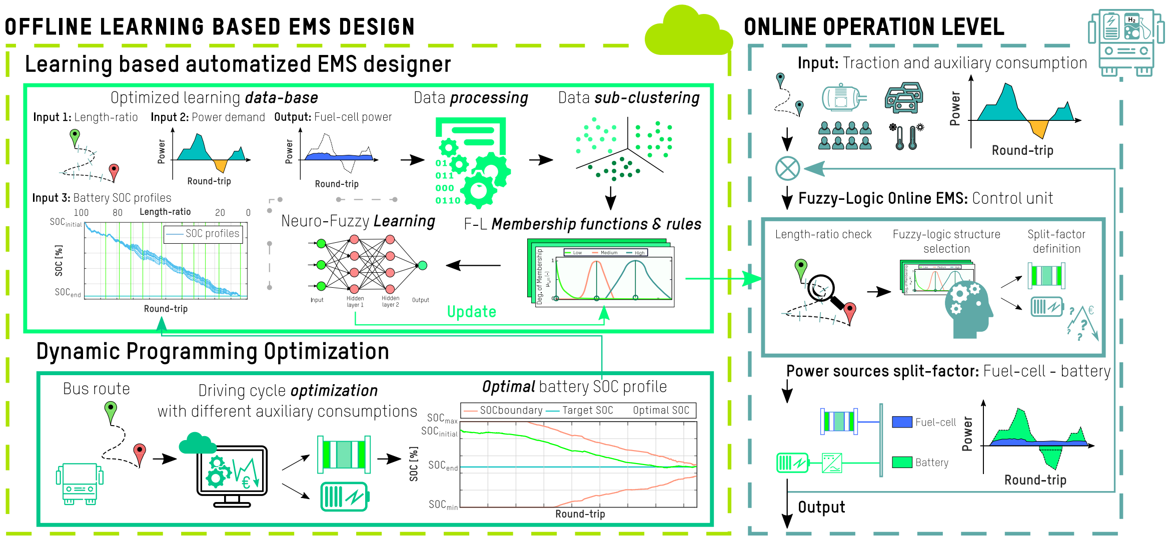

Figure 3.19: Energy management strategy design and operation for FCHEB.

The EMS replication has been tested in two scenarios. The first scenario has been performed with route 4 with a mean auxiliary consumption of 16 kW. The evaluation of the same scenario allows to directly compare both topologies in techno-economic terms. Therefore, a technical analysis for the FCHEB powertrain is carried out. In addition to that, a TCO comparison of the P-HEB and FCHEB with different market penetration hydrogen costs is performed, to evaluate the viability of the FCHEB.

With the aim of validating a route for which the data-sets have to be adjusted and homogenized, as a second case study, applying route 1, has been studied. This route's speed profile is shown in Fig. 3.20. For this case study, all the possible mean auxiliary consumptions from 8 kW to 16 kW have been evaluated.

The EMS has been applied with a step of 1 second.

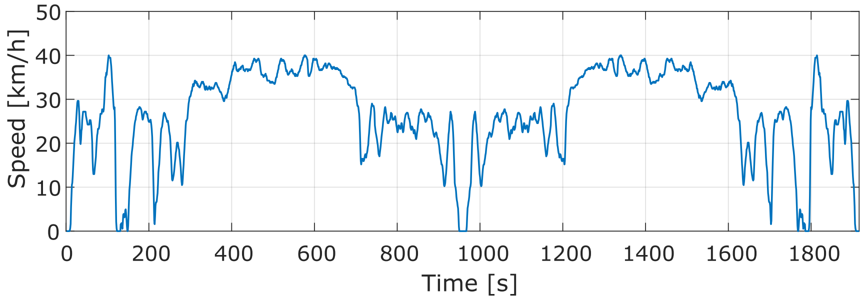

Figure 3.20: Route 1 speed profile.

3.5.1 FCHEB technical evaluation and TCO comparison

The first FCHEB case study has been carried out, considering route 4. The developed ANFIS based EMS has been evaluated in technical and economic terms with the results of the FCHEB in different hydrogen price scenarios. These results have been compared and comparing them with the P-HEB in Subsec. 3.4.1.

Beginning with the power demand split analysis between the available sources, the obtained FC and BT power demands are together shown in Fig. 3.21. Owing to the slower dynamics of the FCs, the power provided by the FC has a constant behavior, avoiding to be switched-off. Since the BT chemistry is LTO with high c-rates, it provides the power peaks. It is noteworthy the FC power increases with the aim of fulfilling the highest power demand, maintaining the OER within the determined operation levels, which is further explained below.

Following with the OER analysis, a comparison between the optimized DP operation and ANFIS based EMS results are shown in Fig. 3.22 A and B respectively. The DP optimization is managed to maintain the OER within the determined limits during the entire the route. On the contrary, in the ANFIS based EMS, as shown in Fig. 3.22, 3 points are below 1, reaching the 0 value. The FC operates outside the operating range 3 seconds in total. The obtained mean OER values for the DP optimization and ANFIS based EMS respectively are 1.75 and 1.74, both within the operation range.

The obtained SOC profile with the ANFIS based EMS replication of the DP optimal SOC profile is evaluated in Fig. 3.23. The evaluation has been done together with the obtained error, got from the comparison with the DP SOC profile as baseline. It is important to highlight the high error at the beginning of the route. These are the points where the OER dropped to the 0 value. The behavior of the ANFIS based EMS tries to correct and match the optimal SOC profile providing three power peaks at the starting point as it has been examined

Figure 3.21: ANFIS based EMS power demand split between the BT (up) and the FC (down).

in the power provided by the FC in Fig. 3.21. The SOC correction is reached along the route. After this deviation, the SOC profile is corrected and the error is minimized. The highest error is 0.738% when the main deviation occurs at the beginning of the route. The obtained mean error is 0.055%.

This behavior is further analyzed in the SOC analysis.

To further validate the ANFIS based EMS, the FC current response has been analyzed. As examined before, it should be emphasized the higher deviation at the beginning of the route, as shown in Fig. 3.24. A zoom has been done in Fig. 3.24 A, to analyze the FC power deviation. The power provided by the FC managed by the ANFIS based EMS is above the optimized one. This behavior occurs when the developed EMS mismatches an input data and gives the wrong FC power response. Once the DP obtained optimal SOC profile is stabilized, the FC power replication accuracy is improved. In a second zoom in Fig. 3.24 B, the developed ANFIS based EMS replicates the DP optimization FC power.

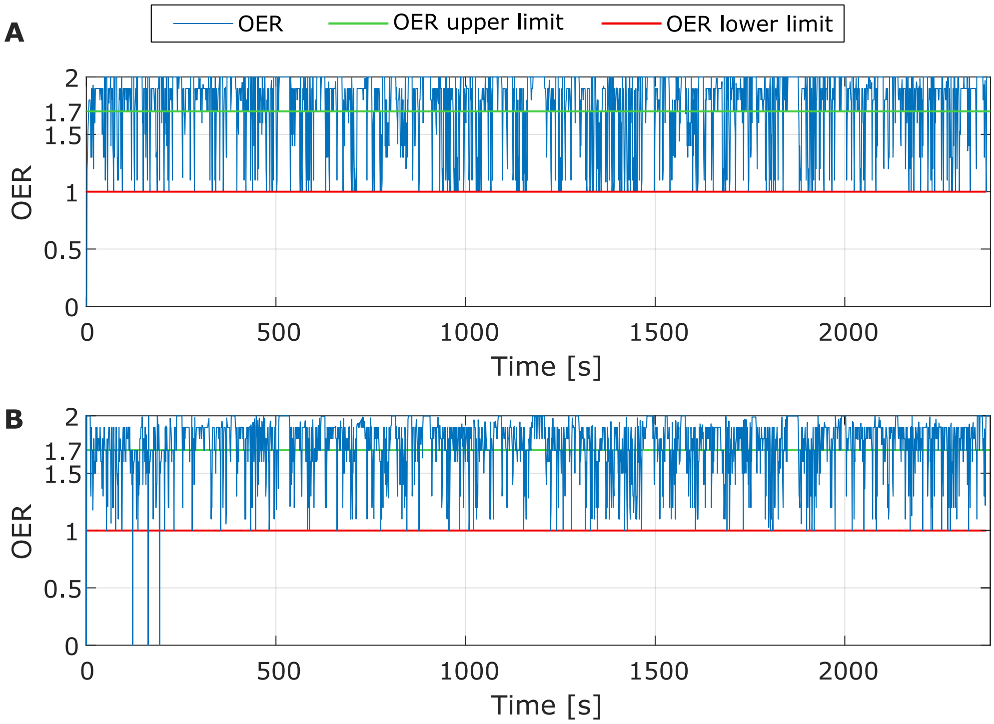

Figure 3.22: OER graphical result for the **A** DP optimization and **B** for the ANFIS based EMS.

Finally, once the technical side has been evaluated, a TCO comparison between the P-HEB and FCHEB in route 4 has been performed. Regarding the BT cost for the P-HEB and FCHEB with LTO BT, the medium cost scenario has been analyzed (1000€$/kWh$). Regarding the hydrogen cost, 5 different cost scenarios have been analyzed, to evaluate FCHEB readiness and competitiveness level. The first 4 scenarios of hydrogen costs have been determined according to the market penetration level, studying the 1%, 10%, 30% and 75% hydrogen technology penetration levels. The last studied scenario has been set to the ideal price as documented in [13].

The TCO comparison results are shown in Fig. 3.25. The P-HEB TCO has been taken as a baseline to directly compare the viability of the FCHEB. The current scenario with a 1% hydrogen market penetration is far from being a viable solution. Indeed, the FCHEB solution is 59.68% more expensive than the P-HEB solution. As the hydrogen price decreases with the increasing hydrogen market penetration, the margin between the P-HEB and the FCHEB reduces, until the 75% of market penetration is reached. Below this point, the FCHEB is a cheaper solution compared to the P-HEB. The ideal hydrogen cost scenario at 5€$/kg$ shows the FCHEB as an attractive solution, being 15.34% less expensive than the

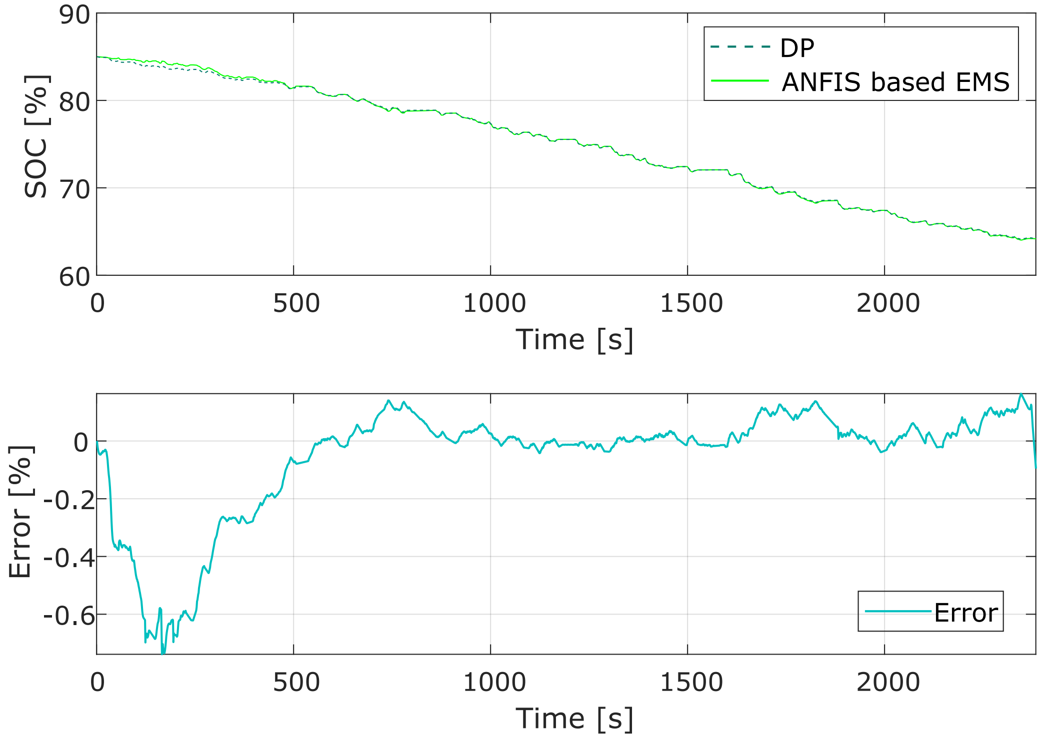

Figure 3.23: DP SOC profile compared to ANFIS based EMS (up) and error (down).

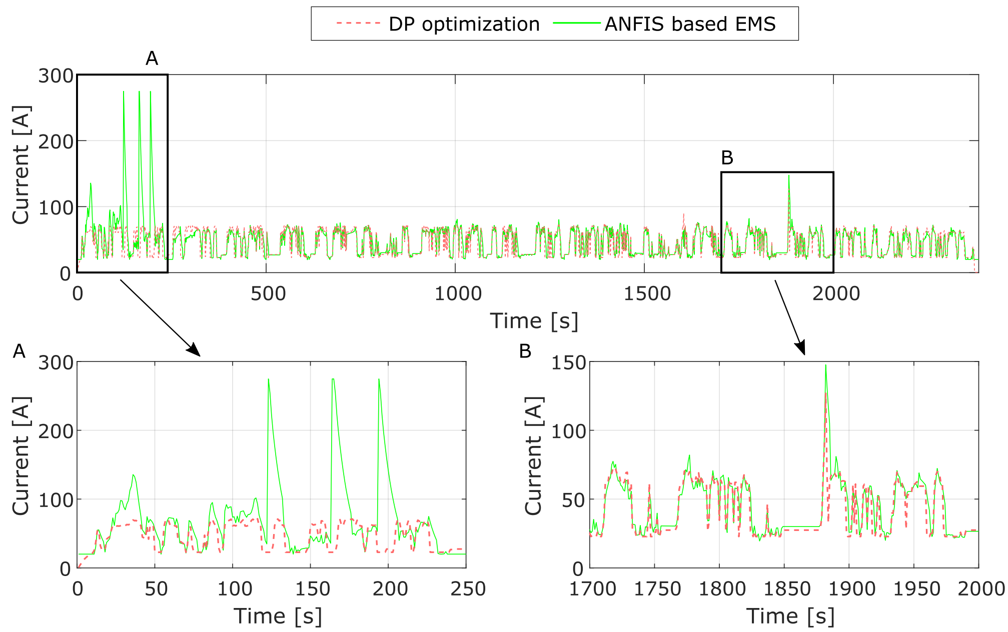

Figure 3.24: fuel-cells current response for the DP optimization and for the ANFIS based EMS.

P-HEB solution. The obtained results have been compared to the study in [13], confirming the feasibility of FCHEBs at 6€/kg.

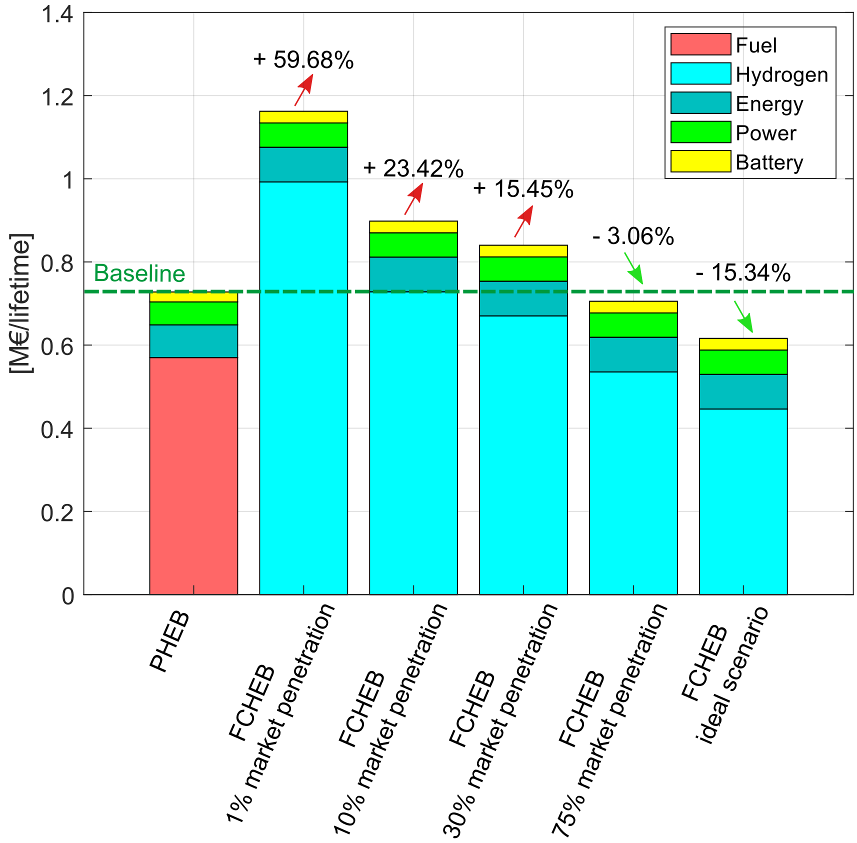

Figure 3.25: TCO comparison in route 4 for the PHEB and FCHEB.

3.5.2 FCHEB ANFIS based EMS Evaluation

A second FCHEB case study has been performed in route 1. This driving cycle is shown in Fig. 3.20. This additional case study has been chosen, due to the particularity of the number of data-sets. This situation is given when the route speed profile is composed of urban and extra-urban cycles (see routes 1, 2, 5 and 9). There, the amount of data is larger at low speeds, hence the 10 % of the length-ratio is larger in time than the cycle parts at high speeds. In this case, the amount of data in each data-set has been homogenized, splitting into 2 steps of 5 % length-ratio the initially considered 10 % steps length-ratio.

For this particular route 1, an example for the 16 kW mean auxiliary consumption DP optimal operation is shown in Fig. 3.26. It is is important to stress that in this route, the length-ratio is split into 14 data-sets. In this case, the data-base is composed of the power demand, BT SOC and length-ratio inputs and the FC power as output.

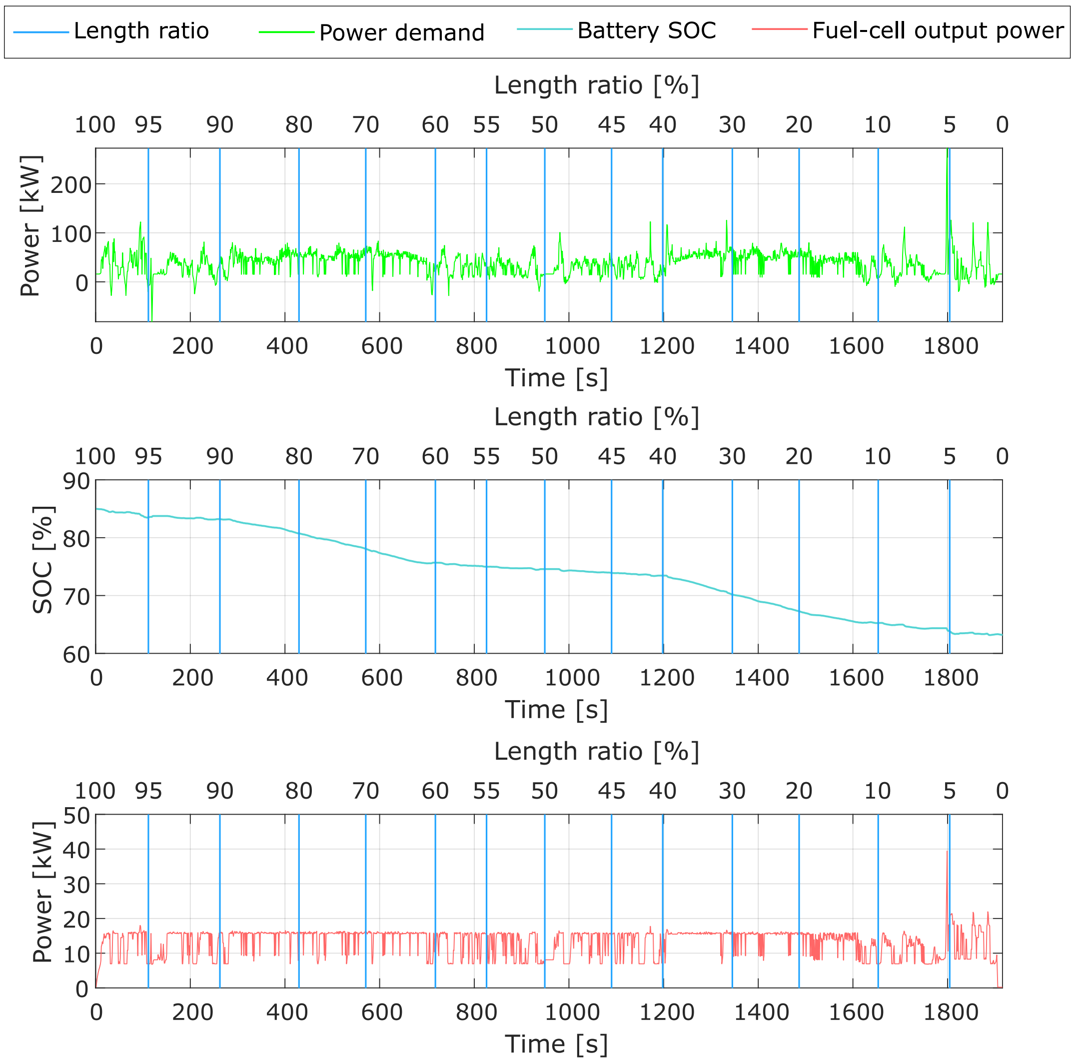

Figure 3.26: Route 1 with 16 kW mean auxiliary consumption: power demand, BT SOC and FC output power profiles, all split by the length-ratio.

This particular optimization case for the 16 kW mean auxiliary consumption has been replicated for all the mean auxiliary consumptions between the minimum and the maximum value, 8 kW and 16 kW respectively, with a power step of 1 kW. A total of 9 optimizations have been performed and data-base has been built. In Fig. 3.27, the obtained optimal operation SOC trajectories for different mean auxiliary consumptions are shown. The initial SOC has been set at the same level, i.e., 85%, and the final SOC has been calculated for fulfilling the charging features following the process explained in Subsec. 3.2.1.

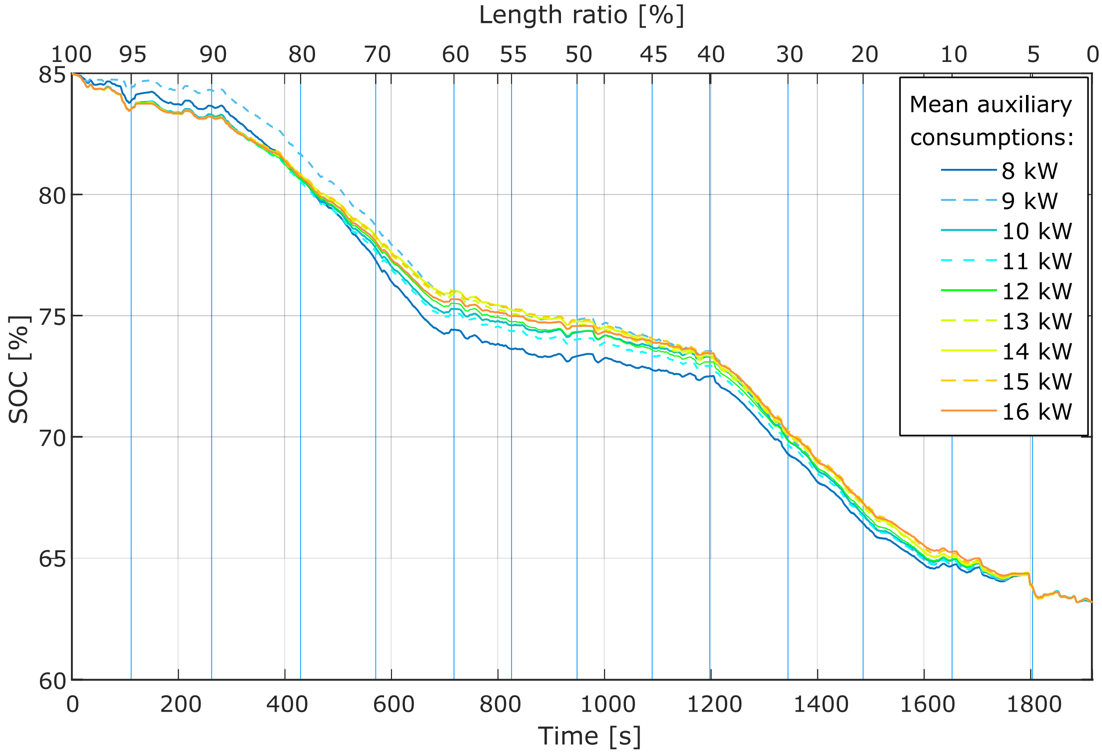

Figure 3.27: DP optimized SOC profiles for different auxiliary consumptions.

For the training data preparation, based on the length-ratio, a first approach of 10% steps was defined to divide the database composed of 17,244 data-points into 10 different training data sets. However, to have a more equally distributed training data sets, for the ranges comprised within 100-90, 60-50, 50-40 and 10-0 an additional step of 5% has been determined, as shown in Tab. 3.3. This decision was made, since these training datasets were identified as weak points. As a result, the accuracy of the tuned fuzzy-logic strategy was improved.

After the training data sets determination, in Tab. 3.3, it is shown the amount of data used for training and testing based on each data-set. For this process, different training and testing percentages were determined. In this case 90% of the data was used for training and 10% of the data was used for testing. This modification has been done due to the obtained lower errors.

The training process performance has been measured by means of the RMSE, as in the previous P-HEB case. However, for the FCHEB powertrain, this value

Table 3.3: Training, testing and all data errors.

Length Ratio [%]	All Data Data	Training Data Data	Training Data RMSE	Testing Data Data	Testing Data RMSE
[100-95)	1,008	882	0.096	126	0.111
[95-90)	1,359	1,189	0.046	170	0.047
[90-80)	1,503	1,202	0.048	301	0.088
[80-70)	1,269	1,015	0.028	254	0.074
[70-60)	1,323	926	0.024	397	0.050
[60-55)	972	680	0.031	292	0.069
[55-50)	1,107	969	0.044	138	0.047
[50-45)	1,269	1,015	0.048	254	0.060
[45-40)	972	851	0.032	121	0.061
[40-30)	1,323	1,158	0.035	165	0.071
[30-20)	1,269	1,110	0.053	159	0.101
[20-10)	1,503	1,315	0.045	188	0.079
[10-5)	1,359	1,189	0.059	170	0.071
[5-0)	1,008	882	0.078	126	0.083

is calculated as follows:

$$RMSE = \sqrt{\frac{1}{n}\sum_{i-1}^{n}(y_i - \widetilde{y}_i)^2} = \sqrt{MSE} = \sqrt{\frac{1}{n}\sum_{i-1}^{n}(P_{FC_{out}(k)} - P_{FC_{target}(k)})^2} \quad (3.14)$$

where n stands for the number of training epochs, $P_{FCoutput}(k)$ the obtained FC power and $P_{FCtarget}(k)$ the FC power training target.

The obtained errors are shown in Tab. 3.3. It is notably the higher error for the testing than for the training. This is the same conclusion as in the P-HEB training. As it has been aforementioned, this behavior indicates that the training overfitting is avoided.

From this point, the operation of this second FCHEB case scenario. For this case study, 14 kW mean auxiliary consumption has been chosen, being at the 2 kW below the maximum (as for the P-HEB scenario). The first step to evaluate the ANFIS based EMS has been to analyze the obtained power split between the available sources. Focusing on the power profile, it is interesting to note that the steady state of the power provided by the FC. On the contrary, the BT provides all the power peaks, as the dynamics are faster than the ones of the FC. This behavior has also been observed, when evaluating route 4 for the FCHEB powertrain. Again a power peak is shown at the beginning of the route, to correct the SOC and another one for fulfilling the high power demand at the end of the route. As it is later analyzed, this causes the OER drop.

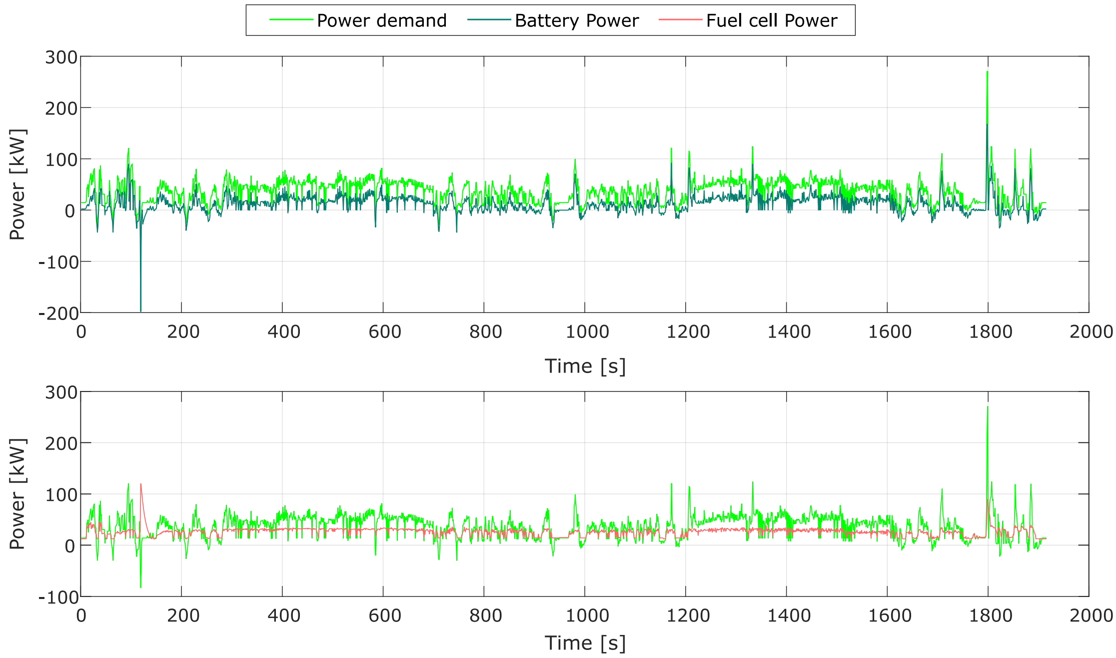

Figure 3.28: Power demand split between the BT and the FC.

The FC dynamics are limited by the OER map (shown in Fig. 2.10 D). The OER has been examined for the 14 kW mean auxiliary consumption, shown in Fig. 3.29. It is significant to note that with the developed DP cost function the OER lower limit is exceeded once and twice applying the ANFIS based EMS. In the case of the ANFIS based EMS, this OER drop is caused owing to the higher power requests to the FC. The obtained mean OER results have been 1.73 and 1.72 for the DP optimization and ANFIS based EMS respectively.

As it has been done in the previous EMS evaluations, for this case study the SOC operation has also been compared to the DP obtained optimal SOC profile. In the first part of the power profiles, as shown in Fig. 3.28, there is a FC power peak. This power peak causes a deviation of the ANFIS profile compared to the optimal DP SOC profile. This behavior happens, due to an incorrect interpretation of the input data into the trained and tested ANFIS based structure. However, this is corrected along the route and finally the desired final SOC is reached.

For having a more accurate evaluation, the error has also been calculated, based on the DP and ANFIS SOC profile differences. The obtained results are shown in Fig. 3.30, having a mean error of -0.092 % and a maximum error of -0.286 %.

Together with the SOC profile evaluation, the FC current obtained with the DP optimization and with the ANFIS based EMS have been compared in Fig.

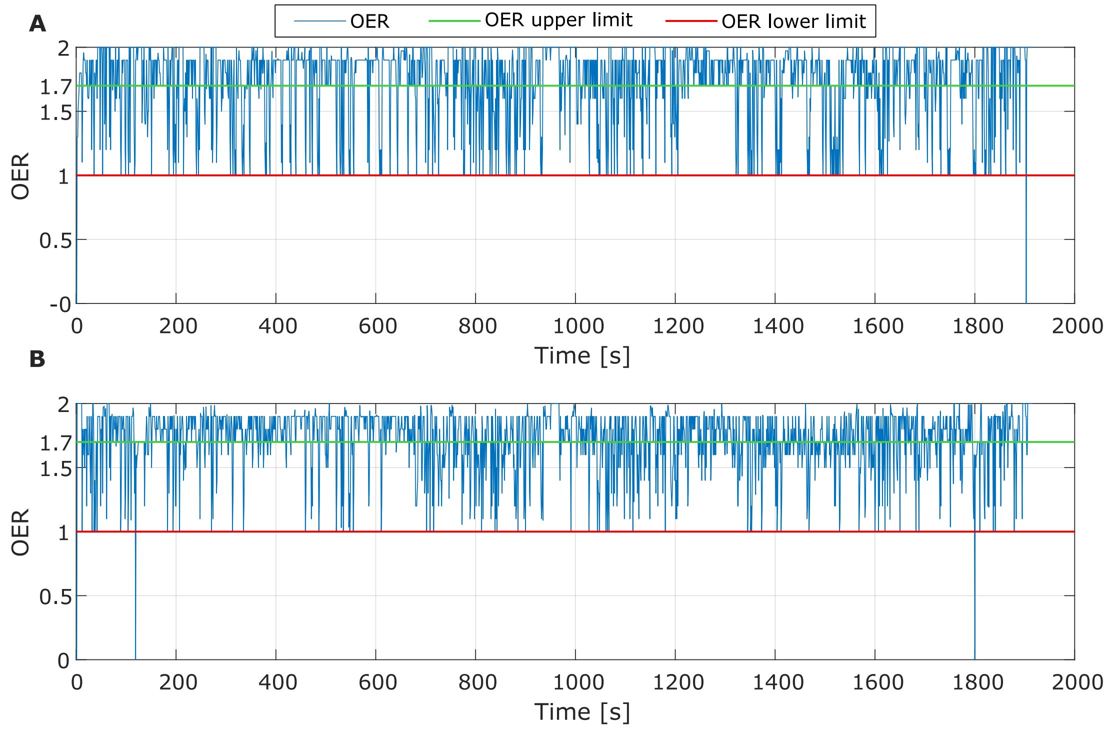

Figure 3.29: OER graphical result for the DP optimization (A) and for the ANFIS based EMS (B).

3.31. The FC current obtained from the ANFIS based EMS follows the obtained optimal FCs utilization from the DP optimization. It is noteworthy the higher power provided by the ANFIS based EMS. This higher FCs utilization generates consequently a higher fuel consumption.

The aforementioned two points where the OER dropped to 0 have been zoomed in Fig. 3.31. The same behavior has been identified at the beginning of the route in the previous case study (route 4), which is shown in Fig. 3.31 A. However, the FC current replication is corrected along the route. The other point where the OER is dropped to 0 is zoomed in Fig. 3.31 B. However, this current increase is given following the optimal the optimal profile.

To evaluate the hydrogen consumption minimization cost function aspect and the OER in depth, all the possible mean auxiliary consumptions have been analyzed and the results are sum up in Tab. 3.4. On the one hand, there is a higher hydrogen consumption for the ANFIS based EMS. This confirms the examined behavior in Fig. 3.31, since a higher FC current output provided by the ANFIS based EMS has been observed. As it has been stated the obtained DP result is the best achievable result, since this optimization is a global optimization.

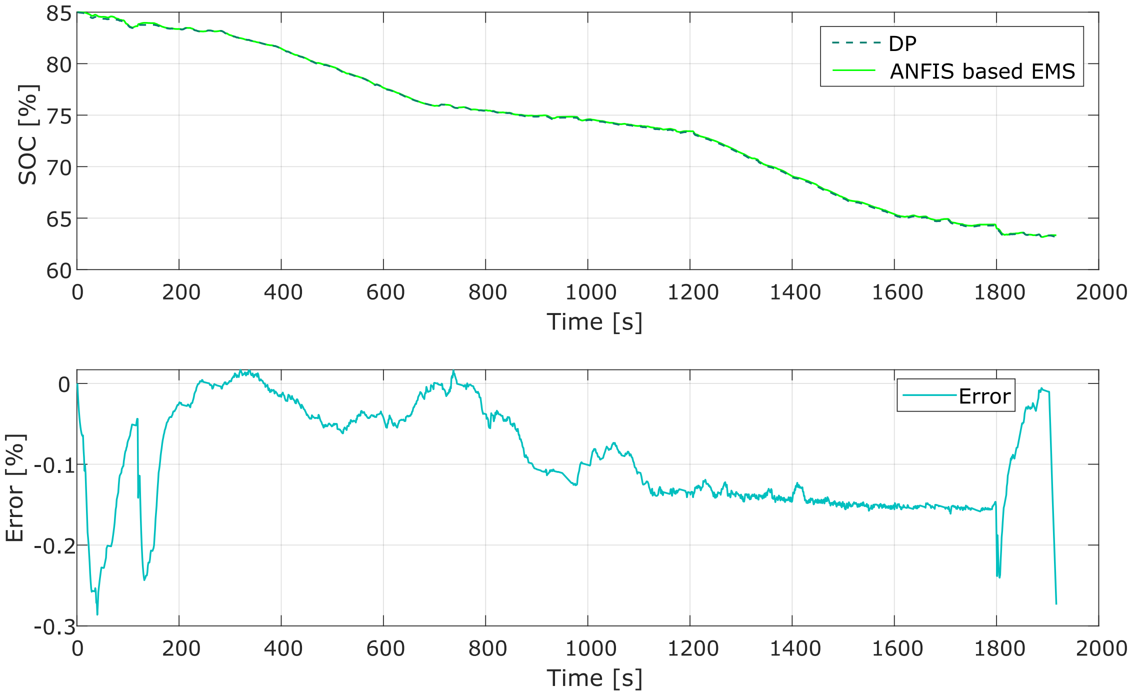

Figure 3.30: DP SOC profile compared to ANFIS based EMS (up) and error (down).

However, the ANFIS based EMS allows to have close results to the DP optimal operation. On the other hand, the OER for the ANFIS based EMS is close to the DP optimal, following the hydrogen consumption behavior.

Table 3.4: Hydrogen consumption and OER technical evaluation of Route 1 with all the possible auxiliary consumptions for the DP optimization and ANFIS based EMS.

Mean Auxiliary consumption [kW]	Hydrogen consumption [kg/100km]		Oxygen Excess Ratio	
	DP optimization	ANFIS based EMS	DP optimization	ANFIS based EMS
8	3.55	3.90	1.76	1.67
9	3.79	4.19	1.71	1.69
10	4.00	4.29	1.78	1.72
11	4.23	4.47	1.75	1.73
12	4.48	4.83	1.72	1.72
13	4.7	4.94	1.72	1.70
14	4.94	5.22	1.72	1.72
15	5.18	5.26	1.73	1.72
16	5.42	6.49	1.74	1.75

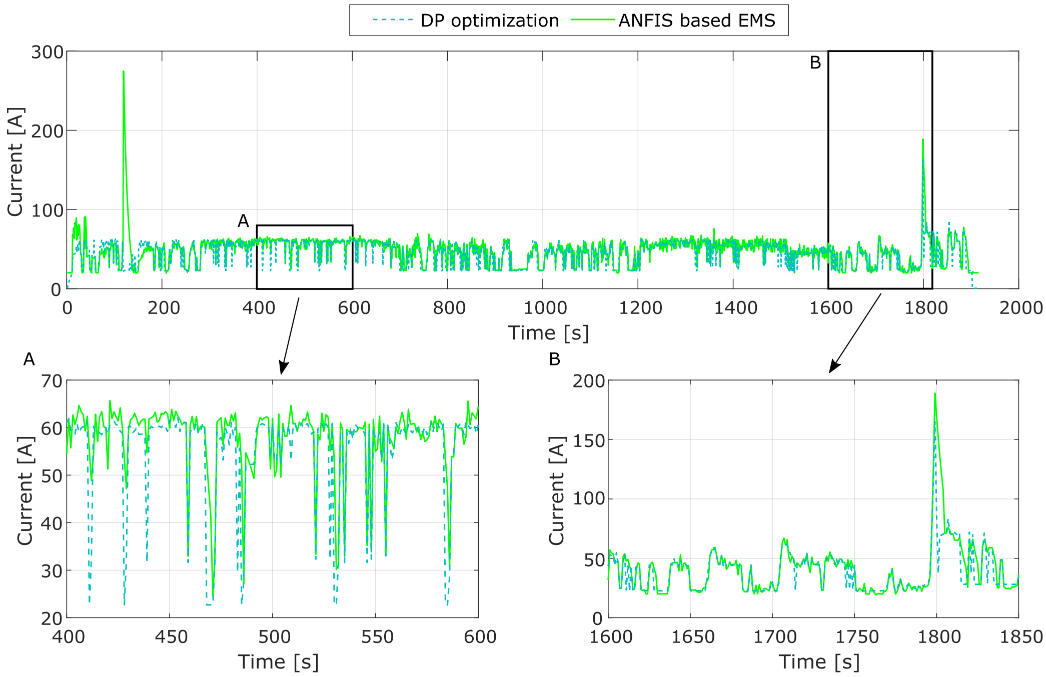

Figure 3.31: Fuel cells current response for the DP optimization and for the ANFIS based EMS.

3.6 Conclusions

In this chapter, a novel adaptive neuro-fuzzy inference system (ANFIS) that learns from and replicates the optimal operation of the DP global optimization has been proposed. The ANFIS artificial intelligence learning technique is a solution that makes use of the solutions offered by the transport digitalization, since it is based on a continuous monitoring, data processing and actuation.

The proposed ANFIS based EMS has been validated at simulation and hardware-in the loop level. The ANFIS based EMS has been applied in two different powertrains, the plug-in hybrid electric bus and the fuel cell hybrid electric bus.

The main qualitative conclusions of the chapter are summarized below:

- The ANFIS based EMS allows to reproduce the optimal operation onboard the vehicle. It manages the power sources determining the optimal power split factor, learned from the DP optimization of a specific route. The replication allows to adapt to each route and not only to reach close fuel consumption results to the optimal operation, but also the BT lifetime management. In the studied scenarios, the proposed ANFIS based EMS improves the vehicle level operation. Benefits in technical and economic terms have been obtain, improving the fuel or hydrogen consumption and supervising and managing the BT lifetime.
- The ANFIS technique tunes the fuzzy-sets and defines the rules of a fuzzy-logic energy management strategy. This process allows to reduce the EMS design complexity, since the design process is automatized. This avoids the utilization of complex design methods or human based expertise designs. The critical part of this energy management strategy design is on the operation optimization and data-base generation and process.
- The ANFIS technique provides a fuzzy-logic based EMS. This strategy has been implemented and tested in real-time operation in a hardware-in-the-loop platform, showing the capability to successfully manage the operation. This is a crucial point, since the EMS has to be run in real-time onboard the bus.
- It has been proven that the plug-in hybrid electric buses developments are directly implementable into the fuel cell hybrid electric buses. In this way, the developed ANFIS based EMS designed for the plug-in hybrid electric bus

has been replicated for a fuel cell hybrid electric bus, replacing the genset output power by the fuel-cell output power. In the analyzed scenarios, the optimal operation obtained with the DP optimization replication has been achieved. Regarding the hydrogen consumption results and fuel-cell dynamics management, results close to the optimal operation have been obtained. This replication demonstrates that all the developments for the plug-in hybrid electric buses will pave the way for the oncoming fuel cell hybrid electric buses, finding viable solutions to further optimize their operation and improve the energy efficiency.

4

Fleet Level Decision Maker for Energy Management based on Battery Aging

Summary

In this chapter the novel hierarchical energy management strategy for TCO management, studied in the previous chapter at vehicle level is elevated at fleet level. The decisions are made from the fleet level point of view to optimize the whole fleet TCO based on the three levels hierarchical decision maker. The outer part is the offline route-to-bus data exploitation and decision maker, to establish the DP optimization design. The next level is the offline optimization bus-to-route, where the neuro-fuzzy learns from the global optimal solutions. Finally, the trained fuzzy-logic strategy is used to manage the online operation. This fleet is then re-organized and the online operation energy management strategy is updated throughout the buses lifetime. These decisions are made based on the evaluated battery lifetime of the fleet, to meet the planned TCO requirements.

4.1 Fleet Level Energy Management Strategy

The main contribution of this Ph.D. thesis lies on an approach for the energy management of a whole fleet, based on the hierarchical decision maker and management structure presented in Chapter 2 [87]. In this chapter, the fleet management methodology is thoroughly described. As shown in Figure 4.1, it is divided into several levels and stages. In a first classification, two offline levels and one online level are distinguished.

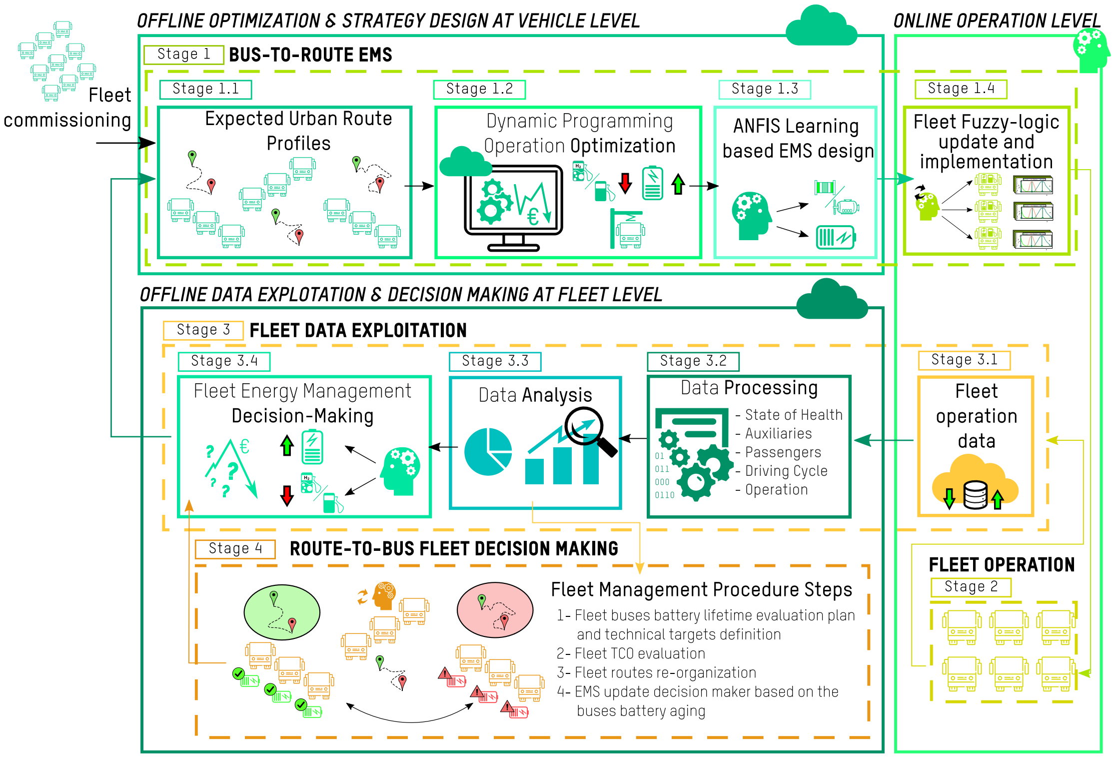

Figure 4.1: Fleet management methodology.

The fleet upper level goal is to manage and improve the operation energy efficiency of the whole fleet, taking decisions based on the whole fleet TCO picture. This approach allows to take decisions with a wider view, which offers additional degrees of freedom further optimize the TCO.

Going deeper into the proposed available degrees of freedom, two TCO management techniques have been differentiated, as shown in Fig. 4.2 [87]: the bus-to-route and the route-to-bus approaches. The bus-to-route approach is given in Stage 1 and lies on a short-term improvement to fulfill the efficiency goals of fuel or hydrogen consumption minimization. This optimization is carried out to optimize the bus according to the route. Once the bus fleet has been operated for a defined period of time, operation data will be available and the initial bus conditions will be different. At this point, in Stage 4, the *route-to-bus* long-term improvement takes place. The compiled historical data is exploited to improve the optimization process. Besides, bus conditions are updated and decisions are made according to the new SOH of the BTs and TCO planning. These decisions are made to fix the operation to the TCO plan. The decisions can imply a fleet re-organization or EMS updating for a combined management of the fuel or hydrogen consumption and BT lifetime.

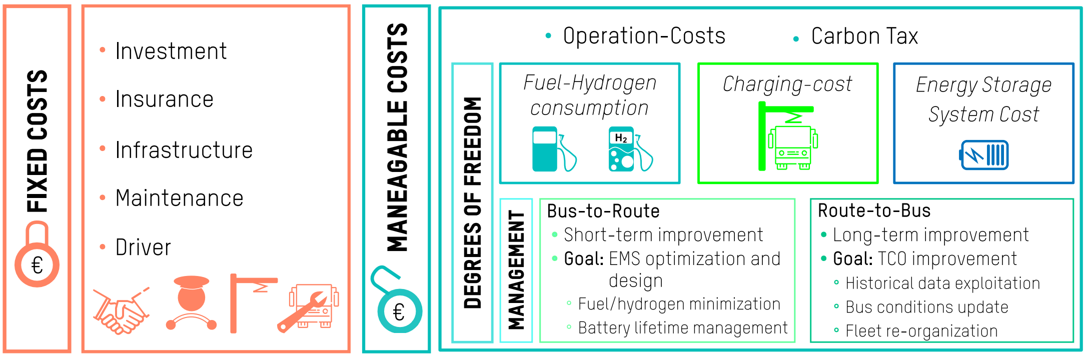

Figure 4.2: TCO fixed and manageable costs based on the degrees of freedom from the energetic manageability point of view.

Once the degrees of freedom have been defined, the whole methodology of Fig. 4.1 is thoroughly explained in the following lines.

Stage 1: Bus-to-route EMS design

In the first stage, the *bus-to-route* optimization scenario is defined and the fleet expected urban route profiles are analyzed. Once the fleet structure and operation are defined, the optimization itself is performed and the ANFIS learning based EMS is designed. The optimization and the EMS design is personalized for each bus, to optimize the operation at vehicle level in each route.

Stage 1.1: *Expected Urban Route Profiles*

In stage 1.1, the optimization scenario is defined and the expected urban route profiles are analyzed.

Regarding the optimization scenario definition, the explained constraints in Subsec. 3.2.1 for each bus are applied. In addition to that, the current bus BT SOH has to be updated for the new optimization scenarios. Regarding the cost function, for the P-HEB γ_{BT} (in Subsec. 3.2.1 Eq. 3.10) and $\triangle SOC_{ref} w_{SOC}$, variables must be defined to manage the BT lifetime, as explained in Subsec. 3.2.1 (Eq. 3.1). For the case of the FCHEB, the variables to determine are α and β, to prioritize the hydrogen consumption or the FC OER management respectively, as explained in Subsec. 3.2.1 (Eq. 3.5).

According to the available data, the mean auxiliary consumptions and mean passengers are updated, if the studied tendency has changed. At this stage, a crucial point for the scenario definition is the final SOC determination, since this variable allows to manage the BT lifetime. Following the procedure introduced in Sec. 3.2.1, the final SOC of each route is determined.

Depending on the fleet status, two pathways are identified to determine the scenario to be optimized. The first path is given when a fleet is commissioned. In this case, there is no compiled fleet operation data and the SOH of the buses BTs are at 100%. At this point, the optimization scenario cost functions γ_{BT} and $\triangle SOC_{ref} w_{SOC}$ for the P-HEB are defined as 1. For the FCHEB, α and β are defined as 1 and 0. This pathway in both powertrains allows to use the whole BT capacity in the optimization, harnessing the BT utilization and minimizing the fuel or hydrogen consumption. The fleet operation is evaluated analyzing the daily operation time, round trips, driven distance, and the yearly driven distance.

The second path is given, when the fleet has been operating for a period of time and operation data is available. In this case, the first step is to update the buses BT SOH. According to the decisions taken in stages 3.4 and 4 (further explained below), the γ_{BT} and $\triangle SOC_{ref} w_{SOC}$ for the P-HEB and α and β for the FCHEB are updated.

Stage 1.2: *Dynamic Programming Operation Optimization*

Once the optimization scenario is defined, in stage 1.2, each bus operation is optimized for each route according to the DP optimization technique. From the pursued optimizations with the chosen mean auxiliary consumptions, the data-base is generated.

For the P-HEB powertrain, the data-base is generated with the power demand, BT SOC profile, length ratio, and GS output power. The variables for generating the FCHEB powertrain data-base are the same, replacing the GS output power for the FC output power. This data is used for the training and testing part of the ANFIS based EMS.

Stage 1.3: *ANFIS Learning based EMS design*

In stage 1.3, the EMS is designed with the ANFIS learning technique. The data-base generated in stage 1.2 is first processed and divided into data-sets according to the length ratio. For both topologies, power demand, BT SOC profile, and length ratio are the input variables. The output variable is the GS output power for the P-HEB and the FC output power for the P-HEB.

Stage 1.4: *Fleet Fuzzy-Logic Update and Implementation*

As a final step of stage 1, the developed FL EMS is implemented in each bus. This last stage is the bridge between the *offline optimization and strategy design at vehicle level* and the *online operation level.*

Stage 2: Fleet operation

In this stage, the implemented EMSs in each bus are operated in their corresponding routes.

The digitalization new techniques allow a continuous monitoring of the buses operation. The most important variables to be registered from the energy management point of view are summarized.

- Driving speed: it allows to analyze the driving cycle and behavior that each driver of the fleet is completing in all the routes. The information of the driving cycle improve the energy efficiency without changing the driver's driving behavior.
- Power demand: it concerns the power derived from the tractive force and the auxiliary power demand. It is a very representative variable for generating the optimization data-base.
- Buses auxiliary consumption: it is the variable that mostly influences the power demand variation [86]. This variable generate the optimization data-base.
- Buses passenger flow: it is the second most affecting variable in the power demand variation [86]. This variable also allows to generate the optimization data-base.
- Fuel or hydrogen mass flow: they are key factors that have direct impact on the TCO. Besides, they are good indicators for evaluating the EMSs effectiveness.
- BT power demand and SOC: they are crucial indicators for evaluating the BT lifetime.

- OER: it is a vital indicator to be managed in order to manage the FC lifetime for FCHEBs.

Stage 3: Fleet data exploitation

In stage 3, the obtained data from the fleet operation is processed for the subsequent fleet data analysis. Based on this analysis, EMS update and/or *route-to-bus fleet decision making* approach is performed.

Stage 3.1: *Fleet operation data*

In this stage, a time period has to be set, to collect enough data for the processing stage. This watching period can be set from weeks to years, depending on the data analysis type. This stage is the bridge between the *online operation level* and the *offline data exploitation and decision making at fleet level*. The evaluated period is known as the period until the evaluation point, which is the moment in which the fleet BT aging is evaluated and decisions are made. The evaluation point is described below and thoroughly analyzed in Appendix A.

Stage 3.2: *Data processing*

The collected data of the previous stage has to be processed, to get valuable information. The factors to be processed are the monitored bus speed, auxiliary consumption, passenger flow, power demand, fuel or hydrogen mass flow, BT power demand, BT SOC and, FC OER.

This data is processed, to acquire additional information for the analysis and decision making stages. On the one hand, the speed, auxiliary consumption, passenger flow, and power demand define the new optimization scenario. On the other hand, the fuel or hydrogen mass flow, BT power demand, BT SOC, and FC OER variables are used for making decisions for the new optimization scenario.

The new information obtained from the data processing is crucial for the following stages. From the speed cycle, the mean speed, maximum speed, acceleration, and route distance are obtained. Mean speed and route distance for evaluate the route demand level and the fleet BT lifetime plan (further explained below).

Finally, the fuel or hydrogen consumptions are calculated and the BT lifetime is processed.

Stage 3.3: *Data analysis*

At this stage, an analysis of the whole fleet is performed by checking the planned TCO goals fulfillment. The first goal is to respect the fuel and hydrogen consumption limits constrained by the fleet operator. The second goal is to respect the planned buses BT lifetime.

Stage 3.4: *Energy management decision making*

Based on the data analysis, in the energy management decision making stage, the new updated EMS design is decided. This stage receives inputs from stage 3.3 and stage 4. From stage 3.3, the bus new operating conditions are received. These new conditions are the ones refereed to the new scenario to be optimized, such as the buses BT SOH at the evaluation point and decisions made for the new optimization final SOC.

From stage 4, based on the fleet management procedure, the new routes re-organization is obtained and the bus re-optimization target is set for the new optimization scenario definition. The re-optimization target is set based on the final SOC, which is modified and determined with the γ_{BT} constant in Eqs. 3.10 and 3.11. The constant γ_{BT}, as it has been aforementioned is used to manage the BT lifetime.

The optimization decisions are made based on the TCO plan to increase or decrease the estimated buses BT lifetime, by adjusting the γ_{BT}. On the one hand, in order to increase the BT lifetime of a bus, the BT utilization must be decreased, increasing γ_{BT} ($\gamma_{BT} > 1$) and consequently increasing the final SOC target. In case the final SOC matches the initial SOC, the BT utilization is constrained with the $\triangle SOC_{ref}$ by means of the w_{SOC}. On the other hand, for the bus BT lifetime to be decreased, γ_{BT} is decreased ($\gamma_{BT} < 1$) and BT utilization is harnessed, consequently decreasing the optimization final SOC target.

For the FCHEB topology, as explained in the cost function in Eq. 3.5, the OER level is managed adjusting α and β weights. Increasing α, hydrogen consumption is minimized. On the contrary, when increasing β above α value, hydrogen consumption increases.

Stage 4: Route-to-bus Fleet Decision Making

The *route-to-bus* stage is the stage dealing with the fleet management itself and it takes place at the evaluation point. It receives inputs from the data analysis of stage 3.3 and it calculates an output for the energy management decision making. At this point, it is decided according to the current lifetime of the BTs of the whole fleet and the buses BT lifetime estimation, whether an EMS update is enough or a re-organization of the fleet is required. The fleet management procedure is implemented in 4 steps as follows.

1- Fleet buses BT lifetime evaluation plan and technical targets definition: In this step, the lifetime of all the BTs of buses from the whole fleet is estimated and the bus BT lifetime plan for the whole fleet is developed. The BT lifetime plan is crucial for making the most of each element of the powertrain and exploit all the degrees of freedom to improve the TCO.

When no BT lifetime plan is developed and applied, two situations are identified, as depicted in Fig. 4.3A. The identified scenarios are characterized by the $P_{FleetEOL}$ fleet service lifetime, $\Psi_{aboveEOL}$ BT lifetime above $P_{FleetEOL}$ and $\Psi_{belowEOL}$ BT lifetime of above. Both scenarios ($\Psi_{aboveEOL}$ and $\Psi_{belowEOL}$) have to be corrected because they influence negatively on the fleet TCO.

On the one hand, when bus BT lifetime is above ($\Psi_{aboveEOL}$) the fleet lifetime horizon ($P_{FleetEOL}$), the BT utilization is misused comparing to the initial forecast. Therefore, this causes an extra fuel or hydrogen consumption. In addition to that, as shown in Fig. 4.3B, the BT SOH at the fleet EOL point ($P_{FleetEOL}$) is half of the begining BT SOH. In this case, an EMS updating is needed in the evaluation point P_{eval}. The EMS is updated in order to fit the fleet EOL point and the BT EOL, maximizing the BT utilization and minimizing the GS or FC and consequently

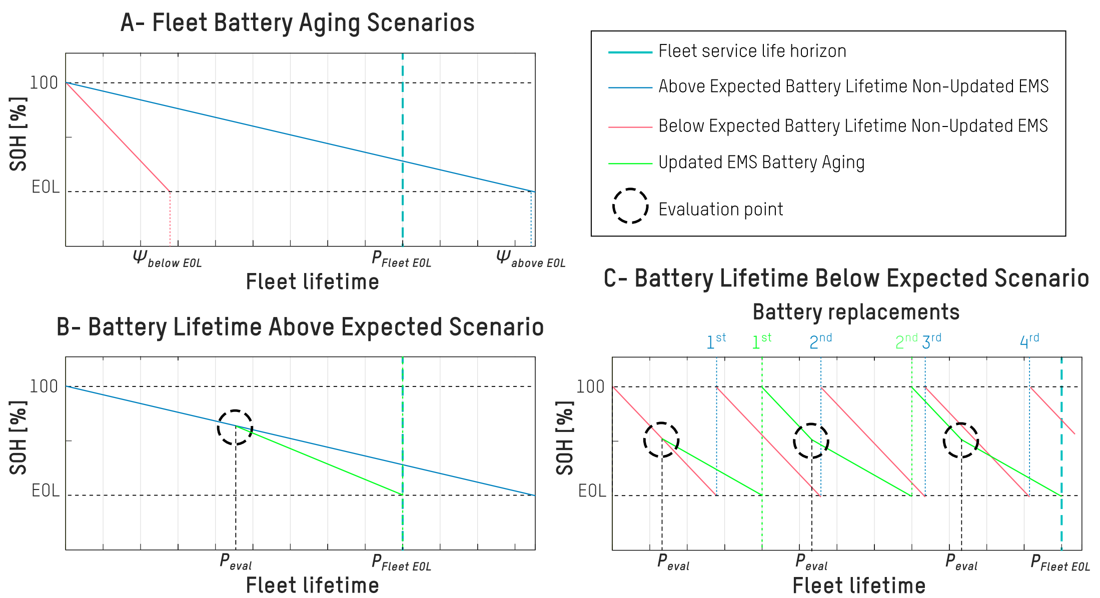

Figure 4.3: A: Fleet BT aging scenarios, **B**: BT lifetime above expected scenario and **C**: Battery lifetime below expected scenario.

fuel or hydrogen consumption.

On the other hand, when the bus BT lifetime is below ($\Psi_{belowEOL}$) the fleet lifetime horizon ($P_{FleetEOL}$), as shown in Fig. 4.3C, the GS or FC is underused and the battery is overused, increasing the number of planned BT replacements. As an example, in this specific case, the EMS is not updated and therefore, the bus service operation has 4 replacements. On the contrary, if the EMS is updated at the evaluation point, the number of BT replacements is reduced to 2. To correct the identified cases and managing the fleet buses BT lifetime and make the most of the fleet TCO, the BT lifetime evaluation plan development is crucial.

The BT lifetime evaluation plan definition is summarized in Fig.4.4. As a first step, from the fleet BT aging scenario, the buses lifetime (bus^n_Ψ bus^m_Ψ), the minimum (min_Ψ), and the maximum (max_Ψ) buses BT lifetime and fleet EOL point ($P_{FleetEOL}$) have to be identified, as depicted in Fig. 4.4A.

The next step consists in defining the evaluation point based on the fleet buses BT aging years. Three evaluation point techniques have been analyzed and presented in Appendix A. As a conclusion, the best results have been obtained applying the evaluation point definition based on the fleet BT aging years. The procedure to follow for the evaluation point definition based on the fleet BT aging

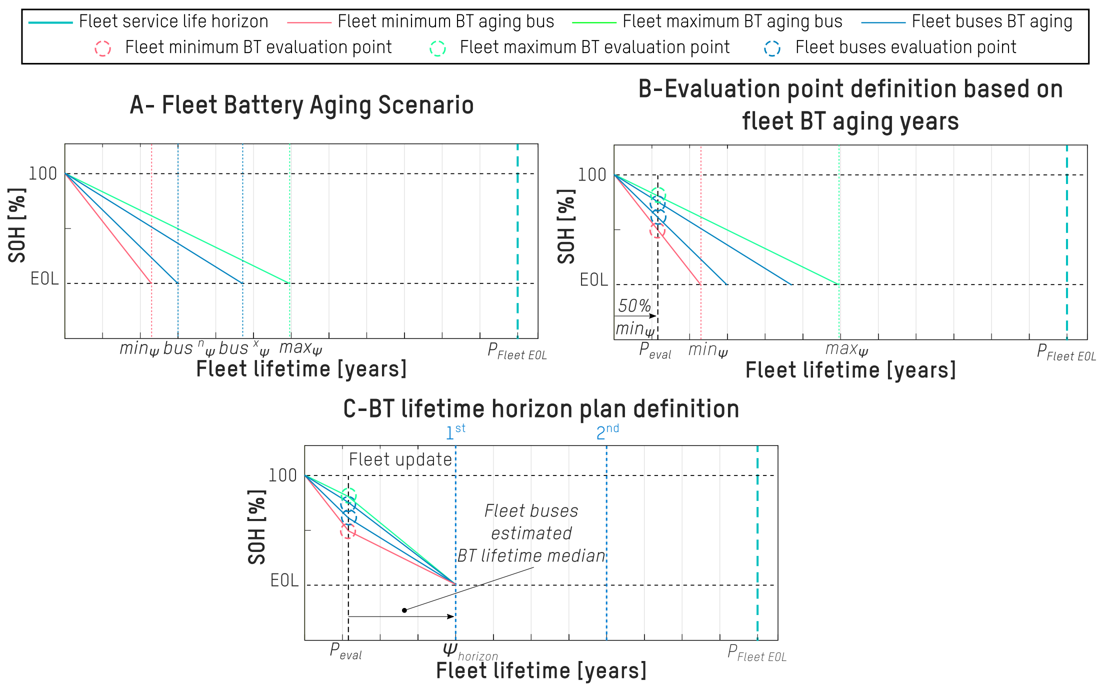

Figure 4.4: Fleet buses BT lifetime evaluation plan development.

years is depicted in Fig. 4.4B. The buses BT lifetime evaluation point is defined in the half of the BT lifetime for the bus with the minimum BT aging. The EOL of the BT is limited at 80% of BT SOH or by the calendar degradation.

To conclude the development of the fleet buses BT lifetime plan, the BT lifetime horizon plan has to be defined. This horizon $\Psi_{horizon}$ sets the fleet buses BT lifetime target. It is obtained based on the fleet buses estimated BT lifetime median, as indicated in Fig. 4.4C.

2- Fleet TCO evaluation: Before the fleet is re-organized and/or the EMS updating decisions are made, the current fleet TCO status has to be calculated and analyzed. This TCO calculation is performed between the fleet commissioning or last evaluation point and the current fleet evaluation point. This information is valuable for the next steps decisions.

3- Fleet routes re-organization: Fleet routes re-organization decisions are made, to balance the BT lifetime of the buses with the best and the worst SOH. The decisions are made based on the fleet buses BT lifetime picture, shown in Fig. 4.5. The fleet buses BT lifetime picture, depicted in Fig. 4.5, contains the information of the estimated buses BT lifetime, BT SOH at the evaluation point, cycle and daily driven distances and the mean route speed.

The routes are grouped, facilitating the decision maker process. They are grouped into three groups: least demanding, most demanding, and average demanding groups. The least and the most demanding routes are those in which the BT lifetime are a 20% above or below from the BT lifetime horizon plan. It is considered that those BT lifetimes cannot be corrected by only adjusting or updating the EMS. Those routes require additional decisions. The rest of the routes are grouped in the average demand.

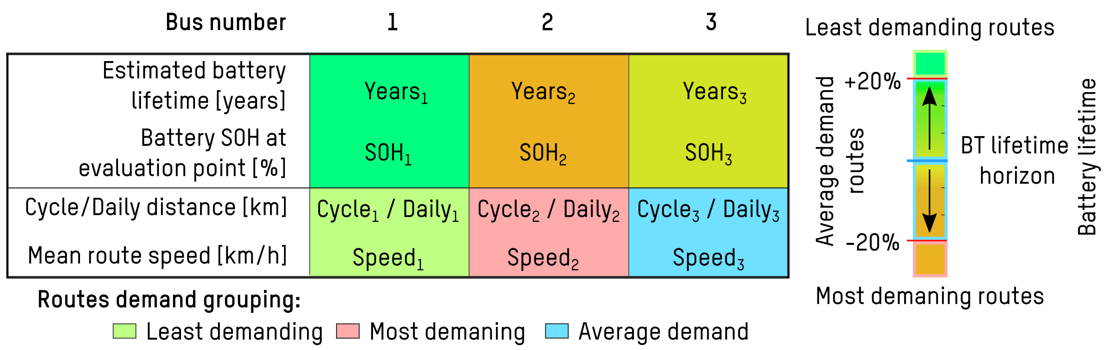

Figure 4.5: Fleet buses battery lifetime picture.

The most demanding and less demanding routes are the routes that are re-organized to fit to the BT lifetime horizon. The re-organization process is executed in the following way. The buses with the best SOH are exchanged for the most demanding lines and the buses with the worst SOH are exchanged for the least demanding lines. In the buses of the re-organized routes and the ones grouped in the average demand the EMSs have to be updated.

4- EMS update decision maker based on the buses BT aging: Once the *route-to-bus* decisions has been made, all the routes are re-optimized with the DP and the buses BT lifetimes are estimated in order to stick to the buses BT lifetime horizon goal. The *route-to-bus* EMS design decision is made to meet the predefined BT aging targets and improve the TCO of the whole fleet. In this way the short-term management to minimize the fuel or hydrogen consumption and the long-term BT lifetime management are merged.

The explained novel fleet management methodology stages have been evaluated in two different case studies. To evaluate different fleet case scenarios, a fleet of P-HEBs with LTO BT chemistry and a fleet of P-HEBs with NMC BT chemistry have been studied. These P-HEBs characteristics have been presented in Tabs. 2.2 and 2.3 respectively.

The fleet management methodology has been evaluated following the methodology itself. First, the expected urban route profiles analysis is performed. The obtained operation with the ANFIS based EMS for each bus driving in specific routes is analyzed and both fleets are compared. Once the fleet scenario is determined, the designed ANFIS based EMSs in the bus-to-route stage are evaluated in techno-economic terms. After that, the obtained fleets operation is processed and analyzed the route-to-bus fleet decision making. In this point, the multiple steps that contains the fleet management stage are performed and evaluated: starting from the fleet BT lifetime evaluation plan development, fleet TCO evaluation, fleet routes re-organization, and EMS update based on the buses BT aging.

4.2 Expected Urban Route Profiles Analysis

In this section, the expected urban route profiles analysis is performed following the first pathway described in Stage 1.1. At this point, each daily operations, round trips, distances, and yearly driven distances are analyzed.

The studied lithium-ion BT chemistries have their characteristics. LTO BT has higher charging c-rates compared to the NMC BT. Owing to this fact, the

LTO BT pack can be charged at a higher power, up to 168 kW, compared with the NMC BT pack that can be charged up to 96 kW. According to the maximum charging power, the t_{cha} constant is 22 for the NMC BT and 9 for the LTO BT. This is translated into a longer charging time for the fleet of buses with NMC BTs compared with the fleet of buses with LTO BTs.

In Tables 4.1 and 4.2, the fleet characteristics with LTO chemistry and NMC chemistry are shown. Starting from the daily operation, it is worth mentioning that all the routes are operated around 16 hours in both fleets, except the route 7 that it is operated 17.18 hours with NMC and 17.12 hours with LTO. The main reason for the longer operation time is that it is the longest route with 32.17 km. The NMC fleet operates over a longer period of time, but with less round-trips, owing to the longer time needed to recharge the buses BT.

The charging time having the constraint of around 16 hour daily operation, it has direct influence on the number of round-trips and consequently the daily kilometers covered by each bus. The two fleets are analyzed at the same time, since the routes are the same, however with different charging times and powers.

Table 4.1: Route characteristics of the fleet with LTO chemistry.

Route	**Distance**	**Mean speed**	**Fleet of buses with LTO chemistry**			
	[km]	**[km/h]**	**Daily operation [hours]**	**Round trips**	**Daily distance[km]**	**Yearly distance[km]**
1	14.25	26.77	16.51	29	413	136,000
2	20.44	25.57	16.20	19	388	128,000
3	9.18	13.84	16.48	24	220	73,000
4	13.63	20.58	16.05	23	314	104,000
5	15.48	17.80	16.37	18	279	92,000
6	18.58	27.00	16.21	22	409	135,000
7	32.17	28.23	17.12	14	450	149,000
8	29.63	28.53	16.74	15	445	147,000
9	17.29	23.45	16.43	21	363	120,000
10	12.16	17.77	16.47	23	280	92,000

The route with the highest number of round trips completed is the first route with 26 and 29 round trips accomplished in one day for the buses with NMC and LTO respectively. It is the shortest route in terms of duration, as shown in Tab. 2.1.

Regarding the daily and yearly distances, they are correlated. The yearly operation has been set at 330 days. It is important to underline that at this characteristic, route 8 has the longest yearly driven distance for the bus with NMC BT and route 7 has the longest yearly driven distance for the bus with LTO

Table 4.2: Route characteristics of the fleet with NMC chemistry.

Route	Distance [km]	Mean speed [km/h]	Fleet of buses with NMC chemistry			
			Daily operation [hours]	Round trips	Daily distance[km]	Yearly distance[km]
1	14.25	26.77	16.19	26	370	122,000
2	20.44	25.57	16.73	18	368	121,000
3	9.18	13.84	16.58	23	211	70,000
4	13.63	20.58	16.47	22	300	99,000
5	15.48	17.80	16.13	17	263	87,000
6	18.58	27.00	16.13	20	372	123,000
7	32.17	28.23	17.18	12	386	127,000
8	29.63	28.53	16.1	14	414	137,000
9	17.29	23.45	16.43	19	329	108,000
10	12.16	17.77	16.76	22	267	88,000

BT. This is due to the fact that route 8 has one less daily round trip in the case of the bus with NMC BT compared with the bus with LTO BT. On the contrary, regarding route 7 round trips, 2 less daily round trips are fulfilled by the bus with NMC BT.

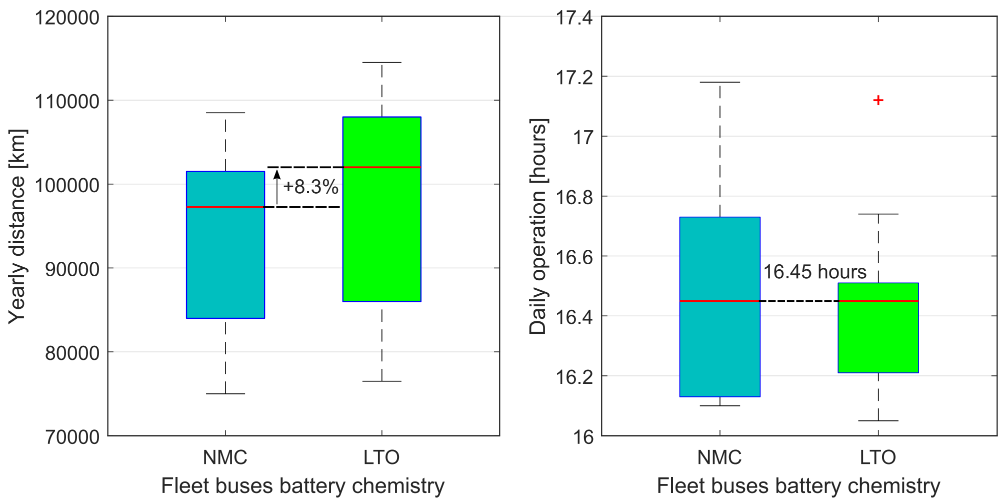

Figure 4.6: Fleets yearly distance and daily operation time comparison.

Finally, the fleets are compared in terms of yearly driven distance and daily operation time in Fig. 4.6. It should be noted that making the comparison with the yearly distance medians, the fleet of buses with LTO covers 8.3% kilometers more that the fleet of buses with NMC (102,100 less covered kilometers) having the same daily operation time median (16.45 hours). This is a significant point, since the fleet of buses with NMC can lead to the need of an additional bus to offer the same service level than the fleet of buses with LTO.

4.3 Bus-to-Route EMS Operation Evaluation

Once the fleet scenario operation has been analyzed, in the *bus-to-route* EMS design stage, the ANFIS based EMSs are developed for each bus of the fleet. The main objective of the developed EMS is to improve the overall efficiency of each bus, as performed at the vehicle level in the previous chapter. However, in this chapter, the study has been extended to the fleet level.

The evaluation is proceed from the fleet commissioning point to the evaluation point for the P-HEBs fleet of buses with LTO and the P-HEBs fleet with NMC. For both fleets, the fuel consumption improvement has been compared with the DP global optimization and with a simple CD-CS EMS. This comparison has been performed for evaluating the proposed ANFIS based EMS range of improvement compared with the most optimal solution and a commercially well known EMS.

For the P-HEB fleet with LTO BT chemistry, the obtained fuel consumption results are shown in Tab. 4.3. As a link with the chapter 3, the obtained fuel consumption and range of improvement for route 4 in Subsec. 3.4.1 and in this subsection is the same. It is worth underlining that a fuel consumption minimization has been achieved in all the routes compared with the CD-CS EMS, obtaining differences between 4.26% and 7.05%. The obtained fuel consumption errors of the ANFIS based EMS compared with the optimized operation with the DP, ranges from 6.10%, up to 11.13%.

The operation study has been extended to the BT SOC profiles comparison for

Table 4.3: Fuel consumption evaluation of the fleet based on P-HEBs with LTO BT.

Buses	Fuel consumption [l/100 km]			DP	ANFIS vs
	DP optimization	ANFIS based EMS	CD-CS EMS	Error [%]	CD-CS diff. [%]
1	31.78	34.41	36.33	8.28	5.43
2	36.32	38.71	40.62	6.58	4.82
3	48.53	53.93	56.28	11.13	4.26
4	35.85	38.81	40.96	8.26	5.25
5	39.69	42.66	46.89	7.48	9.45
6	31.32	33.41	35.58	6.67	7.05
7	32.31	34.28	36.73	6.10	6.90
8	33.10	35.13	36.99	6.13	5.16
9	36.98	39.53	41.81	6.90	5.61
10	40.56	44.08	46.89	8.68	6.18

all the routes and obtained training RMSE results. In Fig. 4.7 the obtained DP optimal SOC profiles are compared to the ones obtained with the developed ANFIS based EMS. It is important to emphasize the capability of the ANFIS based EMS to replicate the DP optimized SOC profiles. The obtained ANFIS training RMSE results are comprised between 0.063 and 0.15, being accurate results for replicating the optimal SOC.

In Tab. 4.4, the obtained fuel consumption results for the P-HEB fleet with NMC BT chemistry are shown. First, comparison has been done with the DP global optimization in order to have a benchmark of the routes. The overall errors are low, ranging from 6.08 % to 11.19 % error. In addition to this, to evaluate the improvement of the proposed ANFIS based EMS performances has been compared with a CD-CS EMS. In the evaluation, fuel consumption minimization is achieved in all the routes, ranging from 4.44 % to 9.59 %. In this way, the *bus-to-route* EMS is technically validated and proved that substantial fuel savings are achieved in both fleets with close results to the DP reference.

Table 4.4: Fuel efficiency evaluation of the fleet based on P-HEBs with NMC BT.

Buses	**Fuel consumption [l/100 km]**			**DP**	**ANFIS vs**
	DP optimization	**ANFIS based EMS**	**CD-CS EMS**	**Error [%]**	**CD-CS diff. [%]**
1	32.01	34.55	36.39	7.94	5.19
2	36.58	38.92	40.71	6.40	4.50
3	48.69	54.14	58.08	11.19	7.02
4	36.02	38.81	41.35	7.75	6.34
5	39.90	42.50	46.78	6.51	9.59
6	31.54	33.52	35.94	6.28	6.97
7	32.59	34.57	37.01	6.08	6.82
8	33.36	35.45	37.06	6.27	4.44
9	37.24	39.98	41.93	7.36	4.76
10	40.75	44.04	47.24	8.07	7.01

The capability of the ANFIS based EMS to replicate the DP optimal SOC profiles has also been proved. The developed ANFIS based EMSs follow the optimal paths with small errors (RMSEs of up to 0.22 % as it can be observed in Fig. 4.8). This global optimization replication allows to achieve both, fuel consumption minimization and BT aging management.

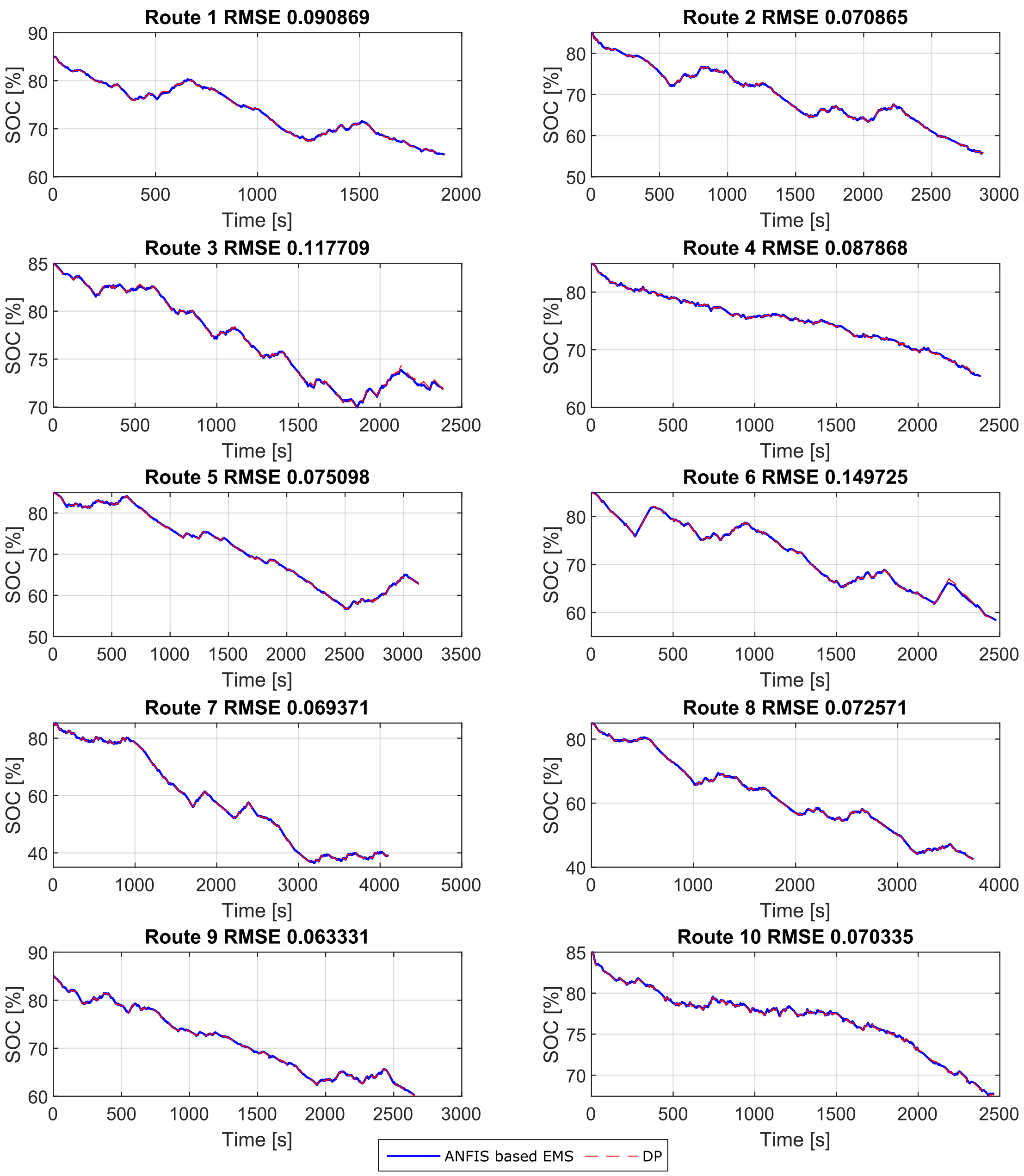

Figure 4.7: Buses SOC profiles comparison and RMSEs for DP and ANFIS based EMS in all the routes with LTO BT.

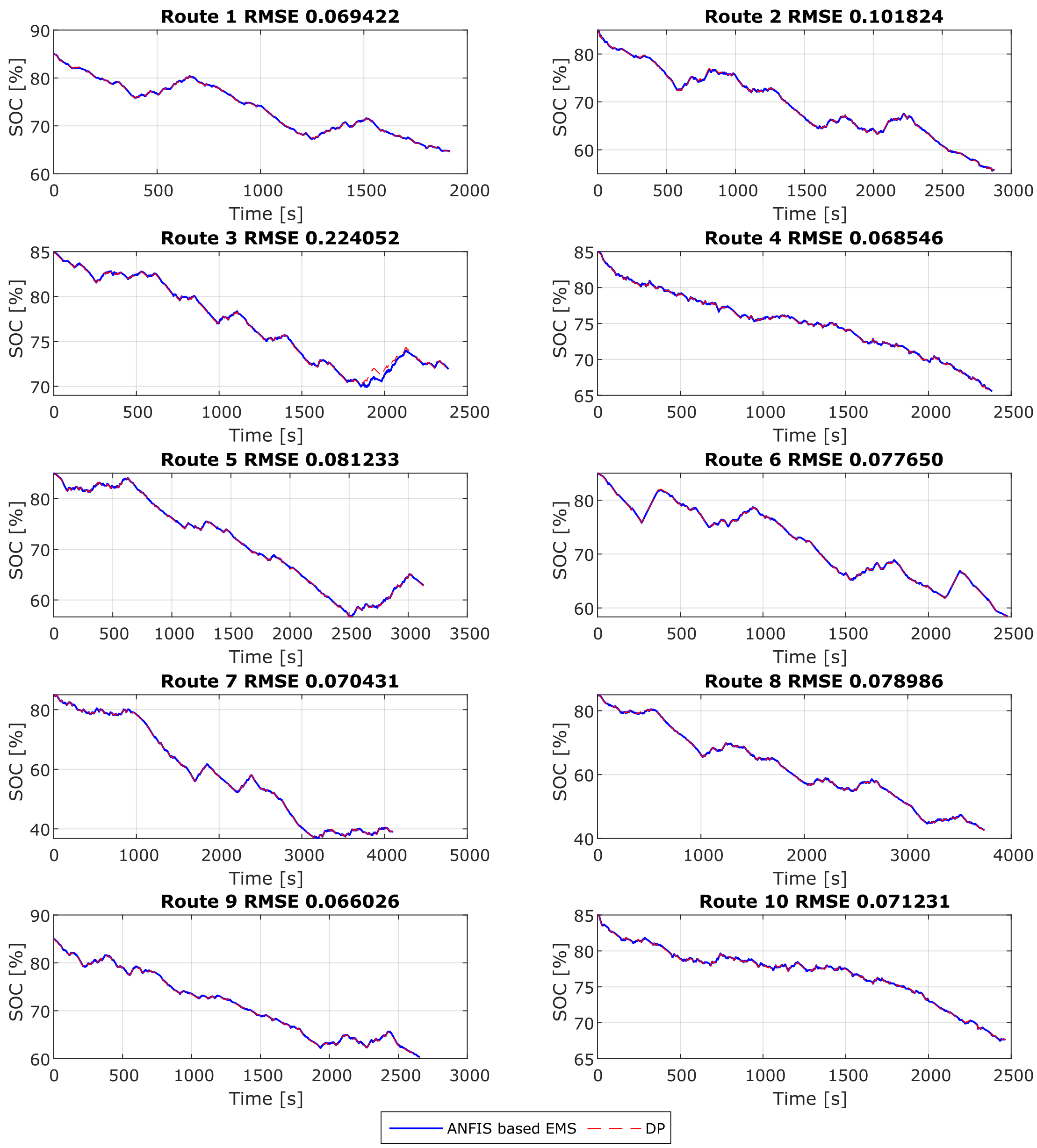

Figure 4.8: Buses SOC profiles comparison and RMSEs for DP and ANFIS based EMS in all the routes with NMC BT.

4.4 Route-to-Bus Fleet Level Decision Making

In this section, the proposed route-to-bus decision making stage 4 is evaluated. In this stage, the proposed fleet energy management is analyzed. This evaluation is performed following the Stage 4 fleet energy management procedure steps.

4.4.1 Fleet Buses Battery Lifetime Evaluation Plan and Technical Targets Definition

The fleet buses BT lifetime evaluation plan has been developed based on the evaluation point definition based on the years. This technique sets the evaluation point at the half of the estimated minimum bus BT lifetime applied to both fleets BT lifetime plan development.

4.4.1.1 Evaluation point and battery plan definition of the fleet with LTO

The bus-to-route operation of the previous section has been processed to estimate the fleet BT lifetime, obtaining the fleet picture shown in Fig. 4.9. Based on the obtained median of the buses BT lifetime, the buses BT lifetime horizon has been set to 12 years. This median is calculated based on the estimated buses BT lifetime. This lifetime horizon matches with the fleet service EOL, avoiding completely BT replacements.

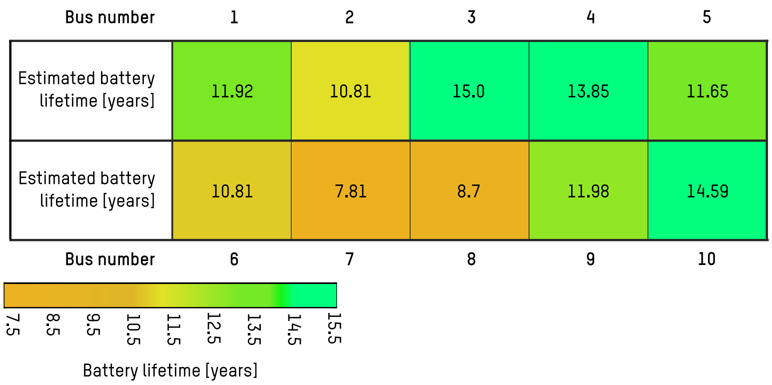

Figure 4.9: LTO based fleet BT lifetime initial picture.

The fleet buses BT lifetime varies from 7.81 to 15 years. On the one hand, the difference between the fleet service lifetime of 12 years and the bus with the minimum BT lifetime estimation is below 5 years (for the bus number 7). On the other hand, the difference between the fleet service lifetime and the bus with the maximum BT lifetime estimation is 3 years above (for the bus number 3). Both cases need a BT operation correction. Based on the minimum bus BT lifetime of 7.81 years (limited by bus 7), the evaluation point has been set to 3.9 years. However, due to the evaluation time step, which is one week, it has been approximated to 3.78 years for all the buses of the fleet.

The fleet status at the evaluation point is shown in Tab. 4.5. All the buses of the fleet have the SOH above 90%. Bus 7 is the closest bus to this value, having 90.01% SOH, even though it is the bus with the longest driven distance. The bus with the shortest driven distance, bus 10, matches with the highest SOH.

Table 4.5: LTO based fleet buses BT status at the evaluation point based on years.

Bus	Years	SOH	Kilometers
1	3.78	93.29	515,000
2	3.78	92.65	484,000
3	3.78	94.66	274,000
4	3.78	94.12	391,000
5	3.78	93.20	347,000
6	3.78	92.75	509,000
7	3.78	90.01	561,000
8	3.78	90.93	554,000
9	3.78	93.29	452,000
10	3.78	94.37	349,000

4.4.1.2 Evaluation point and battery plan definition of the fleet with NMC

For the case study of the fleet of P-HEBs with NMC BT chemistry, the buses BT lifetime fleet status is shown in Fig. 4.10. Based on the minimum BT lifetime of 2.33, the evaluation point has been established in the middle of that lifetime, being 1.17 years and corresponding to the bus number 7.

As in the previous scenario, all the other routes are above 90% of SOH as it can be observed in Tab. 4.6. This BT SOH status allows the buses BT lifetime correction and management to fix to the buses BT lifetime planned horizon. In the previous BT lifetime horizon, BT replacements were avoided. On the contrary, in this case the BT lifetime horizon, based on the fleet buses BT lifetime median has been set to 4 years.

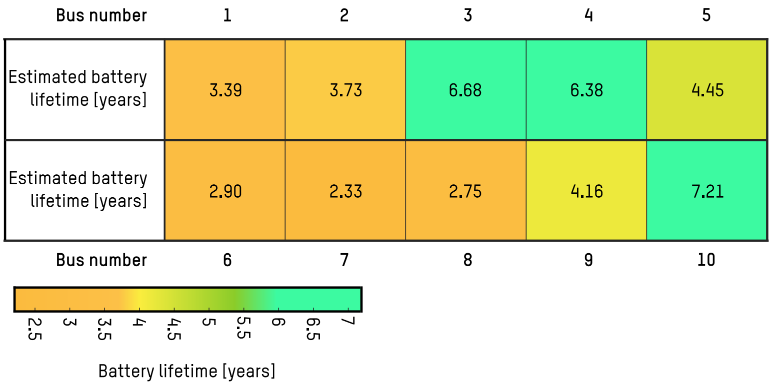

Figure 4.10: NMC based fleet BT lifetime initial picture.

Table 4.6: NMC based fleet BT status at the evaluation point based on years.

Bus	Years	SOH	Kilometers
1	1.17	93.10	159,000
2	1.17	94.03	150,000
3	1.17	96.50	84,800
4	1.17	96.26	120,000
5	1.17	94.69	107,000
6	1.17	91.94	157,000
7	1.17	89.90	173,000
8	1.17	91.48	171,000
9	1.17	94.38	140,000
10	1.17	96.68	108,000

4.4.2 Fleet TCO Evaluation

The TCO of the fleet is updated in every BT lifetime evaluation point. The period starts at the fleet commissioning instant until the defined evaluation point. The obtained fleet TCO applying the ANFIS based EMS has been compared with a fleet operating with the CD-CS EMS.

At this point, no BT replacements are required and all the buses have the same initial BT cost. Therefore, this price has been excluded from the TCO calculation, since it is constant for all buses. The factors taken into account in the TCO calculation have been the fuel cost and the recharging energy and power costs.

The P-HEB fleet with LTO BT chemistry has been firstly evaluated, as depicted in Fig. 4.11. The TCO calculation period has been understood between the fleet commissioning until the evaluation point at the year 3.78. It should be emphasized that for all the routes the operation cost has been minimized with the ANFIS based EMS, decreasing operation cost from 4.11% up to 7.56%. The whole fleet TCO has been improved a 5.06 % applying the ANFIS based EMS.

Following the previous procedure, the P-HEB fleet with NMC BT chemistry has been also evaluated, as shown in Fig. 4.12. The evaluation period in this case has also been understood between the fleet commissioning to the evaluation period, defined at the year 1.17. All the buses TCO has been decreased and savings are reached with the ANFIS EMS compared with the CD-CS EMS. The obtained improvements are ranging from 3.8 % and 7.64 %.

The overall fleet TCO has also been evaluated in the defined time period with an improvement of 4.77 %. It is important to note that a higher improvement has been achieved in the fleet with LTO compared with the fleet with NMC. The main reason for this difference is the evaluation period, which has been longer for the

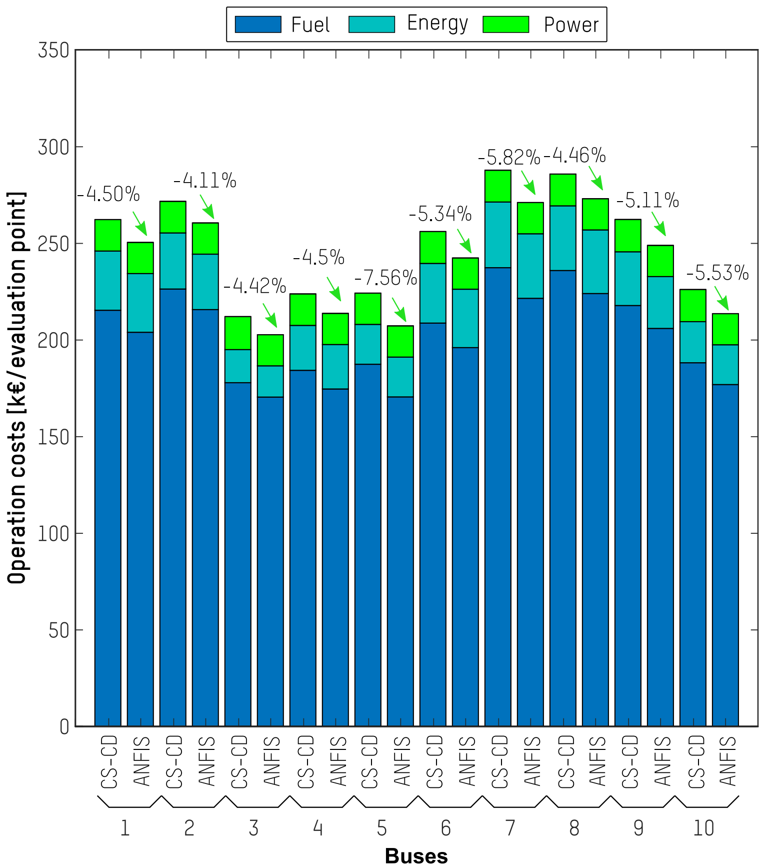

Figure 4.11: TCO comparing ANFIS based EMS with the CD-CS EMS of the fleet with LTO.

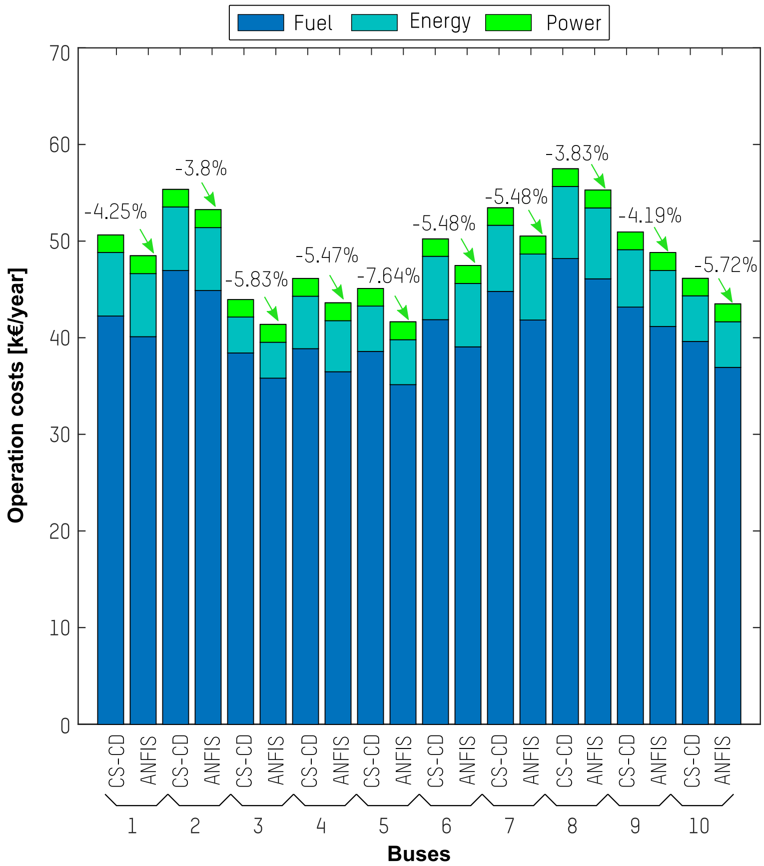

Figure 4.12: TCO comparing ANFIS based EMS with the CD-CS EMS of the fleet with NMC.

LTO case (3.78 years compared with 1.17 years).

Longer operations are better when main minimization target is the fuel or hydrogen consumption. However, in the long-term operation projection, the BT costs play a key role on the fleet TCO. Therefore, according to the current fleet BT lifetime estimation picture, decisions have to be made. In this way, the short-term bus overall efficiency is improved, combined with the long-term fleet buses BT lifetime management.

4.4.3 Fleet Routes Re-Organization

Putting the focus on the long-term operation and fleet buses BT lifetime, in this section, the fleet routes re-organization is performed. This routes re-organization is pursued to manage the buses with the most critical BT SOH. These buses are those where the BT lifetime estimation is far above or below from the buses

BT lifetime horizon. An EMS update is not enough to correct the BT lifetime. Therefore, a routes re-organization has to be applied.

4.4.3.1 Routes Re-Organization of the Fleet with LTO

The BT lifetime picture of the fleet with LTO chemistry is shown in Fig. 4.13. The grouping process of the least demanding, most demanding, and average demanding routes has been performed with the information of the cycle daily distance, mean route speed and routes grouping. The buses with a BT lifetime estimation 20% below (BT lifetime estimation < 9.6 years) or above (BT lifetime estimation > 14.4 years) the defined BT lifetime horizon of 12 years have been grouped in the least or most demanding routes respectively. The rest of the lines within the 20% threshold have been grouped as average demanding.

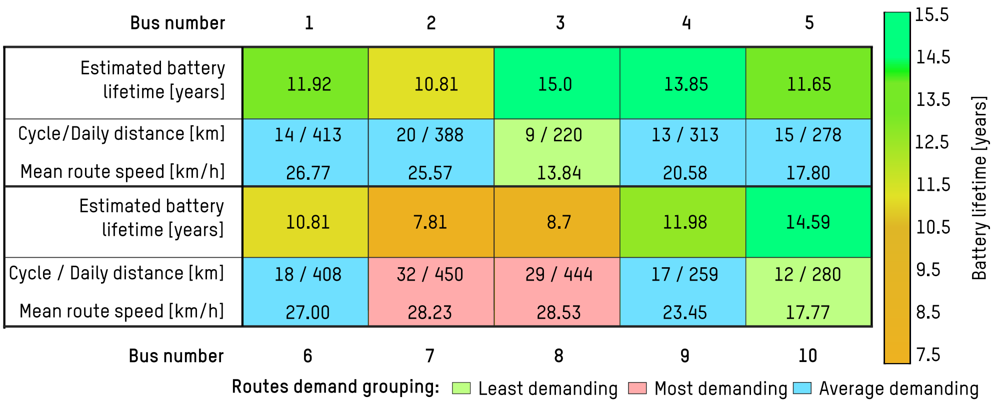

Figure 4.13: BT SOH evaluation and lifetime estimation of the LTO based fleet.

The least demanding routes, in this case, lines 3 and 10, match with the routes that have the shortest cycle and daily driven distance and the lowest average speed. The most demanding routes are the routes that have the longest cycle and daily distance and the higher average speed, identifying routes 7 and 8 in this group and being line 7 the most demanding one. The main reason for being the line 7 the most demanding route in comparison with line 8, is the longer cycle length. The longer cycle length depletes more the BT and consequently, degrades more the BT. Finally, the remaining routes with an average BT degradation within the 20% BT lifetime horizon threshold have been grouped in the average demanding class.

In Table 4.7, the routes re-scheduling is sum-up. Bus 3 that was operating in line 3 has been exchanged for the most demanding line 7. Bus 7 that was operating in the most demanding route has been exchanged for the least demanding route

3. The same decisions have been applied for the subsequent the most and the least demanding lines, 8 and 10 respectively. In the buses driving in the average demanding routes, the EMS has been updated, but they do not require routes re-organization for achieving the buses BT lifetime target of 12 years.

Table 4.7: Buses and routes exchanging of the LTO based fleet.

Group	Bus number	Current line	Exchanged for line
Best SOH	3	3	7
	10	10	8
Worst SOH	7	7	3
	8	8	10

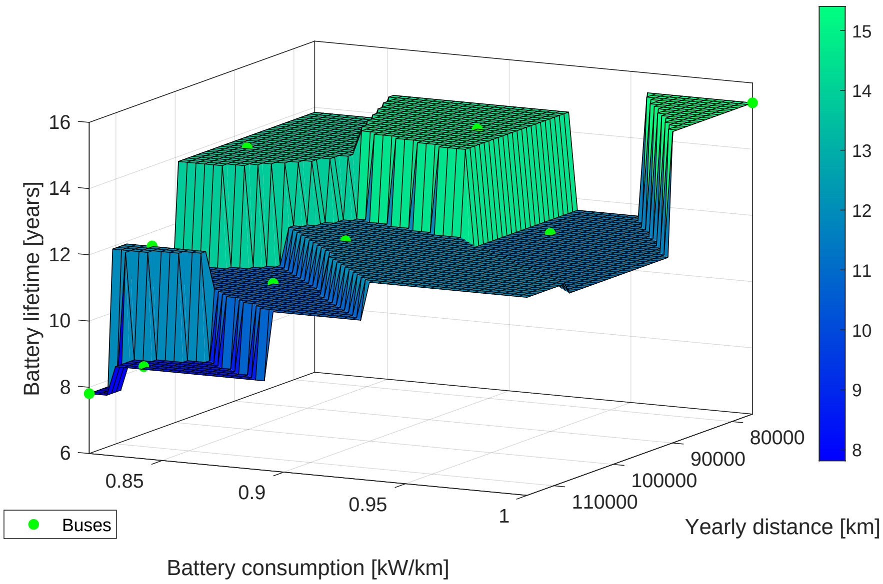

Figure 4.14: BT lifetime, BT consumption and yearly driven distance correlation for the fleet with LTO chemistry.

For the fleet with LTO chemistry the correlation is studied in Figs. 4.14 and 4.15. This study helps to understand and identify the correlation between the different factors that affect to the BT lifetime. First, the BT lifetime, BT consumption, and yearly driven distance have been correlated in Fig. 4.14. The influence of each parameter affecting to the BT lifetime can be evaluated. It is worth highlighting that the yearly driven distance is more critical than an aggressive use of the BT and a high BT consumption per kilometer, if the BT is operated within the operation limits. This is explained by the higher number

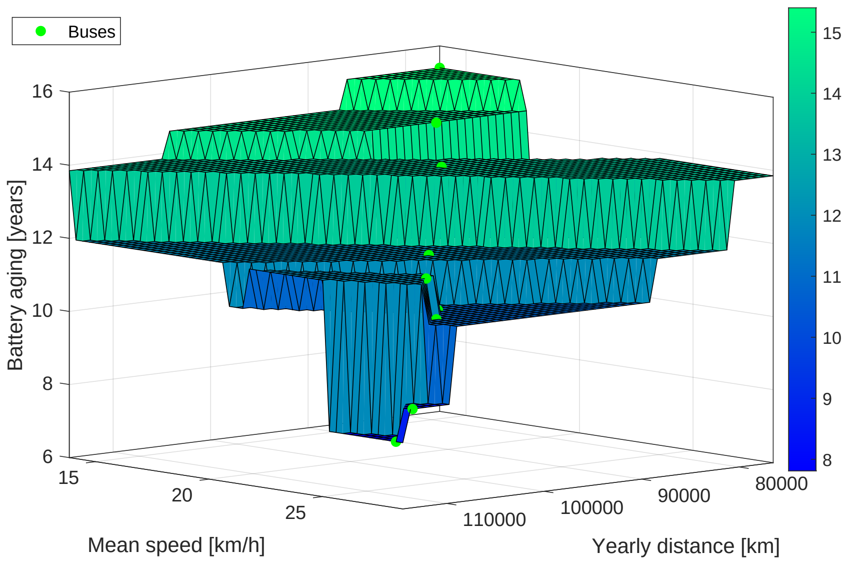

Figure 4.15: BT lifetime, mean speed and yearly driven distance correlation for the fleet with LTO chemistry.

of performed cycles and because the DOD degradation factor has a more negative effect in the degradation rather than the high c-rates. The buses with the lowest BT lifetime are those that have higher yearly driven distances with deeper cycles and lower BT consumption (lower c-rates). The correlation of BT lifetime, mean speed, and yearly driven distance is shown in Fig. 4.15. It is important to highlight that the longest routes match with the highest mean speeds. Higher driven distances involve a higher use of the BT, reducing the lifetime consequently.

4.4.3.2 Routes Re-Organization of the Fleet with NMC

For the fleet with NMC chemistry, the detailed BT lifetime is shown in Fig. 4.16, which varies from the previous LTO based fleet. Based on the buses BT lifetime estimation in Fig. 4.16, buses re-organization is performed. To make the most of the BT, the median of the fleet buses BT lifetime has been set as the BT lifetime horizon of 4 years.

In Fig. 4.16, the least demanding, most demanding and average demanding routes have been grouped. In contrast to the LTO bus fleet, due to the the applied FEC constraint in the NMC BT Wöhler, the least demanding line in NMC bus fleet is the tenth route and not the third one. The least demanding routes match with those routes that have the shortest cycle and daily driven distance and the lowest average speed, in this case lines 3, 4 and 10. Only route 5 has lower mean speed and

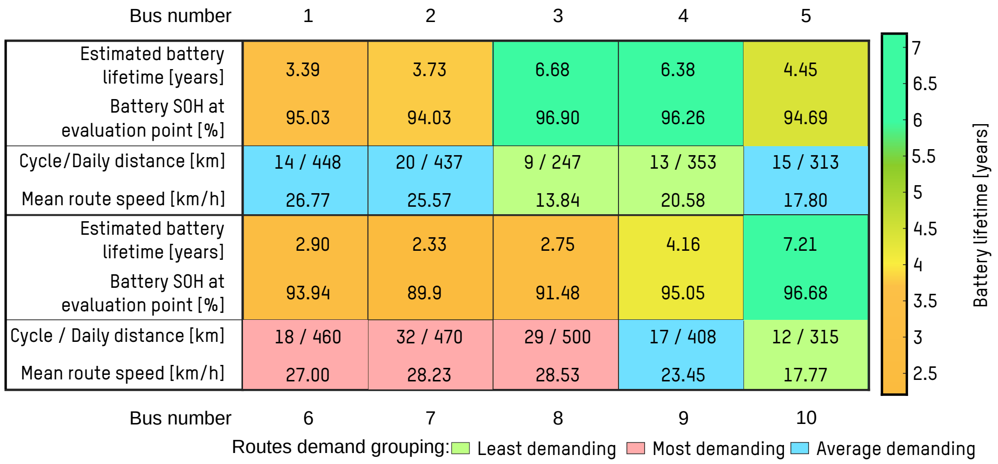

Figure 4.16: BT SOH evaluation and lifetime estimation of the NMC based fleet.

shorter driven distance than line 4. However, line 5 has a lower BT lifetime, due to the higher aggressiveness than the other routes. The most demanding routes are those with a longer cycle, daily distance, and a higher average speed, identifying routes 6, 7 and 8 in this class. The main reason for this fact, in comparison with lines 6 and 8, is the longer cycle length, that depletes more the BT and consequently degrades more the BT. Finally, the remaining routes that have an average BT degradation, have been grouped in the average demanding class. In the buses that operate in these routes, the EMS have been updated, but they do not participate in the route re-organization process, since for achieving the buses BT lifetime target of 4 years their current BT lifetime is within the 20% threshold of the lifetime horizon target.

In Table 4.8, the routes re-scheduling is sum-up. Bus number 10 that was operating in line 10 has been exchanged for the most demanding line 7. Bus number 7 that was operating in the most demanding route, has been exchanged for the least demanding route 10. The same decisions have been applied for the second and third most and least demanding lines, 3, 4, 6 and 8 respectively. Bus number 3 has been exchanged for line 8, bus number 8 for line 3, bus number 4 has been exchanged for line 6 and bus number 6 for line 4.

In Figs. 4.17 and 4.18, the correlation between the buses operation factors affecting to the BT lifetime degradation has been also analyzed. As studied in the fleet of buses with LTO chemistry, first the BT lifetime, BT consumption, and yearly driven distance have been correlated in Fig. 4.17. The obtained picture follows the same pattern as the fleet of buses with LTO chemistry with lower BT lifetimes. The lowest buses BT lifetime is again given in the highest yearly driven

Table 4.8: Buses and routes exchanging of the NMC based fleet.

Group	Bus number	Current line	Exchanged for line
Best SOH	3	3	8
	4	4	6
	10	10	7
Worst SOH	6	6	4
	7	7	10
	8	8	3

distances routes, since the BTs degrade faster owing to the number and depth of the cycles. As shown in Fig. 4.18, the BT lifetime, mean speed, and yearly driven distance correlation follows a very linear pattern, being directly correlated the mean speed, BT lifetime, and yearly driven distance. The longest routes are the extra urban routes with higher mean speeds than the urban routes. The deeper cycles of the extra urban routes affects in a negative way the BT degradation.

4.4.4 EMS Update Decision Maker based on Buses Battery Aging: Technical Analysis

The fleet of buses with LTO chemistry and the fleet of buses with NMC chemistry EMS update have been technically analyzed and compared. In the

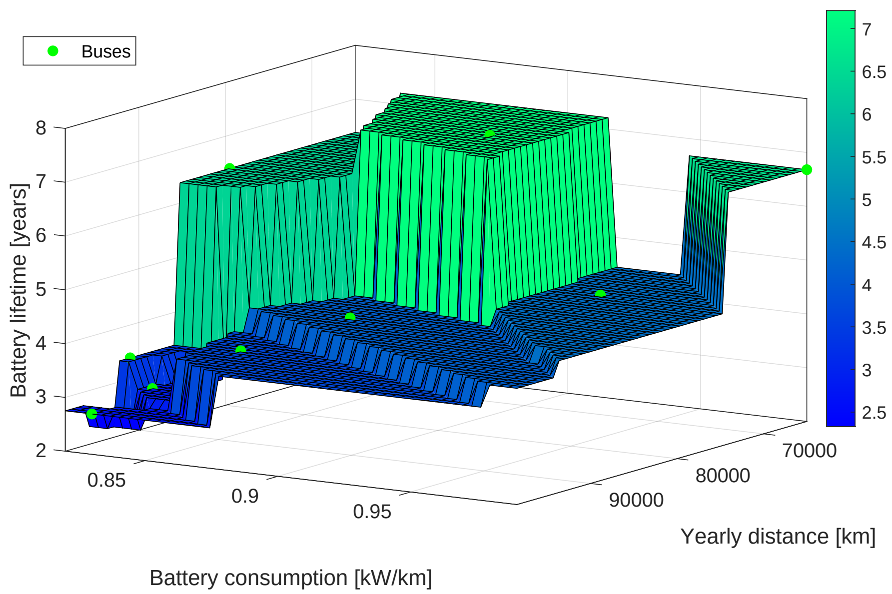

Figure 4.17: BT lifetime, BT consumption and yearly driven distance correlation for the fleet with NMC chemistry.

technical evaluation, the fuel consumption, and BT lifetime have been analyzed. Furthermore, the obtained technical results for both fleets have been compared.

For the long-term *route-to-bus* EMS update, two separate technical analyses have been carried out: first, the technical fuel consumption analysis of the whole fleet and second the buses BT lifetime study of the whole fleet.

The objective is to highlight the importance of updating the EMS with the DP optimization, to make the most of the proposed hierarchical EMS. Therefore, the updated EMS and the non-updated results are technically compared for both fleets, i.e. the fleet of buses based on LTO BT and the fleet of buses based on NMC BT.

4.4.4.1 EMS Update Decision Maker based on Fuel Consumption Technical Impact

The evaluation, in terms of fuel consumption of the two fleets are shown in Tables 4.9 and 4.10. The tendency of the obtained results for the two fleets has been an increase on fuel consumption compared to the not updated fleet. The highest fuel consumption increase matches in both fleets with the buses that have the worst BT SOH. On the contrary, the buses that have been exchanged for a less demanding route have improved their fuel consumption. In spite of the obtained

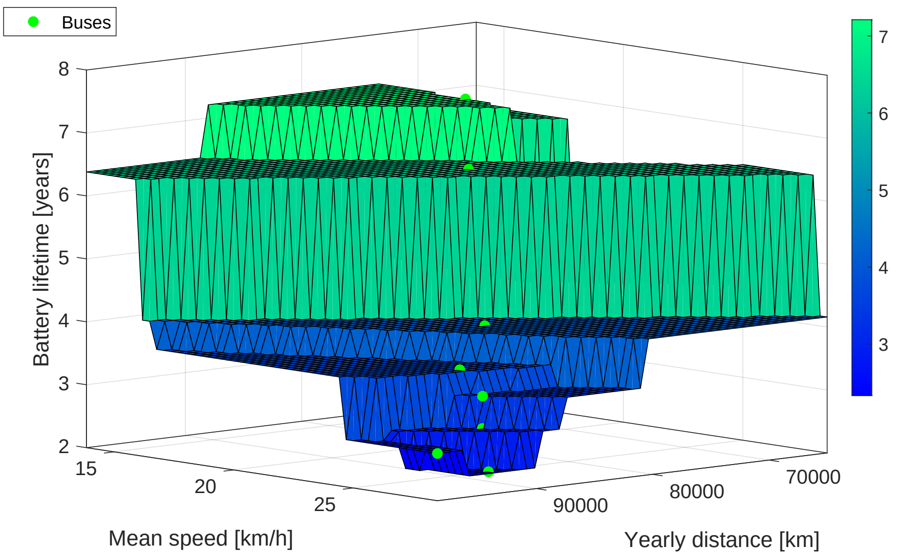

Figure 4.18: BT lifetime, mean speed and yearly driven distance correlation for the fleet with NMC chemistry.

results in terms of fuel consumption, in Subsection 4.4.5, a fleet level overall TCO improvement is shown.

As regards the fuel consumption of the LTO based fleet, the obtained results are shown in Tab. 4.9. It highlights that only the buses that have been exchanged for the less demanding to the most demanding lines (bus 3 and 10) and bus 4 have reduced the fuel consumption. All these three buses have the estimation of BT lifetime above the BT lifetime horizon (bus 3 25%, bus 4 15%, and bus 10 21% above the BT lifetime horizon) and have been corrected to decrease and fit the BT lifetime target. For these buses, the BT utilization is increased, minimizing the fuel consumption. The re-scheduled buses and exchanged for the least demanding routes 7 and 8 have the highest fuel consumption increase. This fuel consumption increase is due to the exchange for the least demanding to the most demanding routes, with an increase of 74.71 % and 31.25 % respectively. The remaining buses BT lifetime estimation was below the BT lifetime horizon, needing to increase the fuel usage in order to manage the BT lifetime to the 12 years target.

In the case of the NMC based fleet, most of the buses BT lifetime estimation are above the BT lifetime horizon, buses 3, 4, 5, 9 and 10. All these buses, except 4, have a fuel consumption decrease. In this scenario, the buses that have been exchanged for a more demanding route (buses 6, 7 an 8) except exchanged bus 6 have a fuel consumption increase. The opposite scenario is identified in the exchanged buses for less demanding routes (buses 3, 4 and 10). In this case, all the buses have a fuel consumption decrease except bus 4. The identified two exceptions matches with a exchange for the route 4 and 6, showing the opposite behavior in terms of fuel consumption. On the one hand, route 4 is in the lower edge of the least demanding group, having the lower BT lifetime estimation of the

Table 4.9: Fuel consumption of the LTO based fleet.

Buses	Fuel consumption [l/100 km] Non-update EMS	DP Re-optimization	Updated EMS	DP Error [%]	Non-updated diff. [%]
1	35.29	40.38	42.34	4.85	+19.98
2	39.81	47.04	47.80	1.62	+20.07
3	55.18	38.96	40.48	3.90	-26.64
4	39.86	35.85	38.55	7.53	-3.29
5	44.10	44.92	46.93	4.47	+6.42
6	34.52	40.24	41.79	3.85	+21.06
7	35.95	60.58	62.81	3.68	+74.71
8	36.42	45.22	47.80	5.70	+31.25
9	40.43	43.76	45.51	4.00	+12.56
10	44.84	41.22	42.34	2.71	-5.58

Table 4.10: Fuel consumption of the NMC based fleet.

Buses	Fuel consumption [l/100 km] Non-update EMS	DP Re-optimization	Updated EMS	DP Error [%]	Non-updated diff. [%]
1	35.11	38.26	40.68	6.33	+14.7
2	39.85	43.81	46.40	5.91	+15.19
3	54.57	34.89	37.01	6.08	-38.35
4	39.31	37.68	39.40	4.56	+0.23
5	43.45	37.94	40.51	6.77	-7.00
6	34.64	32.77	35.72	9.00	-3.07
7	39.19	39.32	42.52	8.14	+8.15
8	36.66	42.01	46.76	11.31	+24.21
9	40.58	36.32	38.75	6.69	-4.61
10	44.28	37.20	38.99	4.81	-12.71

group. On the other hand, route 6 is on the top edge of the most demanding lines group, having the longest BT lifetime estimation of the group. Being in the edges of both groups makes to have an opposite behavior in these two buses. Buses 1 and 2 are below the BT lifetime horizon in the average demanding group. To correct and fulfill the BT lifetime target of 4 years the fuel consumption is increased.

It is important to highlight the higher fuel consumption for the LTO based bus fleet than for the NMC based bus fleet. The higher fuel consumption is due to the higher BT lifetime increase to meet the BT lifetime horizon of 12 years for LTO comparing with the 4 years NMC BT lifetime horizon.

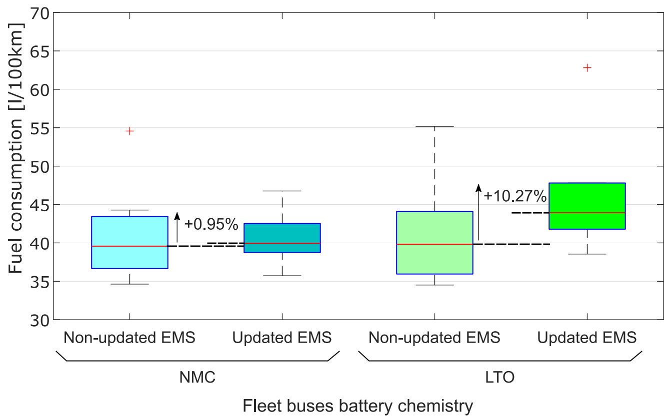

Figure 4.19: Fleets fuel consumption comparison.

Regarding the fleets fuel consumption comparison shown in Fig. 4.19, it is worth stressing the close median fuel consumption. The fuel consumption increase is higher in the case of the LTO based fleet (10.27%) than for the NMC based fleet is (0.95%). The reasoning follows the aforementioned explanation, the BT aging years to be corrected for the LTO based fleet are greater.

Table 4.11: Fleet BT aging technical evaluation of both fleet.

Buses	**LTO BT lifetime [years]**		**Non-updated diff. [%]**	**Buses**	**NMC BT lifetime [years]**		**Non-updated diff. [%]**
	Non-update EMS	**Updated EMS**			**Non-update EMS**	**Updated EMS**	
1	11.92	12.35	+3.61	**1**	3.54	4.35	+22.88
2	10.81	12.15	+12.40	**2**	3.9	4.37	+12.05
3	15.0	12.01	-22.01	**3**	6.87	4.14	-39.74
4	13.85	12.77	-7.80	**4**	6.17	4.22	-31.60
5	11.65	12.15	+9.61	**5**	4.37	4.07	+6.86
6	10.82	12.22	+12.94	**6**	3.03	4.24	+39.93
7	7.81	12.07	+54.55	**7**	2.31	4.07	+76.19
8	8.7	12.07	+38.74	**8**	2.74	4.24	+54.75
9	11.98	12.36	+3.17	**9**	4.33	4.24	-2.08
10	14.59	12.35	-15.35	**10**	6.96	4.09	-41.24

4.4.4.2 EMS Update Decision Maker based on Battery Aging Technical Impact

The applied updated EMS behavior in terms of BT lifetime management has been analyzed. The evaluation period has started in the SOH evaluation point to the end of the fleet service life. The obtained results are shown in Table 4.11. The overall buses BT lifetime of the fleet has increased up to 76.19 %. However, in those buses that have been exchanged for the most demanding lines, the BT lifetime has been reduced.

Updating the EMSs of the LTO and NMC based fleets the BT lifetime targets of 12 and 4 years respectively are fulfilled. On the contrary not updating the EMSs, buses 3, 4, 5, 9 and 10 for the NMC based fleet and buses 3 and 10 for the LTO based fleet met the goal. These buses again match with the buses with the fuel consumption reduction. To sum up, the non-updated EMS have random results, as they were initially designed for specific conditions, and these conditions have changed throughout the bus lifetime. Therefore, to ensure the BT management, the EMS needs to be updated.

In Fig. 4.20, both fleets BT lifetime are compared. The obtained median values indicated with the red line are close compared to the non-updated and updated EMS. In the case of the NMC based fleet, the median lifetime has increased 4.37%. For the case of the LTO based fleet has an increase of 3.48%. Median values so close means that the BT lifetime management is applicable. As conclusion, the fleet BT lifetime median is a good indicator for the fleet buses BT lifetime horizon target definition.

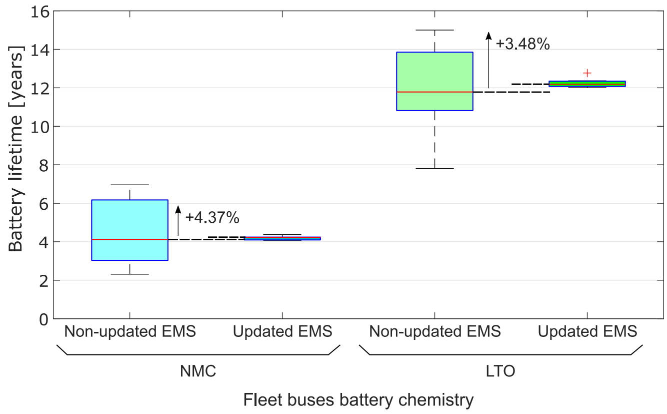

Figure 4.20: Fleets BT aging comparison.

4.4.5 EMS Update Decision Maker based on Buses Battery Aging: TCO Evaluation

After the technical evaluation, a TCO analysis has been performed. The TCO has been evaluated from the SOH evaluation point to the buses BT EOL. For the TCO evaluation of the whole fleet, the medium BT cost scenario has been applied. After this, the three cost scenarios defined in Tab. 2.7 have been analyzed for the *route-to-bus* and fleet TCO improvement rate analysis.

4.4.5.1 TCO evaluation of the Fleet with LTO Chemistry

The LTO based bus fleet TCO at vehicle level has been improved within the range of 1.14 % and 31.84 %, as shown in Fig. 4.21. This improvement has been obtained applying the proposed fleet management methodology. However, those buses that have been exchanged for the most demanding lines (routes 3 and 10) have increased their TCO at vehicle level. However, this is compensated with the avoidance of BT replacement on those buses operating in the initial period on the most demanding lines by means of the fleet manager. It is must be emphasized the operation modification for bus 7. To reach the service life target, the operation has been changed to start and finish nearly at the same SOC. This is the reason for having low energy and power costs.

To analyze the improvement and demonstrate the need to exchange buses, an evaluation for the exchanged and non-exchanged buses has been carried out, as shown in Fig. 4.22. For this analysis, low, medium, and high BT cost scenarios (LTO cost scenarios described in Tab. 2.7) have been studied in the 4 buses where exchanging has been applied. It is important to acknowledge that in the three cost scenarios an improvement is achieved, ranging from 4.19% to 5.62%.

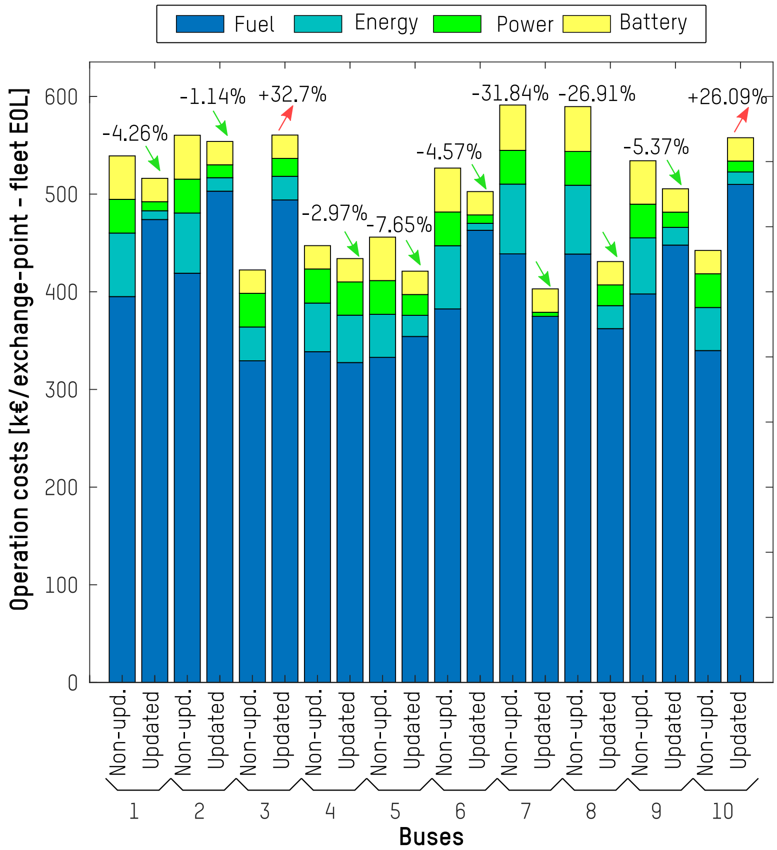

Figure 4.21: TCO of the non-updated and updated buses of the LTO based fleet.

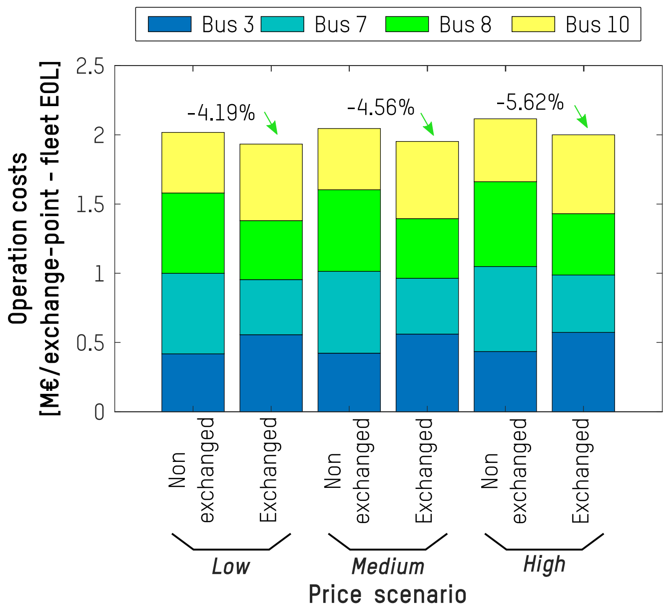

Figure 4.22: TCO analysis of non-exchanged and exchanged buses of the LTO based fleet.

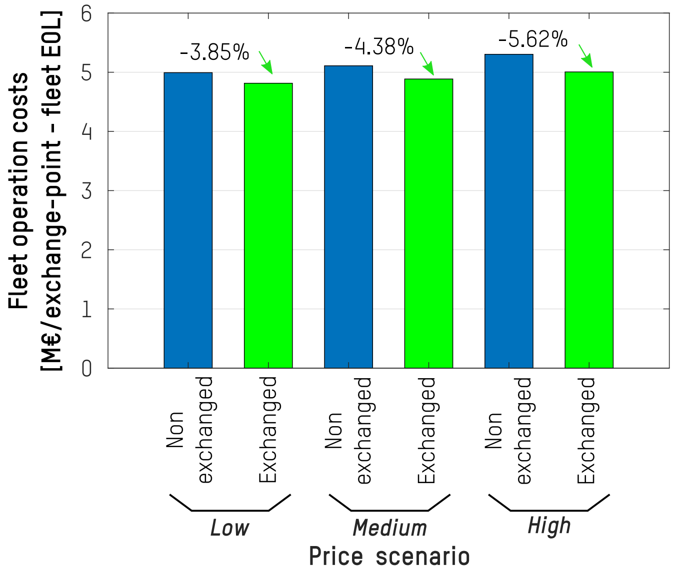

Figure 4.23: LTO based fleet TCO analysis of the non-updated/non-exchanged and updated/exchanged buses.

Regarding the fleet total TCO improvement analysis, the three price scenarios have also been evaluated as depicted in Fig. 4.23. With the proposed approach, the buses BT lifetime requirements are met and a TCO improvement has been achieved. In the low, medium and high BT price scenario a fleet TCO improvement of 3.85%, 4.38% and 5.62% has been achieved respectively .

4.4.5.2 TCO evaluation of the Fleet with NMC Chemistry

The scenario from the evaluation point until the buses EOL has been evaluated, being defined at 12 years.

For the case of NMC based fleet, an improvement from 0.4 % to 29.27 % has been obtained, as shown in Fig. 4.24. As happened for the LTO based fleet, those buses that have been exchanged for the most demanding lines (routes 3, 4 and 10) have increased their TCO. The rest of the buses TCO has been improved managing their BT lifetimes.

As it has been done for the LTO bus fleet, to analyze the improvement and demonstrate the need to exchange some buses, an evaluation of exchanged and non-exchanged buses has been carried out and depicted in Fig. 4.25. For this analysis low, medium, and high BT cost scenarios for NMC have been studied with the 6 buses that have been exchanged. It is important to underscore that in the three cost scenarios an improvement is achieved, ranging from 2.72% to 3.06%.

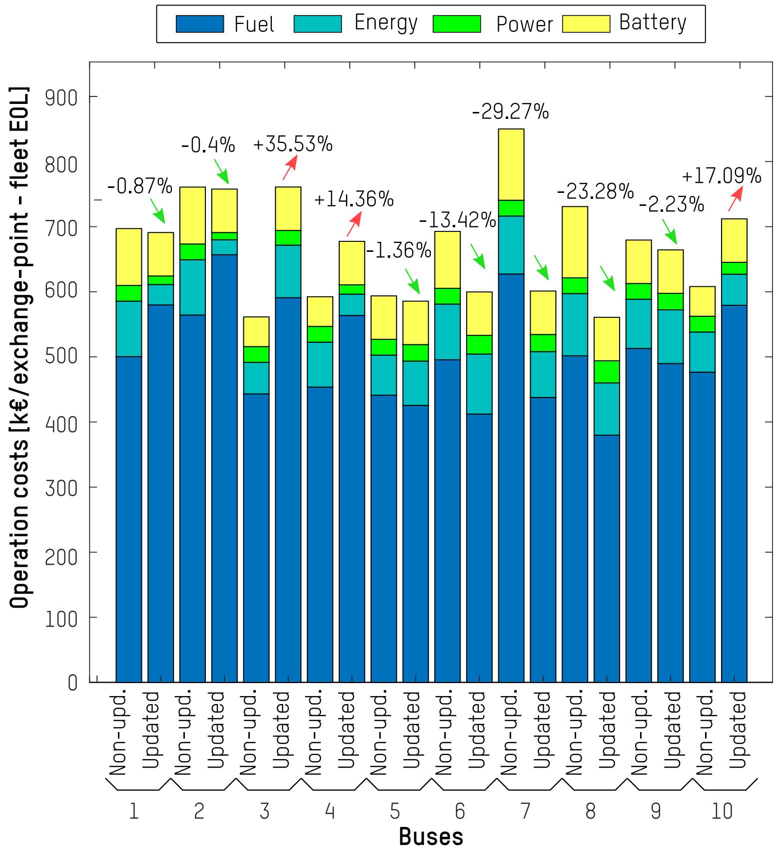

Figure 4.24: TCO of the non-updated and updated buses of the NMC based fleet.

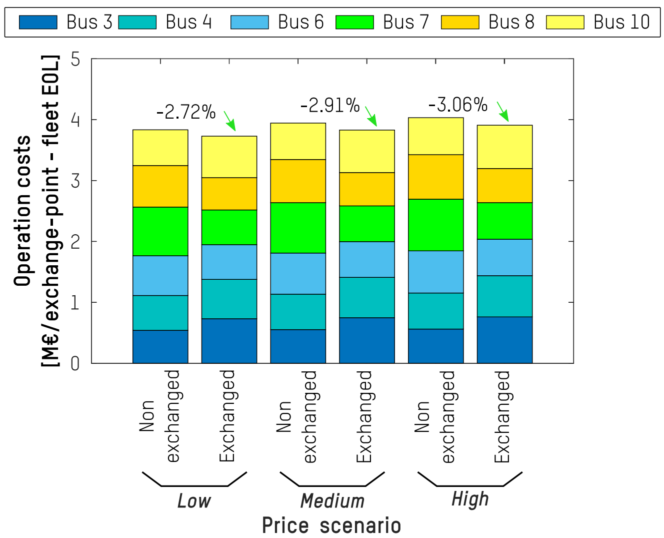

Figure 4.25: TCO analysis of non-exchanged and exchanged buses of the NMC based fleet.

The whole fleet TCO improvement has been represented in Fig. 4.26. In the three BT price scenarios, a TCO improvement has been achieved. The achieved fleet TCO improvement for the low, medium and high BT price scenarios, has been of 1.84%, 2.1%, and 2.3% respectively.

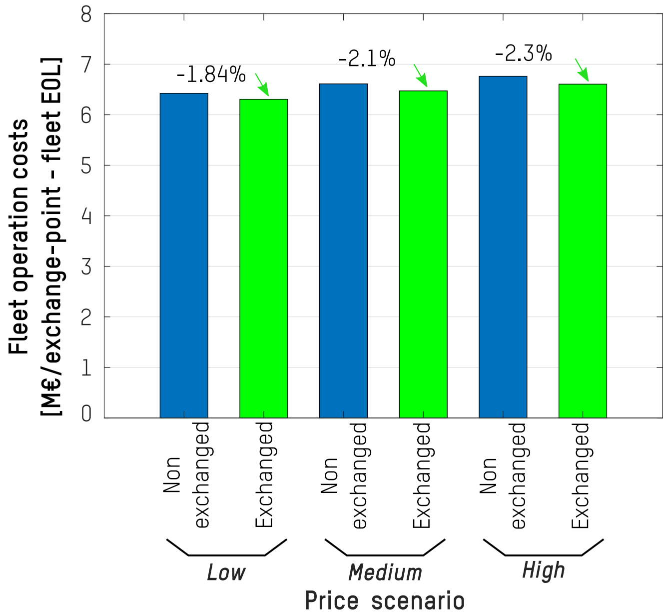

Figure 4.26: NMC based fleet TCO analysis of the non-updated/non-exchanged and updated/exchanged buses.

4.5 Conclusions

In this chapter a hierarchical EMS for TCO management at fleet level has been proposed. The proposed approach is based on a hierarchical decision maker with a management composed of three levels. The upper level is the offline data exploitation and decision making at fleet level, to perform the fleet energetic management with the upper fleet level point of view executed in the cloud. The fleet level makes the decisions for the next lower level, the offline optimization, and strategy design at vehicle level. This intermediate level optimizes the operation and designs the ANFIS based EMS for each bus also in the cloud. Finally, at the lower level, in the online operation level, the developed ANFIS based EMS is operated onboard on each bus in real time. This lower level, to determine the split factor of the available power sources in the bus in the most efficient way.

As a result, three fleet management techniques have been defined. The bus-to-route vehicle level management, the route-to-bus fleet re-organization, and the route-to-bus fleet buses energy management strategy update. Performing the first technique bus-to-route vehicle level management, the fleet of buses can be adapted to the optimal operation of each route. The second route-to-bus fleet re-organization technique, performs a buses re-organization. The third technique updates the online EMS throughout the bus lifetime. These decisions are made based on the developed BT lifetime evaluation plan of the fleet, to meet the planned TCO requirements. The proposed hierarchical EMS has been analyzed in two fleets: LTO BT based fleet and NMC BT based fleet.

The conclusions are summarized as follows:

- The proposed *bus-to-route* approach to adapt each bus operation to each route from the initial moment to the end of the fleet service life, replicating the DP optimal operation by means of the ANFIS based EMS. This EMS improves the local efficiency of each bus composing the fleet. In the studied two case studies, technical and economic improvements have been obtained in both fleets, obtaining close results to the DP optimal operation in terms of fuel consumption.

- The *route-to-bus* fleet re-organization is applied once the fleet operation arrives to the defined evaluation point, targeting to balance the critical BT lifetimes of the buses. The buses with the BT lifetime estimation 20% above the BT lifetime horizon and the buses with the BT lifetime estimation 20% below the BT lifetime horizon are exchanged for manage the BT lifetimes.

Fleet re-organizations have been performed in two different fleet (LTO and NMC) scenarios. In the first scenario, a LTO based fleet of vehicles without replacements has been studied. On the contrary, in the second scenario, a NMC based fleet of vehicles with periodically planned replacements has been analyzed. Three BT cost scenarios have been defined, to analyze different future scenarios. In the analyzed scenarios, the re-organized fleet TCO has been improved compared to the non-re-organized fleet. The fleet re-organization,consequently, provides the possibility to balance those buses with the worst and best BT SOHs, avoiding unnecessary extra BT replacements or buses arriving to the fleet service EOL with a high BT SOH.

- As a secondary fleet energy management measure, the EMS update has been proposed. The ANFIS based EMS update allows to combine the short-term overall vehicle efficiency targets with the long-term BT lifetime objective. In this way, the management takes advantage of all the available resources to improve the TCO of the whole fleet further. As a conclusion, when managing a fleet of vehicles, the fuel consumption minimization is a key factor for short-term management. However, for the whole fleet TCO improvement, the long-term buses BT lifetime must be considered.

5

Conclusions and Future Research

Summary

In this final chapter the main conclusions, key findings, and contributions of the present Ph.D. thesis in the field of the fleet energy management are collected. Finally, future research are pointed out.

5.1 Conclusions

Energy management at vehicle and fleet level has been studied. The focus has been on the road public transport electrification, more specifically on fleet of buses. The digitalization new trend that allows to have additional information of the operation, increased computational resources or decentralized management structures. These new resources make possible to integrate advance energy management strategies and widen the degrees of freedom to optimize the total cost of ownership of a whole fleet. The total cost of ownership is a key aspect to manage to make the best use of the available resources onboard the bus. In this scope, two main potential candidates for the present and near future public transport electrification solutions have been studied: Plug-in Hybrid Electric Buses and Fuel-Cell Hybrid Electric Buses.

The most relevant gaps in the state-of-the-art regarding fleet energy management can be split into two. On the one hand, the digitalization for managing energetically a fleet of vehicles for the total cost of ownership improvement by means of learning based energy management strategies. On the other hand, the exploration and application of the new discovered degrees of freedom derived from the fleet level point of view.

To address an aforementioned first gap, a novel adaptive neuro-fuzzy inference system learning based energy management strategy conscious of the battery aging has been developed for the vehicle level energy management. This learning based energy management strategy allows to combine the short-term and long-term management. On the one hand, the instantaneous power/energy short-term management to achieve close results to the dynamic programming optimal operation. On the other hand, the buses battery state of health long-term management evolution.

The adaptive neuro-fuzzy inference system technique takes advantage of the data acquisition, data storage, and cloud computing solutions provided by the digitalization. It allows to directly learn from the optimized scenario in different operating conditions, adapting the buses operation to each route and managing the power sources in an efficient way.

To address the second gap, a hierarchical fleet energy management strategy, that includes the adaptive neuro-fuzzy inference system energy management strategy as part of the hierarchical architecture has been proposed. The fleet energy management strategy allows to apply the discovered new degrees of freedom from the fleet level point of view. The primary bus-to-route fleet management, aiming to adapt each bus operation to each route. The route-to-bus fleet re-organization has been proposed as the secondary fleet management approach, aiming at balancing the most critical buses batteries lifetime. As a third technique, the bus-to-route adaptive neuro-fuzzy inference system energy management strategy update has been identified. This update allows to take advantage of continuous motorization solutions offered by the digitalization and update the operation to the new conditions of the bus throughout the fleet lifetime.

Therefore, the main contribution of this Ph.D. thesis is *the development of a hierarchical energy management strategy at fleet level to optimize the total cost of ownership of a whole fleet, allowing to ensure the minimum operating cost of vehicles while ensuring the buses battery lifetime for the planned battery replacement horizon.*

The adaptive neuro-fuzzy inference system learning based energy management strategy evaluation at vehicle level has been tested in different scenarios. The adaptive neuro-fuzzy inference system technique enables to replicate and obtain really close results to the dynamic programming optimal operation. Therefore, the obtained results in terms of fuel consumption and battery aging are really close to the optimal ones. The real-time validation of the adaptive neuro-fuzzy inference system based energy management strategy has been performed in a hardware-in-the-loop platform, which proves the ability to run the adaptive neuro-fuzzy inference system based energy management strategy in real-time.

The similarity of the series plug-in hybrid electric bus powertrain to the parallel fuel cell hybrid electric bus powertrain allows to directly apply the developed solutions in both types of vehicles. In this way, it has been demonstrated that the solution for the series plug-in hybrid electric bus powertrain is applicable for the parallel fuel cell hybrid electric bus powertrain. The direct application paves the way and provides solutions for the oncoming fuel-cell hybrid electric buses, facilitating their integration and reducing the offset costs compared to other technologies.

The upper fleet level point of view offers new degrees of freedom, allowing to fulfill the fleet buses battery lifetime evaluation plan. Three techniques have been developed, the bus-to-route, the fleet re-organization, and the adaptive neuro-fuzzy inference system energy management strategy update. The primary bus-to-route fleet management, optimize each bus operation for each route in the fleet. The secondary fleet re-organization exchanges the buses with the best and worst battery state of health, aiming at managing the battery degradation in new routes. As third management technique, the update of the fleet adaptive neuro-fuzzy inference system energy management strategy update has been proposed. This technique is applied to the whole fleet to fulfill the battery lifetime target with the lowest operation costs.

The developed hierarchical fleet energy management strategy has been analyzed in two case studies: a fleet of buses with LTO battery chemistry and a fleet of buses with NMC battery chemistry. These two case studies have allowed to provide and analyze solutions for a fleet of vehicles without battery replacements and a fleet of vehicles with periodically planned battery replacements. For these two scenarios, first, a fleet buses battery lifetime evaluation plan has been defined, based on the fleet battery lifetime estimation. The correct compliance of the developed battery lifetime plan ensures improving the total cost of ownership of the whole.

As a general conclusion, it can be stated that the present Ph.D. thesis has contributed to the topic of energy management, providing solutions for the vehicle and fleet level total cost of ownership improvement, ensuring the minimum operation costs and managing the battery lifetime according to the developed fleet battery lifetime plan. In this regard, evaluations in different scenarios with different battery chemistries, such as LTO and NMC, and with different powertrains, plug-in hybrid electric buses and fuel-cell hybrid electric buses, have been performed. All these scenarios have been analyzed based on the developed Digi e-FLeet simulation platform (registered as software license). This simulation platform allows to study different vehicle types, battery chemistries, and routes. As outputs, the fleet operation and the total cost of ownership are obtained. It is important to underline that the obtained results are closely related to the case studies and developed bus models. In this way, the conclusions have been related to the qualitative results and not to the quantitative results.

5.2 Future Work

From the work developed in the Ph.D. thesis, future research have been:

- The integration of the battery state of health information as an input in the ANFIS based energy management strategy. Optimizations of different state of health levels have to be performed and included in the data-base used for the learning process. This will allow to develop a self adaptive energy management strategy conscious of the battery state of health. This development is under the process to be patented.
- The energy management strategies analysis with a more reliable genset dynamic model and characterized fuel cell model. This integration will allow to take a step closer to the results that will be obtained in a real operation. It is worth mentioning that the obtained results in this Ph.D. thesis are closely related to the case studies and considered bus models and reference data. So, the results are highly dependent on input data. In this regard, the more reliable inputs, the more realistic will be the quantitative results.
- The fuel-cell aging factors have been analyzed and taken into account for the development of the fuel-cell hybrid electric bus ANFIS energy management strategy. However, the lifetime management margin of the fuel-cell was not possible to quantify. The implementation of a fuel-cell aging to the methodology will allow to integrate the fuel-cell lifetime in the battery evaluation plan and manage it throughout the bus lifetime.
- The developments of this Ph.D. thesis have been related to hybrid buses, that have more degrees of freedom owing to the multiple power sources onboard. Regarding the battery electric buses the degrees of freedom are more constrained, limited to the charging and auxiliary consumption efficiency improvement. The continuous monitoring of the digitalization allows to follow closely the auxiliary elements behavior and consumption. Having the auxiliary consumption information will make possible to develop auxiliary elements models. In this regard, the energy management of the auxiliary elements has been identified as a potential point to increase the degrees of freedom. The auxiliary consumption management will allow to improve the overall efficiency of the bus, consequently reducing the energy consumption, recharging time and maximizing the battery lifetime.
- Following the current trend of the development and implementation of new buses solutions, in a near future, a mixed fleet scenario is foreseen. Therefore,

an extended evaluation of the proposed hierarchical fleet energy management strategy on a mixed fleet scenario is proposed.

A

Fleet Buses Battery Aging Evaluation Points Definition for Route-to-Bus Applications

A.1 Fleet Buses Battery Evaluation Point Definition

The battery aging evaluation point definition is crucial, since it is the point where the *route-to-bus* fleet management approach is performed. At this point, the long-term management decisions are made. The BT aging management is considered a long-term management and it has to be performed having the sufficient margin to correct and fulfill the predefined lifetime target. The starting point is with the fleet BT aging scenario, as depicted in Fig. A.1A. In this scenario,

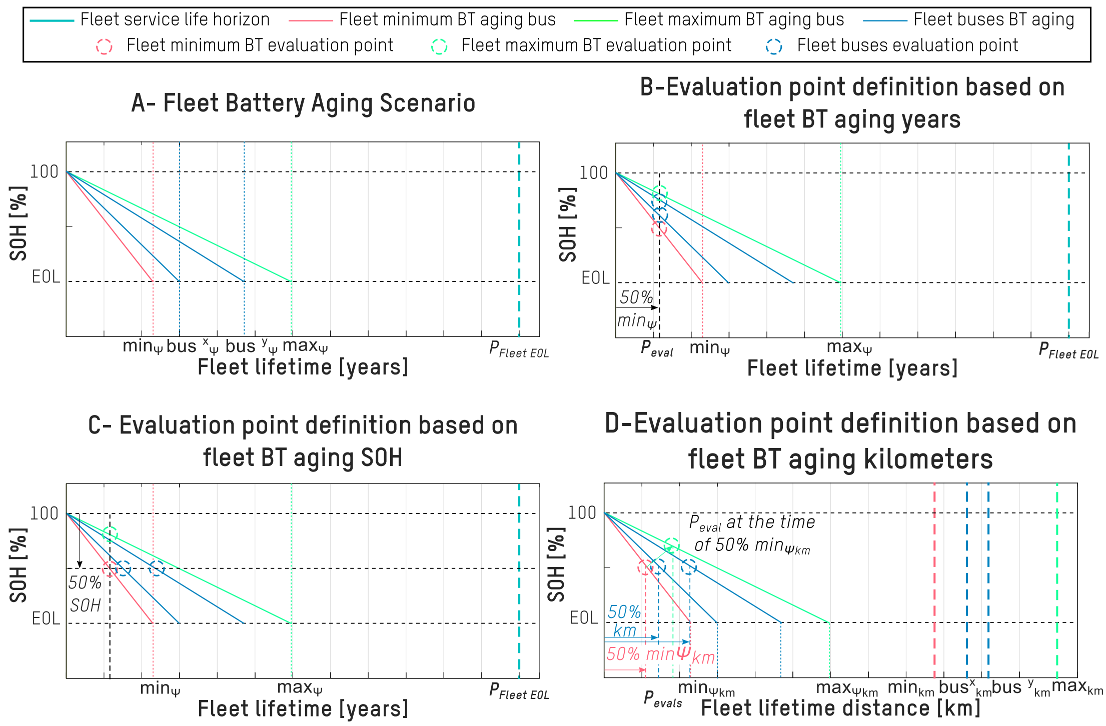

Figure A.1: A: Fleet BT aging scenarios, **B**: Evaluation point definition based on years evaluation, **C**: Evaluation point definition based on SOH evaluation and **D**: Evaluation point definition based on kilometers evaluation.

Bus number	1	2	3	4	5
Estimated battery lifetime [years]	3.39	3.73	6.68	6.38	4.45
Estimated battery lifetime [years]	2.90	2.33	2.75	4.16	7.21
Bus number	6	7	8	9	10

Figure A.2: NMC based fleet BT lifetime initial picture.

the buses lifetime (bus^n_Ψ bus^m_Ψ), minimum (min_Ψ) and maximum (max_Ψ) bus BT lifetimes have to be estimated and fleet EOL point ($P_{FleetEOL}$) has to be defined. With this information, the fleet buses BT lifetime estimation heat map has to be built. In this heat map, the estimated BT lifetimes of the fleet is shown, as depicted in Fig. A.2.

Once the *route-to-bus* evaluation point has been defined, all the routes are re-optimized with DP and the buses BT lifetimes are estimated, to ensure that the buses fulfill the BT lifetime target.

Analyzing the fleet BT lifetime, three evaluation point definition techniques have been studied for the NMC based fleet, with the aim to evaluate the best solution to define the evaluation point. The NMC based fleet allows to study a fleet with multiple replacements. The three evaluation point definition techniques are the following ones: years evaluation, SOH evaluation and kilometers evaluation, which are shown in Fig. A.1 B, C and D respectively.

Evaluation point definition based on fleet BT aging years: When defining the evaluation point based on the buses operating years, the bus with the minimum BT aging (min_Ψ) has to be identified. The evaluation point for all the fleet is defined the half of the minimum BT aging bus, as shown in Fig. A.1B. The EOL of the BT is limited at 80% of BT SOH or calendar degradation, as explained in Sec. 2.4.

Evaluation point definition based on fleet BT aging SOH: The second evaluation point definition method has been based on the SOH monitoring. In this case, the buses with the minimum and maximum BT agings (min_Ψ and max_Ψ) have to be identified. The evaluation point is defined for each bus in the half of SOH, except for those that have to be exchanged. The exchange process is performed for two buses. The bus with the minimum BT aging evaluation point is defined in the half of the SOH. At this point, the evaluation point for the bus with the maximum BT aging is defined. The bus with the best BT SOH will have a greater SOH than the half. Both buses are evaluated and the routes are exchanged.

Evaluation point definition based on fleet BT aging kilometers: The last evaluation point definition is carried out based on the fleet kilometers. Again the buses with the minimum and maximum BT agings (min_Ψ and max_Ψ) have to be identified, however, the estimation has to be done in kilometers. Based on the fleet operation planning, route to drive in, number of round trips and daily operation, the lifetime operation kilometers are calculated. This operation information is used to estimate the kilometers to be performed, until the BT arrives to the EOL. The evaluation point is defined for each bus in the half of the estimated kilometers to be performed without replacements, except for those that have to be exchanged. As it has been explained in the previous case, the exchange of the buses has to be performed for two buses. The bus with the minimum BT SOH sets the evaluation point for the bus to be exchanged. As in the case study for the SOH evaluation point definition, both buses are evaluated and the routes are exchanged.

A.1.1 Evaluation Point Definition Based on Fleet Battery Aging Years

The first case scenario is the one in which the evaluation point is defined by the years. The evaluation point has been established in the year 1.17, since this year the bus 7 (bus with the minimum BT lifetime estimation) arrives to the half of SOH.

In Tab. A.1, it is shown the fleet buses battery status at the evaluation point based on the years.

Table A.1: NMC based fleet BT status at the evaluation point based on years.

Bus	**Years**	**SOH**	**Kilometers**
1	1.17	93.10	159,000
2	1.17	94.03	150,000
3	1.17	96.50	84,800
4	1.17	96.26	120,000
5	1.17	94.69	107,000
6	1.17	91.94	157,000
7	1.17	89.90	173,000
8	1.17	91.48	171,000
9	1.17	94.38	140,000
10	1.17	96.68	108,000

The TCO of each bus has improved from 0.4 % up to 29.27 %, as shown in Fig. A.3, except for the exchanged buses. More specifically the buses that have been exchanged for the most demanding lines (routes 3, 4 and 10) have increased their own TCO. However, the BT aging estimation of the buses operating in the most demanding routes in the initial period have been corrected with the buses exchange. The exchange and EMS update have allowed to replace the BTs at the predefined point..

For analyzing the range of improvement and demonstrate the need for exchange

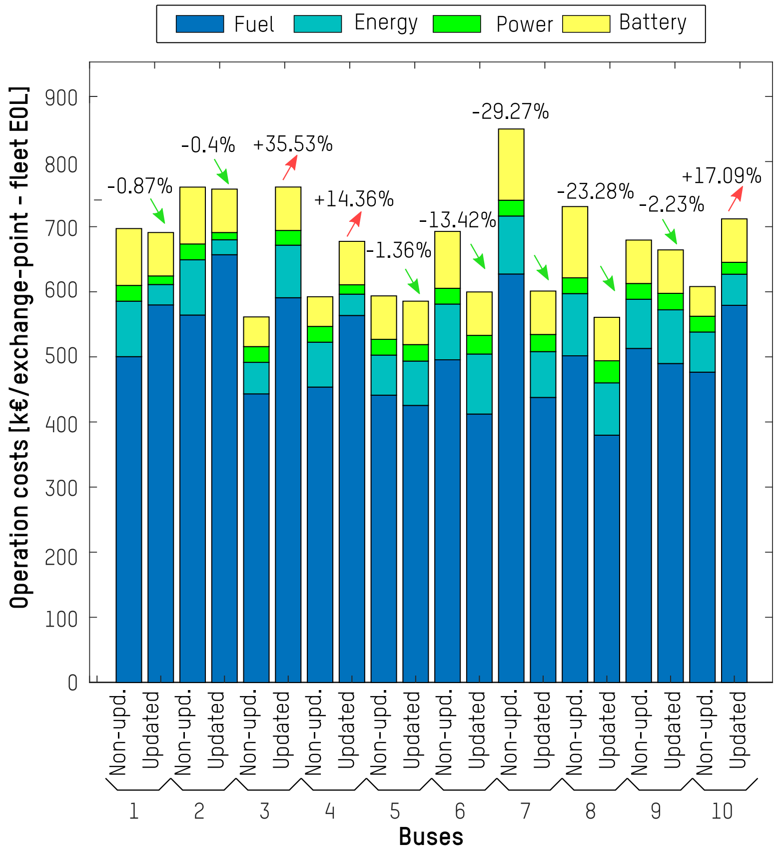

Figure A.3: TCO of non-updated and updated buses.

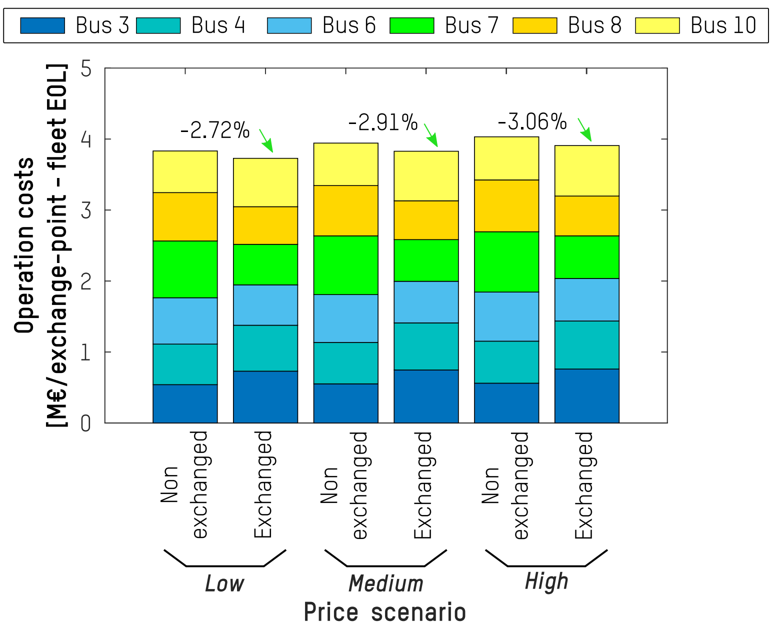

Figure A.4: TCO evaluation exchanged and non-exchanged buses.

the buses, an evaluation of the exchanged and non-exchanged buses has been carried out, as shown in Fig. A.4. Low, medium and high BT cost scenarios (NMC cost scenarios described in Tab. 2.7) have been studied in the 6 buses where exchanging has been applied. It is imporatnt to note that in the three cost scenarios an improvement is achieved, ranging from 2.29% up to 2.62%.

Regarding the overall fleet TCO improvement analysis, the three price scenarios have been evaluated. In the proposed approach, the buses BT lifetime requirements and TCO model are achieved. The obtained TCO at fleet level results for the low, medium, and high BT price scenarios an improvement of 1.84%, 2.1% and 2.3% has been achieved respectively.

A.1.2 Evaluation Point Definition Based on Fleet Battery Aging State of Health

In the second case study, the evaluation point has been defined according to the SOH. The evaluation point has been carried out when the buses BT lifetime arrive at the half of the BT SOH EOL for each bus. Following the previous evaluation point definition, the buses that have to be exchanged for the most demanding lines are excluded. This is the case for buses 3 and 8 at year 1.19, buses 4 and 6 at year 1.34 and bus 10 and 7 at year 1.24, as shown in Tab. A.2.

Table A.2: Fleet buses battery status at the evaluation point based on SOH.

Bus	**Years**	**SOH**	**Kilometers**
1	1.63	90.36	242,000
2	1.70	91.22	245,000
3	1.19	92.23	96,900
4	1.34	91.59	155,000
5	2.57	91.80	265,000
6	1.34	90.76	203,000
7	1.12	90.99	175,000
8	1.19	90.71	196,000
9	1.85	91.09	249,000
10	1.24	96.40	117,000

Compared to the previous evaluation point definition technique, an additional bus to the exchanged buses for a more demanding line (buses 3, 4 and 10) has worsen the TCO, the 9. bus. The obtained improvement ranges are comprised between 0.6 % up to 26.84 %, as shown in Fig. A.5. Even thought worse results than in the previous study have been obtained, an improvement of the TCO in the exchanged buses is achieved compared to the non-exchanged buses. These improvement are comprised between 0.22% up to 0.78%, evaluating the different BT price scenarios.

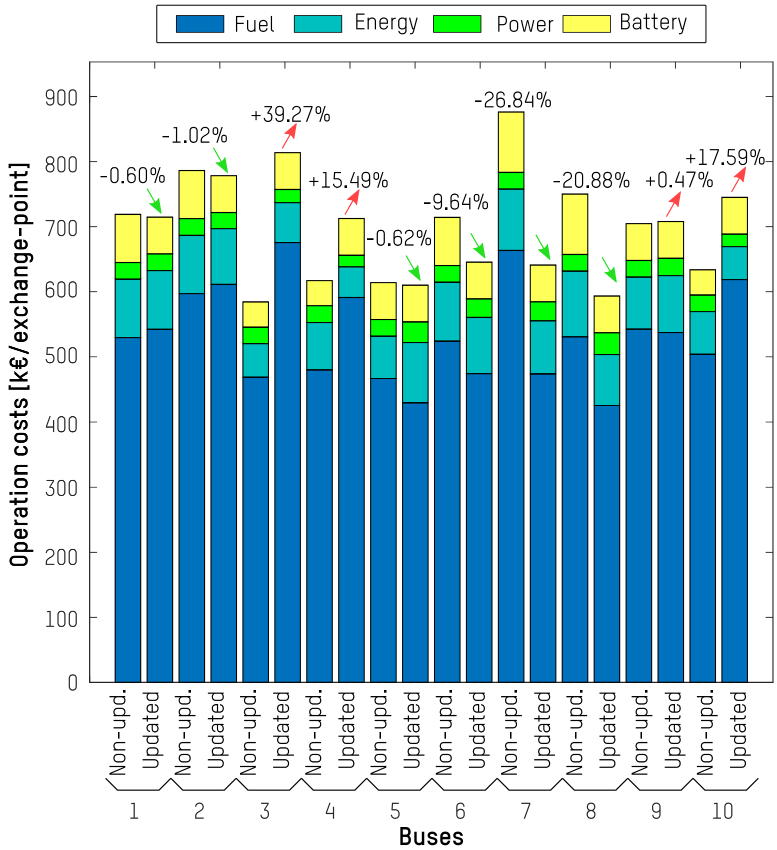

Figure A.5: TCO of non-updated and updated buses.

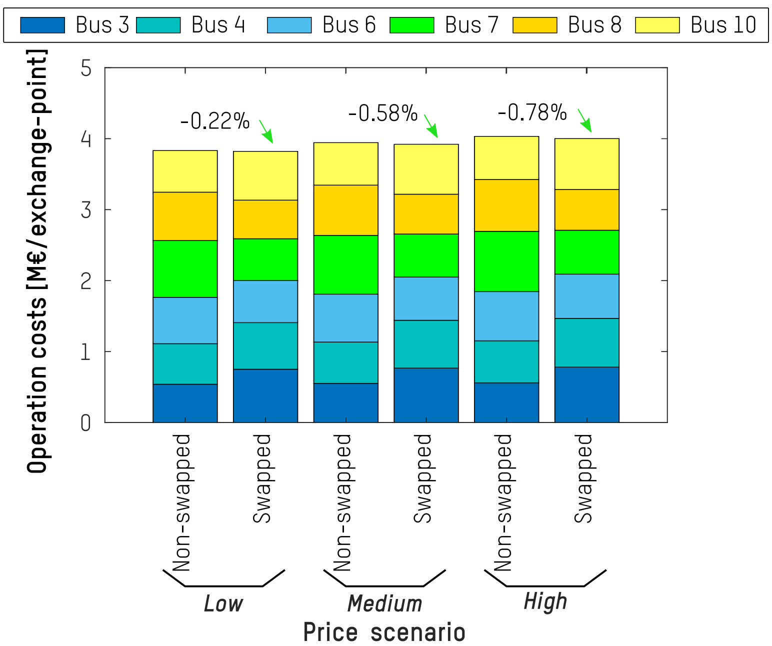

Figure A.6: TCO evaluation exchanged and non-exchanged buses.

The overall fleet TCO improvement obtained for the low, medium and high BT price scenarios has been of 0.04%, 0.33%, and 0.55% respectively.

A.1.3 Evaluation Point Definition Based on Fleet Battery Aging Kilometers

In the last case study, the evaluation point is defined by the kilometers. The kilometers evaluation requires the study performed in Subsec. 4.2, to determine the kilometers to operate each bus. According to this operation, the kilometers performed by each bus until the BT arrives to the BT EOL is estimated. From the estimated kilometers for each BT lifetime, the evaluation point has been defined in the half of kilometers. The buses that have been exchanged are excluded from this evaluation point, to perform the exchange of buses and manage the BT lifetime. This is the case for buses 3 and 8 at year 1.4, buses 4 and 6 at year 1.48 and bus 10 and 7 at year 1.17, as shown in Tab. A.3.

Table A.3: Fleet buses battery status at the evaluation point based on kilometers.

Bus	Years	SOH	Kilometers
1	1.72	89.86	234,000
2	1.87	90.39	239,000
3	1.40	95.81	102,000
4	1.48	95.22	154,000
5	1.21	89.86	203,000
6	1.48	89.80	200,000
7	1.17	89.90	173,000
8	1.40	89.74	205,000
9	1.70	91.83	203,000
10	1.17	96.68	108,000

Analyzing the TCO of each bus, more buses have worsen the TCO compared to the previous two techniques. Applying this technique, in addition to the exchanged buses 3, 4 and 10 for worse routes, buses 1, 5 and 9 have worsen their individual TCO. However, at fleet level an improvement comprised from 0.46 % to 29.52 % has been obtained, as depicted in Fig. A.7.

As analyzed in the previous two case studies, an evaluation for the exchanged and non-exchanged buses has been carried out, as shown in Fig. A.8. For this analysis, the same BT cost scenarios have been studied in the 6 buses where exchanging has been applied. It is should be emphasized that in the three cost scenarios an improvement is achieved, ranging from 0.89% up to 1.32%.

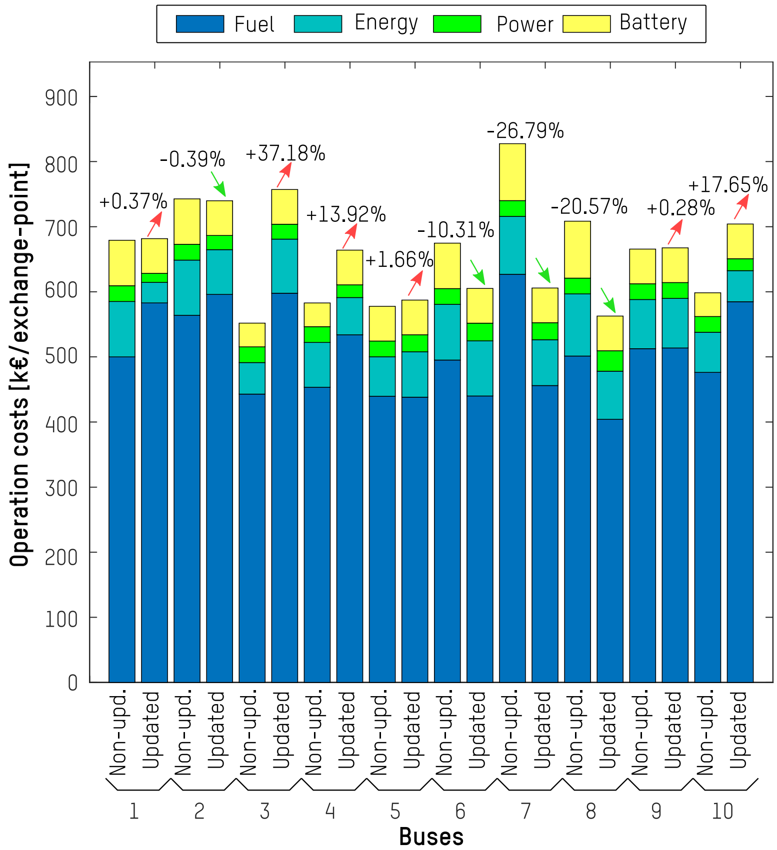

Figure A.7: TCO of non-updated and updated buses.

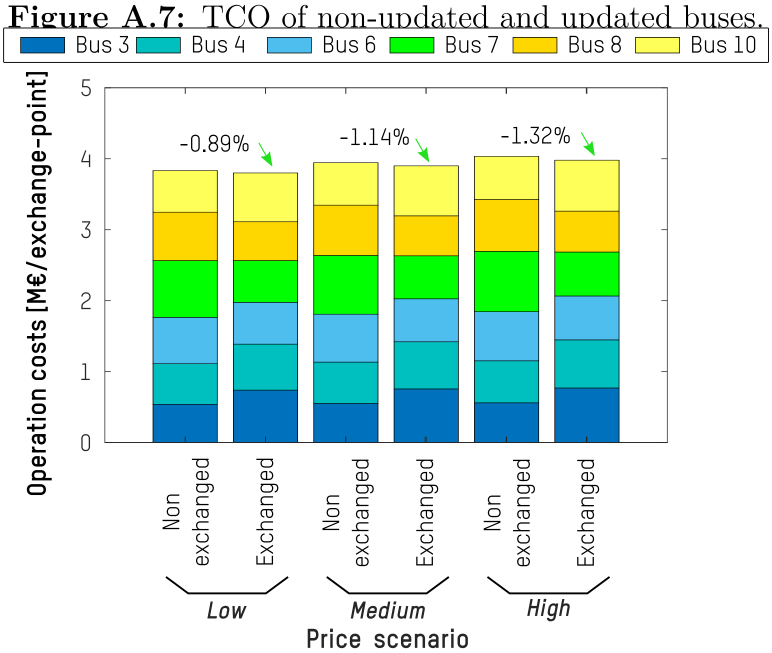

Figure A.8: TCO evaluation exchanged and non-exchanged buses.

With the last technique, even though the worst results have been obtained compared to the previous scenarios, still an improvement of the TCO at fleet level has been obtained. In addition, the planned BT replacements have been achieved. The obtained overall fleet TCO improvement for the studied three BT price scenarios, low, medium, and, high, have been of 0.12%, 0.4%, and 0.62% respectively.

A.1.4 Conclusions

After the three techniques evaluation, the evaluation point definition based on the fleet BT aging years technique has resulted in being the most effective technique. It is important to highlight that it is the technique defining the earliest the evaluation point. This early evaluation allows to manage and correct the fleet BT lifetimes without a high fuel consumption increase.

B

Adaptive Neuro-Fuzzy Inference System Energy Management Strategy

B.1 Adaptive Neuro-Fuzzy Inference System Energy Management Strategy Generated Membership-Functions and Rules

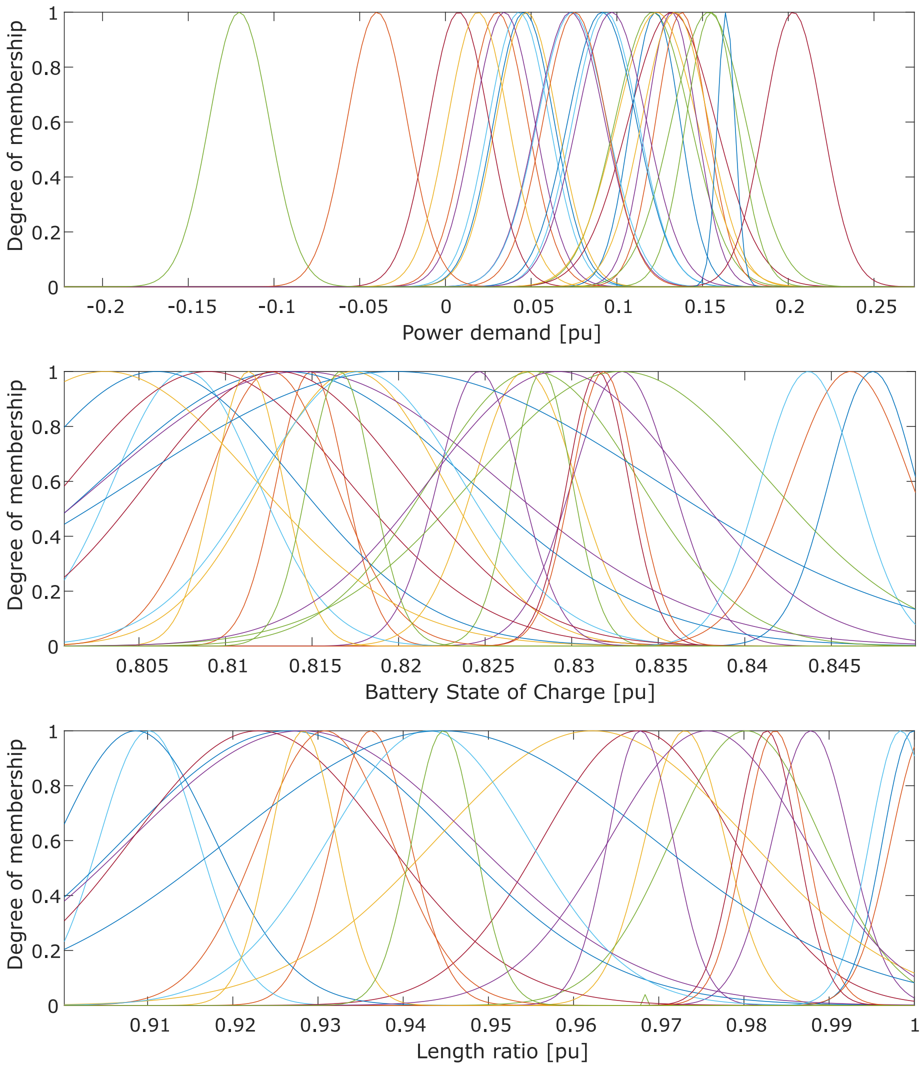

Figure B.1: Power demand, battery state of charge, and length ratio.

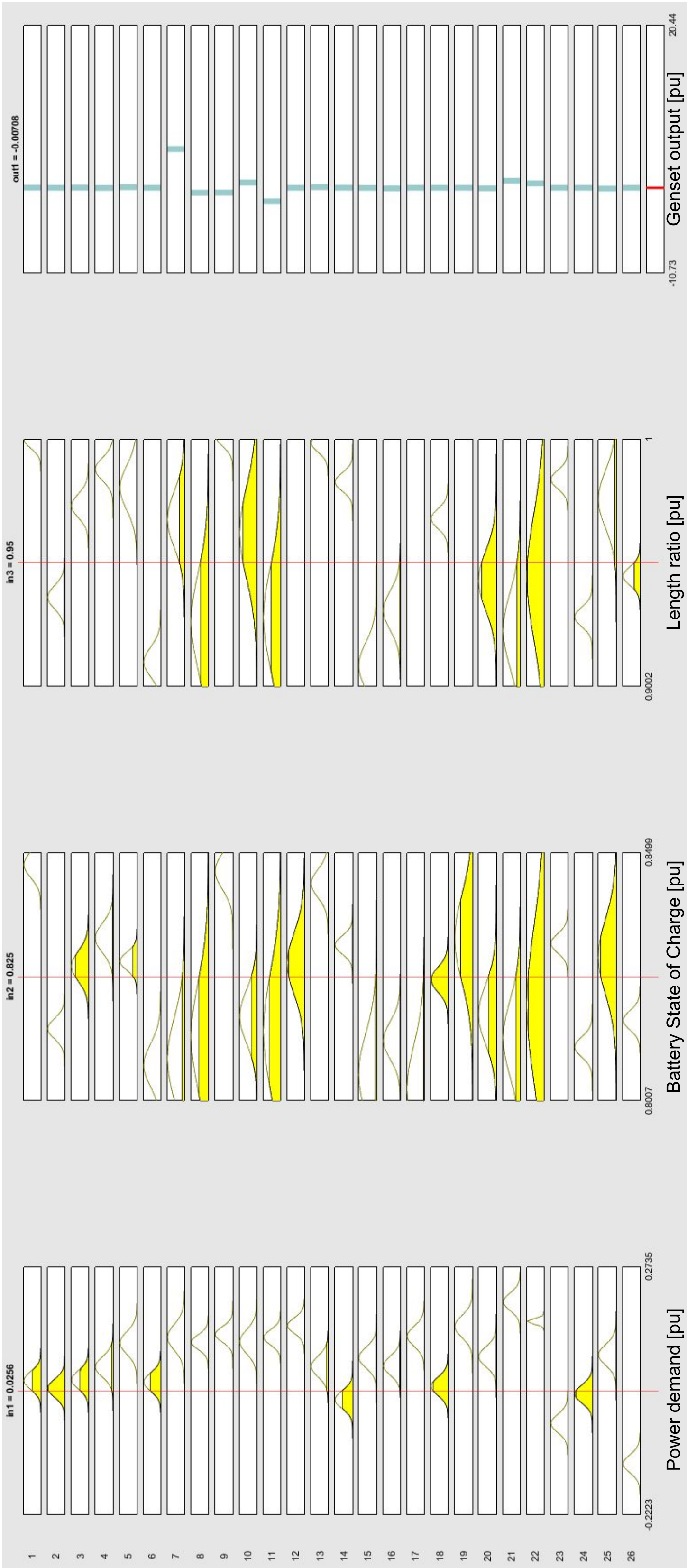

Figure B.2: Rules

Bibliography

[1] Diana Vedlugaite. Greenhouse gas emissions from transport. Technical report, European Environment Agency, 2018.

[2] Heavy-duty vehicles co2 emissions and fuel efficiency, . Available: http://www.europarl.europa.eu/legislative-train/theme-resilient-energy-union-with-a-climate-change-policy/file-heavy-duty-vehicles-co2-emissions-and-fuel-efficiency, 20-04-2018 [Accessed: 21-05-2018].

[3] Mircea Steriu. Local public transport in the european union. Technical report, UITP. Advancing Public Transpot, 2016.

[4] Violeta Bulc. An overview of electric buses in europe. Technical report, 2017.

[5] Reducing co2 emissions from heavy-duty vehicles, . Available:https://ec.europa.eu/clima/policies/transport/vehicles/heavy_en [Accessed: 22-08-2018].

[6] Matthias Rogge, Evelien van der Hurk, Allan Larsen, and Dirk Uwe Sauer. Electric bus fleet size and mix problem with optimization of charging infrastructure. *Applied Energy*, 211(November 2017):282–295, 2018. ISSN 03062619. doi: 10.1016/j.apenergy.2017.11.051. URL https://doi.org/10.1016/j.apenergy.2017.11.051.

[7] Antti Lajunen. Energy consumption and cost-benefit analysis of hybrid and electric city buses. *Transportation Research Part C: Emerging Technologies*, 38:1–15, 2014. ISSN 0968090X. doi: 10.1016/j.trc.2013.10.008. URL http://dx.doi.org/10.1016/j.trc.2013.10.008.

[8] Sjoerd Bakker and Rob Konings. The transition to zero-emission buses in public transport - The need for institutional innovation. *Transportation*

Research Part D: Transport and Environment, (March):0–1, 2017. ISSN 13619209. doi: 10.1016/j.trd.2017.08.023. URL http://dx.doi.org/10.1016/j.trd.2017.08.023.

[9] Kate Palmer, James E. Tate, Zia Wadud, and John Nellthorp. Total cost of ownership and market share for hybrid and electric vehicles in the UK, US and Japan. *Applied Energy*, 209(July 2017):108–119, 2018. ISSN 03062619. doi: 10.1016/j.apenergy.2017.10.089. URL https://doi.org/10.1016/j.apenergy.2017.10.089.

[10] Antti Lajunen. Lifecycle costs and charging requirements of electric buses with different charging methods. *Journal of Cleaner Production*, 172:56–67, 2018. ISSN 09596526. doi: 10.1016/j.jclepro.2017.10.066. URL https://doi.org/10.1016/j.jclepro.2017.10.066.

[11] Bloomberg, 2019. electric vehicle outlook 2019. Available: https://about.bnef.com/electric-vehicle-outlook/#toc-viewreport, 20-05-2019 [Accessed: 03-03-2020].

[12] Moataz Mahmoud, Ryan Garnett, Mark Ferguson, and Pavlos Kanaroglou. Electric buses: A review of alternative powertrains. *Renewable and Sustainable Energy Reviews*, 62:673–684, 2016. ISSN 18790690. doi: 10.1016/j.rser.2016.05.019.

[13] Hydrogen Joint Undertaking. Strategies for joint procurement of fuel cell buses A study for the Fuel Cells and Hydrogen Joint Undertaking. Technical report, Fuel Cells and Hydrogen Joint Undertaking (FCH JU), 2018.

[14] M. F. M. Sabri, K. A. Danapalasingam, and M. F. Rahmat. A review on hybrid electric vehicles architecture and energy management strategies. *Renewable and Sustainable Energy Reviews*, 53:1433–1442, 2016. ISSN 18790690. doi: 10.1016/j.rser.2015.09.036. URL http://dx.doi.org/10.1016/j.rser.2015.09.036.

[15] Yue Hu, Weimin Li, Kun Xu, Taimoor Zahid, Feiyan Qin, and Chenming Li. Energy Management Strategy for a Hybrid Electric Vehicle Based on Deep Reinforcement Learning. *Applied Sciences*, 8(2):187, 2018. doi: 10.3390/app8020187.

[16] He Tian, Shengbo Eben Li, Xu Wang, Yong Huang, and Guangyu Tian. Data-driven hierarchical control for online energy management of plug-in hybrid electric city bus. *Energy*, 142:55–67, 2018. ISSN 03605442. doi: 10.1016/j.energy.2017.09.061.

[17] Nan Xu, Yan Kong, Liang Chu, Hao Ju, Zhihua Yang, Zhe Xu, and Zhuoqi Xu. Towards a smarter energy management system for hybrid vehicles: A comprehensive review of control strategies. *Applied Sciences (Switzerland)*, 9(10), 2019. ISSN 20763417. doi: 10.3390/app9102026.

[18] Hongtao Zhang, Xianguo Li, Xinzhi Liu, and Jinyue Yan. Enhancing fuel cell durability for fuel cell plug-in hybrid electric vehicles through strategic power management. *Applied Energy*, 241(March):483–490, 2019. ISSN 03062619. doi: 10.1016/j.apenergy.2019.02.040. URL https://doi.org/10.1016/j.apenergy.2019.02.040.

[19] Lisiana Nurhadi, Sven Borén, and Henrik Ny. A sensitivity analysis of total cost of ownership for electric public bus transport systems in swedish medium sized cities. *Transportation Research Procedia*, 3(July): 818–827, 2014. ISSN 23521465. doi: 10.1016/j.trpro.2014.10.058. URL http://dx.doi.org/10.1016/j.trpro.2014.10.058.

[20] M Ranta, M Pihlatie, A Pellikka, J Laurikko, P Rahkola, and J Anttila. Analysis and comparison of energy efficiency of commercially available battery electric buses. 2017.

[21] Andrew Harris, Danielle Soban, Beatrice M. Smyth, and Robert Best. Assessing life cycle impacts and the risk and uncertainty of alternative bus technologies. *Renewable and Sustainable Energy Reviews*, 97(April): 569–579, 2018. ISSN 18790690. doi: 10.1016/j.rser.2018.08.045. URL https://doi.org/10.1016/j.rser.2018.08.045.

[22] Mohammad Mesgarpour, Dario Landa-Silva, and Ian Dickinson. Overview of Telematics-Based Prognostics and Health Management Systems for Commercial Vehicles. *Communications in Computer and Information Science*, 395:123–130, 2013. doi: 10.1007/978-3-642-41647-7_16.

[23] Sara Mehar, Sherali Zeadally, Guillaume Remy, and Sidi Mohammed Senouci. Sustainable Transportation Management System for a Fleet of Electric Vehicles. *IEEE Transactions on Intelligent Transportation Systems*, 16(3):1401–1414, 2015. ISSN 1524-9050. doi: 10.1109/TITS.2014.2367099. URL http://ieeexplore.ieee.org/document/6975190/.

[24] Clara Marina Martinez, Xiaosong Hu, Dongpu Cao, Efstathios Velenis, Bo Gao, and Matthias Wellers. Energy Management in Plug-in Hybrid Electric Vehicles: Recent Progress and a Connected Vehicles Perspective. *IEEE Transactions on Vehicular Technology*, PP(99):1–1, 2016. ISSN

0018-9545. doi: 10.1109/TVT.2016.2582721. URL http://ieeexplore.ieee.org/document/7496906/.

[25] E. D. Tate, Michael O. Harpster, and Peter J. Savagian. The Electrification of the Automobile: From Conventional Hybrid, to Plug-in Hybrids, to Extended-Range Electric Vehicles. *SAE International Journal of Passenger Cars - Electronic and Electrical Systems*, 1(1):2008–01–0458, 2008. ISSN 1946-4622. doi: 10.4271/2008-01-0458. URL http://papers.sae.org/2008-01-0458/.

[26] Guang Wu, Xing Zhang, and Zuomin Dong. Powertrain architectures of electrified vehicles: Review, classification and comparison. *Journal of the Franklin Institute*, 352(2):425–448, 2015. ISSN 00160032. doi: 10.1016/j.jfranklin.2014.04.018.

[27] Lino Guzzella and Antonio Sciarretta. *Vehicle Propulsion Systems*. 2005. ISBN 9783540251958.

[28] Haiping Du Hui Zhang, Dongpu Cao. *Modelling, Dynamics, and Control of Electrified Vehicles*. Joe Hayton, 2018. ISBN 9780444535658.

[29] Heide Budde-Meiwes, Julia Drillkens, Benedikt Lunz, Jens Muennix, Susanne Rothgang, Julia Kowal, and Dirk Uwe Sauer. A review of current automotive battery technology and future prospects. *Proceedings of the Institution of Mechanical Engineers, Part D: Journal of Automobile Engineering*, 227(5):761–776, 2013. ISSN 09544070. doi: 10.1177/0954407013485567.

[30] Meiling Yue, Samir Jemei, and Rafael Gouriveau. Review on health-conscious energy management strategies for fuel cell hybrid electric vehicles: Degradation models and strategies. *International Journal of Hydrogen Energy*, 44(13):6844–6861, 2019. ISSN 0360-3199. doi: 10.1016/j.ijhydene.2019.01.190. URL https://doi.org/10.1016/j.ijhydene.2019.01.190.

[31] Jon Ander López-ibarra, Nerea Goitia-zabaleta, Aitor Milo, Haritza Camblong, and Haizea Gaztañaga. Battery and Fuel Cell Aging Conscious Intelligent Energy Management Battery and Fuel Cell Aging Conscious Intelligent Energy Management Strategy for Hydrogen Hybrid Electric Buses. In *Transport Research Arena*, number April, pages 0–10, Helsinki, Finland, 2020. URL https://www.traficom.fi/sites/default/files/media/publication/TRA2020-Book-of-Abstract-Traficom-research-publication.pdf.

[32] Antti Lajunen. Powertrain design alternatives for electric city bus. *2012 IEEE Vehicle Power and Propulsion Conference, VPPC 2012*, pages 1112–1117, 2012. ISSN 1938-8756. doi: 10.1109/VPPC.2012.6422622.

[33] Roberto Sommariva. Sustainable bus magazine. Technical report, April 2020.

[34] Roberto Sommariva. Sustainable bus magazine. Technical report, September 2020.

[35] Zicheng Bi, Lingjun Song, Robert De Kleine, Chunting Chris Mi, and Gregory A. Keoleian. Plug-in vs. wireless charging: Life cycle energy and greenhouse gas emissions for an electric bus system. *Applied Energy*, 146 (February):11–19, 2015. ISSN 03062619. doi: 10.1016/j.apenergy.2015.02.031. URL http://dx.doi.org/10.1016/j.apenergy.2015.02.031.

[36] Rodolfo Dufo-López. Optimisation of size and control of grid-connected storage under real time electricity pricing conditions. *Applied Energy*, 140: 395 – 408, 2015. ISSN 0306-2619. doi: https://doi.org/10.1016/j.apenergy.2014.12.012.

[37] Jiuyu Du, Xiaobin Zhang, Tianze Wang, Ziyou Song, Xueqing Yang, Hewu Wang, Minggao Ouyang, and Xiaogang Wu. Battery degradation minimization oriented energy management strategy for plug-in hybrid electric bus with multi-energy storage system. *Energy*, 165:153–163, 2018. ISSN 0360-5442. doi: 10.1016/j.energy.2018.09.084. URL https://doi.org/10.1016/j.energy.2018.09.084.

[38] Jang Wook Choi and Doron Aurbach. Promise and reality of post-lithium-ion batteries with high energy densities. *Nature Reviews Materials*, 1, 2016. ISSN 20588437. doi: 10.1038/natrevmats.2016.13.

[39] J. M. Tarascon and M. Armand. Issues and challenges facing rechargeable lithium batteries. *Nature*, 414(6861):359–367, 2001. ISSN 00280836. doi: 10.1038/35104644.

[40] M. A. Hannan, M. M. Hoque, A. Mohamed, and A. Ayob. Review of energy storage systems for electric vehicle applications: Issues and challenges. *Renewable and Sustainable Energy Reviews*, 69(November 2016): 771–789, 2017. ISSN 18790690. doi: 10.1016/j.rser.2016.11.171. URL http://dx.doi.org/10.1016/j.rser.2016.11.171.

[41] D. H. Doughty and E. P. Roth. A General Discussion of Li Ion Battery Safety. *Interface magazine*, 21(2):37–44, 2012. ISSN 1064-8208. doi: 10.1149/2.F03122if. URL http://interface.ecsdl.org/cgi/doi/10.1149/2.F03122if.

[42] Gwyn Griffiths. Review of developments in lithium secondary battery technology. *Underwater Technology*, 33(3):153–163, 2016. ISSN 17560551. doi: 10.3723/ut.33.153.

[43] Languang Lu, Xuebing Han, Jianqiu Li, Jianfeng Hua, and Minggao Ouyang. A review on the key issues for lithium-ion battery management in electric vehicles. *Journal of Power Sources*, 226(March):272–288, 2013. ISSN 03787753. doi: 10.1016/j.jpowsour.2012.10.060. URL http://dx.doi.org/10.1016/j.jpowsour.2012.10.060.

[44] Ephrem Chemali, Matthias Peindl, Pawel Malysz, and Ali Emadi. Electrochemical and Electrostatic Energy Storage and Management Systems for Electric Drive Vehicles: State-of-the-Art Review and Future Trends. *IEEE Journal of Emerging and Selected Topics in Power Electronics*, 4(3): 1117–1134, 2016. ISSN 2168-6777. doi: 10.1109/JESTPE.2016.2566583.

[45] S. J. Peighambardoust, S. Rowshanzamir, and M. Amjadi. Review of the proton exchange membranes for fuel cell applications. 35(17):9349–9384, 2010. ISSN 03603199. doi: 10.1016/j.ijhydene.2010.05.017. URL http://dx.doi.org/10.1016/j.ijhydene.2010.05.017.

[46] L. van Biert, M. Godjevac, K. Visser, and P. V. Aravind. A review of fuel cell systems for maritime applications. *Journal of Power Sources*, 327(X): 345–364, 2016. ISSN 03787753. doi: 10.1016/j.jpowsour.2016.07.007. URL http://dx.doi.org/10.1016/j.jpowsour.2016.07.007.

[47] Omer Berkehan Inal and Cengiz Deniz. Assessment of fuel cell types for ships: Based on multi-criteria decision analysis. *Journal of Cleaner Production*, 265:121734, 2020. ISSN 09596526. doi: 10.1016/j.jclepro.2020.121734. URL https://doi.org/10.1016/j.jclepro.2020.121734.

[48] Colin McKerracher Aleksandra O'Donovan, James Frith. Electric buses in cities. driving towards cleaner air and lower co_2. Technical report, Bloomberg New Energy Finance, 2018.

[49] Hans Pohl. Prequisites for fuel cell vehicles. Research Institutes of Sweden, December, 2017. Rise Viktoria. URL

https://energiforskmedia.blob.core.windows.net/media/23563/6-prerequisites-for-fuel-cell-vehicles-hans-pohl-rise.pdf.

[50] Leon Rosario and P. C K Luk. Applying management methodology to electric vehicles with multiple energy storage systems. *Proceedings of the Sixth International Conference on Machine Learning and Cybernetics, ICMLC 2007*, 7(August):4223–4230, 2007. doi: 10.1109/ICMLC.2007.4370888.

[51] V. Herrera. Optimized energy management strategies and sizing of hybrid storage systems for transport applications, 2017.

[52] Jari Vepsäläinen, Antti Ritari, Antti Lajunen, and Klaus Kivekäs. Energy Uncertainty Analysis of Electric Buses. 2018. doi: 10.3390/en11123267.

[53] Ximing Wang, Hongwen He, Fengchun Sun, Xiaokun Sun, and Henglu Tang. Comparative Study on Different Energy Management Strategies for Plug-In Hybrid Electric Vehicles. *Energies*, 6(11):5656–5675, oct 2013. ISSN 1996-1073. doi: 10.3390/en6115656. URL http://www.mdpi.com/1996-1073/6/11/5656.

[54] Jon Ander Lopez, Victor Herrera, Aitor Milo, Haizea Gaztañaga, and Haritza Camblong. Energy Management improvement based on Fleet Learning for Hybrid Electric Buses. In *IEEE Vehicle Power and Propulsion Conference (VPPC)*, Chicago, 2018.

[55] Weiwei Xiong, Yong Zhang, and Chengliang Yin. Optimal energy management for a series-parallel hybrid electric bus. *Energy Conversion and Management*, 50(7):1730–1738, 2009. ISSN 01968904. doi: 10.1016/j.enconman.2009.03.015. URL http://dx.doi.org/10.1016/j.enconman.2009.03.015.

[56] Morteza Montazeri-Gh, Zeinab Pourbafarani, and Mehdi Mahmoodi-k. Comparative study of different types of PHEV optimal control strategies in real-world conditions. *Proceedings of the Institution of Mechanical Engineers, Part D: Journal of Automobile Engineering*, page 095440701773285, 2017. ISSN 0954-4070. doi: 10.1177/0954407017732858. URL http://journals.sagepub.com/doi/10.1177/0954407017732858.

[57] Jian Chen, Chenfeng Xu, Chengshuai Wu, and Weihua Xu. Adaptive Fuzzy Logic Control of Fuel-Cell-Battery Hybrid Systems for Electric Vehicles. *IEEE Transactions on Industrial Informatics*, 14(1):292–300, 2018. ISSN 15513203. doi: 10.1109/TII.2016.2618886.

[58] Victor Isaac Herrera, Aitor Milo, Haizea Gaztanaga, Amaia Gonzalez-Garrido, Haritza Camblong, and Andres Sierra. Design and Experimental Comparison of Energy Management Strategies for Hybrid Electric Buses Based on Test-Bench Simulation. *IEEE Transactions on Industry Applications*, 55(3):3066–3075, 2019. ISSN 00939994. doi: 10.1109/TIA.2018.2886774.

[59] M. Essoufi, B. Hajji, and A. Rabhi. Fuzzy Logic based Energy Management Strategy for Fuel Cell Hybrid Electric Vehicle. *2020 International Conference on Electrical and Information Technologies, ICEIT 2020*, 2020. doi: 10.1109/ICEIT48248.2020.9113162.

[60] A. Tani, M.B. Camara, and B. Dakyo. Energy management based on frequency approach for hybrid electric vehicle applications: Fuel-cell/lithium-battery and ultracapacitors. *IEEE Transactions on Vehicular Technology*, 61(8):3375–3386, 2012. doi: 10.1109/TVT.2012.2206415. URL https://www.scopus.com/inward/record.uri?eid=2-s2.0-84867774193&doi=10.1109%2fTVT.2012.2206415&partnerID=40&md5=65e4f87336d1a98cfc6ccf9ff9577873. cited By 88.

[61] S. Tavakol-Sisakht and S.M. Barakati. Energy manegement using fuzzy controller for hybrid electrical vehicles. *Journal of Intelligent and Fuzzy Systems*, 30(3):1411–1420, 2016. doi: 10.3233/IFS-152054. URL https://www.scopus.com/inward/record.uri?eid=2-s2.0-84961223451&doi=10.3233%2fIFS-152054&partnerID=40&md5=fc262b0c3cdf2a9d2914c6e1b8b42591. cited By 11.

[62] M. Dawei, Z. Yu, Z. Meilan, and N. Risha. "Intelligent fuzzy energy management research for a uniaxial parallel hybrid electric vehicle". *Computers and Electrical Engineering*, 58:447–464, 2017. ISSN 0045-7906. doi: 10.1016/j.compeleceng.2016.03.014. URL http://dx.doi.org/10.1016/j.compeleceng.2016.03.014.

[63] Olle Sundström, Lino Guzzella, and Patrik Soltic. Optimal Hybridization in Two Parallel Hybrid Electric Vehicles using Dynamic Programming. *Proceedings of the 17th IFAC World Congress*, 1:4642–4647, 2008. ISSN 14746670. doi: 10.3182/20080706-5-KR-1001.00781. URL http://www.nt.ntnu.no/users/skoge/prost/proceedings/ifac2008/data/papers/2452.pdf.

[64] Emilia Silvas, Theo Hofman, Nikolce Murgovski, L F Pascal Etman, and Maarten Steinbuch. Review of Optimization Strategies for System-Level Design in Hybrid Electric Vehicles. *Ieee Transactions on Vehicular*

Technology, 66(1):57–70, 2017. ISSN 0018-9545. doi: 10.1109/TVT.2016.2547897.

[65] Liang Li, Chao Yang, Yahui Zhang, Lipeng Zhang, and Jian Song. Correctional DP-Based Energy Management Strategy of Plug-In Hybrid Electric Bus for City-Bus Route. *IEEE Transactions on Vehicular Technology*, 64(7):2792–2803, 2015. ISSN 00189545. doi: 10.1109/TVT.2014.2352357.

[66] Ximing Wang, Hongwen He, Fengchun Sun, and Jieli Zhang. Application study on the dynamic programming algorithm for energy management of plug-in hybrid electric vehicles. *Energies*, 8(4):3225–3244, 2015. ISSN 19961073. doi: 10.3390/en8043225.

[67] Raphael Wegmann, Volker Döge, Jan Becker, and Dirk Uwe Sauer. Optimized operation of hybrid battery systems for electric vehicles using deterministic and stochastic dynamic programming. *Journal of Energy Storage*, 14:22–38, 2017. ISSN 2352152X. doi: 10.1016/j.est.2017.09.008. URL http://linkinghub.elsevier.com/retrieve/pii/S2352152X17301925.

[68] Heeyun Lee, Jongryeol Jeong, Yeong-il Park, and Suk Won Cha. Energy Management Strategy of Hybrid Electric Vehicle Using Battery State of Charge Trajectory Information. 4(1):79–86, 2017. doi: 10.1007/s40684-017-0011-4.

[69] Victor Isaac Herrera, Aitor Milo, Haizea Gaztanaga, Javier Ramos, and Haritza Camblong. Adaptive and Non-Adaptive Strategies for Optimal Energy Management and Sizing of a Dual Storage System in a Hybrid Electric Bus. *IEEE Transactions on Intelligent Transportation Systems*, 20(9):3435–3447, 2018. ISSN 15249050. doi: 10.1109/TITS.2018.2874092.

[70] Lars Johannesson, Stefan Pettersson, and Bo Egardt. Predictive energy management of a 4QT series-parallel hybrid electric bus. *Control Engineering Practice*, 17(12):1440–1453, 2009. ISSN 09670661. doi: 10.1016/j.conengprac.2009.07.004. URL http://dx.doi.org/10.1016/j.conengprac.2009.07.004.

[71] Lulu Guo, Bingzhao Gao, Ying Gao, and Hong Chen. Optimal Energy Management for HEVs in Eco-Driving Applications Using Bi-Level MPC. *IEEE Transactions on Intelligent Transportation Systems*, 18(8):2153–2162, 2017. ISSN 15249050. doi: 10.1109/TITS.2016.2634019.

[72] Peter Mell and Timothy Grance. The NIST Definition of Cloud. Technical report, National Institute of Standards and Technology, US Dept. of Commerce, Special Publication 800-145, DC, USA, 2011.

[73] Engin Ozatay, Simona Onori, James Wollaeger, Umit Ozguner, Giorgio Rizzoni, Dimitar Filev, John Michelini, and Stefano Di Cairano. Cloud-based velocity profile optimization for everyday driving: A dynamic-programming-based solution. *IEEE Transactions on Intelligent Transportation Systems*, 15(6):2491–2505, 2014. ISSN 15249050. doi: 10.1109/TITS.2014.2319812.

[74] Hamid Khayyam and Alireza Bab-Hadiashar. Adaptive intelligent energy management system of plug-in hybrid electric vehicle. *Energy*, 69:319–335, 2014. ISSN 03605442. doi: 10.1016/j.energy.2014.03.020. URL http://dx.doi.org/10.1016/j.energy.2014.03.020.

[75] Zheng Chen, Chunting Chris Mi, Jun Xu, Xianzhi Gong, and Chenwen You. Energy management for a power-split plug-in hybrid electric vehicle based on dynamic programming and neural networks. *IEEE Transactions on Vehicular Technology*, 63(4):1567–1580, 2014. ISSN 00189545. doi: 10.1109/TVT.2013.2287102.

[76] He Tian, Ziwang Lu, Xu Wang, Xinlong Zhang, Yong Huang, and Guangyu Tian. A length ratio based neural network energy management strategy for online control of plug-in hybrid electric city bus. *Applied Energy*, 177: 71–80, 2016. ISSN 03062619. doi: 10.1016/j.apenergy.2016.05.086. URL http://dx.doi.org/10.1016/j.apenergy.2016.05.086.

[77] He Tian, Xu Wang, Ziwang Lu, Yong Huang, and Guangyu Tian. Adaptive Fuzzy Logic Energy Management Strategy Based on Reasonable SOC Reference Curve for Online Control of Plug-in Hybrid Electric City Bus. *IEEE Transactions on Intelligent Transportation Systems*, 19(5):1607–1617, 2018. ISSN 15249050. doi: 10.1109/TITS.2017.2729621.

[78] Zheng Chen, Liang Li, Bingjie Yan, Chao Yang, Clara Marina Martinez, and Dongpu Cao. Multimode Energy Management for Plug-In Hybrid Electric Buses Based on Driving Cycles Prediction. *IEEE Transactions on Intelligent Transportation Systems*, 17(10):2811–2821, 2016. ISSN 15249050. doi: 10.1109/TITS.2016.2527244.

[79] Chao Yang, Liang Li, Sixiong You, Bingjie Yan, and Xian Du. Cloud computing-based energy optimization control framework for plug-in hybrid

electric bus. *Energy*, 125:11–26, 2017. ISSN 03605442. doi: 10.1016/j.energy.2017.02.102. URL http://dx.doi.org/10.1016/j.energy.2017.02.102.

[80] Teng Liu, Bo Wang, and Chenglang Yang. Online Markov Chain-based energy management for a hybrid tracked vehicle with speedy Q-learning. *Energy*, 160:544–555, 2018. ISSN 03605442. doi: 10.1016/j.energy.2018.07.022. URL https://doi.org/10.1016/j.energy.2018.07.022.

[81] Teng Liu, Xiaosong Hu, Weihao Hu, and Yuan Zou. A Heuristic Planning Reinforcement Learning-Based Energy Management for Power-Split Plug-in Hybrid Electric Vehicles. *IEEE Transactions on Industrial Informatics*, 15 (12):6436–6445, 2019. ISSN 19410050. doi: 10.1109/TII.2019.2903098. URL 10.1109/TII.2019.2903098.

[82] H. Shin, S. Park, J. Pi, J. Choi, S. Lee, and H. Kim. "Energy Management Strategy Considering Cabin Heating for Plug-in Hybrid Electric Vehicle". In *EVS 28 International Conference Vehicle Symposium and Exhibition*, pages 1–7, Kintex, Korea, 2015.

[83] Qi. Li, W. Chen, Y. Li, S. Liu, and J. Huang. "Energy management strategy for fuel cell/battery/ultracapacitor hybrid vehicle based on fuzzy logic". *International Journal of Electrical Power & Energy Systems*, 43(1):514–525, December 2012. ISSN 01420615. doi: 10.1016/j.ijepes.2012.06.026. URL https://linkinghub.elsevier.com/retrieve/pii/S0142061512002888.

[84] Tom Fletcher, Rob Thring, and Martin Watkinson. An Energy Management Strategy to concurrently optimise fuel consumption & PEM fuel cell lifetime in a hybrid vehicle. *International Journal of Hydrogen Energy*, 41(46): 21503–21515, 2016. ISSN 03603199. doi: 10.1016/j.ijhydene.2016.08.157. URL http://dx.doi.org/10.1016/j.ijhydene.2016.08.157.

[85] Lu Li, Hong K. Lo, Feng Xiao, and Xuekai Cen. Mixed bus fleet management strategy for minimizing overall and emissions external costs. *Transportation Research Part D: Transport and Environment*, 60:104–118, 2018. ISSN 13619209. doi: 10.1016/j.trd.2016.10.001.

[86] Jon Ander López-Ibarra, Nerea Goitia-Zabaleta, Victor Isaac Herrera, Haizea Gazta ñaga, and Haritza Camblong. Battery aging conscious intelligent energy management strategy and sensitivity analysis of the critical factors for plug-in hybrid electric buses. *eTransportation*, 5(2016):100061, aug 2020. ISSN 25901168. doi: 10.1016/j.etran.2020.100061. URL https://linkinghub.elsevier.com/retrieve/pii/S2590116820300187.

[87] Jon Ander López-Ibarra, Haizea Gaztañaga, Andoni Saez-de Ibarra, and Haritza Camblong. Plug-in hybrid electric buses total cost of ownership optimization at fleet level based on battery aging. *Applied Energy*, 280 (March):115887, 2020. ISSN 03062619. doi: 10.1016/j.apenergy.2020.115887. URL https://doi.org/10.1016/j.apenergy.2020.115887.

[88] Shaobo Xie, Xiaosong Hu, Shanwei Qi, Xiaolin Tang, Kun Lang, Zongke Xin, and James Brighton. Model predictive energy management for plug-in hybrid electric vehicles considering optimal battery depth of discharge. *Energy*, 173: 667–678, 2019. ISSN 03605442. doi: 10.1016/j.energy.2019.02.074. URL https://doi.org/10.1016/j.energy.2019.02.074.

[89] M. Lucu, E. Martinez-Laserna, I. Gandiaga, K. Liu, H. Camblong, W. D. Widanage, and J. Marco. Data-driven nonparametric Li-ion battery ageing model aiming at learning from real operation data - Part B: Cycling operation. *Journal of Energy Storage*, 30(May):101410, 2020. ISSN 2352152X. doi: 10.1016/j.est.2020.101410. URL https://doi.org/10.1016/j.est.2020.101410.

[90] L. Tang, G. Rizzoni, and S. Onori. "Energy management strategy for HEVs including battery life optimization". *IEEE Transactions on Transportation Electrification*, 1(3):211–222, 2015. ISSN 23327782. doi: 10.1109/TTE.2015.2471180.

[91] G. Tang, L.; Rizzoni. "Energy Management Strategy Including Battery Life Optimization for a HEV with a CVT". *2016 IEEE Transportation Electrification Conference and Expo, Asia-Pacific (ITEC Asia-Pacific)*, pages 549–554, 2016. doi: 10.1109/ITEC-AP.2016.7513014.

[92] A. Ravey, B. Blunier, and A. Miraoui. Control strategies for fuel-cell-based hybrid electric vehicles: From offline to online and experimental results. *IEEE Transactions on Vehicular Technology*, 61(6):2452–2457, 2012. ISSN 00189545. doi: 10.1109/TVT.2012.2198680. URL https://www.scopus.com/inward/record.uri?eid=2-s2.0-84863895603&doi=10.1109%2fTVT.2012.2198680&partnerID=40&md5=32033a60bb0f18df8ed140639ecb6fe0. cited By 64.

[93] A. Santucci, A. Sorniotti, and C. Lekakou. "Power split strategies for hybrid energy storage systems for vehicular applications". *Journal of Power Sources*, 258:395–407, 2014. ISSN 0378-7753. doi: 10.1016/j.jpowsour.2014.01.118. URL http://dx.doi.org/10.1016/j.jpowsour.2014.01.118.

[94] F. Jin, M. Wang, and C. Hu. "A fuzzy logic based power management strategy for hybrid energy storage system in hybrid electric vehicles considering battery degradation". In *2016 IEEE Transportation Electrification Conference and Expo (ITEC)*, pages 1–7. IEEE, jun 2016. ISBN 978-1-5090-0403-4. doi: 10.1109/ITEC.2016.7520207. URL http://ieeexplore.ieee.org/document/7520207/.

[95] O. Gomozov, J.P.F. Trovao, X. Kestelyn, and M.R. Dubois. Adaptive energy management system based on a real-time model predictive control with nonuniform sampling time for multiple energy storage electric vehicle. *IEEE Transactions on Vehicular Technology*, 66(7):5520–5530, 2017. ISSN 00189545. doi: 10.1109/TVT.2016.2638912. URL https://www.scopus.com/inward/record.uri?eid=2-s2.0-85029216763&doi=10.1109%2fTVT.2016.2638912&partnerID=40&md5=87825613773d68efc10a0f568fc39e8b. cited By 34.

[96] Nicolas Sockeel, Masood Shahverdi, and Michael Mazzola. Impact of the State of Charge Estimation on Model Predictive Control Performance in a Plug-In Hybrid Electric Vehicle Accounting for Equivalent Fuel Consumption and Battery Capacity Fade. *ITEC 2019 - 2019 IEEE Transportation Electrification Conference and Expo*, 2019. doi: 10.1109/ITEC.2019.8790581.

[97] Xuerui Ma, Yong Zhang, Chengliang Yin, and Shifei Yuan. Multi-objective optimization considering battery degradation for a multi-mode power-split electric vehicle. *Energies*, 10(7), 2017. ISSN 19961073. doi: 10.3390/en10070975.

[98] Pei Zhang, Fuwu Yan, and Changqing Du. A comprehensive analysis of energy management strategies for hybrid electric vehicles based on bibliometrics. *Renewable and Sustainable Energy Reviews*, 48(205):88–104, 2015. ISSN 18790690. doi: 10.1016/j.rser.2015.03.093. URL http://dx.doi.org/10.1016/j.rser.2015.03.093.

[99] Jiankun Peng, Hongwen He, and Rui Xiong. Rule based energy management strategy for a series–parallel plug-in hybrid electric bus optimized by dynamic programming. *Applied Energy*, 185:1633–1643, 2017. ISSN 03062619. doi: 10.1016/j.apenergy.2015.12.031. URL http://dx.doi.org/10.1016/j.apenergy.2015.12.031.

[100] Imad Matraji, Salah Laghrouche, Samir Jemei, and Maxime Wack. Robust control of the PEM fuel cell air-feed system via sub-optimal second order

sliding mode. *Applied Energy*, 104:945–957, 2013. ISSN 03062619. doi: 10.1016/j.apenergy.2012.12.012. URL http://dx.doi.org/10.1016/j.apenergy.2012.12.012.

[101] Li Sun, Jiong Shen, Qingsong Hua, and Kwang Y. Lee. Data-driven oxygen excess ratio control for proton exchange membrane fuel cell. *Applied Energy*, 231(April):866–875, 2018. ISSN 03062619. doi: 10.1016/j.apenergy.2018.09.036. URL https://doi.org/10.1016/j.apenergy.2018.09.036.

[102] Olle Sundström and Anna G. Stefanopoulou. Optimal Power Split in Fuel Cell Hybrid Electric Vehicle with different Battery Sizes, Drive Cycles, and Objectives. *Proceedings of the IEEE International Conference on Control Applications*, pages 1681–1688, 2006. doi: 10.1109/CACSD-CCA-ISIC.2006.4776894.

[103] Y. Wang, Zhendong Sun, and Zonghai Chen. Energy management strategy for battery/supercapacitor/fuel cell hybrid source vehicles based on finite state machine. *Applied Energy*, 254(May):113707, 2019. ISSN 03062619. doi: 10.1016/j.apenergy.2019.113707. URL https://doi.org/10.1016/j.apenergy.2019.113707.

[104] Yujie Wang, Xiyun Li, Li Wang, and Zhendong Sun. Multiple-grained velocity prediction and energy management strategy for hybrid propulsion systems. *Journal of Energy Storage*, 26(September), 2019. ISSN 2352152X. doi: 10.1016/j.est.2019.100950.

[105] Yujie Wang, Zhendong Sun, Xiyun Li, Xiaoyu Yang, and Zonghai Chen. A comparative study of power allocation strategies used in fuel cell and ultracapacitor hybrid systems. *Energy*, 189:116142, 2019. ISSN 03605442. doi: 10.1016/j.energy.2019.116142. URL https://doi.org/10.1016/j.energy.2019.116142.

[106] Stephen Teang Soo Thong, Tien Han Chua, and Tharek Abdul Rahman. Intelligent fleet management system with concurrent GPS & GSM real-time positioning technology. *ITST 2007 - 7th International Conference on Intelligent Transport Systems Telecommunications, Proceedings*, pages 136–141, 2007. doi: 10.1109/ITST.2007.4295849.

[107] D.Srinivasan Balaji P. G, Gaurav Sachdeva and Chen khong Tham. Multi-agent System based Urban Traffic Management. *2007 IEEE Congress on Evolutionary Computation (CEC 2007)*, 117576:1740–1747, 2007. doi: 10.1109/CEC.2007.4424683.

[108] Baisravan HomChaudhuri, Runing Lin, and Pierluigi Pisu. Hierarchical control strategies for energy management of connected hybrid electric vehicles in urban roads. *Transportation Research Part C: Emerging Technologies*, 62:70–86, 2016. ISSN 0968090X. doi: 10.1016/j.trc.2015.11.013. URL http://dx.doi.org/10.1016/j.trc.2015.11.013.

[109] Janos Grantner, Bradley Bazuin, Liang Dong, Jumana Al-shawawreh, Richard Hathaway, Claudia Fajardo, Matthew P. Castanier, and Shabbir Hussain. Condition based maintenance for light trucks. *Conference Proceedings - IEEE International Conference on Systems, Man and Cybernetics*, pages 336–342, 2010. ISSN 1062922X. doi: 10.1109/ICSMC.2010.5641796.

[110] Robin Haycock and Colin Ferguson. Creating demand in fleets for EVs, infrastructure and demand driven energy supply through enabling software that can significantly improve the TCO model of the complete system. *2013 World Electric Vehicle Symposium and Exhibition, EVS 2014*, pages 1–9, 2014. doi: 10.1109/EVS.2013.6914926.

[111] Anthony Barré, Frederic Suard, Mathias Gerard, and Delphine Riu. Battery Capacity Estimation and Health Management of an Electric Vehicle Fleet. In *2014 IEEE Vehicle Power and Propulsion Conference (VPPC)*, volume 16, pages 1–6. IEEE, oct 2014. ISBN 978-1-4799-6783-4. doi: 10.1109/VPPC.2014.7007025. URL http://ieeexplore.ieee.org/document/7007025/.

[112] Adnan Nuhic, Jonas Bergdolt, Bernd Spier, Michael Buchholz, and Klaus Dietmayer. Battery health monitoring and degradation prognosis in fleet management systems. *World Electric Vehicle Journal*, 9(3):1–20, 2018. ISSN 20326653. doi: 10.3390/wevj9030039.

[113] Jochen Eisner, Stefan Funke, and Sabine Storandt. Optimal Route Planning for Electric Vehicles in Large Networks. *Aaai*, pages 1108–1113, 2011. URL http://www.aaai.org/ocs/index.php/AAAI/AAAI11/paper/viewPDFInterstitial/3637/4005.

[114] Martin Sachenbacher, Martin Leucker, Andreas Artmeier, and Julian Haselmayr. Efficient Energy-Optimal Routing for Electric Vehicles. *Proc. Twenty-Fifth AAAI Conference on Artificial Intelligence*, (January 2011): 1402–1407, 2011.

[115] Guillaume Remy, Sara Mehar, Tonino Sophy, Sidi Mohammed Senouci, Francois Jan, and Yvon Gourhant. Green fleet management architecture:

Application to economic itinerary planning. *2012 IEEE Globecom Workshops, GC Wkshps 2012*, (December):369–373, 2012. ISSN 2166-0077. doi: 10.1109/GLOCOMW.2012.6477599.

[116] Timo Duchrow, Martin Schroer, Britta Griesbach, Sebastian Kasperski, Fabian Maas Genannt Bermpohl, Stefan Kramer, and Frank Kirchner. Towards electric mobility data mining. *2012 IEEE International Electric Vehicle Conference*, (March):1–6, 2012. doi: 10.1109/IEVC.2012.6183199. URL http://ieeexplore.ieee.org/document/6183199/.

[117] Hua Qin and Wensheng Zhang. Charging scheduling with minimal waiting in a network of electric vehicles and charging stations. *Proceedings of the Eighth ACM international workshop on Vehicular inter-networking - VANET '11*, (May 2014):51, 2011. doi: 10.1145/2030698.2030706. URL http://dl.acm.org/citation.cfm?doid=2030698.2030706.

[118] Michael Wittmann, Jürgen Lohrer, Johannes Betz, Benedikt Jäger, Maria Kugler, Manfred Klöppel, Adam Waclaw, Moritz Hann, and Markus Lienkamp. A holistic framework for acquisition, processing and evaluation of vehicle fleet test data. *IEEE Conference on Intelligent Transportation Systems, Proceedings, ITSC*, pages 1–7, 2017. doi: 10.1109/ITSC.2017.8317637.

[119] Emission test cycles, worldwide engine and vehicle test cycles, . Available: https://www.dieselnet.com/ standards/cycles/index.php, 10-07-2017 [Accessed: 26-04-2018].

[120] V. Herrera. Optimized energy management strategies and sizing of hybrid storage systems for transport applications, 2017.

[121] Jon Ander López-Ibarra, Victor Isaac Herrera, Haritza Camblong, Aitor Milo, and Haizea Gaztañaga. Energy Management Improvement Based on Fleet Digitalization Data Exploitation for Hybrid Electric Buses. In Blondin Maude Josée, Panos M. Pardalos, and Javier Sanchis Sáez, editors, *Computational Intelligence and Optimization Methods for Control Engineering Energy*, chapter 14, pages 321–355. Springer Nature Switzerland AG 2019, 2019. ISBN 978-3-030-25446-9. doi: 10.1007/978-3-030-25446-9_14. URL http://link.springer.com/10.1007/978-3-030-25446-9_14.

[122] Victor Isaac Herrera, Aitor Milo, Haizea Gaztañaga, Ion Etxeberria-Otadui, Igor Villarreal, and Haritza Camblong. Adaptive energy management strategy and optimal sizing applied on a battery-supercapacitor based tramway. *Applied Energy*, 169:831–845, 2016. ISSN 03062619.

[123] Kokam li-ion/polymer cell, . Available: http://kokam.com/data/Kokam_Cell_Brochure_V.4.pdf, [Accessed: 26-04-2018].

[124] Samppa Jenu, Ivan Deviatkin, Ari Hentunen, Marja Myllysilta, Saara Viik, and Mikko Pihlatie. Reducing the climate change impacts of lithium-ion batteries by their cautious management through integration of stress factors and life cycle assessment. *Journal of Energy Storage*, 27(November 2019): 101023, 2020. ISSN 2352152X. doi: 10.1016/j.est.2019.101023. URL https://doi.org/10.1016/j.est.2019.101023.

[125] Norio Takami, Hiroki Inagaki, Yoshinao Tatebayashi, Hidesato Saruwatari, Keizoh Honda, and Shun Egusa. High-power and long-life lithium-ion batteries using lithium titanium oxide anode for automotive and stationary power applications. *Journal of Power Sources*, 244:469–475, 2013. ISSN 03787753. doi: 10.1016/j.jpowsour.2012.11.055. URL http://dx.doi.org/10.1016/j.jpowsour.2012.11.055.

[126] R. Dufo. Dimensionamiento y control optimo de sistemas híbridos aplicando algorítmos evolutivos, 2007.

[127] Victor Herrera, Aitor Milo, Haizea Gaztañaga, and Haritza Camblong. Multi-objective Optimization of Energy Management and Sizing for a Hybrid Bus with dual Energy Storage System. 2016.

[128] W. A. Facinelli. Modeling and Simulation of Lead-acid Batteries for Photovoltaic Systems. 1983.

[129] Dirk Uwe Sauer and Heinz Wenzl. Comparison of different approaches for lifetime prediction of electrochemical systems-Using lead-acid batteries as example. *Journal of Power Sources*, 176(2):534–546, 2008. ISSN 03787753. doi: 10.1016/j.jpowsour.2007.08.057.

[130] Mitch Mabrey. Advantages and Marine Applications of Various Lithium Ion Battery Chemistries. In *Battery Propulsion Conference*, USA, December, 2016. IEEE. URL maritime.dot.gov/sites/marad.dot.gov/files/docs/innovation-research/meta/3376/spear-lithiumionchemistries.pdf.

[131] M. Pihlatie, S. Kukkonen, T. Halmeaho, V. Karvonen, and N. O. Nylund. Fully electric city buses - The viable option. *2014 IEEE International Electric Vehicle Conference, IEVC 2014*, 2015. doi: 10.1109/IEVC.2014.7056145.

[132] Björn Nykvist and Måns Nilsson. Rapidly falling costs of battery packs for electric vehicles. *Nature Climate Change*, 5(4):329–332, 2015. ISSN 17586798. doi: 10.1038/nclimate2564.

[133] Huajie Ding, Zechun Hu, and Yonghua Song. Value of the energy storage system in an electric bus fast charging station. *Applied Energy*, 157:630–639, 2015. ISSN 18729118. doi: 10.1016/j.apenergy.2015.01.058. URL http://dx.doi.org/10.1016/j.apenergy.2015.01.058.

[134] Orhan Topal and İsmail Nakir. Total cost of ownership based economic analysis of diesel, CNG and electric bus concepts for the public transport in Istanbul City. *Energies*, 11(9), 2018. ISSN 19961073. doi: 10.3390/en11092369.

[135] Ivan Mareev, Jan Becker, and Dirk Uwe Sauer. Battery dimensioning and life cycle costs analysis for a heavy-duty truck considering the requirements of long-haul transportation. *Energies*, 11(1), 2018. ISSN 19961073. doi: 10.3390/en11010055.

[136] Yu Miao, Patrick Hynan, Annette Von Jouanne, and Alexandre Yokochi. Current li-ion battery technologies in electric vehicles and opportunities for advancements. *Energies*, 12(6):1–20, 2019. ISSN 19961073. doi: 10.3390/en12061074.

[137] Fabian Meishner, Bonjad Satvat, and DIrk Uwe Sauer. Battery electric buses in european cities: Economic comparison of different technological concepts based on actual demonstrations. *2017 IEEE Vehicle Power and Propulsion Conference, VPPC 2017 - Proceedings*, 2018-January:1–6, 2018. doi: 10.1109/VPPC.2017.8331012.

[138] Bernd Emonts, Markus Reuß, Peter Stenzel, Lara Welder, Felix Knicker, Thomas Grube, Klaus Görner, Martin Robinius, and Detlef Stolten. Flexible sector coupling with hydrogen: A climate-friendly fuel supply for road transport. *International Journal of Hydrogen Energy*, 44(26):12918–12930, 2019. ISSN 03603199. doi: 10.1016/j.ijhydene.2019.03.183.

[139] Olle Sundstr and Lino Guzzella. A Generic Dynamic Programming Matlab Function. *18th IEEE International Conference on Control Applications, Saint Petersburg, Russia*, (7):1625–1630, 2009.

[140] Olle Sundström, D Ambühl, and Lino Guzzella. On Implementation of Dynamic Programming for Optimal Control Problems with Final State Constraints. *Oil & Gas Science and Technology – Revue de l'Institut*

Français du Pétrole, 65(1):91–102, 2009. ISSN 1294-4475. doi: 10.2516/ogst/2009020.

[141] Jon Ander Lopez-Ibarra, Nerea Goitia-Zabaleta, Aitor Milo, Haizea Gaztañaga, and Haritza Camblong. Intelligent and Adaptive Fleet Energy Management Strategy for Hybrid Electric Buses. In *IEEE Vehicle Power and Propulsion Conference (VPPC)*, pages 1–6, Hanoi, Vietnam, 2019.

[142] Stephen L. Chiu. Fuzzy model identification based on cluster estimation. *Journal of Intelligent and Fuzzy Systems*, 2(3):267–278, 1994. ISSN 18758967. doi: 10.3233/IFS-1994-2306.

[143] Jyh-SShing Roger Jang. ANFIS: Adaptive-Network-Based Fuzzy Inference System. IEEE Transactions on Systems. *Man and Cybernetics*, 23(3): 665–685, 1993. ISSN 00189472.

[144] M Sugeno and G.T Kang. Structure identification of fuzzy model. *Fuzzy Sets and Systems*, 28(1):15 – 33, 1998. ISSN 0165-0114. doi: https://doi.org/10.1016/0165-0114(88)90113-3. URL http://www.sciencedirect.com/science/article/pii/0165011488901133.

[145] A. Bouscayrol. Different types of Hardware-In-the-Loop simulation for electric drives. *IEEE International Symposium on Industrial Electronics*, pages 2146–2151, 2008. doi: 10.1109/ISIE.2008.4677304.

[146] Rahul C. Basole and Douglas A. Bodner. *Modeling and Simulation in the Systems Engineering Life Cycle*. 2015. ISBN 9781447156338. doi: 10.1007/978-1-4471-5634-5_10.